Regulation of RECQL4, the Rothmund-Thomson-, RAPADILINO- and Baller-Gerold-Syndrome Gene Product, by p300 Mediated Acetylation

Dissertation

zur

Erlangung der naturwissenschaftlichen Doktorwürde
(Dr.sc.nat.)

vorgelegt der

Mathematisch-naturwissenschaftlichen Fakultät

der

Universität Zürich

von

Tobias Dietschy

aus

Rheinfelden (AG), Schweiz

Promotionskomitee

Prof. Dr. Josef Jiricny (Vorsitz)
Prof. Dr. Igor Stagljar (Leitung der Dissertation)
Prof. Dr. Michael Hottiger

Zürich, 2007

Contents

Contents ii

Summary v

Zusammenfassung vii

Abbreviations x

1 Helicases 1

2 RecQ Family of DNA Helicases 5

2.1 RECQL1 8

2.1.1 General Information 8

2.1.2 Biochemical Properties of RECQL1 Protein 8

2.1.3 RECQL1 Interacting Partners 9

2.2 BLM 10

2.2.1 Bloom Syndrome 10

2.2.2 BLM Mouse Models 11

2.2.3 BLM Interacting Partners 12

2.2.4 Biochemical Properties of the BLM Protein 15

2.2.5 Posttranslational Modifications of BLM Protein 16

2.3 WRN 17

2.3.1 Werner Syndrome 17

2.3.2 WRN Mouse Models 18

2.3.3 WRN Interacting Partners 19

2.3.4 Biochemical Properties of WRN Protein 23

2.3.5 Posttranslational Modifiactions of WRN Protein 23

2.4 RECQL4.....25
2.4.1 Rothmund-Thomson Syndrome..... 25
2.4.2 RAPADILINO Syndrome.....26
2.4.3 Baller-Gerold Syndrome.....27
2.4.4 RECQL4 Mouse Models.....28
2.4.5 RECQL4 in the Context of DNA Replication.....29
2.4.6 RECQL4 Interacting Partners..... 29
2.4.7 Subcellular Localization of RECQL4.....32
2.4.8 Biochemical Properties of the RECQL4 Protein..... 33
2.5 RECQL5.....35
2.5.1 General Information.....35
2.5.2 Biochemical Properties of the RECQL5β Protein.....35
2.5.3 RECQL5β Interacting Proteins.....36

3 Posttranslational Modifiaction of Proteins 37

3.1 General Introduction.....37
3.2 Protein Acetylation.....38
3.2.1 Reversible N^{ε}- Acetylation of Lysine Residues..... 38
3.2.2 Acetylation of Serine and Threonine Residues..... 39
3.2.3 Acetylations of Histones.....40
3.2.4 Histone Acetyltransferases..... 41
3.2.5 Histone Deacetylases.....43
3.3 Histone Acetyltransferase p300/CBP.....45
3.3.1 Structure and Function of p300/CBP.....45
3.3.2 p300/CBP and Human Disease..... 46
3.3.3 p300/CBP Acetylation of Traget Proteins.....47

4 Results 49

Article I: The human Rothmund-Thomson syndrome gene product, RECQL4, localizes to distinct nuclear foci that coincide with proteins involved in the maintenance of genome stability..... **50**

Article II: The molecular role of the Rothmund-Thomson-,RAPADILINO- and Baller-Gerold-gene product, RECQL4: recent progress..... **60**

Article III: Physical and functional interactions between Werner syndrome helicase and mismatch-repair initiation factors..... **68**

Article IV: Acetylation of RECQL4, the Rothmund-Thomson-, RAPADILINO- and Baller-Gerold-Syndrome gene product, by the histone acetyltransferase p300 regulates its subcellular localization.....**80**

5 Conclusion and Perspectives **105**

6 References **109**

7 Appendix **124**

Article V: The Werner syndrome protein is required for recruitment of chromatin assembly factor 1 following DNA damage.....**125**

Article VI: The Bloom's syndrome helicase (BLM) interacts physically and functionally with p12, the smallest subunit of human DNA polymerase δ.....**138**

8 Acknowledgements **161**

9 Curriculum Vitae **162**

Summary

The RecQ family of DNA helicases is conserved from bacteria to human and members play an important role in the maintenance of genome stability. Humans possess five RecQ homologues: *RECQL1*, *BLM*, *WRN*, *RECQL4*, and *RECQL5*. Five autosomal recessive disorders, characterized by genomic instability, cancer progression, and developmental abnormalities, are associated with defects in the BLM (Bloom syndrome), WRN (Werner syndrome), and RECQL4 (Rothmund-Thomson (RTS), RAPADILINO, and Baller-Gerold syndromes (BGS) genes products. While the distinct molecular functions of BLM and WRN helicases have been widely characterized in the last decade, the precise molecular and cellular role of the RECQL4 protein has not yet been elucidated.

The aim of this thesis was to investigate if RECQL4 is subject to reversible acetylation and how this post-translational modification influences RECQL4 function *in vivo*. To this end, we overexpressed RECQL4 with different human histone acetyltransferases (HATs) in human embryonic kidney (HEK) 293T cells and examined RECQL4 acetylation *in vivo* using whole cell extracts and an α-acetyl-lysine antibody. This experiment revealed that only p300, a human transcriptional co-activator and histone acetyltransferase, specifically acetylated RECQL4 *in vivo*. A RECQL4/p300 interaction was confirmed by co-immunoprecipitation and ELISA-based protein binding assays and the interaction regions were mapped using GST-pull down experiments. The N-terminal amino acids 1-408 of RECQL4 and residues 1459–1892 of p300 were necessary and sufficient for the interaction of RECQL4 with p300.

We investigated the biochemical consequences of RECQL4/p300 interaction. Therefore, RECQL4 and p300 were recombinantly expressed, purified and subsequently used to test RECQL4 ATPase activity. We showed that p300 specifically stimulated the RECQL4 ATPase activity *in vitro*, while acetylation of RECQL4 decreased this effect.

We used an *in vitro* acetylation assay with purified recombinant p300, different GST-RECQL4 fragments, and ^{14}C-labeled Acetyl-Coenzyme A (Ac-CoA) to identifiy several lysine residues (K 376, 380, 382, 385, 386) of the previously characterized RECQL4 nucleolar localization signal (NOS) (aa 376-386) as targets of p300 mediated acetylation. This finding was confirmed since RECQL4 (K 376, 380, 382, 385, 386 R) mutant was no longer acetylated by p300 *in vivo*.

We next analyzed RECQL4 localization in human cells using immunofluorescence. As previously shown, overexpressed His-RECQL4 was predominantly localized to the nucleus in different human cell lines. Interestingly, mutation of the NOS lysine residues to alanine (K 376, 380, 382, 385, 386 A), but not to arginine (K 376, 380, 382, 385, 386 R), completely abolished the nuclear import of RECQL4 in human cells. Additionally, the fusion of the RECQL4 NOS (aa 376-386) to the N-terminus of β-galactosidase led to the nuclear import of this 100kDa protein in mammalian cells, indicating the importance of positively charged amino acid residues for the nuclear import of the RECQL4 protein.

Finally, we investigated the consequence of p300 mediated RECQL4 acetylation on its subcellular localization. Immunofluorescence experiments showed that overexpression of p300, but not its catalytic dead mutant, enhanced about three-fold the number of cells in which RECQL4 was mainly cytoplasmic. No difference was seen when the corresponding RECQL4 mutant (K 376, 380, 382, 385, 386 R) was used. The same effect was observed when cells were treated with the histone deacetylase (HDAC) inhibitors Trichostatin A (TSA) and nicotin amide (NA) indicating that protein acetylation drives RECQL4 from the nucleus to the cytoplasm.

Our results provide the first evidence of a post-translational modification of the RECQL4 protein and suggest that acetylation of RECQL4 by p300 regulates the trafficking of RECQL4 between the nucleus and the cytoplasm.

Zusammenfassung

RecQ Helikasen spielen eine entscheidende Rolle in der Aufrechterhaltung genomischer Stabilitaet. Die Mitglieder der Familie der RecQ Helikasen sind hochkonserviert und es wurden im Menschen fuenf homologe Gene identifiziert: *RECQL1, BLM, WRN, RECQL4* und *RECQL5*. Es ist bekannt, dass Mutationen in den *BLM*, *WRN* und *RECQL4* Genen zu verschiedenen autosomal rezessiven Krankheiten führen: Mutationen im *BLM* Gen fuehren zum Bloom Syndrom, *WRN* Mutationen sind verantwortlich fuer das Werner Syndrom und *RECQL4* Mutationen werden mit drei verschiedenen Krankheiten assoziiert: Dem Rothmund-Thomson-, RAPADILINO- und Baller-Gerold Syndrom. Patienten mit diesen Krankheiten haben Anomalien waehrend der Entwicklung und ein erhoehtes Krebsrisiko, hervorgerufen durch genomische Instabilitaet in den Zellen. Waehrend die BLM- und WRN Helikasen gut erforscht sind und ihre zellulaeren Aufgaben zu einem grossen Teil charakterisiert wurden, ist die Rolle von RECQL4 weitgehend unbekannt.

Das Ziel dieser Dissertation war es, herauszufinden, ob RECQL4 reversibel aceyliert wird. Verschiedene Histon Acetyltransferasen (HATs) wurden zusammen mit RECQL4 in menschlichen Zellen (HEK 293T) ueberexprimiert und die Zellextrakte mittels einem α- Acetyl-Lysin Antikoerpers auf acetyliertes RECQL4 hin untersucht. Diese Experimente zeigen, dass RECQL4 spezifisch von der HAT p300 *in vivo* acetyliert wird. Die Interaktion zwischen RECQL4 und p300 konnten wir durch Co-immunopräzipitations- und ELISA Experimente bestaetigen. Des Weiteren bestimmten wir die interagierenden Regionen von RECQL4 und p300. Mit *GST-pull down* Experimenten haben wir nachgewiesen, dass das RECQL4 Fragment von Aminosaure 1 bis 408 und das p300 Fragment von Aminosaeure 1459 bis 1893 fuer die Interaktion der beiden Proteine ausreichen.

Zur Untersuchung der Funktion dieser Interaktion testeten wir den Einfluss von p300 auf die ATPase Aktivitaet von RECQL4. Wir verwendeten dazu rekombinant exprimierte und aufgereinigte RECQL4 und p300 Proteine. Wir konnten nachweisen, dass p300 die ATPase Aktivitaet von RECQL4 stimuliert, waehrend die Acetylierung von RECQL4 durch p300 eine leicht hemmende Wirkung hat.

Als Naechstes untersuchten wir, welche RECQL4 Lysine von p300 acetyliert werden. Mittels *in vitro* Acetylierungsassays mit aufgereinigtem p300, verschiedenen GST-RECQL4 Fragmenten und ^{14}C-Acetly-Coenzym A identifizierten wir mehrere Lysine (K 376, 380, 382, 385, 386) innerhalb des RECQL4 Nukleolar Lokalisation Signal (NOS) als moegliche Ziele der Acetylierung. Die Tatsache, dass die RECQL4 (K 376, 380, 382, 385, 386 R) Mutante von p300 nicht laenger *in vivo* acetyliert wurde, bestaetigte dies.

Des Weiteren untersuchten wir die Lokalisation von RECQL4 in humanen Zellen mittels Immunofluoreszenz. Wie bereits von anderen Gruppen gezeigt, ist endogenes sowie ueberexprimiertes RECQL4 Protein vor allem im Nukleus lokalisiert. Wir untersuchten zwei RECQL4 NOS Lysin Mutanten, (K 376, 380, 382, 385, 386 A) und (K 376, 380, 382, 385, 386 R), auf ihre Lokalisation. Interessanterweise war die (K 376, 380, 382, 385, 386 A) Mutante ausschliesslich im Zytoplasma lokalisiert, waehrend sich die (K 376, 380, 382, 385, 386 R) Mutante wie der RECQL4 Wildtyp verhielt. Die N-terminale Fusion des RECQL4 NOS (aa376-386) an β-Galaktosidase fuehrt zum Import in den Nukleus dieses 100kDa Proteins, was die Relevanz der RECQL4 Aminosaeuresequenz 376-386 fuer den nuklearen Import weiter unterstreicht.

Zu guter Letzt wollten wir den Einfluss p300-vermittelter Acetylierung auf die Lokalisation von RECQL4 studieren. Immunfluoreszenz Experimente zeigen, dass die Ueberexprimierung von p300 die RecQL4 Lokalisation im Zytoplasma signifikat erhoehte, waehrend die ueberexprimierte katalytisch-inaktive p300 Mutante keinen Einfluss hatte. Derselbe Effekt wurde erzielt, wenn die Zellen mit Histon Deacetylase Inihbitoren Trichostatin A und Nikotinamid behandelt wurden.

Wir schliessen daraus, dass die Acetylierung von RECQL4 fuer die zytoplasmatische Lokalisation von RECQL4 verantwortlich ist.
Die hier gezeigte Acetylierung von RECQL4 durch p300 ist der erste Nachweis einer posttranslationeller Modifikation von RECQL4. Des Weiteren zeigen wir, dass sie eine wichtige Rolle in der Lokalisation von RECQL4 spielt.

Abbreviations

4NQO	4-nitroquinoline 1-oxide
aa	Amino acid
Ac-CoA	Acetyl Co-enzyme A
APE-1	Apurinic/apyrimidinic endonuclease 1
ATP	Adenosine 5′-triphosphate
BASC	BRCA1 associated genome surveillance complex
β-Gal	β-Galactosidase
bp	Base pair
BGS	Baller-Gerold syndrome
BS	Bloom syndrome
BSA	Bovine serum albumin
CAF-1	Chromatin assembly factor 1
CBP	CREB-binding protein
Cdc	Cell division cycle
DHJ	Double holliday junction
DNA	Deoxyribonucleic acid
DNA-PK	DNA-dependent protein kinase
dNTP	Deoxyribonucleoside 5′-triphosphate
DSB	Double-strand break
dsDNA	Double-stranded DNA
E.coli	*Escherichia coli*
ELISA	Enzyme linked immunoabsorbent assay
ES	Embryonic stem
FAT	Factor acetyltransferase
Fen1	Flap endonuclease
GFP	Green fluorescence protein

GST	Glutathione S-transferase
HAT	Histone acetyltransferase
HDAC	Histone deacetylase
HEK	Human embryonic kidney
HJ	Holliday junction
Hprt	Hypoxantine phosphoribosyltransferase
HR	Homologous recombination
HRDC	Helicase RNase D C-terminal
HU	Hydroxy urea
IF	Immunofluorescence
IR	Ionizing radiation
kb	Kilobase pair
kDa	Kilodalton
MAPK	Mitogen-activated protein kinase
MEF	Mouse embryonic fibroblast
MMS	Methyl methanesulfonate
mRNA	messenger RNA
NA	Nicotin amide
NER	Nucleotide excision repair
NHEJ	Nonhomologous end-joining
NLS	Nuclear localization signal
NOS	Nucleolar localization Signal
NTP	Nucleoside 5′-triphosphate
PARP-1	Poly(ADP-ribose) polymerase-1
PCNA	Proliferating cell nuclear antigen
PGK	Phosphoglycerate kinase
PML	Promyelocytic leukaemia
pol β	Polymerase β
pol δ	Polymerase δ
RFC	Replication factor C

RNA	Ribonucleic acid
RNAi	RNA interference
RPA	Replication protein A
RQC	RecQ family C-terminal
RTS	Rothmund-Thomson syndrome
RTS	Rubenstein-Taby syndrome
SCE	Sister-chromatid exchange
SF	Superfamily
ssDNA	Single-stranded DNA
TRF	Telomeric repeat binding factor
TSA	Trichostatin A
UV	Ultraviolet
WS	Werner syndrome
YTH	Yeast two-hybrid

1 Helicases

Helicases are motor proteins that can transiently catalyze the unwinding of energetically stable duplex nucleic acids (DNA-DNA, RNA-DNA, RNA-RNA) using NTP hydrolysis as the energy source. They are important enzymatic tools for the cellular DNA machinery and play essential roles in nearly all aspects of nucleic acid metabolism, such as DNA replication, repair, recombination, and transcription (1, 2).

In 1976, the first helicase was discovered in *Escherichia coli* (*E. coli*) (3) and since then, a large number of these enzymes have been identified and characterized in many different organisms. Helicases can be classified according to sequence homology and directionality. Most helicases require a single-stranded nucleic acid region to bind and initiate the action of strand separation. Once loaded on the strand, they show a directional bias and translocate either 5'→3' or 3'→5' (Fig. 1). The directionality is defined with respect to the nucleic acid strand on which the enzyme translocates.

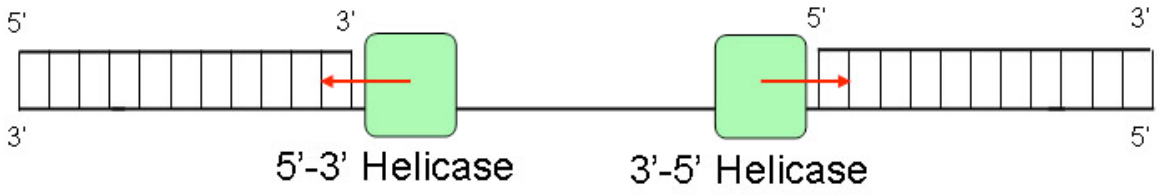

Figure 1: Polarity of protein translocation along a DNA strand

Based on conserved amino acid sequence motifs, helicases are classified into families and superfamilies (SF1-4) (4). Helicases from different families share similarities in their three-dimensional folds (RecA-like folds) (5-7). SF1 and SF2 represent the largest and most closely related groups of helicases, and contain at

least seven conserved motifs (I, Ia, II-VI), SF3 helicases have three motifs (A, B and C), and SF4 members have five motifs (1, 1a, 2-4) (8). All helicases, irrespective of the superfamily to which they belong, contain motifs that are equivalent to the so-called Walker A and B motifs, characteristic of NTP-binding and/or hydrolyzing enzymes, which were first identified in mitochondrial F_1-ATPase (9).

Figure 2 shows the organization of the conserved DEAD box helicase domains. Motif I is necessary for ATP binding (10) and referred to as the Walker A motif found in ATPases (9). The motif Ia is present in most SF1 and SF2 helicases (11) and binds ssDNA in the UL9 helicase from the Herpes Simplex Virus (HSV) (11). DEAD and DExH helicases exhibit an additional motif named Ib, which has the consensus sequence of TxGx (2). Motif II, also named the Walker B motif, is also found in other ATPases. Based on the sequence of this motif, helicases are further classified into the DExH and the DEAD families. The highly conserved aspartate residue (D of DE) in this motif coordinates Mg^{2+}, and is required for ATP hydrolysis (10). Motif III reveals a role in coupling ATP hydrolysis to strand separation (12). Motif IV seems to be essential for the later steps of the ATPase reaction as it binds ADP. Motif V makes contacts with the sugar-phosphate backbone and is therefore likely to serve as an additional DNA binding domain (8). Motif VI has been proposed to be required for the helicase to move along the DNA by mediating conformational changes associated with nucleotide binding (2).

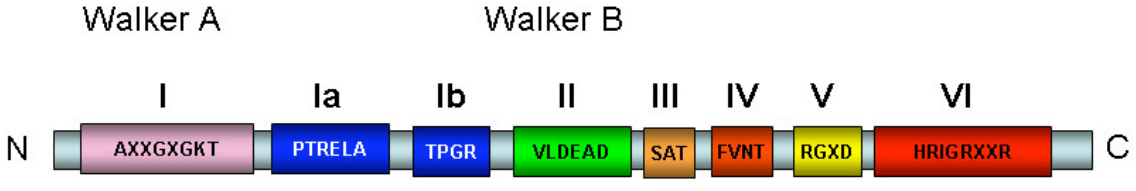

Figure 2: Schematic representation of conserved helicase motifs of the DEAD box helicases. The colored boxes represent the conserved helicase motifs, and the consensus amino acid sequence of each motif is shown by the single letter code inside the boxes (Adapted from (2)).

Much effort has been made in the past to understand how DNA helicases are able to simultaneously interact with NTP and nucleic acids, hydrolyze NTP, and couple the energy resulting from nucleotide hydrolysis to DNA unwinding. Different models have been proposed to describe the helicase catalyzed mechanism of unwinding (13-17) (Fig. 3).

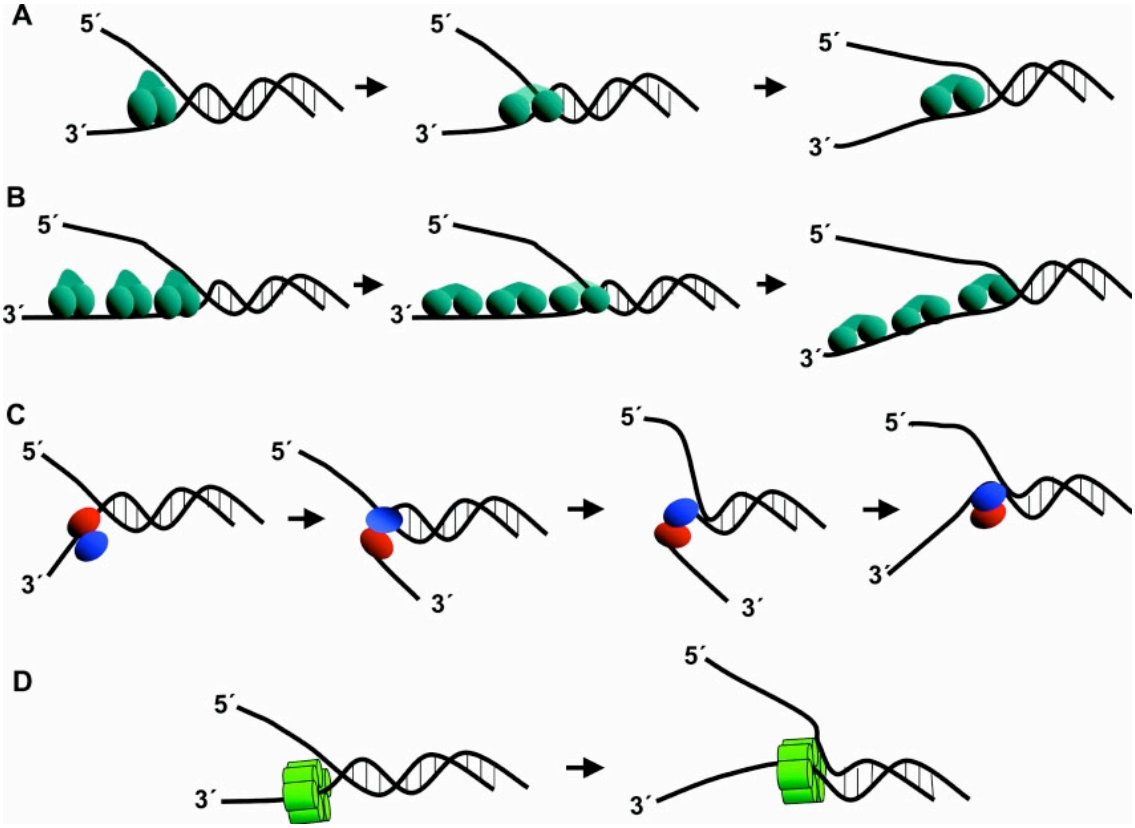

Figure 3: Different proposed models for the active unwinding mechanisms for DNA helicases. For all of the mechanisms depicted, DNA unwinding is fuelled by the energy of helicase-catalysed NTP hydrolysis (18).

In the inchworm model (19) (Fig. 3A), the functional helicase has two non-identical DNA-binding sites that bind with a defined polarity; the leading site interacts with the duplex region during successive cycles of unwinding, whereas the tail site interacts with the ssDNA. A co-operative inchworm mechanism has been proposed in

which multiple helicase molecules line up along the ssDNA lattice (20, 21) (Fig. 3B). The rolling model requires at least two identical DNA-binding sites, both of which can bind to ssDNA and dsDNA, in an alternating fashion (Fig. 3C). The rolling model requires a dimeric protein, whereas the inchworm model is consistent with any oligomeric state, including a monomer. An alternative multimeric form is the hexameric helicase, which is believed to have a ring structure that encircles one strand of the duplex leaving the other extruded outside the ring (Fig. 3D). The hexameric helicase may have an advantageous design to prevent.

2 RecQ Family of DNA Helicases

RecQ DNA helicases are wide spread in nature and have been identified in organisms ranging from bacteria to humans. All RecQ homologues tested to date unwind paired DNA, translocating in a 3′→5′ direction (22). A single family member exists in bacteria and budding or fission yeast, whereas there are generally multiple representatives in higher eukaryotes, including five identified RecQ proteins in humans: RECQL1, BLM, WRN, RECQL4, RECQL5 (Fig. 4).

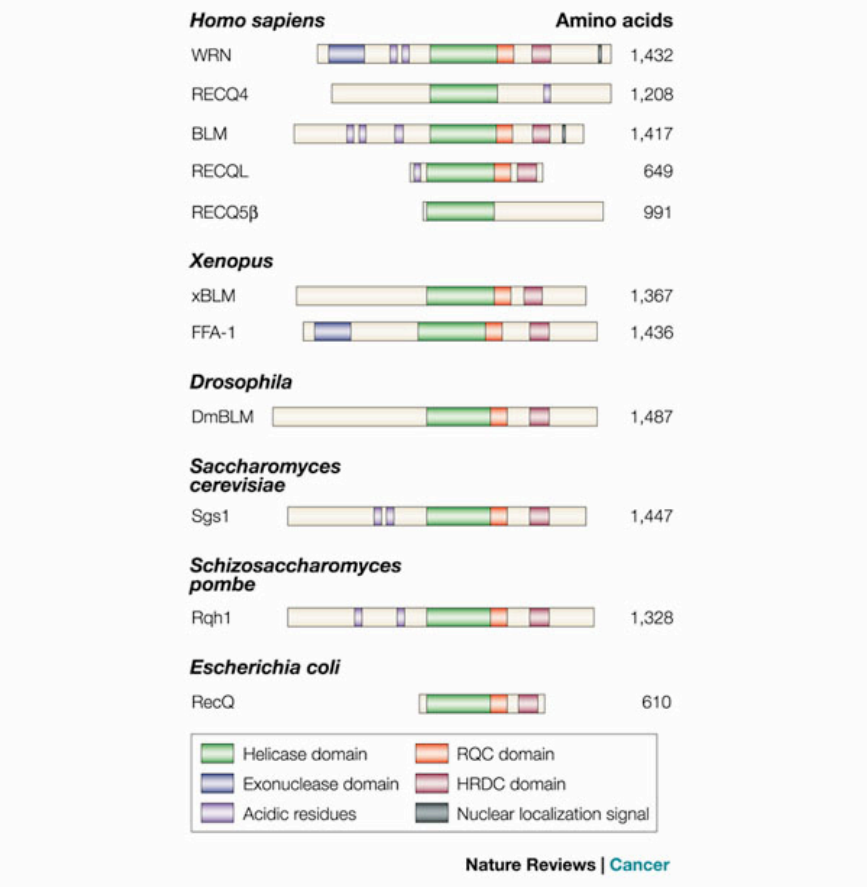

Figure 4: Representation of selected members of the RecQ family of DNA helicases.
The name of this family derived from the bacterial (*E. coli*) DNA helicase RecQ. Proteins are aligned by their conserved helicase domains (green boxes). Poorly conserved regions of each protein are shaded in light grey. Three splice variants of the human RECQL5 protein are expressed, only one of which is shown. The size of each protein in amino acids is indicated on the right. (Adapted from (23)).

All members share a central helicase domain, comprised of approximately 450 amino acids, which contains the seven conserved motifs including the Walker A and B boxes involved in ATP binding, and a DEXH box that defines this helicase family (24). In most RecQ helicases, the region that is carboxy-terminal to this domain contains two motifs: the RecQ C-terminal (RQC) domain, which is also a characteristic of the RecQ family and appears to mediate protein-protein interactions and the HRDC domain that might be involved in DNA binding (24). Some of the RecQ family members contain a highly acidic region at the N-terminus, which may mediate protein interactions DNA interactions, or both. Finally, human WRN helicase contains an exonuclease domain. Outside of these domains, there is little sequence similarity between family members.

The first RecQ helicase was identified over 20 years ago in *E. coli* through a screen for mutants resistant to thymineless-death (25). Recently, the 1.8 Å resolution structure of the catalytic core of *E. coli* RecQ was determined (26). The RecQ core comprises four conserved subdomains, two of these combine to form its helicase region, while the others form Zn^{2+} -binding and winged-helix motifs (Fig. 5).

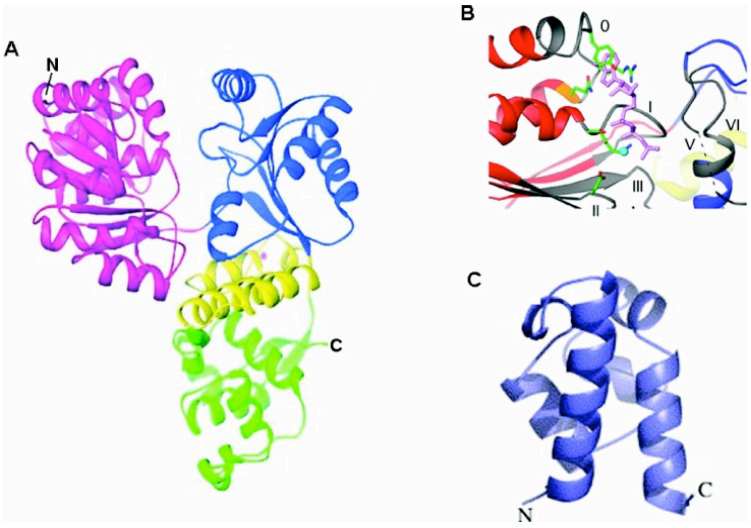

Figure 5: Structures of conserved RecQ domains
(**A**) Crystal structure of the *E. coli* RecQ catalytic core. Helicase lobes are coloured pink and blue, the Zn2+-binding domain and winged helix domain of the RQC region are in yellow and green respectively. (**B**) Close-up of the ATP binding site in the structure of the ATP[S]-bound *E. coli* RecQ catalytic core. A bound Mn2+ ion is shown as a cyan sphere. (**C**) Crystal structure of the *E. coli* RecQ HRDC domain (18).

The winged-helix motif shares significant structural similarity with other DNA binding proteins, thus identifying a likely DNA binding site in *E. coli* RecQ. It was shown that *E. coli* RecQ is a component of the RecF pathway of recombinational repair (25). Additionally, RecQ helicase activity has also been shown to function in suppressing illegitimate recombination, rescuing stalled replication forks and promoting induction of the SOS response in *E.coli* (27-29). Thus, *E.coli* RecQ is important for cellular genome maintenance and its activities are linked by its helicase function. Members of the RecQ family of DNA helicases are involved in processes linked to DNA replication, DNA recombination, and gene silencing (30).

Out of the five human RecQ homologues, three have been shown to be associated with five autosomal recessive disorders characterized by genomic instability and cancer predisposition. Werner syndrome (WS) has been linked with mutations in the WRN gene (31) and mutations in the BLM gene have been found to cause Bloom syndrome (BS) (32). Interestingly, three different human disorders have been associated with mutations in the RECQL4 gene: Rothmund-Thomson (RTS), RAPADILINO and Baller-Gerold (BGS) syndromes (33-35). In the last decade a huge effort was made to understand the underlying molecular mechanisms of these disorders.

Below, is a summary of the recent findings and highlighting the importance of studying human RecQ family members in order to understand their role in the maintenance of genome stability.

2.1 RECQL1

2.1.1 General Information

RECQL1 is the smallest human RecQ family member, being only slightly larger in size than *E.coli* RecQ (36). The RECQL1 gene is located on chromosome 12p11-12 and encodes a 649 amino acid protein. It was originally cloned by two independent groups (37, 38). So far, no genetic disease has been linked to mutations in the RECQL1 gene and the cellular function of the RECQL1 protein remains mainly elusive.

2.1.2 Biochemical Properties of RECQL1 Protein

Purified RECQL1 exhibits low processivity helicase activity and was originally found as a dimer in solution (39). RECQL1 alone is capable of unwinding short DNA duplexes (<110 bp) but requires human replication protein A (hRPA) in order to unwind longer substrates (501 bp) (40). Additional biochemical studies revealed that RECQL1 is able to unwind homlogous recombination (HR) intermediates such as Holliday junctions (HJ) and D-loop structures (41). Furthermore, RECQL1 catalyzes efficient strand annealing between complementary ssDNA molecules and this activity is inhibited by ATP binding (41). Very recent size exclusion chromatography and transmission electron microscopy data indicate that RECQL1 is found in two quaternary forms: higher-order oligomers consistent with pentamers or hexamers, and smaller oligomers consistent with monomers or dimers. RECQL1 seems to anneal ssDNA as a pentamer or hexamer, while it unwinds DNA as a monomer or dimer (42).

2.1.3 RECQL1 Interacting Partners

In 1997, Qip1 and Rch1, two human importin α homologues involved in nuclear-cytoplasmic transport, were identified as RECQL1 interacting partners in a yeast two-hybrid (YTH) screen (43) (Fig. 6). This interaction was confirmed by the finding that Qip1 is able to mediate nuclear transport of bovine serum albumin (BSA) when conjugated to the RECQL1 nuclear localisation signal (NLS) (44). RECQL1 is also reported to physically interact with topoisomerase IIIα (Top3α) (45), but the functional importance of RECQL1 interactions with Top3α has not been demonstrated. In 2005, Doherty *et* al. showed that RECQL1 is associated with several mismatch repair proteins. RECQL1 stimulates the incision activity of human exonuclease 1 and the mismatch repair recognition complex MSH2/6 stimulated RECQL1 helicase activity *in vitro*, suggesting a role of RECQL1 in the context of mismatch repair.

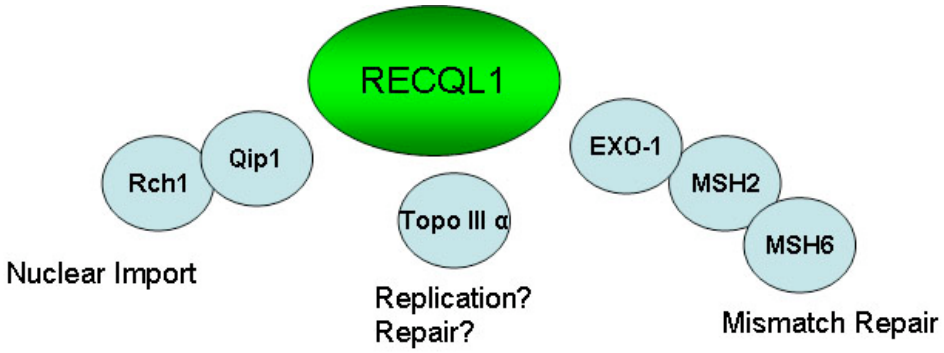

Figure 6: RECQL1-interacting partners and their function
The few interacting partners of RECQL1 identified so far suggest different roles in replication and mismatch repair.

2.2 BLM

2.2.1 Bloom Syndrome

Bloom syndrome (BS) was originally described 1954 by the dermatologist David Bloom (46). It is an extremely rare, autosomal recessive genetic disorder characterized by proportional dwarfism, skin erythema (skin lesion), immune deficiency, type II diabetes mellitus and very high incidence of cancers of most types, with a very early average age of onset. Male patients are sterile, while female patients are subfertile (47).

Source: Yale Pediatrics Resident's Website (48).

Source: Geneva Foundation for Medical Education and Research

Figure 7: Bloom syndrome patients
Both patients suffer from telangiectatic erythema caused by UV hypersensitivity.

BS is caused by various mutations in the *BLM* gene, located on chromosome 15q26.1 (49). These mutations are predominantly nonsense or frameshift mutations, leading to a premature termination codon and expression of truncated BLM protein.

Truncated BLM protein is found in the cytoplasm due to the lack of its C-terminal NLS. Approximately 15% of BS cases are due to missense mutations in *BLM*, and these mostly map to exons encoding the helicase domain resulting in catalytic inactive BLM protein.

Cell lines established from BS patients show elevated levels of gaps, breaks and structurally rearranged chromosomes (50, 51). However, the hallmark feature of BS cells, which is used in diagnosis in humans, is the approximately 10-fold increase in the frequency of sister-chromatid exchanges (SCEs) (52). The SCEs are generally thought to represent HR events occurring between sister chromosomes during S phase or G2.

2.2.2 BLM Mouse Models

In 1998, Chester *et* al. created the first BLM knockout mouse model (53). Gene disruption resulted in integration of the phosphoglycerate kinase (PGK)–*neo* cassette upstream of the BLM helicase homology region. *Blm*$^{-/-}$ mice were developmentally delayed and died by embryonic day 13.5. Fibroblasts derived frome these embryos showed elevated levels of SCE.

Two years later Luo *et* al. generated viable Bloom mice that were prone to a wide variety of cancers (54). They used embryonic stem (ES) cell technology to replace exon 2 with a loxP-PGK-*neo* cassette. This Bloom mouse model was a good tool for studying the underlying mechanism leading to genomic instability and cancer predisposition in Bloom syndrome. Their study showed that, in the absence of BLM function, mouse ES cells had an increased frequency of gene targeting, indicative of an increased frequency of homologous recombination. This is consistent with the high SCE rate observed from cells derived from these *BLM* deficient mice.

The third BLM mouse model was generated by Goss *et* al. in 2002 (55). In contrast to the mouse models mentioned above, they used a gene targeting construct in which exons 10, 11, and 12 of *Blm* were replaced with a hypoxanthine

phosphoribosyltransferase (Hprt) cassette, mimicking a mutation that is widespread among BS patients. These mice developed lymphoma earlier than wild-type littermates in response to challenge with murine leukemia virus and developed twice the number of intestinal tumors when crossed with mice carrying a mutation in the *Apc* tumor suppressor. These observations indicate that *Blm* is a modifier of tumor formation, a finding with important implications for cancer risk in humans.

2.2.3 BLM Interacting Partners

According to countless interaction studies of BLM and associated proteins, numerous models for BLM function have been proposed and BLM may be involved in DNA repair, homologous recombination, DNA replication, apoptosis and telomere maintenance (47). A complete list of all BLM interacting partners is found in Figure 8. Below, the most relevant BLM interacting partners are discussed.

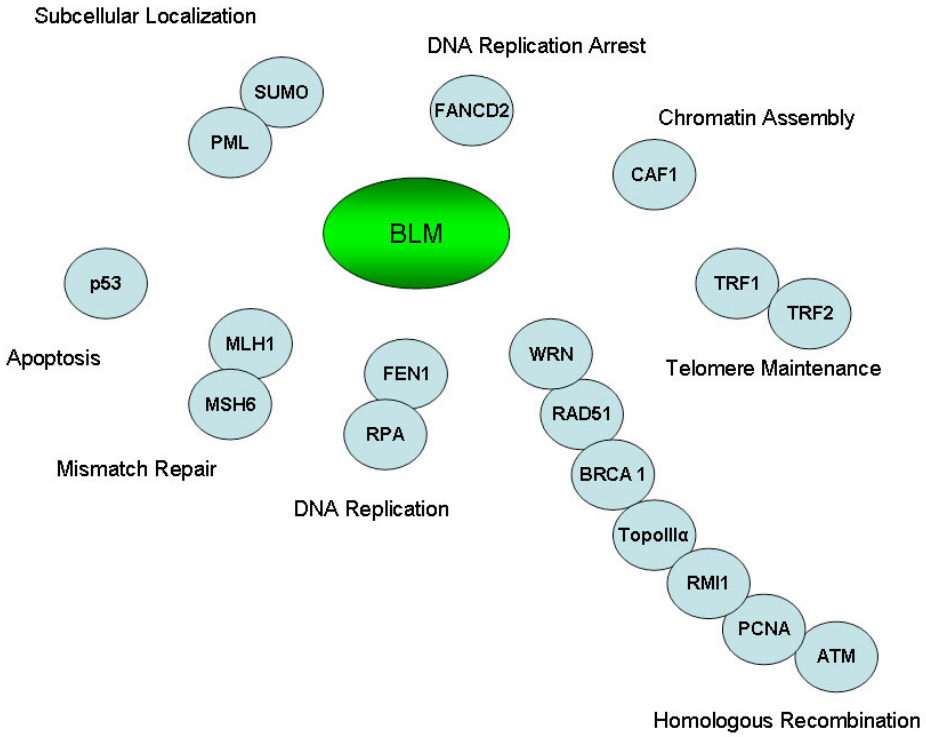

Figure 8: BLM-interacting partners and their function
BLM binds to a variety of proteins, suggesting roles for BLM in many aspects of DNA transactions

The *PML* gene was originally identified as the site of translocations in cases of acute promyelocytic leukaemia (56). The PML protein functions as a tumor suppressor and was found to localize into specific structures called PML bodies, where many proteins involved in DNA metabolism are localized (57-59). BLM co-localizes with PML in most cells, but co-localization is never complete (60). This suggests a regulated association of the two proteins, and that PML bodies might, therefore, be temporary storage sites for BLM. It seems that BLM shuttles to and from PML bodies while effecting its function.

Wang *et al.* have identified a high-order complex consisting of many DNA repair factors, BLM amongst them, and called it BASC, standing for BRCA1-associated genome surveillance complex (61). Many tumor suppressors and DNA damage repair proteins are found in this complex: ATM, BLM, BRCA1, MSH2, MSH6, MLH1, RAD50-MRE11-Nbs1 (MRN complex) and RFC. Members of the BASC complex have roles in recognition of abnormal DNA structures or damaged DNA, which implicates that BASC might play a role as a DNA damage sensor. Upon hydroxyl urea (HU) treatment, BLM, BRCA1 and PCNA co-localize, suggesting a common role in replication repair (61, 62).

Upon Immunoprecipitation of BLM from HeLa cells, Meetei *et al.* identified by masspectrometric methods a complex that includes BLM, Top3α, RPA and the five core Fanconi anemia (FA) proteins FANCA, FANCC, FANCE, FANCF and FANCG and called this complex BRAFT. BLM is responsible for the unwinding activity in this complex (63). Pichierri *et al.* have shown that BLM and FANCD2 colocalise and co-immunoprecipitate upon treatment with DNA crosslinkers or agents inducing replication fork arrest, again indicating a functional interaction (64). The features of the BS are very different to those of the FA, but some aspects of genomic instability in these diseases are similar.

Rad51 protein is an ortholog of the bacterial RecA protein, which plays a central role in HR and DNA repair. Rad51 forms a nucleoprotein filament on ssDNA to mediate strand exchange, an important step in the initiation of HR. BLM and the human Rad51 have been shown to interact both *in vivo* and *in vitro* (65) and they co-

localize in certain untreated cells. Upon IR or aphidicolin treatment, the number of BLM and RAD51 co-localizing foci increases (66). This data suggest a role of BLM in the context of DNA DS repair by HR.

BLM and p53 interact physically and functionally *in vitro* and *in vivo* (67-69). p53 inhibits the unwinding activity of BLM on HJs, but not on standard oligonucleotide substrates, indicating that p53 might be involved in the regulation of HR through modulating the interaction of BLM with recombination intermediates (69). Additionally, Wang *et al.* found that BLM and p53 might regulate apoptosis because ectopically expressed p53 induces apoptosis in normal cells but not in BS cells. Furthermore, BS cells show normal Fas-induced apoptosis, and therefore the effect seems to be specific for the p53 apoptotic pathway (68).

The replication protein A (RPA) is a heterotrimeric ssDNA binding protein that is formed by subunits of 14, 32 and 70 kDa. BLM interacts physically with RPA through the p70 subunit (70, 71) and co-localizes with RPA (72). RPA stimulates helicase activity of BLM (70).

Top3α catalyses the interconversion of different topological isomers of DNA. BLM and Top3α co-localize to PML nuclear bodies in fibroblasts (73) but Top3α is not localized correctly in BS cells (45). In addition, BLM interacts functionally with Top3α and it stimulates the relaxation of negatively supercoiled plasmid DNA catalyzed by Top3α.

Human RMI1 cooperates with BLM and Top3α to catalyze double Holliday junction (DHJ) dissolution (74). Moreover, the role of RMI1 is mediated through a specific interaction with Top3α and RMI1 promotes the recruitment of Top3α to DHJs. The mechanistic significance of the BLM/ Top3α interaction is discussed in detail in the BLM Biochemistry section below.

Different data suggest that BLM might also be involved in the maintenance of telomere stability. TRF1 and TRF2 are homodimeric proteins that have been shown to bind exclusively to double-stranded telomeric DNA. BLM has been shown to interact with TRF2 *in vitro* and *in vivo* and TRF2 stimulates BLM helicase activity

(75). Both of these proteins co-localize with BLM in atypical, telomere-associated PML bodies (76).

Our group demonstrated the physical and functional interaction between BLM and the chromatin assembly factor 1 (CAF-1) (77). BLM and hp150, the largest subunit of CAF-1, are found in complex *in vivo* and they co-localize upon DNA damage treatment. Furthermore, BLM inhibits CAF-1 mediated chromatin assembly during DNA repair *in vitro* (77). These findings point out the coordinate way of BLM and CAF-1 function to promote cell survival in response to DNA damage and replication blockade.

2.2.4 Biochemical Properties of the BLM Protein

In 1997, Karow *et* al. purified recombinant human BLM protein from *S. cerevisiae.* BLM was shown to possess ATP and Mg^{+2} dependent 3'→5' helicase activity (78). Electron microscopy and size exclusion experiments indicated that BLM protein is a hexamer in its active form and the N-terminal domain is crucial for the oligomerization (79).

Different studies indicate that BLM can unwind several DNA substrates such as synthetic HJs, G4 DNA and D-loop structures (80, 81). Additionally, BLM promotes the annealing of ssDNA, an activity that does not require Mg^{2+}, is inhibited by ssDNA binding proteins and ATP, and is dependent on DNA length (82).

The most important biochemical finding on BLM was discovered by Ian Hickson's group. They describe that BLM, in conjunction with Topo IIIα, is able to resolve double holliday junctions (DHJ) via a strand passage mechanism that prevents exchange between flanking sequences (83). The underlying mechanism was called DHJ dissolution. DHJs are intermediates in meiotic recombination (84) and are predicted to form in mitotic cells during repair of DSBs by HR.

2.2.5 Posttranslational Modifications of BLM Protein

BLM is posttranslationally modified by phosphorylation (85-89) and sumoylation (90). Originally, data indicate that BLM, in response to ionizing radiation, is phosphorylated and accumulates through an ATM-dependent pathway, suggesting that BLM acts as an ATM kinase downstream effector (85). In addition, BLM is phophorylated by ATR following exposure of cells to HU (88). BS cells ectopically expressing a BLM mutant unable to be phosphorylated, fail to recover from HU-induced replication blockade.

Recent findings identified BLM as a phosphorylation substrate for two other kinases: The mitotic Cdc2 kinase and the spindle assembly checkpoint kinase MPS-1 (86, 89) suggesting additional roles for BLM in the context of mitosis and accurate chromosome segregation.

In 2005, Eladad *et* al. showed that BLM is sumoylated on several lysine residues (90). BLM proteins that are mutated on their SUMO modification site fail to localize to PML nuclear bodies and they induce formation of DNA damage induced (DDI) foci in the absence of treatment with DNA damaging agents, suggesting that sumoylation of BLM regulates its intra-nuclear trafficking (90).

2.3 WRN

2.3.1 Werner Syndrome

Werner syndrome (WS) was first described by the medical student Otto Werner within his dissertation in 1904. He reported three cases of young WS patients who showed ocular cataract accompanying hard scleroderma-like changes in the skin. In 1992, the causative gene locus was mapped (8p12) (91) and four years later, after extensive positional cloning, *WRN* was identified as the gene encoding a DNA helicase (31).

Figure 9: Werner syndrome and accelerated aging (Adapted from (92)).

WS is a rare autosomal recessive disorder characterized by many clinical features, however, the hallmark of WS is accelerated aging (93-95). WS patients often suffer from bilateral ocular cataracts, type 2 diabetes mellitus, osteoporosis, various forms of arteriosclerosis, and hypogonadism at a relatively young age. The aged appearance is due to short stature, premature graying and loss of hair, scleroderma-like skin changes, and regional atrophy of subcutaneous fat. WS subjects have an elevated risk of various cancers, particularly sarcomas (96). The age of death varies between approximately 30 and 65 years, with a mean of 47 years, and usually results from cancer or cardiovascular disease (94, 97, 98).

All mutations in the WRN gene examined so far are either nonsense or frameshift mutations, leading to premature stop codons and expression of truncated WRN protein lacking the C-terminal NLS. These findings imply that both WS and BS are not only helicase diseases but in molecular terms they are also nuclear transportation disorders.

Fibroblasts derived from WS patients display limited replicative potential, prolongation of S-phase and hypersensitivity to 4-nitroquinoline-1-oxide (4-NQO) (99). Chromosomal analysis of WS cells revealed an overall genomic instability including frequent pseudodiploidy, with variable structural rearrangements associated with a high proportion of deletions. WRN primarily localizes to the nucleolus in all cells examined, and translocates to the nucleoplasm upon genotixic stress (100, 101).

2.3.2 WRN Mouse Models

Three *WRN* mutant mice have been created by several groups thus far (102-104). The first model consists of a deletion of part of the helicase domain of the murine *WRN* homologue (102). These mice exhibited an enhanced sensitivity to camptothecin (the DNA topoisomerase 1 inhibitor), increased genomic instability, telomere attrition, and increased tumor occurrence (in particular in a poly (ADP-ribosyl) polymerase-1 null or p53 null background). Cells derived from these mice showed premature loss of their proliferative capacity (102, 105). Although the tumor spectrum has been studied extensively in this model, the other phenotypes normally associated with human WS have not been analyzed.

The second model consists of a mutation that eliminates the expression of the C-terminal region of *WRN* (103). The resulting mouse model is a *WRN*-null mutant as no WRN protein was detected using antibodies against either the N- or the C-terminal region of the protein.

The phenotypes reported for WS patients were not observed in these mice. However, crosses between *WRN*-null and *TERC*-null mice (knock out for the gene encoding the telomerase RNA component) recapitulated several symptoms associated with WS in humans in a subset of mice (106).

Wang et al. generated a third model by introducing a human cDNA with a dominant-negative mutation in the helicase domain into mice (104). Although the *in vivo* phenotype was not reflecting the situation in humans, cells derived from these transgenic mice exhibited a slow growth phenotype in culture and a hypersensitivity to the DNA damaging agent 4-NQO.

Taken together, no animal model of WS to date accurately mimics the human disorder. This might be due to differences between humans and mice in maintaining genomic stability.

2.3.3 WRN Interacting Partners

Although different genetic and biochemical studies have so far failed to establish a definite cellular role of WRN, characterizing the interaction with different protein partners might help to delineate the principal pathways in which WRN participates. WRN physically and functionally interacts with a variety of proteins (Fig. 10), suggesting a role for WRN in telomere maintenance, DNA replication, recombination, and repair. Below, the most prominent WRN interacting partners are discussed.

One of the first physical and functional interactions was found in co-immunoprecipitation studies identifying PCNA and topoisomerase I as two WRN-interacting components. PCNA acts as a processivity factor for DNA polymerase delta in eukaryotic cells. Since DNA polymerase δ (pol δ) is also involved in resynthesis of excised damaged DNA strands during DNA repair, PCNA is important for both DNA synthesis and DNA repair (107).

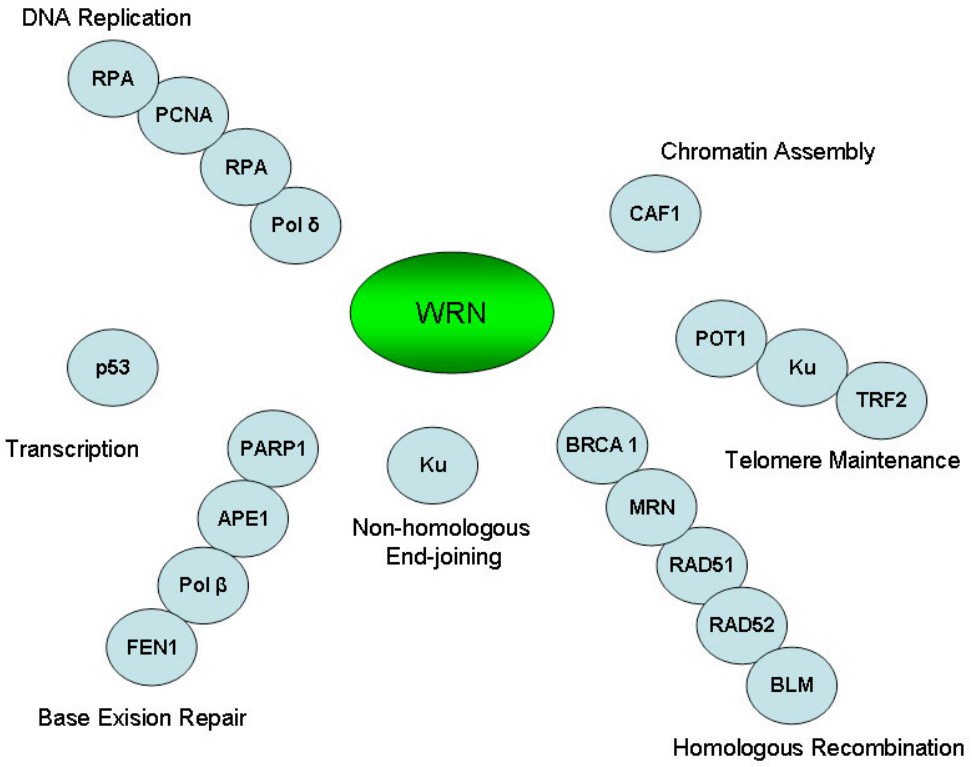

Figure 10: WRN-interacting partners and their function
WRN binds to a variety of proteins, suggesting roles for WRN in many aspects of DNA metabolism (112).

The WRN exonuclease domain contains a region that is homologous to the PCNA binding motif (108, 109) found in many proteins involved in DNA replication and repair, such as FEN-1 and DNA ligase 1 (110, 111). WRN co-localizes with PCNA at replication foci of primary cells, suggesting a possible role in DNA replication.

Topoisomerases change the linking number of DNA during DNA replication in order to relive torsional stress caused by the advancing replication fork. Recent studies reveal that WRN physically interacts with topoisomerase I. WRN stimulates topoisomerase I to relax negatively supercoiled DNA while topoisomerase I inhibits WRN ATPase activity (113). Furthermore, WS cells are hypersensitive camptothecin during G2 and S phases of the cell cycle (114, 115).

WRN has also shown to be associated with the major replicative DNA pol δ (116). WRN stimulates yeast pol δ primer extension *in vitro*, but has no effect on PCNA-pol δ complex processivity, indicating that WRN is not directly involved in normal processive DNA synthesis mediated by pol δ. It was shown that WRN instead helps pol δ by unwinding physical barriers like quadruplex DNA that block pol δ-catalyzed DNA synthesis (117).

Another important protein that associates with WRN is human RPA, a heterotrimeric, single-stranded DNA binding protein required for DNA replication, recombination, and repair (118). Co-immunoprecipitation- and ELISA-based protein binding assays revealed a direct physical interaction between the two proteins. RPA markedly stimulates the DNA helicase activity of the WRN protein (119, 120) and increases its ability to unwind forked telomeric DNA structures (121, 122). While WRN alone cannot unwind partial duplexes longer than 40 bp, its interaction with RPA allows it to unwind substrates as long as 849 bp, the longest substrate tested (119).

FEN-1 is an interesting replication protein that directly interacts with WRN (123). FEN-1 possesses 5'-endonuclease/5'–3'-exonuclease activity and is involved in Okazaki fragment maturation during lagging strand DNA replication (124), long-patch base excision repair (BER) (125), as well as non-homologous DNA end joining (NHEJ) (126). WRN greatly stimulates (more than 80-fold) the nucleolytic activity of FEN-1 in a concentration-dependent manner, even if the helicase and exonuclease activities of WRN are abolished (123). Additionally, WRN stimulates the cleavage of DNA structures that are poor substrates of FEN-1 alone, indicating that these two proteins are likely to act together *in vivo.*

The DNA-dependent protein kinase (DNA-PK), consisting of Ku70/Ku80 heterodimer and DNA-PK_{cs}, is an important player in processes like NHEJ and VDJ recombination (127, 128). WRN was found to interact physically with the Ku complex and DNA-PK_{cs} *in vitro* and *in vivo* (129-134). The Ku complex stimulates the WRN exonuclease activity but does not affect its helicase activity (129).

WRN protein seems to be involved in the process of DNA DSB repair.

WRN binds to DNA polymerse β (pol β) and stimulates strand-displacement DNA synthesis of pol β *in vitro* in a reaction requiring the helicase domain of WRN (135). pol β is a key polymerase in BER (136). Additionally, GST-pulldown- , ELISA-, as well as dot blot assays and immunofluorescence experiments show that WRN forms a complex with the human apurinic/apyrimidinic endonuclease-1 (APE-1), a key player in the early stages of BER. However, the exact molecular role of WRN in BER remains elusive.

p53, the key tumor suppressor, directly associates with the C-terminal portion of WRN, and inhibits its exonuclease activity (137, 138). Wild type p53 diminishes WRN helicase activity and abolishes its ability to unwind synthetic HJ *in vitro*. This inhibition is dependent upon the phosphorylation of p53 (69). On a cellular level, p53 is a repressor of the WRN gene transcription (139).

The physical association of telomeric repeat binding factor 2 (TRF-2) and WRN protein (140) in conjunction with biochemical data demonstrating the disruption of D loops (structures formed at telomeres) by WRN protein (141, 142), suggests that WRN may participate in the maintenance of telomeres. Furthermore, WRN protein has been shown to be involved in the synthesis of the lagging strand of telomeres (143).

Another protein complex that has been shown to cooperate with WRN is the MRN complex (144), a three-subunit complex that is composed of Mre11, Rad50, and Nbs1/Xrs2 (145). Mutations in these genes lead to sensitivity to DNA damage, genomic instability, telomere attrition, and aberrant meiosis (145). WRN co-localizes and physically interacts with the MRN complex at stalled replication forks (62) and the interaction is mediated by Nbs1. Furthermore, MRE11 promotes WRN helicase activity (146). Since depletion of Mre11 by RNAi knockdown does not enhance chromosomal breakage and cell death in WS cells, it is proposed that WRN and Mre11 act in a common pathway in response to replication fork arrest (147).

Jiao *et* al. show that WRN interacts physically with the largest subunit of CAF-1, hp150, *in vitro* and *in vivo* (148). In the absence of WRN, hp150 does not re-localize to form nuclear foci following treatment of cells with hydroxyurea (HU), whereas in hp150 RNAi knockdown cells, WRN localization was unaffected. These

results indicate that before CAF-1, WRN responds to DNA damage and WRN may recruit CAF-1, via hp150, to DNA damage sites to assemble the newly synthesized DNA into chromatin following DNA synthesis.

2.3.4 Biochemical Properties of WRN Protein

The human WRN protein is a 1432 amino acid protein with a predicted molecular mass of 170 kDa. Size exclusion chromatography data suggest oligomerization of WRN *in vivo,* most likely as a trimer (149). WRN protein is unique among the five human RecQ members in that it is a bipartite and bifunctional Enzyme: In addition to ATP-dependent 3′-5′ helicase and ssDNA-dependent ATPase activities, it also possesses a functional 3′-5′ exonuclease domain, which is similar to the exonuclease domain of *E. coli* DNA polymerase I. The WRN enzymatic activities are separable from each other (150). As a helicase, WRN shows poor processivity and preferentially unwinds bubble substrates, forked structures and G-quadruplex DNA (80). As shown for BLM, WRN is also capable of branch migrating HJs over distances of several kb (151). WRN exonuclease activity displays low processivity on substrates such as ds duplexes with blunt ends. The preferred WRN exonuclease substrate is a partial duplex with a single 3' mismatch, suggesting a role analogous to the proofreading exonuclease activity of replicative DNA polymerases (150).

2.3.5 Posttranslational Modifications of WRN Protein

WRN was found to be phosphorylated *in vivo* after bleomycin treatment or in replication stress (146, 152, 153). Several studies revealed that four kinases seem to be involved in WRN serine/threonine and tyrosine phosphorylation *in vivo*: ATM/ATR, DNA-$PK_{cs,}$ and c-Abl. On the basis of the consensus of ATM phosphorylation sites, WRN has been predicted to be a substrate of this kinase (154) and Pichierri *et* al. suggested an ATR dependent phosphorylation of WRN following replication arrest and DNA damage induced during the S phase of the cell cycle

(153). DNA-PK_{cs} phosphorylates WRN together with Ku70/Ku80 as a heterotrimeric complex *in vitro* and *in vivo* (133, 152, 155), leading to inhibition of WRN helicase and exonuclease activity. WRN was found to be constitutively associated with c-Abl and upon bleomycin treatment WRN is phosphorylated on a tyrosine residue and dissociates from c-Abl. Furthermore, c-Abl phosphorylation also inhibits WRN exonuclease and helicase activity (146). It will be of particular interest to unravel the role of ATM in WRN phosphorylation and its impact on the role of WRN in DNA damage response.

Using a yeast two-hybrid approach, Ubc9 was found as a prominent WRN interacting partner. Ubc9 belongs to the family of ubiquitin ligases and is required for WRN sumoylation *in vivo* (156). It has been proposed that SUMO modification may play a role in the WRN nuclear re-localization (157). Nevertheless, the functional consequence of WRN sumoylation needs to be further characterized.

In addition to phosphorylation and sumoylation, acetylation of WRN has been reported (158). WRN is acetylated by the histone acetyltransferse p300 *in vivo,* and this results in translocation of WRN protein from the nucleolus to nuclear foci (158).

2.4 **RECQL4** (adapted from Dietschy et al.)

2.4.1 Rothmund-Thomson Syndrome

RTS was originally described in 1868 by the German ophthalmologist Rothmund (159) and subsequently confirmed by the English dermatologist Thomson in 1936 (160). It is an unusual autosomal recessive defect composed of diverse symptoms like poikiloderma, growth deficiency, juvenile cataracts, premature aging and a predisposition to malignant tumours, particularly osteosarcomas (161).

Source: University of Erlangen, Department of Dermatology

Figure 11: Rothmund-Thomson Syndrome Patient
Depicted is the skin rash (poikiloderma pigmentosum) phenotype, a hallmark of RTS.

Despite its long history, only about 300 cases of RTS have been reported in the scientific literature thus far (161, 162). Interestingly, mutations in the *RECQL4* gene cause only 60% of all RTS cases (163). Accordingly, RTS seems to be a heterogenous disease and mutations in other, yet unidentified gene(s) seem to be responsible for the phenotype of the remaining 40% of RTS patients. The number of mutations found in *RECQL4* is quite low, ranging from nonsense, frameshift and

splice site mutations to intronic insertions and deletions (34). Most of them result in premature termination of protein translation and truncated RECQL4 proteins that often lack a large part of the helicase domain (164). Cells derived from RTS patients show genomic instability, including trisomy, aneuploidy and chromosomal rearrangements (161, 165). Additionally, RTS cells are sensitive to ionizing radiation and oxidative stress/damage (166, 167).

2.4.2 RAPADILINO Syndrome

Another autosomal recessive disease associated with mutations in the *RECQL4* gene is RAPADILINO syndrome (34). The syndrome was originally described in 14 patients from Finland. To date, additional 3 cases of RAPADILINO syndrome have been reported (34). The acronym stands for the characteristic clinical features: RAdial hypo-/aplasia, Patellae hypo-/aplasia and cleft or highly arched PAlate, DIarrhoea and DIslocated joints, LIttle size and LImb malformation, NOse slender and NOrmal intelligence.

Figure 12: RAPADILINO Syndrome Patient
This patient is 12 years old. Note the hand and facial features (168).

The most common mutations of the *RECQL4* gene in RAPADILINO patients represent in-frame deletions of exon 7 which do not affect the helicase domain of RECQL4 protein (34). Although RAPADILINO patients share some clinical features with RTS patients, like photosensitivity with extra pigmentation of skin, or growth deficiency, there are unique diagnostic findings such as joint dislocations and patellar hypo/aplasia. In contrast to RTS, RADADILINO is more common in females, and only 7% of the current RAPADILINO patients carry malignant tumors, mainly osteosarcomas (169).

2.4.3 Baller-Gerold Syndrome

BGS, originally discovered in 1950 (170), is the third recently reported autosomal recessive disorder linked to mutations in the *RECQL4* gene (35). Approximately 20 cases of BGS have been reported in the scientific literature thus far (35). The clinical hallmarks of BGS are radial aplasia/hypoplasia and craniosynostosis.

Figure 13: Baller-Gerold Syndrome Patients
Left picture: First characterization of the clinical phenotype of BGS 1950 (170)
Right picture: Craniosynostosis phenotype of BGS patient (35)

To date, most mutations of *RECQL4* found in BGS patients represent a R1021W missense mutation and a 2886 delta T frameshift mutation of exon 9.

Surprisingly, none of the 24 BGS patients reported so far show any predisposition for cancer (35).

2.4.4 RECQL4 Mouse Models

In 2002, the Furuichi group created the first *RECQL4* knock-out mouse model (171). These mice were embryonic lethal, showing severe proliferation defects and therefore could not be used as a model for RTS. One year later, the Kito group generated another *RECQL4* knock-out mouse model by deleting exon 13 of the *RECQL4* gene, which encodes part of the central RecQ-helicase domain. Exon 13 is a hot spot for mutations identified in RTS patients (172). This *RECQL4* deficient mouse showed severe growth retardation and several tissue abnormalities that resemble those of RTS patients. Additionally, the proliferation rate of Mouse Embryonic Fibroblasts (MEFs) derived from this *RECQL4* deficient mouse was decreased. Only 5% of the mutant mice survived the first 14 days, and these mice failed to develop poikiloderma and malignancies, both characteristics of RTS (172).

One year ago, the Luo group generated the third RECQL4-knock-out mouse by deleting the *RECQL4* coding region including exons 9-13 (173). 84% of all homozygous *RECQL4*$^{-/-}$ progeny survived to adulthood, with some exhibiting typical clinical features of RTS like hypo-/hyper-pigmented skin, skeletal limb defects and palatal patterning defects. Furthermore, chromosomal analysis using different cell types derived from this *RECQL4* deficient mouse displayed an overall aneuploidy phenotype and a significant increase in the frequency of premature centromere separation, suggesting that this *RECQL4*$^{-/-}$ mouse is a good model for human RTS (173).

Taken together, the results derived from the experiments with various *RECQL4*$^{-/-}$ mice showed that these mice accumulate defects that clearly reflect the situation in humans, i.e. different mutations in the *RECQL4* gene lead to different phenotypes. It would therefore be of particular interest to investigate whether the

genotype-phenotype correlations seen in humans could be observed in mice by mimicking mutations causing RAPADILINO and BGS syndromes.

2.4.5 RECQL4 in the Context of DNA Replication

In the past 2 years, analyses of RECQL4 in *Xenopus laevis* have indicated an interesting novel role for RECQL4 in the initiation of DNA replication. The *Xenopus laevis* RECQL4 protein (xRTS) is 60% identical to human RECQL4 and shares the central helicase domain common among all RecQ family members. The N-terminal region of xRTS shows 20% identity to two yeast proteins, Sld2 and Drc1, which are both required for the establishment of replication forks (174-176). This feature makes xRTS unique among the members of the RecQ family. The Venkitaraman lab showed that immunodepletion of xRTS from *Xenopus laevis* egg extracts leads to a reduction and delay of sperm chromatin replication, an effect that can be rescued by complementing the extracts with the purified recombinant wild-type human RECQL4 (177). These findings were recently confirmed by the Takisawa group, showing that purified N-terminal fragments of xRTS were able to rescue the DNA replication activity of RECQL4-depleted extracts (178). Accordingly, by knocking down the murine homologue of xRTS with shRNA in primary MEFs, the proliferation rate and DNA replication of these primary cells was highly perturbed. Together, these results suggest that RECQL4 has a role in DNA replication and that this function is conserved during evolution.

2.4.6 RECQL4 Interacting Partners

Several attempts have been made thus far to identify proteins that associate with RECQL4 (Fig. 14). Recent studies in the Wang group have revealed that RECQL4 isolated from HeLa cells is found in a complex with UBR1 and UBR2 (179). These two 200 kDa proteins share high sequence similarities to each other and

belong to the family of E3 ubiquitin ligases of the N-end rule pathway, which is part of the Ubiquitin-proteasome system (180). The N-end rule pathway exists in all organisms examined, from mammals to fungi and bacteria. In eukaryotes it is part of the ubiquitin system. By the action of the three ubiquitin-ligases (E1, E2 and E3), a substrate protein is polyubiquitylated and subsequently degraded by the 26S proteasome (180). Surprisingly, the Wang group found that RECQL4 is not ubiquitylated *in vivo.* In addition, newly synthesized RECQL4 was shown to be a stable protein (half-life of 2h) and the level of RECQL4 protein was not increased by inhibiting the proteasome with different drugs. Despite these discoveries, the functionality of the physical interaction between RECQL4 and UBR1/UBR2 remains unknown and further investigations are needed to elucidate a novel function of ubiquitin ligases in the maintenance of genome stability.

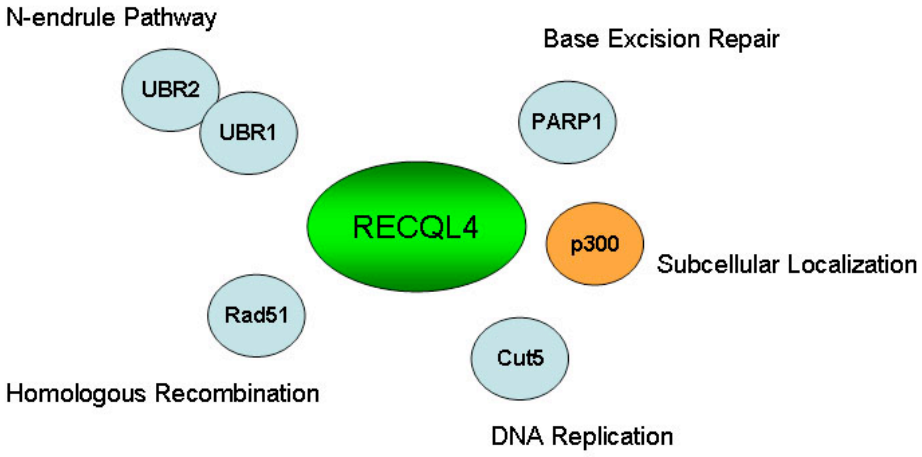

Figure 14: RECQL4-interacting partners and their function
The few interacting partners of RECQL4 identified so far suggest different roles for RECQL4 in DNA metabolism

Our group found that RECQL4 is in a complex with Rad51 *in vivo* (181). It has been previously reported that Rad51 foci, which are important for DNA repair by homologous recombination, accumulate at sites of single stranded DNA after

induction of DNA double strand breaks (DSB) (182). In response to the induction of DSBs by treatment with etoposide, a portion of RECQL4 and Rad51 nuclear foci colocalized, suggesting that RECQL4 plays a role in the repair of DSBs by homologous recombination (181). The precise role of RECQL4 in DSB repair via its interaction with Rad51 is currently being investigated in our lab.

Recently, Cut5 was shown to interact with the *Xenopus laevis* homologue of RECQL4 both, *in vitro* and *in vivo* (178). Cut5, the metazoan homologue of *S. cerevisiae* Dpb11, is required for the loading of DNA polymerases onto chromatin (183, 184). As mentioned above, the N-terminus of RECQL4 has similarity to Sld2 ("synthetically lethal with *dpb11"*), one of six Sld family members found to interact with Dpb11 (185). Thus, these findings provide an additional hint that RECQL4 may function during DNA replication.

The Frank group reported the physical interaction between RECQL4 and poly(ADP-ribose) polymerase-1 (PARP-1) (186). PARP-1 is involved in different pathways of DNA metabolism such as recombination, repair and transcriptional regulation (187). Additionally, PARP-1 is part of the base excision repair (BER) pathway and is activated in response to DNA breaks (188)**.** The authors showed complex formation between RECQL4 and PARP-1 *in vitro* and *in vivo.* Additionally, PARP-1 was able to poly(ADP-ribosyl)ate RECQL4 *in vitro* (186). However, the functional relevance of this posttranslational modification of RECQL4 has to be confirmed by further *in vitro* and *in vivo* experiments.

In summary, the current data from several different protein interaction assays indicate that RECQL4 is involved in DNA repair and replication processes. However, further studies are needed to identify additional RECQL4-interacting proteins in order to draw a more precise picture of the exact cellular pathways RECQL4 might be involved in. The extended N- and C-terminal domains of all RecQ helicases studied so far show very little sequence identity and are therefore thought to confer specificity to these proteins by mediating protein-protein interactions (23). For this reason, N- and C-terminal fragments of RECQL4 could be used as baits in a yeast two-hybrid screen in order to find novel RECQL4 interacting partners. On the other hand, different RECQL4 specific antibodies have been raised in the last couple of years

that could be used to co-immunprecipitate RECQL4-interacting partners from mammalian cells extracts, followed by mass spectrometry analysis.

2.4.7 Subcellular Localization of RECQL4

Four different groups have thus far examined the subcellular localization of RECQL4 in different mammalian cells and their observations are contradictory. The Furuichi group overexpressed full length FLAG-tagged RECQL4 in HeLa cells and immunfluorescence analysis suggested RECQL4 is localized exclusively to the nucleus (163). In 2004, the Wang group extensively studied the subcellular localization of RECQL4 using different cell types and three polyclonal anti-RECQL4 antibodies (179). Western blot analysis of HeLa, MCF7 and Jurkat cell extracts revealed that RECQL4 was found predominantly in the cytoplasm, while indirect immunfluorescence experiments using HeLa cells displayed RECQL4 localization to both the nucleus and the cytoplasm. In contrast, RECQL4 was largely present in the nuclear fraction derived from untransformed WI-38 fibroblasts.

Our group raised two antibodies, against the N- and C-termini of RECQL4, and used them in immunofluorescence experiments on several exponentially growing human cell lines. Although we found that the majority of RECQL4 protein is detected in the nucleus, a small amount of it was found in the cytosolic fraction of HeLa cell extracts (181). Furthermore, we found that endogenous RECQL4 localized exclusively in discrete nuclear foci in HeLa, WI-38/VA13 and primary skin fibroblast cells, and that the number of these does not significantly change during the cell cycle or upon the induction of DNA DSBs. In addition, we found that RECQL4 foci partially coincide with those formed by promyelotic leukemia (PML) bodies and Rad51 as well as with regions of single-stranded DNA (ssDNA) upon induction of DSBs. PML bodies and Rad51 foci have been shown to regulate the response to and repair of DSBs (58, 189). These findings suggested a role for RECQL4 in the repair of DSBs by homologous recombination (HR) and indicated a completely novel function for RECQL4 in human cells (181).

Very recently, the Frank group investigated the localization of RECQL4 in living cells by fusing EGFP to the N-terminus of the RECQL4 sequence (186). RECQL4 displayed nucleoplasmic staining in most of the cells examined and no significant cytoplasmic staining was observed. Using different EGFP deletion mutants of RECQL4 the authors further characterized the domain structure. Their data suggests that RECQL4 contains at least two N-terminal nuclear localization signals (NLS) and one nucleolar localization signal (NOS) spanning amino acids 376-386. Furthermore, RECQL4 nucleolar enrichment was observed after treating cells with H_2O_2 or streptonigrin which leads to oxidative damage of DNA. Interestingly, RECQL4 localization did not change after treating cells with other DNA damage agents such as γ irradiation, etoposide, bleomycin, or UV irradiation (186).

2.4.8 Biochemical Properties of the RECQL4 Protein

Compared to all other human RecQ family members, the biochemical properties of the RECQL4 protein are thus far only poorly understood. This is mainly due to the inability to purify the RECQL4 protein. Many groups including ours have attempted to purify full-length RECQL4 protein using different expression systems but all efforts resulted in production of truncated RECQL4 protein. Consequently, the first enzymatic activity assays were performed by the Wang group with immunoprecipitated RECQL4 protein from HeLa cell extracts (179). RECQL4 coupled to protein-A sepharose beads showed DNA dependent ATPase activity, however, RECQL4 failed to unwind any of the tested DNA substrates, although BLM helicase purified by the same way possessed DNA helicase and translocase activity.

One year ago, the Sung group purified full-length RECQL4 protein from *E.coli* (190). Although the yield of purified RECQL4 protein was low, the authors demonstrated that RECQL4 has no detectable helicase activity, but possesses ssDNA-stimulated ATPase activity. In addition, the authors showed that RECQL4 binds to ssDNA, an effect that could be inhibited by ssDNA binding protein RPA (190).

Taken together, the current studies indicate that RECQL4 is not an active helicase, however, it still remains possible that RECQL4 needs a co-activator protein(s) and/or a particular post-translational modification(s) in order to accomplish a DNA unwinding function. To this end, it would be interesting to test if RECQL4 purified from mammalian or insect cells possesses helicase activity.

2.5 RECQL5

2.5.1 General Information

As with *RECQL1,* no human genetic disease has been linked to a deficiency in the *RECQL5* gene. The RECQL5 gene is located on chromosome 17q25.2. The 19 exons of the human *RECQL5* gene give rise to alternatively spliced mRNA species which encode the three designated RecQL5α, RecQL5β and RecQL5γ isoforms. They have predicted molecular masses of 46 kDa, 108.9 kDa and 49 kDa respectively (191). The different RecQL5 isoforms seem to be expressed ubiquitously in human tissues, with a very high abundance in the testis. Their subcellular localization has been studied using ectopically expressed proteins. The small isoforms, RecQL5α and RecQL5γ, are entirely cytoplasmic, while RecQL5β is transported to the nucleus, consistent with the presence of a putative NLS (192). All biochemical and cell biological studies to date have been performed with the largest isoform RECQL5β.

2.5.2 Biochemical Properties of the RECQL5β Protein

Garcia *et* al. described the first biochemical properties of the human RECQL5β in 2004 (193). Like BLM and WRN, RECQL5β was shown to be an ATP-dependent 3'-5' DNA helicase that can promote migration of Holliday junctions. RECQL5β required the single-stranded DNA-binding protein RPA in order to mediate unwinding of DNA substrates. In contrast to BLM and WRN that form oligomeric structures (194, 195), the RECQL5β helicase exists as a monomer. The most important finding, which has been confirmed for all human RecQ helicases is that RECQL5β exhibits an efficient DNA strand annealing activity, residing in the C-terminal half of the protein (193).

Furthermore, RECQL5β helicase possesses the ability to promote strand exchange on synthetic forked DNA structures that mimic a stalled replication fork (196).

2.5.3 RECQ5Lβ Interacting Proteins

Immunoprecipitation and co-localization studies revealed that RECQL5β is found in complex with topoisomerase 3α and 3β (192), suggesting a specific role for RECQL5β in DNA metabolism.

Recent findings indicate physical interaction of RECQL5β and PCNA in human cells (196). RECQL5β and PCNA co-localize in distinct DNA replication foci in S phase nuclei, suggesting a role in regression of stalled replication forks *in vivo* (Fig. 15).

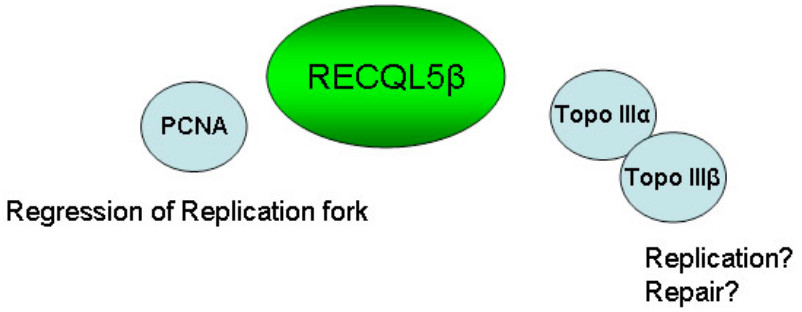

Figure 15: RECQL5β-interacting partners and their function
The cellular role of RECQL5β remains to be elucidated

3 Posttranslational Modifications of Proteins

3.1 General Introduction

At the time when the human genome was sequenced, researchers were surprised that it only contained approximately 30,000 genes and not 100,000 as had been predicted. It became more and more clear, that evolution had favored the existence of a limited number of genes with inducible functions over the existence of multiple genes with very specific functions. A large number of gene products are posttranslationally modified, therefore fine-tuning the roles of the corresponding proteins. The ensemble of covalent changes are termed post translational modifications to reflect that these changes are introduced after translation of mRNA nucleotide sequences into amino acid-based protein sequences at ribosomes (197). Posttranslational modifications can be divided into two broad categories. The first is the covalent addition of one or more groups, such as phosphoryl, acetyl, or glycosyl, to amino acid side chains of proteins. The second category is the hydrolytic cleavage of peptide bonds by proteases.

It has been estimated that about 5% of the human genome codes for enzymes that are involved in the posttranslational modification of target proteins. Posttranslational modifications can influence protein stability, protein-protein interactions, protein-DNA interactions, catalytic activities, and protein localization.

In the following section, I will exclusively focus on the acetylation of target proteins by different acetyltransferases and the functional consequences of this specific posttranslational modification.

3.2 Protein Acetylation

3.2.1 Reversible N^{ε}- Acetylation of Lysine Residues

Protein acetylation is a widely used mechanism in eukaryotes. The irreversible N^{α}-terminal acetylation occurs co-translationally and is one of the most abundant eukaryotic protein modifications with 85% of all proteins being modified (198). In addition, proteins can be acetylated on their N^{ε}-lysine (199) and two basic enzymatic mechanisms are known to be used by lysine acetyltransferases in order to add an acetyl group to the N^{ε}-lysine of substrate proteins (Fig. 16).

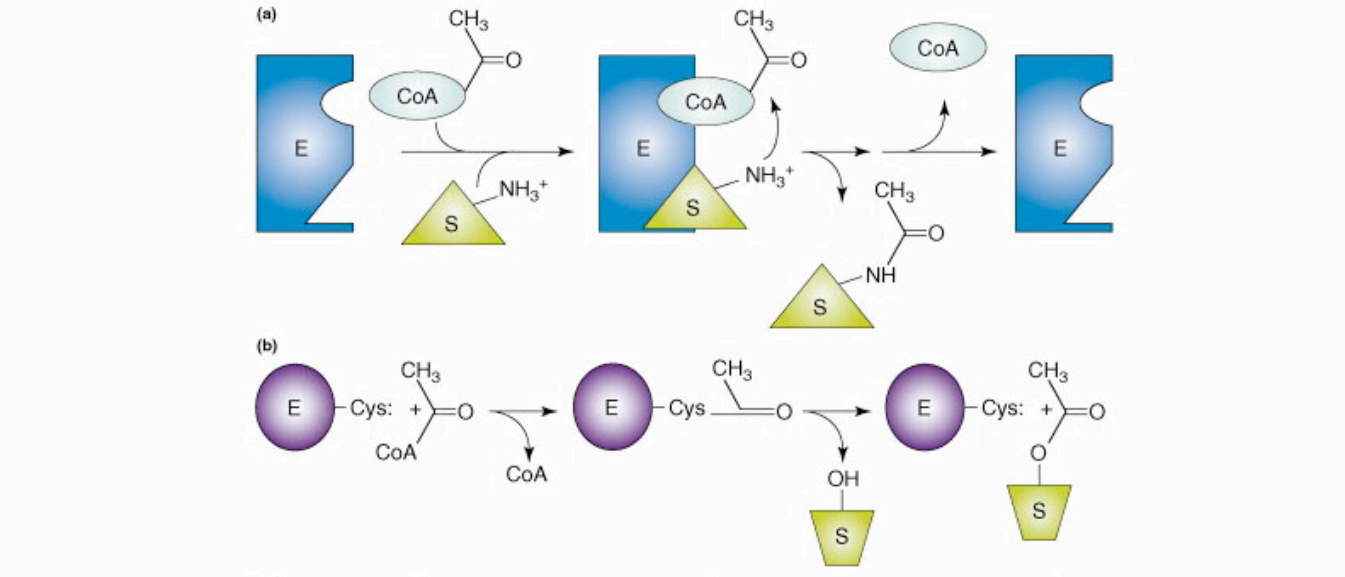

Figure 16: **Two distinct enzymatic mechanisms used for acetylation**
(a) Acetylation by direct transfer mechanism. **(b)** Acetylation by ping-pong mechanism. (Adapted from (200))

The first mechanism involves the formation of a tertiary complex composed of the enzyme, acetyl coenzyme A (Ac-CoA) and the protein substrate. The enzyme bound Ac-CoA binds a protein substrate and positions one of the lysine residues of the substrate for nucleophilic attack of Ac-CoA. The modified substrate is released

followed by release of CoA (Fig. 16a). The second mechanism is a ping-pong mechanism, used by the p300 family of acetyltransferases (discussed in section XY). Ac-CoA binds and is attacked by a catalytic residue of the enzyme, resulting in the formation of a covalent acetyl-enzyme intermediate, while CoA is released. In a second step, the substrate protein binds to coordinate a nucleophilic attack by a lysine residue on the acetyl-enzyme intermediate. The acetyl group is transferred and the modified substrate is released (Fig. 16b).

Unlike N^{α}-terminal acetylation, N^{ε}-acetylation is a reversible process providing dynamic responses to extra- and intracellular signaling events. The proteins involved in the opposing reactions are the histone deacetylases (HDACs), they are able to remove the acetyl group from the lysine residue reestablishing the positive charge.

3.2.2 Acetylation of Serine and Threonine Residues

Recent studies by Mukherjee *et* al. identified serine and threonine as new targets for acetlytransferase mediated acetylation (200). The authors determined the mechanism by which the bacterium *Yersinia* prevents the activation of mitogen-activated protein kinase (MAPK) and the nuclear factor kappaB (NFkappaB) signaling pathway in host cells. They showed that YopJ, one of six bacterial effectors secreted into the host cell, acts as an acetyltransferase, using acetyl-coenzyme A (CoA) to modify critical serine and threonine residues in the activation loop of MAPKK6 thereby blocking its phosphorylation. The acetylation on MAPKK6 directly competed with phosphorylation, preventing activation of the modified protein. It will be of particular interest to further elucidate if this covalent modification may be used as a general regulatory mechanism in biological signaling.

3.2.3 Acetylation of Histones

More than 40 years ago histones derived from calf thymus were reported to be acetylated *in vivo* (201). Originally, histone acetylation was associated with highly active transcription, while silent regions appeared to be hypoacetylated (202, 203). Acetylation neutralizes the positive charge of the lysine residue side chains and it was suggested that the interaction with the negatively charged sugar-phosphate backbone of the DNA is weakened, thus negatively influencing the nucleosomal stability and facilitating transcription. Acetylated histone N-terminal tails influence transcription on two levels i) by inducing chromatin structure changes and subsequent accessibility and ii) by serving as interaction platforms for specific protein modules (bromo domains).

However, it's inexpedient to focus on the acetylation of histones and subsequent functional consequences without a more global view of histone modifications. In the last couple of years it has been shown that histones are targets for extensive posttranslational modifications such as phosphorylation, methylation, ubiquitination, SUMOylation, and acetylation (204). These modifications decorate the canonical histones (H2A, H2B, H3 and H4), as well as variant histones (such as H3.1, H3.3 and HTZ.1). Most modifications take place at the amino- and carboxy-terminal histone tails, and only a few localize to the histone globular domains. Some of the functional outcomes of these modifications are clear. For example, there is abundant evidence that acetylation is activating, whereas SUMOylation seems to be repressing transcription, and these two types of modification may mutually interfere. On the other hand, methylation and ubiquitylation have variable effects, depending on the precise residues and contexts (Table 1).

Table 1: A list of histone modifications and their role in transcription

Mark*	Transcriptionally relevant sites†	Transcriptional role‡
DNA methylation		
Methylated cytosine (meC)	CpG islands	Repression
Histone PTMs		
Acetylated lysine (Kac)	H3 (9, 14, 18, 56), H4 (5, 8, 13, 16), H2A, H2B	Activation
Phosphorylated serine/threonine (S/Tph)	H3 (3, 10, 28), H2A, H2B	Activation
Methylated arginine (Rme)	H3 (17, 23), H4 (3)	Activation
Methylated lysine (Kme)	H3 (4, 36, 79) H3 (9, 27), H4 (20)	Activation Repression
Ubiquitylated lysine (Kub)	H2B (123§/120¶) H2A (119¶)	Activation Repression
Sumoylated lysine (Ksu)	H2B (6/7), H2A (126)	Repression
Isomerized proline (Pisom)	H3 (30–38)	Activation/repression

*The modification on either DNA or a histone.
†Well-characterized sites with regard to genomic location for DNA methylation or residues within histones for PTMs.
‡Whether the epigenetic mark is associated with activation or repression.
§Yeast (*Saccharomyces cerevisiae*).
¶Mammals.

(Adapted from (205))

Accordingly, transcriptional regulation is much more complex than just static on/off switches and more work has to be done in order to understand the nuanced chromatin 'language'. For more detailed information see (205).

3.2.4 Histone Acetyltransferases

Histone acetyltransferases (HATs) can be divided into two groups; the B-type HATs that are found in the cytoplasm and the nuclear A-type HATs. In 1995, *S. cerevisiae* Hat1 was the first HAT identified (206). Hat1 was shown to be a B-type HAT, involved in the acetylation of soluble but not nucleosomal histones in the cytoplasm that are subsequently incorporated into chromatin during replication (207). One year later, the first A-type HAT was identified in the ciliate *Tetrahymena thermophila* showing strong sequence homologies to the yeast transcriptional co-activator GCN5 (General control non-derepressible-5) (208). This discovery provided the first molecular evidence for a

direct link between histone acetylation and transcriptional regulation. This concept received rapid experimental support through the identification of several other adaptor/coactivator proteins with intrinsic HAT activity, including mammalian GCN5 (209-211) and its ortholog, PCAF (211), CREB-binding protein (CBP) (212, 213), p300 (213), and TAFII250 (214, 215). Table 2 gives an overview of the different HATs and their potential functions. Recent studies show that some HATs have factor acetyltransferase (FAT) activity. FAT activity has been demonstrated for the histone acetyltransferases p300/CBP, PCAF and TAFII250 with substrates ranging from transcriptional activators and basal transcription factors to non-histone chromosomal proteins and different DNA repair factors (216). The section below will concentrate on p300, which is the relevant acetyltransferase for this thesis.

Table 2: A list of histone acetyltransferase

Group	HAT	Organism	Complex	Possible function
Gcn5 family	Gcn5	Yeast	SAGA, SILK, SALSA, ADA, HAT-A2	Transcriptional activation
	GCN5L	Mammal/fly	STAGA, TFTC	Transcriptional activation
	PCAF	Mammal	PCAF complex	Transcriptional activation
MYST family	Esa1	Yeast	NuA4	Transcriptional activation
	Sas2	Yeast	SAS-I	Anti-silencing
	Sas3	Yeast	NuA3	Transcriptional activation
	Tip60	Mammal	Tip60 complex	Transcriptional activation/DNA repair
	HBO1	Mammal	HBO1 complex	Gene expression?/DNA replication
	MORF	Mammal		Transcriptional activation
	MOZ	Mammal		Transcriptional activation
	CLOCK	Mammal		Transcriptional activation (circadian rhythm)
	NCOAT	Mammal		Transcriptional activation
	MOF	Mammal/fly	MSL	Dosage compensation
Others	HAT1	Yeast	HAT1/2 complex	Histone deposition
	Elp3	Yeast	Elongator	Transcriptional elongation
	Hpa2	Yeast		
	Nut1	Yeast	Mediator	RNA pol II transcription
	$TAF_{II}250$ (TAF1)	Yeast/mammal/fly	TFIID	RNA pol II transcription
	p300/CBP	Mammal		Transcriptional activation
	hTFIIICII0	Mammal	TFIIIC	Transcriptional activation
	hTFIIIC90	Mammal	TFIIIC	Transcriptional activation
	ACTR/SRC-1	Mammal		Transcriptional activation
	ATF-2	Mammal		Transcriptional activation

(Adapted from (217))

3.2.5 Histone Deacetylases

Acetylated lysine residues are deacetylated by a specific class of enzymes called histone deacetylases (HDACs). In the same year that the first HAT was identified as transcriptional coactivator Schreiber's group purified and cloned human HDAC1 (218). Based on sequence homologies to yeast proteins, human histone deacetylases (HDACs) are subdivided into four classes (217) (Table 3). Class I HDACs display sequence homology to yeast Rpd3, which deacetylates all four core histones (HDAC1, 2, 3 and 8). Class II HDACs (HDAC 4, 5, 6, 7, 9 and 10) are similar to yeast Hda1, which deacetylates histones H2B and H3 (219). The activities of the members of classes I and II are Zn^{2+}-dependent. Class III HDACs (SIRT1-7) are (NAD+)-dependent and are related to yeast Sir2, which is involved in the regulation of gene silencing and aging (220). Class IV consists of the recently identified HDAC11 (221). Structurally HDAC11 is most closely related to the class I HDACs.

Table 3: A list of histone deacetylases

Class	HDAC	Organism	Complex	Possible function
Class I	Hos1	Yeast		Transcriptional repression/activation
	Hos2	Yeast	Set3C	Transcriptional repression
	Rpd3	Yeast	Rpd3S, L	Transcriptional repression/activation
	HDAC1	Mammal	mSin3-HDAC, NuRD, Co-REST, N-CoR-2	Transcriptional repression
	HDAC2	Mammal	mSin3-HDAC, NuRD, Co-REST, N-CoR-2	Transcriptional repression
	HDAC3	Mammal	N-CoR-1	Transcriptional repression
	HDAC8	Mammal		Transcriptional repression
Class II	Hda1	Yeast	Hda1-associated complex	Transcriptional repression
	Hos3	Yeast	Homo dimmer	
	HDAC4	Mammal		Transcriptional repression
	HDAC5	Mammal		Transcriptional repression
	HDAC6	Mammal		Transcriptional activation/cell motility
	HDAC7	Mammal		Transcriptional repression/activation
	HDAC9	Mammal		Transcriptional repression
	HDAC10	Mammal		Transcriptional repression
Class III	Hst1	Yeast	Set3C	Silencing
	Hst2	Yeast		Silencing
	Hst3	Yeast		Silencing
	Hst4	Yeast		Silencing
	Sir2	Yeast	Sir4, RENT	Silencing
	SIRT1	Mammal		Transcriptional repression
	SIRT2	Mammal		Mitotic exit
	SIRT3	Mammal		Metabolic regulation
	SIRT4	Mammal		
	SIRT5	Mammal		
	SIRT6	Mammal		DNA repair
	SIRT7	Mammal		Pol I transcriptional activation
Class IV	HDAC11	Mammal		

(Adapted from (217))

Transcriptional repression is either achieved by the sequestring of transcriptional activators or by occupancy of enhancer binding sites and does not require enzymatic activity (222). Furthermore, HDACs are active repressors and remove the acetyl group from lysine residues. Mutations in their conserved catalytic domain release the repressive effect of HDACs (223).

Surprisingly, it was shown that HDACs can also function as transcriptional activators. Deletion of Rpd3 or Hda1 in yeast negatively effected the transcription of certain genes and increased gene silencing (224).

These finding provide evidence that the regulation of transcription by acetylation is a complex and dynamic process.

3.3 Histone Acetyltransferase p300/CBP

3.3.1 Structure and Function of p300/CBP

p300 and its homologue CBP are present in many multicellular organisms, including flies, worms and plants, but not in lower eukaryotes such as yeast (225-227). In the last decade, they have been the most studied HATs in the context of transcriptional regulation. Originally isolated as adenoviral E1A interacting (228) and CREB interacting protein (cAMP-response-element-binding protein) (229), p300 and CBP function as global transcriptional co-activators for more than 40 different transcription factors, supporting their role as key players in different signaling pathways (230).

As depicted in Figure 17, p300 and CBP share several conserved regions, including three cysteine-histidine rich regions CH (CH1, -2, and -3), the binding site for the CREB transcription factor, referred to as the KIX domain, the bromodomain important for the binding of acetylated lysines (BD), the HAT domain and the steroid receptor coactivator-1 interaction domain (SID). CBP and p300 interact directly with the basal transcription factors TATA-binding protein (TBP) (231), TFIIB (231, 232) and TFIID (233) and form a complex with RNA polymerase II (234-237). Additionally, CBP and p300 can bind to a variety of diverse transcription factors and other proteins, through their CH-1, CH-3, KIX and SID domains (238, 239).

Figure 17: Schematic representation of the p300/CBP gene
Colored boxes represent shared conserved regions important for protein- and DNA interactions.

One important cellular role of p300/CBP is to work as “molecular bridges” mediating and stabilising the interaction between sequence-specific transcription factors and the

RNA polymerase II transcription machinery (238). The second important aspect of the coactivator function of p300/CBP is their ability to serve as 'protein scaffolds' for the assembly of other chromatin modifying and remodelling complexes. The interaction with other HATs such as SRC-1 (240, 241), P/CAF (213) and SRC-3 (ACTR) (242) has been described. Protein scaffolds increase the local concentration of cofactors around the transcription start sites facilitating protein-protein and protein-DNA interactions.

Thirdly, p300 and CBP acetylate promoter proximal nucleosomal histones, resulting in increased accessibility of the DNA for other essential regulators (212, 213, 243). Soon after the discovery of their enzymatic activities the first non-histone protein (p53) was reported to be acetylated by p300 (244). The increasing number of non-histone proteins acetylated by p300 and CBP is discussed in further detail in section 3.3.3

3.3.2 p300/CBP and Human Disease

The importance of CBP and p300 is supported by evidence that genetic alterations in their genes and subsequent functional inactivation of the proteins are associated with human disease (245-247). Mutation of one copy of the CBP gene results in a congenital developmental disorder called Rubenstein-Taybi-Syndrome (RTS), which is characterized by retarded growth and mental function, broad thumbs and typical facial abnormalities (248). Furthermore, RTS patients have an increased tumor risk (249).

Heterozygous chromosomal translocations involving CBP or p300 are found in patients suffering from acute myeloid leukaemia (ALM) (250). In addition, heterozygous mutations in the p300 gene have been detected in primary solid tumors and tumor cell lines, mainly of epithelial origin (251-254). Most of the mutations lead to truncated p300 protein and in the majority of the cases the second allele was inactivated through deletion (loss of heterozygosity), silencing (hemizygosity), or a different mutation (compound heterozygosity), qualifying p300 as a classical tumor suppressor gene, according to Knudson's two-hit model (255).

In summary, findings on CBP and p300 in human disease indicated that the dosage of these proteins is essential in the regulation of normal differentiation, growth control and homeostasis in humans.

3.3.3 p300/CBP Acetylation of Target Proteins

In 1996, Ogryzko *et* al. demonstrated that p300/CBP was not only a transcriptional adaptor but also a histone acetyltransferase, acetylating all four histones in nucleosomes (213). Two years later, Schiltz *et* al. described that the preferred p300 *in vitro* sites of acetylation on the N-terminal histone tails are lysine 12 (K12) and K15 in histone H2B, K14 and K18 in histone H3 and K5 and K8 in histone H4 (256).

In addition to their ability to acetylate histones, CPB and p300 have also been shown to acetylate a variety of other proteins and have therefore been called factor acetyltransferases (FAT) (216, 250). The list of acetylated non-histone proteins involved in transcription, including site-specific transcription factors, general transcription factors, cofactors and chromatin remodellers grew exponentially. A selection of these acetylation target proteins will be discussed.

In 1997, Gu and co-workers identified the tumor suppressor p53 as the first non-histone acetylation target of p300 (244). p53 was found to be acetylated *in vitro* and *in vivo* on its C-terminal domain known to be critical for the regulation of DNA binding. The acetylation of p53 dramatically stimulated its sequence-specific DNA-binding activity, thus positively influencing p53 transcriptional activation activity.

Some acetylated non-histone proteins are important for DNA repair such as the flap endonuclease 1 (Fen1) (257). Hasan *et* al. demonstrated that the DNA binding and endonuclease activity of Fen1 was reduced upon acetylation by p300. The same authors could also identify polymerase β (pol β) as a non-histone acetylation target of p300. p300 and pol β co-localize and physically interact in human cells. Acetylated Pol β showed an impaired AP lyase activity essential for proper base excision repair (258).

Acetylation of the thymine DNA glycosylase (TDG) by p300/CBP did not affect the TDG DNA cleavage activity but released CBP from the DNA bound complex and

abolished interaction with the AP-endonuclease (259). Additionally, acetylation of human DNA glycosylase NEIL2 on lysine 49 inhibited the base excision as well as the AP lyase activity of NEIL2 and extended the list of modified repair proteins (260).

Acetylation of non-histone substrates can result in either positive or negative effects on transcription by affecting, for example, protein–protein interactions (e.g. the activator of thyroid and retinoid receptors ACTR (261)), protein–DNA interactions (e.g. the high mobility group protein HMGI(Y) (262)), or protein half-life (e.g. E2F (263)).

Recently, protein acetylation has been proposed as a new mechanism for modulating subcellular localization (131, 264-270). Acetylation target lysine residues that are located in the nuclear localization signal (NLS) of several proteins. This can directly modulate NLS function (265) and disrupt its association with the import machinery leading to cytoplasmic localization of proteins (267). Alternatively, acetylation inside NLSs, rather than affecting the NLS function itself, can cause a conformational change that impairs the function of the nuclear export signal (NES), promoting protein accumulation in the nucleus (131, 267, 269).

Taken together, protein acetylation seems to be a widespread mechanism to control a variety of different cellular mechanisms.

4 Results

Article I

The human Rothmund-Thomson syndrome gene product, RECQL4, localizes to distinct nuclear foci that coincide with proteins involved in the maintenance of genome stability.

Maja Petkovic, Tobias Dietschy, Raimundo Freire, Renjie Jiao, and Igor Stagljar

(2005) Journal of Cell Science *118, 4261-4269*

My contribution to this work was helping with protein-protein interaction and the experiment for figure 5c.

Research Article 4261

The human Rothmund-Thomson syndrome gene product, RECQL4, localizes to distinct nuclear foci that coincide with proteins involved in the maintenance of genome stability

Maja Petkovic[1], Tobias Dietschy[1], Raimundo Freire[2], Renjie Jiao[1,*] and Igor Stagljar[1,‡,§]

[1]Institute of Vet. Biochemistry and Molecular Biology, University of Zürich, Winterthurerstr. 190, 8057 Zürich, Switzerland
[2]Unidad de investigacion, Hospital Universitario de Canarias, Ofra s/n, La Cuesta, 38071 Tenerife, Spain
*Present address: Institute of Biophysics, The Chinese Academy of Sciences, Datun Road 15, Chaoyang District, Beijing 100101, China
‡Present address: Department of Biochemistry and Department of Medical Genetics and Microbiology, The Terrence Donnelly Centre for Cellular and Biomolecular Research, University of Toronto, 1 Kings College Circle, Toronto, ON, Canada, M5S 1A8
§Author for correspondence (e-mail: stagljar@utoronto.ca)

Accepted 14 June 2005
Journal of Cell Science 118, 4261-4269 Published by The Company of Biologists 2005
doi:10.1242/jcs.02556

Summary

Rothmund-Thomson syndrome (RTS) is a human genetic disorder characterized by genome instability, cancer susceptibility and premature aging. The gene defective in a subset of RTS cases, *RECQL4*, encodes a member of the RecQ family of DNA helicases. To better define the function of the RECQL4 protein, we have determined its subcellular localization. We have raised antibodies against the N- and C-terminal parts of RECQL4 and could show that in various human cells endogenous RECQL4 forms discrete nuclear foci that colocalize with promyelotic leukaemia protein (PML). The number of foci and their colocalization with PML does not significantly change after induction of different types of DNA damages. Silencing of RECQL4 expression by siRNA causes a significant reduction in RECQL4 nuclear foci formation. Furthermore, we demonstrate that RECQL4 foci coincide with foci formed by human Rad51 and regions of single-stranded DNA after induction of DNA double-strand breaks. In agreement with this, we also show that RECQL4 and Rad51 form a complex in human cells. Our findings suggest a role for RECQL4 in the repair of DNA double-strand breaks by homologous recombination and shed new light onto RECQL4's function in human cells.

Supplementary material available online at
http://jcs.biologists.org/cgi/content/full/118/18/4261/DC1

Key words: Genome stability, Rothmund-Thomson syndrome (RTS), RecQ helicases, Immunofluorescence, Promyelotic leukaemia protein (PML), Rad51

Introduction

Genome instability is thought to play a major role in the development and progression of cancer, and has also been implicated in the aging process. One important family of proteins required to maintain genome stability is the RecQ family of DNA helicases (Hickson, 2003). This highly-conserved protein family includes *Escherichia coli* RecQ (Nakayama et al., 1984), *Saccharomyces cerevisiae* Sgs1p (Gangloff et al., 1994), *Schizosaccharomyces pombe* Rqh1p (Enoch et al., 1992), and at least five human homologs named *RECQL1* (Puranam and Blackshear, 1994; Seki et al., 1994), *WRN* (Yu et al., 1996), *BLM* (Ellis et al., 1995), *RECQL4* and *RECQL5* (Kitao et al., 1998). Common to all RecQ family members is a helicase domain that comprises seven highly conserved motifs of the DExH-box family that are found in many DNA and RNA helicases (Singleton and Wigley, 2002). During the past decade, there has been increasing interest in the RecQ family of DNA helicases because a group of rare, autosomal recessive human disorders has been linked to mutations in some of its members. These disorders include Werner's syndrome (WS), the premature aging disease caused by mutations in *WRN* gene (Yu et al., 1996); Bloom's syndrome (BS), a cancer predisposition disease caused by mutations in *BLM* gene (Ellis et al., 1995), and a subset of cases of RTS characterized by mutations in the *RECQL4* gene (Kitao et al., 1999b).

RTS displays heterogeneous clinical profiles that include growth-deficiency, photosensitivity with poikiloderma, cataracts, early graying and loss of hair, as well as the early development of cancers of many types, in particular osteosarcoma (Lindor et al., 2000). The gene mutated in a subset of RTS patients, *RECQL4*, contains 21 exons spanning only 6 kb of genomic DNA sequence and is located on human chromosome 8q24.3 (Kitao et al., 1999a). In addition to RTS, mutations in the *RECQL4* gene can also cause an RTS-similar disease termed RAPADILINO syndrome (Siitonen et al., 2003). The latter is an autosomal recessive disorder characterized by short stature, radial ray defects and other malformations, as well as infantile diarrhoea, but not by a significant cancer risk (Jam et al., 1999). The most common mutations of the *RECQL4* gene in RAPADILINO patients represent in-frame deletions of exon 7 (Siitonen et al., 2003). On the other hand, most alternations

of *RECQL4* found in RTS patients represent nonsense or frameshift mutations, resulting in a truncated polypeptide and map to the helicase domain (Kitao et al., 1999b; Wang et al., 2003). Somatic cells isolated from RTS individuals are sensitive to ionizing radiation (IR) (Vennos and James, 1995) and show genomic instability, including trisomy, aneuploidy and chromosomal rearrangements (Der Kaloustian et al., 1990). In agreement with this notion, targeted disruption of *RECQL4* in mice results in abnormalities similar to those in RTS patients (Hoki et al., 2003). During G1 arrest, the promoter of the *RECQL4* gene is repressed by p53 that forms a complex with the transcription factor SP1 in concert with histone deacetlyase 1 (HDAC1) (Sengupta et al., 2005). In human cells, RECQL4 is associated with ubiquitin ligases UBR1 and UBR2, thus indicating a potential role of RECQL4 in the N-end rule pathway (Yin et al., 2004).

Numerous studies on Sgs1p, Rqh1, BLM and WRN have revealed that RecQ helicases are involved in the maintenance of genome stability by functioning at the interface between DNA replication, recombination and repair (Hickson, 2003). However, the biochemical properties, interaction partners and subcellular localization of RECQL4 have to date been largely unexplored. In this study, we have carried out a cellular localization analysis of the human RECQL4 protein. To achieve this goal, we have raised two different anti-RECQL4 antibodies that recognize a RECQL4-specific band from human cell extracts. We show that RECQL4 forms nuclear foci in several human cell lines, the number of which does not significantly change after induction of different types of DNA damages. Importantly, downregulation of RECQL4 by siRNA causes reduction in RECQL4 nuclear foci formation. The RECQL4 foci coincide with those formed by PML nuclear bodies and the number of colocalizing foci slightly decreases after induction of DNA double-strand breaks (DSBs). In addition, RECQL4 forms a complex with the human Rad51 protein and colocalizes with Rad51 and regions of single-stranded DNA (ssDNA) upon induction of DNA DSBs. These findings suggest a role for RECQL4 in the repair of DSBs by homologous recombination and indicate a novel function for RECQL4 in human cells.

Materials and Methods

Cell culture and indirect immunofluorescence assays

The HeLa, 293T and WI38/VA13 cells were from the American Type Culture Collection (ATCC), AG18371 cells from Coriell and the primary skin fibroblasts were a kind gift from Silvio Hemmi, University of Zurich, Switzerland. Cells were cultured in Dulbecco's modified Eagle's medium (Life Technologies) and 10% FBS. For some experiments cells were exposed to 10 μM etoposide for 1 hour at 37°C, washed, given drug-free medium, and collected 10-12 hours later. For detection of ssDNA after damage, cells were grown on slides in medium containing 10 μg/ml BrdU, exposed to 10 μM etoposide for 1 hour in BrdU-free medium and fixed after 10 hours. For HU treatment cells were incubated with 10 mM HU for 24 hours, UV treatment was performed with 50 J/m^2 at 254 nm, cells were fixed 16 hours after the treatment; for ionizing-radiation treatment cells were exposed to 5 Gy and fixed 4 hours later. For the indirect immunofluorescence assays, cells growing on glass slides were incubated with 0.5% Triton X-100 in PBS for 5 minutes, fixed with 2% paraformaldehyde in PBS (20 minutes at RT), and permeabilized with 0.5% Triton X-100 in PBS (20 minutes at RT). After the blocking step (0.1% Tween-20, 5% BSA in PBS, 20 minutes at RT), slides were incubated with a mixture of different rabbit and mouse antibodies. Rabbit antibodies were detected with Cy3-conjugated goat anti rabbit IgG (Jackson Laboratories; 1:200 in blocking buffer), and mouse antibodies were detected with FITC-conjugated goat anti mouse IgG (Jackson Laboratories; 1:100 in blocking buffer). To visualize nuclear DNA, slides were incubated with DAPI (0.4 μg/ml). After washing, slides were mounted in Vectashield (Vector Laboratories) and viewed under confocal microscope Leica TCS 4D. Images were processed by Imaris software. For statistical analysis a minimum of 200 cells was counted in two independent experiments.

Antibody production

The rabbit polyclonal RECQL4 N-t and RECQL4 C-t antisera were raised against recombinant human RECQL4 fragments comprising amino acid residues 359 to 478 and 911 to 1208, respectively. For that, the corresponding cDNA fragments were cloned in pET-30 (RecQL4 N-t) or pET-28 (RECQL4 C-t) expression vectors (Novagen) and recombinant proteins fused to a histidine tag were purified using Ni-NTA resin (Qiagen) following the manufacturer's instructions.

RECQL4 N-t and C-t antibodies were affinity-purified using hexahistidine-tagged RECQL4 N-t and C-t recombinant proteins as an affinity matrix, respectively. The purified proteins were fractionated by SDS-PAGE and transferred to nitrocellulose membranes. The membranes were stained with Ponceau S, and the corresponding 6xHis-RECQL4 band was excised. The strips were blocked for 1 hour with 2% bovine serum albumin in TBS (10 mM Tris, pH 7.4, 150 mM NaCl) containing 0.1% Tween 20. The strips were then incubated overnight with rabbit antiserum and washed with TBS containing 0.1% Tween 20 and 1 M NaCl. Anti-RECQL4 antibodies were eluted by incubation in 100 mM glycine pH 2.3, for 5 minutes. The eluate was then immediately neutralized with 1 M Tris-HCl pH 8.8.

Antibodies

In immunofluorescence experiments, anti-PML antibody (Santa Cruz, PG-M3) was used in a 1:50 dilution, anti-Rad51 antibody (abcam, ab1837) in a 1:50 dilution, anti-BrdU antibody (Pharmingen, 3D4) in a 1:50 dilution, anti-RECQL4 N-t antibody in a 1:200 dilution. For western blots, anti-RECQL4 N-t and anti RECQL4 C-t antibodies were used in a 1:2000 dilution, anti-tubulin antibody (Santa Cruz, TU-02) in a 1:1000 dilution, anti-PARP1 antibody (Petrilli et al., 2004) in a 1:2000 dilution, anti-BLM antibody (Wu et al., 2000) in a 1:1500 dilution, anti-GRB2 antibody (BD Transduction, G10111) in a 1:2000 dilution, anti-FLAG antibody (Sigma, M2) in a 1:2000 dilution and anti-Rad51 antibody (Tan et al., 1999) in a dilution 1:20,000.

Total cell and nuclear extracts

Total cell extracts were prepared from exponentially growing HeLa cells by lysis in lysis buffer (50 mM Hepes, pH 7.6; 500 mM NaCl; 1% Triton X-100, protease inhibitors) for 15 minutes with rolling at 4°C and centrifugation at 14,000 rpm for 15 minutes at 4°C. Nuclear extracts were prepared from HeLa cells, which were washed in PBS and re-suspended in buffer A (10 mM Hepes, pH 7.9; 1.5 mM $MgCl_2$; 10 mM KCl; protease inhibitors) and then centrifuged for 1 minute at 2000 rpm. The cell pellet was re-suspended in buffer A+ (buffer A; 0.1% Nonidet P 40) for 5 minutes on ice and centrifuged at 10,000 rpm, for 5 minutes. The supernatant contained cytosolic extract. The pellet was washed in buffer A and then re-suspended in buffer C (20 mM Hepes, pH 7.9; 420 mM NaCl; 1.5 mM $MgCl_2$; 25% glycerol, protease inhibitors) for 15 minutes, with rolling at 4°C. The samples were then centrifuged at 14,000 rpm, for 5 minutes. The supernatant contained nuclear extract and the NaCl concentration was adjusted to 120 mM with buffer D (20 mM Hepes, pH 7.9, protease inhibitors).

Transfection of cells and immunoprecipitation assay

293T cells were transiently transfected with p3xFLAG-myc-CMV-23 (Sigma) expressing RECQL4 or vector alone. Preparation of nuclear extracts was described in previous section. Aliquots (120 μg) of nuclear extracts were incubated with 3 μg of anti-FLAG antibody coupled to magnetic tosylactivated Dynabeads (Dynal Biotech, M-280) according to manufacturer's instructions in immunoprecipitation buffer (20 mM Hepes, pH 7.5; 120 mM NaCl; 5 mM $MgCl_2$; 0.1% Nonidet P 40; protease inhibitors) at 4°C overnight. As a control, nuclear extracts from untransfected cells were used. The beads were washed three times in immunoprecipitation buffer before the protein complexes bound to the beads were eluted and analysed by sodium dodecyl sulfate-polyacrylamide (SDS) gel electrophoresis. A 12 μg aliquot of nuclear extract was used as input control. For the reverse immunoprecipitation assay, an aliquot of nuclear extracts (120 μg) was incubated with 3 μl (approximately 2 μg) of polyclonal anti-Rad51 antibody (kind gift of Roland Kanaar, Erasmas University, Rotterdam, The Netherlands) in immunoprecipitation buffer for 3 hours, to which 20 μl of protein G sepharose 4 fast flow (Amersham Biosciences) beads were added and incubated for an additional for 2 hours. As a control, nuclear extracts were incubated with 1.2 μg of rabbit IgG (Santa Cruz). The beads were washed three times in immunoprecipitation buffer before the protein complexes bound to the beads were eluted and analysed by SDS gel electrophoresis.

RNA-mediated interference

For short interfering RNA (siRNA) experiments, RECQL4-1 5′-aacuucugaucccuggugagu-3′ and control-1 5′-aaucuagcucuccuguagggu-3′ with dTdT overhang (Qiagen, Operon) were used. The siRNAs were transfected in HeLa cells using a 200 nM siRNA concentration with Oligofectamine (Invitrogen) according to manufacturer's instruction and harvested after 24 hours.

Results

Generation of anti-RECQL4 antibodies

Antibodies against N- and C-termini of RECQL4 were raised in rabbits using chimeric proteins consisting of 6xHis-tag fused to residues 359-478 and 911-1208 of RecQL4. These regions of RECQL4 were chosen because they show no sequence homology to other human RecQ helicases. These sera, designated anti-RECQL4 N-t and anti-RECQL4 C-t, respectively, were affinity-purified as described in Materials and Methods. In western blots, both sera recognized their protein fragments used for immunization (data not shown), and a major protein band in HeLa nuclear, cytosolic and total cell extracts with a molecular mass of approximately 150 kDa (Fig. 1A). To control our cell fractionation experiments, we examined the distribution of the endogenous human nuclear proteins PARP1 and BLM as well as a cytosolic protein GRB2. As expected, a band corresponding to PARP1 and BLM was detected in the nuclear extract only, whereas the band corresponding to GRB2 was detected only in the cytosolic extract (Fig. 1A, three lower panels).

In addition, both RECQL4 antisera also recognized FLAG-epitope-tagged RECQL4, expressed in 293T cells, with the expected molecular mass (Fig. 1B). No such protein was detected in HeLa nuclear and total cell extracts with preimmune serum (data not shown) or cell in extracts derived from the RTS-patient cell line AG18371, using both of the anti-RECQL4 sera (Fig. 1A). Likewise, both RECQL4 antibodies did not cross-react with purified recombinant BLM and WRN helicases (data not shown). These results, and the results from the siRNA experiments (discussed below), show that both antisera are specific for the RECQL4 protein.

RECQL4 forms discrete nuclear foci in various human cells

Next, we used the affinity purified anti-RECQL4 N-t antiserum to visualize the in situ distribution of RECQL4 in human cells. Indirect immunofluorescence staining analysis by confocal microscopy of exponentially growing HeLa, WI38/VA13 and primary skin fibroblast cell lines revealed a punctate nuclear staining in all three cell lines, which was observed in the majority of the cells (Fig. 2A-C). No cytoplasmic staining was evident in any of the examined cells, which is contradictory to our western blot results. This can be explained by the difference in sample preparation and detection methods used in these two assays, and that the protocol used for our immunofluorescence assays presumably removes the RECQL4 protein – which is not bound to the nuclear matrix. The calculated average number of RECQL4 foci formed per cell is 25. Furthermore, no specific fluorescence was seen in the cells with pre-immune serum (Fig. 2D).

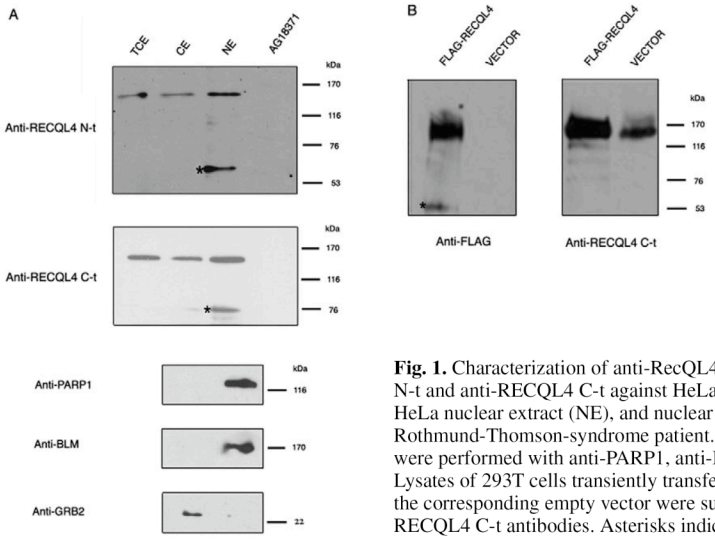

Fig. 1. Characterization of anti-RecQL4 antibodies. (A) Western blot using the anti-RECQL4 N-t and anti-RECQL4 C-t against HeLa total cell extract (TCE), HeLa cytosolic extracts (CE), HeLa nuclear extract (NE), and nuclear extracts from AG18371 fibroblasts derived from a Rothmund-Thomson-syndrome patient. Control western blots against HeLa CE and HeLa NE were performed with anti-PARP1, anti-BLM and anti-GRB2 antibodies, respectively. (B) Lysates of 293T cells transiently transfected with a vector expressing FLAG-RECQL4 or with the corresponding empty vector were subjected to western blot with anti-FLAG and anti-RECQL4 C-t antibodies. Asterisks indicate breakdown products.

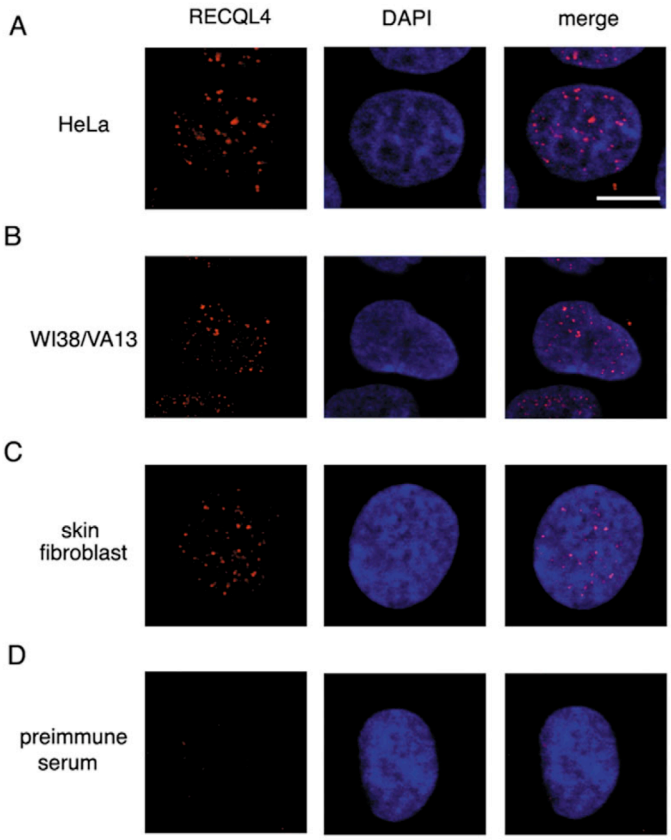

Fig. 2. RECQL4 localizes to nuclear foci in different cell lines. The foci were detected with anti-RECQL4 N-t antibody (red). DAPI-staining shows nuclear DNA. Bar, ~10 μm. (A) HeLa cell. (B) WI38/VA13 cell. (C) Primary skin fibroblast. (D) Preimmune serum, HeLa cell.

To further confirm the specificity of RECQL4 nuclear foci staining, we silenced RECQL4 using RNA interference. We transiently transfected HeLa cells with siRNA RECQL4-1 directed against the RECQL4 mRNA, and control-1 siRNA containing a scrambled sequence of RECQL4-1. We first examined the efficiency of silencing of RECQL4 by immunoblotting. As shown in Fig. 3A, silencing of RECQL4 occurred only in cells transfected with RECQL4-1 siRNA, in which approximately a 70% decrease in the level of endogenous RECQL4 was detected compared with the cells transfected with a control-1 siRNA. An even more pronounced effect was observed after immunofluorescence staining analysis (Fig. 3B). We detected a significant reduction of RECQL4 nuclear foci in the cells transfected with siRNA RECQL4-1, which was not the case for the cells treated with the control-1 siRNA (Fig. 3B,C).

We also examined whether the RECQL4 nuclear foci staining changes after induction of DNA damage. For that purpose, HeLa and WI38/VA13 human fibroblasts were treated with different DNA damaging agents including ionizing radiation (IR), which produces DSBs; ultraviolet light (UV), which generates predominantly pyrimidine dimers and 6-4 photoproducts; and hydroxyurea (HU), an inhibitor of DNA replication. As shown in supplementary material Fig. S1, indirect immunofluorescence analysis showed that there was no significant change in the number of RECQL4 foci after these treatments.

RECQL4 colocalizes with promyelotic leukaemia protein (PML) nuclear bodies

Previous reports have identified a dynamic association of BLM with promyelotic leukaemia protein (PML) (Bischof et al., 2001; Zhong et al., 1999). PML functions as a tumor suppressor, and localizes to nuclear foci termed PML nuclear bodies (PML NBs) (Hodges et al., 1998). It has been suggested that these localization sites function as protein-storage sites, sites where multi-subunit complexes form and post-translational modification of regulatory factors occur, and that are modified in response to a variety of stresses including oncogenes (Dellaire and Bazett-Jones, 2004), and DNA breaks (Carbone et al., 2002). We have therefore analyzed whether the degree to which RECQL4 foci colocalized with PML in exponentially growing, untreated HeLa, WI38/VA13 and primary skin fibroblast cells. In these cells, we observed a partial colocalization between RECQL4 and PML (Fig. 4, upper panel). On average, 14% of RECQL4 foci colocalized with PML foci and 27% of PML foci colocalized with RECQL4 foci, an observation seen in 90% of cells. We then wanted to test whether the number of colocalizing RECQL4 and PML foci changes after treatment of cells with DNA-damaging agents. Upon treatment with a DNA-DSB-inducing agent, etoposide, the number of colocalizing foci was slightly reduced (Fig. 4, lower panel). In 90% of treated cells, 10% of RECQL4 foci colocalized with PML foci and 18% of PML foci colocalized with RECQL4 foci. Collectivelly, these data indicate that at least a portion of RECQL4 foci is associated with PML NBs and that, after induction of DNA DSBs, a minor portion of RECQL4 foci relocalizes from PML NBs.

RECQL4 colocalizes with regions of ssDNA

We next wanted to determine whether RECQL4 is present at regions of ssDNA after the induction of DSBs. For that purpose, 5-bromo-2′-deoxyuridine (BrdU), was used to visualize sites of ssDNA that are often associated with DSB repair. BrdU is inaccessible to an anti-BrdU antibody when present in duplex DNA, but readily accessible to the antibody when the DNA is denatured or single-stranded (Raderschall et al., 1999). HeLa cells that were grown in medium containing BrdU, then fixed with paraformaldehyde and stained under non-denaturing conditions, showed no significant staining, confirming that the antibody does not detect BrdU in duplex DNA (Fig. 5A, upper panel). The same cells, however, showed the expected pattern of RECQL4 foci, indicating that BrdU does not perturb RECQL4 localization. After exposing BrdU-labelled cells to etoposide, BrdU foci appeared in the majority of the cells (Fig. 5A, lower panel). These foci formed because of DNA DSBs, where they presumably identify sites of repair. To determine whether RECQL4 localizes with BrdU, we co-

stained for RECQL4 and BrdU 10 to 12 hours after etoposide treatment. We could detect partial colocalization between RECQL4 and regions of ssDNA as determined by anti-BrdU staining (Fig. 5A, lower panel). There were 9% of RECQL4 foci colocalizing with BrdU foci and 18% of BrdU foci colocalizing with RECQL4 foci. The RECQL4/BrdU colocalization was evident in 46% of cells. Similar results were obtained after cell treatment with IR (data not shown). These results suggest that a portion of RECQL4 foci can associate with regions of ssDNA after exposure to DSB-inducing agent, and might represent sites of ongoing DNA repair.

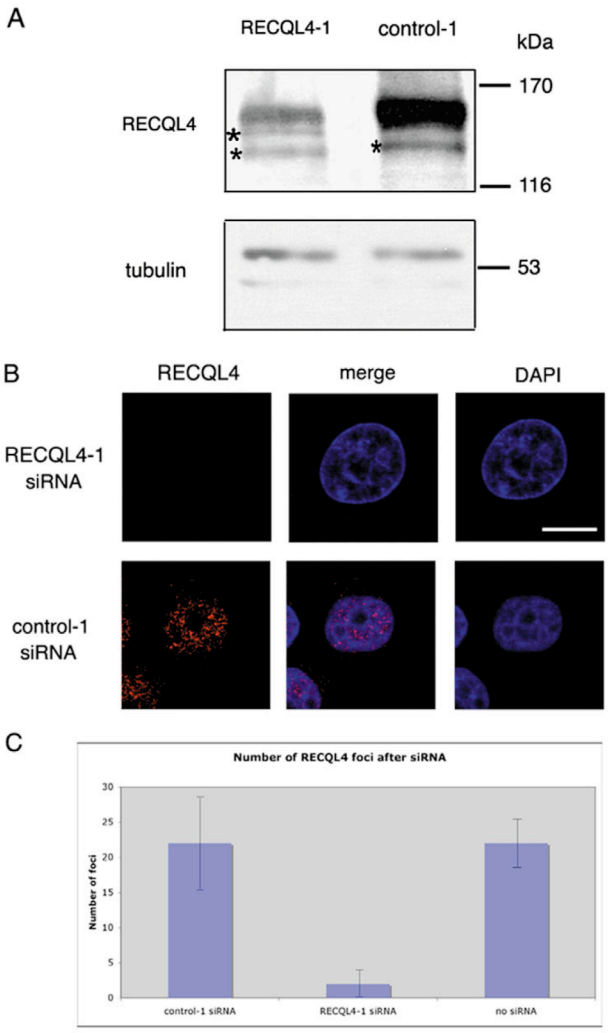

Fig. 3. Determination of the specificity of the RECQL4 antibodies by siRNA. (A) Western blot with anti-RECQL4 C-t antibody (upper panel) or anti-tubulin antibody (lower panel) using total cell extracts from HeLa cells transfected with 200 nM RECQL4-1 or control-1 siRNA. Asterisks indicate breakdown products. (B) RECQL4 knock-down leads to a loss of RECQL4 nuclear foci. Immunofluorescence analysis with anti-RECQL4 N-t antibody (red) on exponentially growing HeLa cells transfected with 200 nM RECQL4-1 or control-1 siRNA, DAPI-staining shows nuclear DNA (blue). Bar, ~10 μm. (C) The mean number of RECQL4 foci per cell after siRNA treatment is displayed in histograms (standard error of the mean is indicated in the columns).

RECQL4 forms a complex in human cells and colocalizes with human Rad51 after the induction of DNA double-strand breaks

It has been previously reported that Rad51 foci, which are important for DNA repair by homologous recombination, accumulate at sites of ssDNA after induction of DSBs (Raderschall et al., 1999). The colocalization of RECQL4 and regions of ssDNA after induction of DSBs prompted us to test whether RECQL4 is a component of Rad51 foci after the same treatment. In exponentially growing, untreated asynchronous WI38/VA13 cells, no Rad51 foci were observed (Fig. 5B, upper panel). This is in agreement with previous studies, which showed that Rad51 foci are detectable only in S phase and/or after induction of DSBs (Tashiro et al., 1996; Thompson and Schild, 2001). However, after we treated the cells with etoposide, the percentage of cells with focally concentrated Rad51 increased. We found that in 43% of these cells, 29% of Rad51 foci colocalized with RECQL4 foci and 10% of RECQL4 foci colocalized with Rad51 foci, indicating that at least a portion of RECQL4 nuclear foci is recruited to sites of DNA-damage-induced ssDNA (Fig. 5B, lower panel). Similar results were obtained with HeLa cells and primary skin fibroblast cells after exposure to etoposide (data not shown). Additionally, in etoposide-treated HeLa cells transfected with RECQL4-1 siRNA, but not in cells transfected with the control siRNA, there was a significant reduction in the formation of RECQL4 foci and thus no colocalization of RECQL4 with Rad51 (supplementary material Fig. S2).

We next analysed whether RECQL4 and Rad51 interact in human cells using a co-immunoprecipitation assay. To that end, the FLAG-RECQL4 was transiently transfected into 293T cells. Nuclear extracts were then immunoprecipitated with anti-FLAG resin and analysed by immunoblotting using the anti-Rad51 antibody. As can be seen in the left panel of Fig. 5C, endogenous Rad51 was efficiently co-precipitated by the anti-FLAG antibody (lane 3), but was not detected when the control IgG antibody was used (lane 2). The reciprocal co-immunoprecipitation experiment was also carried out with an anti-Rad51 polyclonal antibody, to immunoprecipitate FLAG-RECQL4 from 293T nuclear extracts. As shown in the right panel of Fig. 5C, RECQL4 could be specifically co-immunoprecipitated with endogenous anti-Rad51 (lane 6), but not with the control IgG antibody (lane 5). Taken together, these data indicate that RECQL4 and Rad51 form a complex in human cells and that, in response to the induction of DSBs, a portion of RECQL4 and Rad51 nuclear foci colocalize to sites that represent sites of undergoing repair by homologous recombination.

BRCA1, a multifunctional protein with proposed roles in the repair of DSBs by homologous recombination, transcriptional activation, cell-cycle regulation and apoptosis (Narod and Foulkes, 2004), has been shown to colocalize with Rad51 in S-phase foci (Scully et al., 1997)

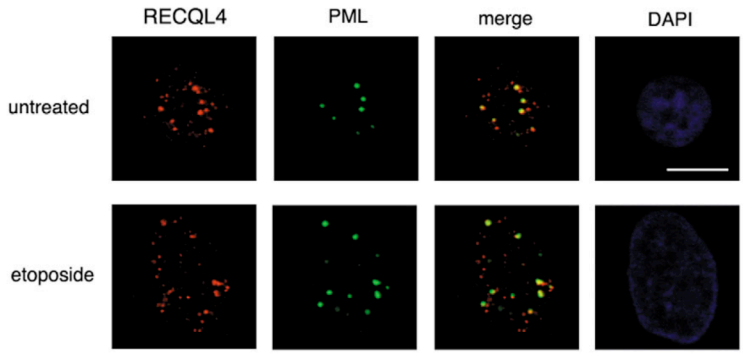

Fig. 4. RECQL4 colocalizes with PML. HeLa cells were stained with anti-RECQL4 (red) and anti-PML (green) antibodies. Where red and green signals overlap, a yellow pattern is seen, indicating colocalization of RECQL4 and PML. DAPI-staining shows nuclear DNA. Bar, ~10 μm. (Upper panel) Colocalization of RECQL4 and PML in untreated HeLa cells. (Lower panel) Colocalization of RECQL4 and PML after 10 μM etoposide treatment of HeLa cells.

and IR-inducible foci (Bhattacharyya et al., 2000). We therefore wanted to determine whether RECQL4 protein colocalizes with BRCA1, by performing double immunolabeling in untreated HeLa cells and cells treated with 10 μM etoposide. In contrast to the partial RECQL4/Rad51 colocalization, a very weak colocalization of RECQL4 with BRCA1 was observed (Fig. 5D). Namely, 2% of RECQL4 foci colocalized with BRCA1 foci and 5% of BRCA1 foci colocalized with RECQL4 foci, an observation made in only 11% of cells. We conclude from this result that RECQL4 foci differ from BLM foci, which colocalize with the BRCA1 protein (Jiao et al., 2004; Wang et al., 2000).

Discussion

Numerous genetic, biochemical and cell biological studies in yeast and human cells have suggested that the members of the RecQ helicase family play a pivotal role in maintaining genome stability (Hickson, 2003). Along with this notion, mutations in the *RECQL4* gene have been shown to cause some cases of the Rothmund-Thomson and RAPADILINO syndromes, which have severe physiological consequences in humans, the most prominent of which are cancer susceptibility and premature aging. At the cellular level, defects in *RECQL4* cause genome instability particularly trisomy, aneuploidy, deletions, translocations and high frequencies of chromosomal rearrangements. Despite this knowledge, the molecular function of RECQL4, as well as the cellular pathways in which it is involved, remain poorly understood. In the current study, we have shown for the first time that endogenous RECQL4 localizes to distinct nuclear foci in various human cell lines. This nuclear foci staining pattern is specific for RECQL4 because silencing of RECQL4 through RNA interference markedly decreases the RECQL4 nuclear foci formation. In contrast to previous studies involving BLM and WRN helicases, which have shown their presence in the nucleus (Bischof et al., 2001; Jiao et al., 2004; Pedrazzi et al., 2001; Sakamoto et al., 2001; Yankiwski et al., 2000), our cellular fractionation experiments showed that, although a majority of RECQL4 is present in the nucleus, a small amount of it can be found in the cytosolic fraction of HeLa cell extracts. A similar result has also been recently reported by Yin and colleagues, who showed that the greater portion of RECQL4 protein is present in the cytosol compared to the nucleus of transformed human cells (Yin et al., 2004). At the present time, the precise role of such 'cytosolic RECQL4' is not known and remains to be determined. Our data that RECQL4 forms nuclear foci seemingly contrasts with the data of Yin and colleagues, who reported that RECQL4 is present in both the cytoplasm and the nucleus of human cells, with a punctate and uniform distribution of RECQL4 in both compartments (Yin et al., 2004). These differences are probably the result of different cell fixation approaches and antibodies that have been employed in these two studies.

Furthermore, we have provided evidence that the number of RECQL4 foci does not significantly change upon cellular treatment with different DNA damaging agents including IR, UV light and HU. Interestingly, these data differ from those obtained for BLM and WRN helicases, and may thus suggest that RECQL4 has a different function in human cells. Namely, previous studies have shown that BLM assembles into nuclear foci specifically in response to agents that cause DNA DSBs (Bischof et al., 2001; Davalos and Campisi, 2003) and block replication (Jiao et al., 2004; Sengupta et al., 2004). However, WRN was shown to traffic between the nucleolus and nucleoplasm, and to form nuclear foci in response to treating cells with various DNA-damaging agents (Gray et al., 1998; Sakamoto et al., 2001).

We have also found that a portion of RECQL4 foci colocalizes with PML NBs in untreated human cells. PML NBs have been shown to be the sites of BLM, RAD51, MRE11 and p53 assembly during late S-G2 phase and following the induction of DSBs (Bischof et al., 2001; Carbone et al., 2002). It has therefore been suggested that these foci represent sites of presumptive homologous recombinational repair after induction of DSBs (Bischof et al., 2001). Given the fact that a portion of RECQL4 foci colocalizes with PML NBs, our findings suggest that RECQL4 plays an active role in DSB repair. Furthermore, we have observed a slight decrease in the number of RECQL4- and PML-colocalizing foci after treatment of cells with the DSB-inducing agent etoposide. Similarly to this observation, it has recently been reported that, BLM helicase relocalizes from PML NBs after replication stall due to HU treatment (Davalos et al., 2004). Thus, our results also suggest that RECQL4 leaves PML foci and, after induction of DNA damage, relocalizes in a similar manner as BLM. In other words, there are different pools of RECQL4 foci in the cell that have a different function after induction of DNA damage.

We have also demonstrated that RECQL4 is a component of

Journal of Cell Science

a portion of Rad51 foci that is thought to be crucial for the repair of DSBs by homologous recombination. We found that RECQL4 forms a complex with Rad51 in human cells and partially colocalizes with Rad51 and regions of ssDNA after induction of DSBs. Nuclear foci containing the Rad51 protein were shown to include other recombination proteins, such as Rad52, Rad54, the single-strand-binding-protein RPA, and the tumor suppressors BRCA1 and BRCA2 (Tarsounas et al., 2004). Given the fact that the processing of DSBs frequently involves the formation of long 3′ single-stranded regions and that Rad51 is tightly associated with these structures in vivo, which promote pairing and strand-exchange between ssDNA and homologous dsDNA (Raderschall et al., 2002; Raderschall et al., 1999), one possible interpretation of the RECQL4/Rad51 complex formation, and RECQL4/PML as well as RECQL4/Rad51 colocalization is that, these structures represent the physical sites where the repair of DSBs by homologous recombination is coordinated and monitored. In agreement with this observation it has previously been shown that cultured cells from RTS patients are sensitive to IR, which further suggests that RECQL4 might participate in DSB repair (Vennos and James, 1995). However, it should be noticed that, it remains to be determined whether RECQL4 has a direct or indirect role in DSB

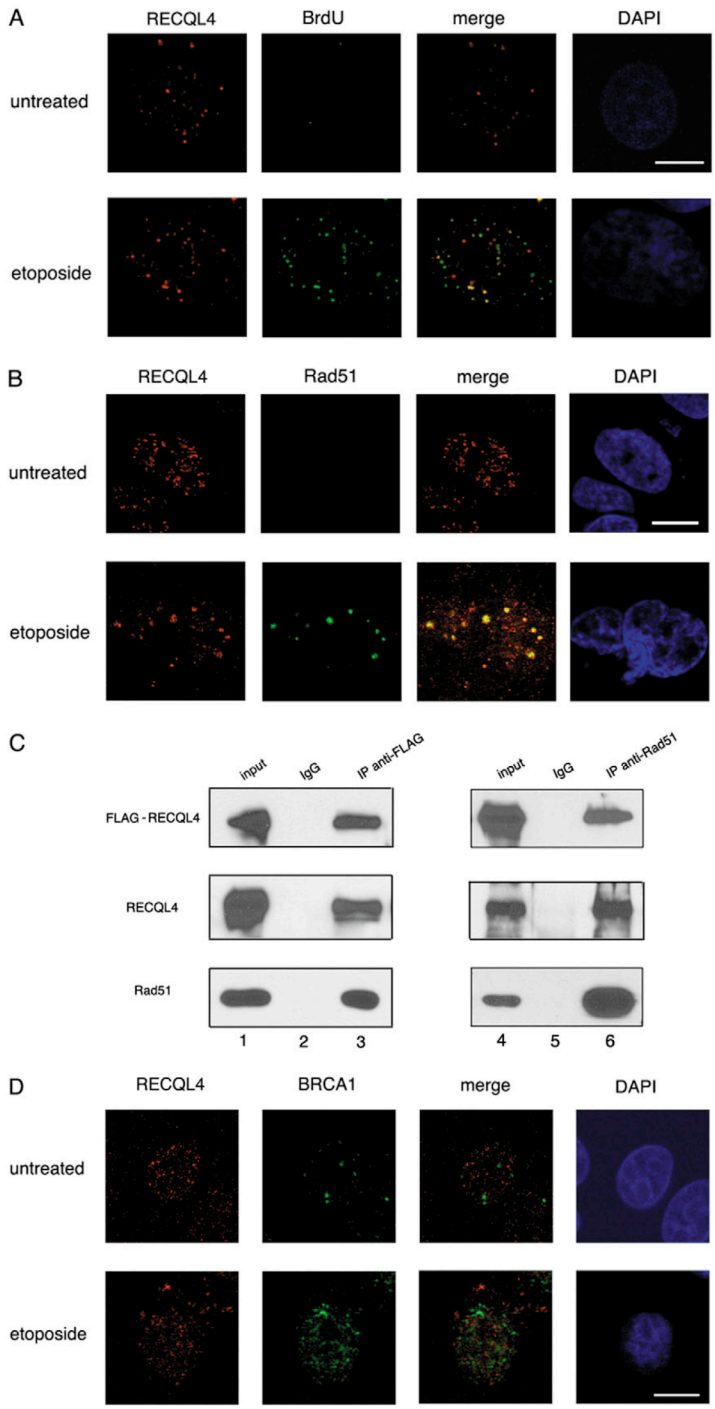

Fig. 5. RECQL4 is associated with regions of ssDNA and colocalizes with Rad51, but it does not colocalize with BRCA1. (A) HeLa cells were grown in BrdU-containing medium and stained for RECQL4 (red), BrdU (green) and nuclear DNA (blue). Bar, ~10 μm. (Upper panel) RecQL4 and BrdU staining in untreated cells. (Lower panel) RECQL4 colocalizes with ssDNA after treatment with 10 μM etoposide. (B) RECQL4 colocalizes with Rad51. WI38/VA13 cells were stained with anti-RECQL4 (red) and anti-Rad51 antibodies (green), and DAPI (blue). RECQL4 and Rad51 antibody-staining in untreated cells (upper panel) and after 10 μm etoposide treatment (lower panel). Bar, ~10 μm. (C) RECQL4 and Rad51 form a complex in human cells. 293T cells were transiently transfected with FLAG-RECQL4, nuclear extracts derived from these cells were immunoprecipitated with the anti-FLAG antibody, and analysed by SDS-polyacrylamide gel electrophoresis. One-tenth of the same nuclear extract was used as input control (lane 1). Immunoprecipitated FLAG-RECQL4 (upper and middle panels) and Rad51 (lower panel) were detected by western blotting with the anti-FLAG, anti-RECQL4 C-t and anti-Rad51 antibodies, but not with the control IgG (lane 2). Reciprocal co-immunoprecipitation is shown in lanes 4-6; lane 4, input; lane 5, immunoprecipitation with the control IgG; lane 6, immunoprecipitation with an anti-Rad51 antibody. (D) Colocalization of RECQL4 with BRCA1 in untreated HeLa cells (upper panel) and in HeLa cells treated with 10 μM etoposide (lower panel). RECQL4 (red), BRCA1 (green), DAPI-staining shows nuclear DNA. Bar, ~10 μm.

repair by homologous recombination. Similarly to BLM and WRN helicases, RECQL4's function could be to resolve aberant DNA structures that are formed during DNA replication and recombinational repair processes. Alternatively, RECQL4 could have a signalling function during the same processes through interactions with other proteins. Either hypothesis or a combination of the two would explain the genome instability displayed by RTS cells and the high incidence of cancer seen in RTS patients.

Our results also show that RECQL4 foci, unlike BLM foci, do not coincide with BRCA1 (Jiao et al., 2004). Previous work has revealed that BRCA1 colocalizes and resides in a so-called 'BASC' (BRCA1-associated genome surveillance complex) that consists of 40 different proteins, including BLM, RAD50, ATM, RAD50/MRE11/NBS1 complex, MSH6, MSH2, MLH1 and three subunits of the replication factor C (RFC) complex (namely p140, p37 and p34) (Wang et al., 2000). BLM and BRCA1 foci do not coincide in untreated human cells; however, their colocalization is greatly enhanced in those cells that are in mid-to-late S phase or in G2 phase after treatment with HU or IR, which suggests a specific requirement for BLM/BRCA1 in replication and/or repair of late-replicating DNA (Wang et al., 2000). In this way, our results imply that RECQL4 foci are distinct from the BLM foci, suggesting that RECQL4 does not participate in the same damage response pathway as BLM.

In conclusion, we have shown that endogenous human RECQL4 localizes to distinct nuclear foci that coincide with PML NBs, Rad51 and regions of ssDNA, suggesting that RECQL4 plays a role in the repair of DSBs by homologous recombination. Further confirmation of the above mentioned results will come from genetic, biochemical and protein-protein-interaction assays performed on RECQL4. These approaches, along with the cell biological approach described in this study, will ultimately help to understand the function of RECQL4 protein in human cells and to understand how genome instability influences cancer predisposition and aging.

We thank Silvio Hemmi for the gift of primary skin fibroblast cell line, Roland Kanaar for the gift of the anti-Rad51 antibody, Paul Hassa and Michael Hottiger for the gift of the anti-PARP1 antibody, Veronique Smits for the gift of the anti-GRB2 antibody, Ian Hickson for the gift of the anti-BLM antibody and Vilhelm Bohr, Michael Fetchko, Ian Hickson, Orlando Schärer, Caroline Zbinden and other members of the Stagljar group for helpful discussions. We are grateful to the Elektronenmikroskopisches Zentrallaboratorium der Universität Zürich for providing confocal facilities for this study. I.S.'s group is financed by grants from the Union Bank of Switzerland (im Auftrag eines Kunden), Gebert Rüf Foundation, EU Grant HPRN-CT-2002-00240, Schweizer Bundesamt für Bildung und Wissenschaft BBW Nr. 01-0528, the Swiss Cancer League (OCS-01310-02-2003) and the Swiss National Science Foundation (Nr. 3100A0-100256/1). R.F. is supported by the EU Grant HPRN-CT-2002-00240 and the GEN2003-20243-C08-07 from the Spanish Ministry of Education and Science.

References

Bhattacharyya, A., Ear, U. S., Koller, B. H., Weichselbaum, R. R. and Bishop, D. K. (2000). The breast cancer susceptibility gene BRCA1 is required for subnuclear assembly of Rad51 and survival following treatment with the DNA cross-linking agent cisplatin. *J. Biol. Chem.* **275**, 23899-23903.

Bischof, O., Kim, S. H., Irving, J., Beresten, S., Ellis, N. A. and Campisi, J. (2001). Regulation and localization of the Bloom syndrome protein in response to DNA damage. *J. Cell Biol.* **153**, 367-380.

Carbone, R., Pearson, M., Minucci, S. and Pelicci, P. G. (2002). PML NBs associate with the hMre11 complex and p53 at sites of irradiation induced DNA damage. *Oncogene* **21**, 1633-1640.

Davalos, A. R. and Campisi, J. (2003). Bloom syndrome cells undergo p53-dependent apoptosis and delayed assembly of BRCA1 and NBS1 repair complexes at stalled replication forks. *J. Cell Biol.* **162**, 1197-1209.

Davalos, A. R., Kaminker, P., Hansen, R. K. and Campisi, J. (2004). ATR and ATM-dependent movement of BLM helicase during replication stress ensures optimal ATM activation and 53BP1 focus formation. *Cell Cycle* **3**, 1579-1586.

Dellaire, G. and Bazett-Jones, D. P. (2004). PML nuclear bodies: dynamic sensors of DNA damage and cellular stress. *BioEssays* **26**, 963-977.

Der Kaloustian, V. M., McGill, J. J., Vekemans, M. and Kopelman, H. R. (1990). Clonal lines of aneuploid cells in Rothmund-Thomson syndrome. *Am. J. Med. Genet.* **37**, 336-339.

Ellis, N. A., Groden, J., Ye, T. Z., Straughen, J., Lennon, D. J., Ciocci, S., Proytcheva, M. and German, J. (1995). The Bloom's syndrome gene product is homologous to RecQ helicases. *Cell* **83**, 655-666.

Enoch, T., Carr, A. M. and Nurse, P. (1992). Fission yeast genes involved in coupling mitosis to completion of DNA replication. *Genes Dev.* **6**, 2035-2046.

Gangloff, S., McDonald, J. P., Bendixen, C., Arthur, L. and Rothstein, R. (1994). The yeast type I topoisomerase Top3 interacts with Sgs1, a DNA helicase homolog: a potential eukaryotic reverse gyrase. *Mol. Cell. Biol.* **14**, 8391-8398.

Gray, M. D., Wang, L., Youssoufian, H., Martin, G. M. and Oshima, J. (1998). Werner helicase is localized to transcriptionally active nucleoli of cycling cells. *Exp. Cell Res.* **242**, 487-494.

Hickson, I. D. (2003). RecQ helicases: caretakers of the genome. *Nat. Rev. Cancer* **3**, 169-178.

Hodges, M., Tissot, C., Howe, K., Grimwade, D. and Freemont, P. S. (1998). Structure, organization, and dynamics of promyelocytic leukemia protein nuclear bodies. *Am. J. Hum. Genet.* **63**, 297-304.

Hoki, Y., Araki, R., Fujimori, A., Ohhata, T., Koseki, H., Fukumura, R., Nakamura, M., Takahashi, H., Noda, Y., Kito, S. et al. (2003). Growth retardation and skin abnormalities of the Recql4-deficient mouse. *Hum. Mol. Genet.* **12**, 2293-2299.

Jam, K., Fox, M. and Crandall, B. F. (1999). RAPADILINO syndrome: a multiple malformation syndrome with radial and patellar aplasia. *Teratology* **60**, 37-38.

Jiao, R., Bachrati, C. Z., Pedrazzi, G., Kuster, P., Petkovic, M., Li, J. L., Egli, D., Hickson, I. D. and Stagljar, I. (2004). Physical and functional interaction between the Bloom's syndrome gene product and the largest subunit of chromatin assembly factor 1. *Mol. Cell. Biol.* **24**, 4710-4719.

Kitao, S., Ohsugi, I., Ichikawa, K., Goto, M., Furuichi, Y. and Shimamoto, A. (1998). Cloning of two new human helicase genes of the RecQ family: biological significance of multiple species in higher eukaryotes. *Genomics* **54**, 443-452.

Kitao, S., Lindor, N. M., Shiratori, M., Furuichi, Y. and Shimamoto, A. (1999a). Rothmund-thomson syndrome responsible gene, RECQL4: genomic structure and products. *Genomics* **61**, 268-276.

Kitao, S., Shimamoto, A., Goto, M., Miller, R. W., Smithson, W. A., Lindor, N. M. and Furuichi, Y. (1999b). Mutations in RECQL4 cause a subset of cases of Rothmund-Thomson syndrome. *Nat. Genet.* **22**, 82-84.

Lindor, N. M., Furuichi, Y., Kitao, S., Shimamoto, A., Arndt, C. and Jalal, S. (2000). Rothmund-Thomson syndrome due to RECQ4 helicase mutations: report and clinical and molecular comparisons with Bloom syndrome and Werner syndrome. *Am. J. Med. Genet.* **90**, 223-228.

Nakayama, H., Nakayama, K., Nakayama, R., Irino, N., Nakayama, Y. and Hanawalt, P. C. (1984). Isolation and genetic characterization of a thymineless death-resistant mutant of Escherichia coli K12: identification of a new mutation (recQ1) that blocks the RecF recombination pathway. *Mol. Gen. Genet.* **195**, 474-480.

Narod, S. A. and Foulkes, W. D. (2004). BRCA1 and BRCA2: 1994 and beyond. *Nat. Rev. Cancer* **4**, 665-676.

Pedrazzi, G., Perrera, C., Blaser, H., Kuster, P., Marra, G., Freire, R., Ryu, G.-H., Jiricny, J. and Stagljar, I. (2001). Direct association of Bloom's syndrome gene product with the human mismatch repair protein MLH1. *Nucleic Acids Res.* **29**, 4378-4386.

Petrilli, V., Herceg, Z., Hassa, P. O., Patel, N. S., Di Paola, R., Cortes, U., Dugo, L., Filipe, H. M., Thiemermann, C., Hottiger, M. O. et al. (2004). Noncleavable poly(ADP-ribose) polymerase-1 regulates the inflammation response in mice. *J. Clin. Invest.* **114**, 1072-1081.

Puranam, K. L. and Blackshear, P. J. (1994). Cloning and characterization of RECQL, a potential human homologue of the Escherichia coli DNA helicase RecQ. *J. Biol. Chem.* **269**, 29838-29845.

Raderschall, E., Golub, E. I. and Haaf, T. (1999). Nuclear foci of mammalian recombination proteins are located at single-stranded DNA regions formed after DNA damage. *Proc. Natl. Acad. Sci. USA* **96**, 1921-1926.

Raderschall, E., Bazarov, A., Cao, J., Lurz, R., Smith, A., Mann, W., Ropers, H. H., Sedivy, J. M., Golub, E. I., Fritz, E. et al. (2002). Formation of higher-order nuclear Rad51 structures is functionally linked to p21 expression and protection from DNA damage-induced apoptosis. *J. Cell Sci.* **115**, 153-164.

Sakamoto, S., Nishikawa, K., Heo, S. J., Goto, M., Furuichi, Y. and Shimamoto, A. (2001). Werner helicase relocates into nuclear foci in response to DNA damaging agents and co-localizes with RPA and Rad51. *Genes Cells* **6**, 421-430.

Scully, R., Chen, J., Ochs, R. L., Keegan, K., Hoekstra, M., Feunteun, J. and Livingston, D. M. (1997). Dynamic changes of BRCA1 subnuclear location and phosphorylation state are initiated by DNA damage. *Cell* **90**, 425-435.

Seki, M., Miyazawa, H., Tada, S., Yanagisawa, J., Yamaoka, T., Hoshino, S., Ozawa, K., Eki, T., Nogami, M., Okumura, K. et al. (1994). Molecular cloning of cDNA encoding human DNA helicase Q1 which has homology to Escherichia coli Rec Q helicase and localization of the gene at chromosome 12p12. *Nucleic Acids Res.* **22**, 4566-4573.

Sengupta, S., Robles, A. I., Linke, S. P., Sinogeeva, N. I., Zhang, R., Pedeux, R., Ward, I. M., Celeste, A., Nussenzweig, A., Chen, J. et al. (2004). Functional interaction between BLM helicase and 53BP1 in a Chk1-mediated pathway during S-phase arrest. *J. Cell Biol.* **166**, 801-813.

Sengupta, S., Shimamoto, A., Koshiji, M., Pedeux, R., Rusin, M., Spillare, E. A., Shen, J. C., Huang, L. E., Lindor, N. M., Furuichi, Y. et al. (2005). Tumor suppressor p53 represses transcription of RECQ4 helicase. *Oncogene* **24**, 1738-1748.

Siitonen, H. A., Kopra, O., Kaariainen, H., Haravuori, H., Winter, R. M., Saamanen, A. M., Peltonen, L. and Kestila, M. (2003). Molecular defect of RAPADILINO syndrome expands the phenotype spectrum of RECQL diseases. *Hum. Mol. Genet.* **12**, 2837-2844.

Singleton, M. R. and Wigley, D. B. (2002). Modularity and specialization in superfamily 1 and 2 helicases. *J. Bacteriol.* **184**, 1819-1826.

Tan, T. L., Essers, J., Citterio, E., Swagemakers, S. M., de Wit, J., Benson, F. E., Hoeijmakers, J. H. and Kanaar, R. (1999). Mouse Rad54 affects DNA conformation and DNA-damage-induced Rad51 foci formation. *Curr. Biol.* **9**, 325-328.

Tarsounas, M., Davies, A. A. and West, S. C. (2004). RAD51 localization and activation following DNA damage. *Philos. Trans. R. Soc London Ser. B* **359**, 87-93.

Tashiro, S., Kotomura, N., Shinohara, A., Tanaka, K., Ueda, K. and Kamada, N. (1996). S phase specific formation of the human Rad51 protein nuclear foci in lymphocytes. *Oncogene* **12**, 2165-2170.

Thompson, L. H. and Schild, D. (2001). Homologous recombinational repair of DNA ensures mammalian chromosome stability. *Mutat. Res.* **477**, 131-153.

Vennos, E. M. and James, W. D. (1995). Rothmund-Thomson syndrome. *Dermatol. Clin.* **13**, 143-150.

Wang, L. L., Gannavarapu, A., Kozinetz, C. A., Levy, M. L., Lewis, R. A., Chintagumpala, M. M., Ruiz-Maldanado, R., Contreras-Ruiz, J., Cunniff, C., Erickson, R. P. et al. (2003). Association between osteosarcoma and deleterious mutations in the RECQL4 gene in Rothmund-Thomson syndrome. *J. Natl. Cancer Inst.* **95**, 669-674.

Wang, Y., Cortez, D., Yazdi, P., Neff, N., Elledge, S. J. and Qin, J. (2000). BASC, a super complex of BRCA1-associated proteins involved in the recognition and repair of aberrant DNA structures. *Genes Dev.* **14**, 927-939.

Wu, L., Davies, S. L., North, P. S., Goulaouic, H., Riou, J. F., Turley, H., Gatter, K. C. and Hickson, I. D. (2000). The Bloom's syndrome gene product interacts with topoisomerase III. *J. Biol. Chem.* **275**, 9636-9644.

Yankiwski, V., Marciniak, R. A., Guarente, L. and Neff, N. F. (2000). Nuclear structure in normal and Bloom syndrome cells. *Proc. Natl. Acad. Sci. USA* **97**, 5214-5219.

Yin, J., Tae Kwon, Y., Varshavsky, A. and Wang, W. (2004). RECQL4, mutated in the Rothmund-Thomson and RAPADILINO syndromes, interacts with ubiquitin ligases UBR1 and UBR2 of the N-end rule pathway. *Hum Mol Genet.* **13**, 2421-2430.

Yu, C. E., Oshima, J., Fu, Y. H., Wijsman, E. M., Hisama, F., Alisch, R., Matthews, S., Nakura, J., Miki, T., Ouais, S. et al. (1996). Positional cloning of the Werner's syndrome gene. *Science* **272**, 258-262.

Zhong, S., Hu, P., Ye, T. Z., Stan, R., Ellis, N. A. and Pandolfi, P. P. (1999). A role for PML and the nuclear body in genomic stability. *Oncogene* **18**, 7941-7947.

Journal of Cell Science

Article II

The molecular role of the Rothmund-Thomson-, RAPADILINO- and Baller-Gerold-gene product, RECQL4: recent progress.

Tobias Dietschy, Igor Shevelev and Igor Stagljar

Cell. Mol. Life Sci. *64, 796 – 802*

In this review article, I have done the organization and the writing.

Cell. Mol. Life Sci. 64 (2007) 796 – 802
1420-682X/07/070796-7
DOI 10.1007/s00018-007-6468-5

Cellular and Molecular Life Sciences

Visions & Reflections (Minireview)

The molecular role of the Rothmund-Thomson-, RAPADILINO- and Baller-Gerold-gene product, RECQL4: recent progress

T. Dietschy, I. Shevelev and I. Stagljar*

Terrence Donnelly Centre for Cellular and Biomolecular Research (CCBR), Department of Biochemistry and Department of Medical Genetics and Microbiology, Faculty of Medicine, University of Toronto, 160 College Street, Toronto, Ontario, M5S 3E1 (Canada), Fax: +1 416 978 82 87; e-mail: igor.stagljar@utoronto.ca

Received 31 October 2006; received after revision 4 January 2007; accepted 5 February 2007
Online First 15 March 2007

Abstract. The RecQ family of DNA helicases is highly conserved throughout evolution and plays an important role in the maintenance of genomic stability in all organisms. Mutations in three of the five known family members in humans, *BLM, WRN* and *RECQL4*, give rise to disorders that are characterized by predisposition to cancer and premature aging, emphasizing the importance of studying the RecQ proteins and their cellular activities. Interestingly, three autosomal recessive disorders have been associated with mutations in the *RECQL4* gene: Rothmund-Thomson, RAPADILINO, and Baller-Gerold syndromes, thus making RECQL4 unique within the RecQ family of DNA helicases. To date, however, the molecular function of RECQL4 and the possible cellular pathways in which it is involved remain poorly understood. Here, we present an overview of recent findings in connection with RECQL4 and try to highlight different directions the field could head, helping to clarify the role of RECQL4 in preventing tumorigenesis and maintenance of genome integrity in humans.

Keywords. Genome stability, cancer, RecQ helicases, RECQL4, Rothmund-Thomson syndrome, RAPADILINO syndrome, Baller-Gerold syndrome.

Introduction

The maintenance of the genetic material (so called 'genome stability') is an essential process in every living organism, and the failure of this process can lead to the development and progression of cancer. If we are to understand the causes of genome instability in humans, we must first understand the function of proteins that normally act to keep the genetic material intact. One family of proteins required to maintain genome stability is the RecQ helicase family [1]. Five human RecQ homologues, called RECQL1, BLM, WRN, RECQL4, and RECQL5, have been identified so far, and three of them have been shown to be associated with five autosomal recessive disorders characterized by genomic instability and cancer predisposition. Werner syndrome (WS), linked to a defect in the WRN protein, is characterized by the appearance of unusually accelerated aging (progeria) [2]. Bloom syndrome (BS), which is associated with a defect in the BLM protein, is characterized by stunted

* Corresponding author.

growth, developmental problems, immunodeficiency, male infertility and, at the cellular level, a slowing of S-phase progression and a dramatic increase in sister chromatid exchange and genomic instability [3]. Interestingly, three different human disorders have been associated with mutations in the *RECQL4* gene: Rothmund-Thomson (RTS), RAPADILINO and Baller-Gerold (BGS) syndromes [4–6]. Below, we review the recent findings and highlight the importance of studying RECQL4 in order to understand its role in the maintenance of genome stability in humans.

RECQL4 and genetic diseases

RTS was originally described in 1868 by the German ophthalmologist Rothmund [7] and subsequently confirmed by the English dermatologist Thomson in 1936 [8]. It is an unusual autosomal recessive condition associating poikiloderma, growth deficiency, juvenile cataracts, premature aging and a predisposition to malignant tumours, particularly osteosarcomas [9]. Despite its long history, only about 300 cases of RTS have been reported in the scientific literature thus far [9, 10]. Interestingly, mutations in the *RECQL4* gene cause only 60% of all RTS cases [11]. Accordingly, RTS seems to be a heterogeneous disease and mutations in other, yet unidentified, gene(s) seem to be responsible for the phenotype of the remaining 40% of RTS patients. The number of mutations found in *RECQL4* is quite low, ranging from nonsense, frameshift and splice site mutations to intronic insertions and deletions [5]. Most of these mutations result in premature termination of protein translation and truncated RECQL4 proteins that often lack a large part of the helicase domain [12]. Cells derived from RTS patients show genomic instability, including trisomy, aneuploidy and chromosomal rearrangements [9, 13]. Additionally, RTS cells are sensitive to ionizing radiation and oxidative stress/damage [14, 15].

Another autosomal recessive disease associated with mutations in the *RECQL4* gene is RAPADILINO syndrome [5]. The syndrome was originally described in 14 patients from Finland. To date, three additional cases of RAPADILINO syndrome have been reported [5]. The acronym stands for the characteristic clinical features: RAdial hypo-/aplasia, Patellae hypo-/aplasia and cleft or highly arched PAlate, DIarrhoea and DIslocated joints, LIttle size and LImb malformation, NOse slender and NOrmal intelligence. The most common mutations of the *RECQL4* gene in RAPADILINO patients represent in-frame deletions of exon 7 which do not affect the helicase domain of RECQL4 protein [5]. Although RAPADILINO patients share some clinical features with RTS patients, like photosensitivity with extra pigmentation of skin, or growth deficiency, there are unique diagnostic findings such as joint dislocations and patellar hypo/aplasia. In contrast to RTS, RADADILINO is more common in females, and only 7% of current RAPADILINO patients carry malignant tumors, mainly osteosarcomas [16].

BGS, originally discovered in 1950 [17], is the third recently reported autosomal recessive disorder linked to mutations in the *RECQL4* gene [6]. Approximately 20 cases of BGS have been reported in the scientific literature thus far [6]. The clinical hallmarks of BGS are radial aplasia/hypoplasia and craniosynostosis. To date, most mutations of *RECQL4* found in BGS patients represent an R1021W missense mutation and a 2886 delta T frameshift mutation of exon 9. Surprisingly, none of the 24 BGS patients reported so far show any predisposition for cancer [6]. Thus, the cumulative set of data suggests that RECQL4 has roles independent of helicase activity. Whether the role of the RECQL4 N-terminal domain is independent of the helicase domain, or whether it is sufficient to perform a partial function remains to be elucidated in future experiments.

Further studies are needed to characterize different symptoms and evaluate whether the three *RECQL4* associated diseases are separate disorders or whether it would be more appropriate to combine them under a new name. Furthermore, the identification of *RECQL4* mutations and their effects on the *RECQL4* transcript is of particular importance. It will therefore be interesting to test whether certain mutations always lead to distinct phenotypes or whether the correlation is more complex. In addition, investigating the genetic causes of RTS, RAPADILINO and BGS that have arisen due to mutations in proteins other than RECQL4 might help to identify additional genes/proteins involved in the same pathway(s).

RECQL4 mouse models

In 2002, the Furuichi group created the first *RECQL4* knockout mouse model [18]. These mice were embryonic lethal, showing severe proliferation defects and therefore could not be used as a model for RTS. One year later, the Kito group generated another *RECQL4* knockout mouse model by deleting exon 13 of the *RECQL4* gene, which encodes part of the central RecQ-helicase domain. Exon 13 is a hot spot for mutations identified in RTS patients [19]. This *RECQL4*-deficient mouse showed severe growth retardation and several tissue abnormalities that

resemble those of RTS patients. Additionally, the proliferation rate of Mouse Embryonic Fibroblasts (MEFs) derived from this *RECQL4*-deficient mouse was decreased. Even though no poikiloderma was observed, other epidermal symptoms such as brittle skin, hair loss and hair color loss were noticed. These mice had hypoplasia of the epidermis, dermis and subcutaneous tissue. Only 5% of the mutant mice survived the first 14 days, and these mice failed to develop malignancies, a unique characteristic of RTS [19].

One year ago, the Luo group generated the third RECQL4 knockout mouse by deleting the *RECQL4* coding region, including exons 9–13 [20]. 84% of all homozygous *RECQL4*$^{-/-}$ progeny survived to adulthood, with some exhibiting typical clinical features of RTS, such as hypo-/hyperpigmented skin, skeletal limb defects and palatal patterning defects. Furthermore, chromosomal analysis using different cell types derived from this *RECQL4*-deficient mouse displayed an overall aneuploid phenotype and a significant increase in the frequency of premature centromere separation, suggesting that this *RECQL4*$^{-/-}$ mouse is a good model for human RTS [20]. In summary, deletion of exon 13 resulted in only 5% survival of the mice, while deletion of exons 9–13 resulted in 84% survival. It seems that the protein remaining after the 9–13 exon deletion appears to be more functional than the protein remaining after deletion of exon 13. This effect might be due to misfolding of the RECQL4 protein after deletion of exon 13, but not after exon 9–13 deletion, which may result in a more stable mutant RECQL4 protein.

Taken together, the results derived from experiments with various *RECQL4*$^{-/-}$ mice showed that these mice accumulate defects that clearly reflect the situation in humans, i.e. different mutations in the *RECQL4* gene lead to different phenotypes. It would therefore be of particular interest to investigate whether the genotype-phenotype correlations seen in humans could be observed in mice by mimicking mutations causing RAPADILINO and BGS syndromes and whether systematic mutation of particular regions of the *RECQL4* gene could be made in cell lines or in other mouse models.

RECQL4 in the context of DNA replication

In the past 2 years, analyses of RECQL4 in *Xenopus laevis* have indicated an interesting novel role for RECQL4 in the initiation of DNA replication. The *Xenopus laevis* RECQL4 protein (xRTS) is 60% identical to human RECQL4 and shares the central helicase domain common among all RecQ family members. The N-terminal region of xRTS shows 20% identity to two yeast proteins, Sld2 and Drc1, which are both required for the establishment of replication forks [21–23]. This feature makes xRTS unique among the members of the RecQ family. The Venkitaraman lab showed that immunodepletion of xRTS from *Xenopus laevis* egg extracts leads to reduction and delay of sperm chromatin replication, an effect that can be rescued by complementing the extracts with the purified recombinant wild-type human RECQL4 [24]. These findings were recently confirmed by the Takisawa group, showing that purified N-terminal fragments of xRTS were able to rescue the DNA replication activity of RECQL4-depleted *Xenopus laevis* egg extracts [25]. Accordingly, by knocking down the murine homologue of xRTS with small hairpin RNA (shRNA) in primary MEFs, the proliferation rate and DNA replication of these primary cells was highly perturbed. Together, these results suggest that RECQL4 has a role in DNA replication and that this function is conserved during evolution.

RECQL4-interacting partners

Several attempts have been made thus far to identify proteins that associate with RECQL4. Recent studies in the Wang group have revealed that RECQL4 isolated from HeLa cells is found in a complex with UBR1 and UBR2 [26]. These two 200-kDa proteins share high sequence similarities to each other and belong to the family of E3 ubiquitin ligases of the N-end rule pathway, which is part of the ubiquitin-proteasome system [27]. The N-end rule pathway exists in all organisms examined, from mammals to fungi and bacteria. In eukaryotes it is part of the ubiquitin system. By the action of the three ubiquitin-ligases (E1, E2 and E3), a substrate protein is polyubiquitylated and subsequently degraded by the 26S proteasome [27]. Surprisingly, the Wang group found that RECQL4 is not ubiquitylated *in vivo*. In addition, newly synthesized RECQL4 was shown to be a stable protein (half-life of 2 h), and the level of RECQL4 protein was not increased by inhibiting the proteasome with different drugs. Despite these discoveries, the functionality of the physical interaction between RECQL4 and UBR1/UBR2 remains unknown, and further investigations are needed to elucidate a novel function of ubiquitin ligases in the maintenance of genome stability. For example, it would be interesting to investigate RECQL4 function in cells derived from Johanson-Blizzard syndrome patients, which are deficient in UBR1 protein.

Our group found that RECQL4 is in a complex with Rad51 *in vivo* [28]. It has previously been reported

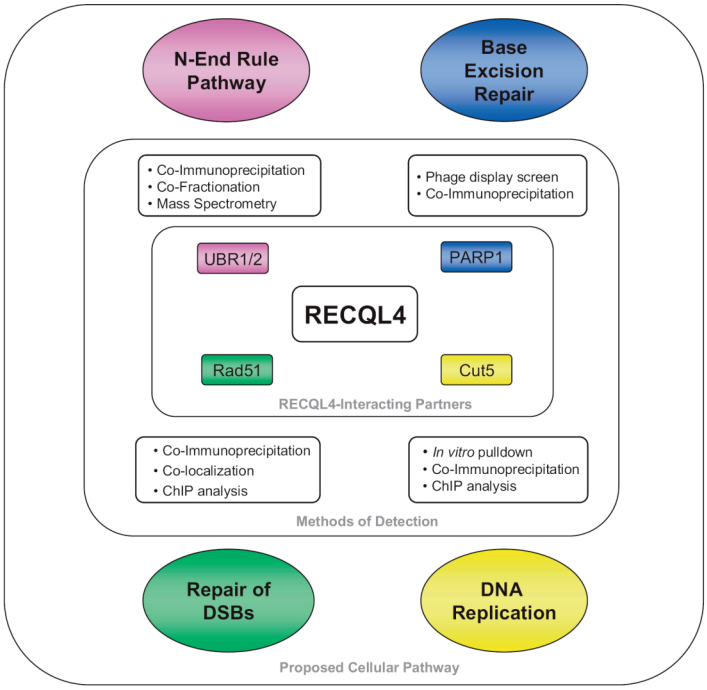

Figure 1. Schematic representation of cellular pathways RECQL4 may be involved in: different RECQL4-interacting partners and corresponding methods of detection.

that Rad51 foci, which are important for DNA repair by homologous recombination, accumulate at sites of single-stranded DNA after induction of DNA double strand breaks (DSBs) [29]. In response to the induction of DSBs by treatment with etoposide, a portion of RECQL4 and Rad51 nuclear foci colocalized, suggesting that RECQL4 plays a role in the repair of DSBs by homologous recombination [28]. The precise role of RECQL4 in DSB repair via its interaction with Rad51 is currently being investigated in our lab.

Recently, Cut5 was shown to interact with the *Xenopus laevis* homologue of RECQL4 both *in vitro* and *in vivo* [25]. Cut5, the metazoan homologue of *Saccharomyces cerevisiae* Dpb11, is required for loading DNA polymerases onto chromatin [30, 31]. As mentioned above, the N-terminus of RECQL4 has similarity to Sld2 ('synthetically lethal with *dpb11*'), one of six Sld family members found to interact with Dpb11 [32]. Thus, these findings provide additional evidence that RECQL4 functions during DNA replication.

The Frank group reported the physical interaction between RECQL4 and poly(ADP-ribose) polymerase-1 (PARP-1) [33]. PARP-1 is involved in different pathways of DNA metabolism, such as recombination, repair and transcriptional regulation [34]. Additionally, PARP-1 is part of the base excision repair (BER) pathway and is activated in response to DNA breaks [35]. The authors showed complex formation between RECQL4 and PARP-1 *in vitro* and *in vivo*. Additionally, PARP-1 was able to poly(ADP-ribosyl)ate RECQL4 *in vitro* [33]. Therefore, RECQL4 might be among a large spectrum of proteins whose deficiencies induce cellular sensitivity to the inhibition of poly(ADP-ribose) polymerase activity. However, the functional relevance of this posttranslational modification of RECQL4 has to be confirmed by further *in vitro* and *in vivo* experiments. For example, it would be interesting to test whether various RTS cells show deficiency in the PARP1 poly(ADP-ribosyl)ation pathway after exposure to DNA damaging agents like hydrogen peroxide (H_2O_2) or methyl methanesulfonate (MMS).

In summary, the current data from several different protein interaction assays indicate that RECQL4 is involved in DNA repair and replication processes (Fig. 1). However, further functional studies are needed to characterize in more detail the exact role of RECQL4 in these processes, as well as to identify additional RECQL4-interacting proteins in order to draw a more precise picture of the exact cellular pathways RECQL4 might be involved in. Finally, it will be important to determine whether RECQL4 interacts with multiple protein partners simultaneously or independently in different pathways.

The extended N- and C-terminal domains of all RecQ helicases studied so far show very little sequence identity and are therefore thought to confer specificity to these proteins by mediating protein-protein interactions [1]. For this reason, N- and C-terminal fragments of RECQL4 could be used as bait in a yeast two-hybrid screen in order to find novel RECQL4-interacting partners. On the other hand, different RECQL4-specific antibodies have been raised in the last couple of years that could be used to co-immunoprecipitate RECQL4-interacting partners from mammalian cells extracts, followed by mass spectrometry analysis.

Subcellular localization of RECQL4

Four different groups have examined the subcellular localization of RECQL4 in different mammalian cells, and their observations are contradictory. The Furuichi group overexpressed full-length FLAG-tagged RECQL4 in HeLa cells, and immunofluorescence analysis suggested that RECQL4 is localized exclusively to the nucleus [11]. In 2004, the Wang group extensively studied the subcellular localization of RECQL4 using different cell types and three polyclonal anti-RECQL4 antibodies [26]. Western blot analysis of HeLa, MCF7 and Jurkat cell extracts revealed that RECQL4 was found predominantly in the cytoplasm, while indirect immunofluorescence experiments using HeLa cells found RECQL4 localization to both the nucleus and the cytoplasm. In contrast, RECQL4 was largely present in the nuclear fraction of untransformed WI-38 fibroblasts.

Our group raised two antibodies, against the N- and C-termini of RECQL4, and used them in immunofluorescence experiments on several exponentially growing human cell lines. Although we found that the majority of RECQL4 protein is detected in the nucleus, a small amount of it was found in the cytosolic fraction of HeLa cell extracts [28]. Furthermore, we found that endogenous RECQL4 localized exclusively in discrete nuclear foci in HeLa, WI-38/VA13 and primary skin fibroblast cells, and that the number of these does not significantly change during the cell cycle or upon the induction of DNA DSBs. We found that RECQL4 foci partially coincide with those formed by promyelocytic leukemia (PML) bodies and Rad51 as well as with regions of single-stranded DNA (ssDNA) upon induction of DSBs. PML bodies and Rad51 foci have been shown to regulate the response to, and repair, of DSBs [36, 37]. These findings suggested a role for RECQL4 in the repair of DSBs by homologous recombination (HR) and indicated a completely novel function for RECQL4 in human cells [28]. The data from our group suggests that RECQL4 forms nuclear foci and that this is contradictory to the findings by Yin et al., who showed uniform distribution of RECQL4 in both the cytoplasm and the nucleus of human cells [26, 28]. These discrepancies can be explained by the use of different fixation methods and antibodies. The immunofluorescence method that we used results in the elimination of all RECQL4 that is not bound to the nuclear matrix, and this may not be the case for other techniques [28]. Very recently, the Frank group investigated the localization of RECQL4 in living cells by fusing EGFP to the N-terminus of the RECQL4 sequence [33]. RECQL4 displayed nucleoplasmic staining in most of the cells examined, and no significant cytoplasmic staining was observed. Using EGFP fused to different deletion mutants of RECQL4, the authors further characterized the RECQL4-domain structure. Their data suggest that RECQL4 contains at least two N-terminal nuclear localization signals (NLSs) and one nucleolar localization signal (NOS) spanning amino acids 376–386. Furthermore, RECQL4 nucleolar enrichment was observed after treating cells with H_2O_2 or streptonigrin, which leads to oxidative damage of DNA. Interestingly, RECQL4 localization did not change after treating cells with other DNA damage agents such as γ irradiation, etoposide, bleomycin, or UV irradiation [33].

Biochemical properties of the RECQL4 Protein

Compared with all other human RecQ family members, the biochemical properties of the RECQL4 protein are thus far only poorly understood. This is mainly due to the inability to purify the RECQL4 protein. Many groups, including ours, have attempted to purify full-length RECQL4 protein using different expression systems, but all efforts resulted in production of truncated RECQL4 protein. Consequently, the first enzymatic activity assays were performed by the Wang group, with immunoprecipitated RECQL4 protein from HeLa cell extracts [26]. RECQL4 coupled to protein-A sepharose beads showed DNA-dependent ATPase activity; however, RECQL4 failed to unwind any of the tested DNA substrates, although BLM helicase purified by the same way possessed DNA helicase and translocase activity.

One year ago, the Sung group purified full-length RECQL4 protein from *Escherichia coli* [38]. Although the yield of purified RECQL4 protein was low, the authors found that this RECQL4 has no detectable helicase activity, but possesses ssDNA-stimulated ATPase activity. In addition, the authors showed that

RECQL4 binds to ssDNA, an effect that could be inhibited by the ssDNA binding protein RPA [38]. Taken together, the current studies indicate that RECQL4 is not an active helicase; however, it still remains possible that RECQL4 needs a co-activator protein(s) and/or a particular post-translational modification(s) in order to accomplish a DNA unwinding function. To this end, it would be interesting to test whether RECQL4 purified from mammalian or insect cells possesses helicase activity.

Conclusions and future directions

The RecQ helicases have received a considerable amount of attention during the past 15 years, primarily owing to their link with premature aging and cancer susceptibility syndromes. While most of the studies involving human RecQ helicase members have thus far been performed on BLM and WRN helicases, only in the past 2 years have we seen increased interest in RECQL4. Although RTS, RAPADILINO and BGS syndromes caused by mutations in RECQL4 are rare (i.e. they currently affect ~400 individuals in total), it will be interesting to figure out how faulty RECQL4 hinders the normal process of DNA repair and replication, and how defects in these processes lead to such a broad spectrum of clinical features, as observed in RTS, RAPADILINO and BGS patients [39, 40]. There are many questions to be answered, and it is certain that new data regarding the identification of RECQL4-interacting partners, determination of RECQL4's post-translational modifications as well as its precise role during DNA metabolism will be forthcoming in the near future.

Acknowledgments. We thank Grant Brown and Tania Roberts for valuable comments on the manuscript. The Stagljar group is supported by grants from the Canadian Government, Canadian Foundation for Innovation, Canadian Institute for Health Research, Genome Canada and the Ontario Genomics Institute, Gebert Rüf Foundation, Novartis, and the Swiss Cancer League (OCS-01310–02–2003).

1 Hickson, I. D. (2003) RecQ helicases: caretakers of the genome. Nat. Rev. Cancer 3, 169 – 178.
2 Yu, C. E., Oshima, J., Fu, Y. H., Wijsman, E. M., Hisama, F., Alisch, R., Matthews, S., Nakura, J., Miki, T., Ouais, S., Martin, G. M., Mulligan, J., and Schellenberg, G. D. (1996) Positional cloning of the Werner's syndrome gene. Science 272, 258 – 262.
3 Ellis, N. A., Groden, J., Ye, T. Z., Straughen, J., Lennon, D. J., Ciocci, S., Proytcheva, M., and German, J. (1995) The Bloom's syndrome gene product is homologous to RecQ helicases. Cell 83, 655 – 666.
4 Kitao, S., Shimamoto, A., Goto, M., Miller, R. W., Smithson, W. A., Lindor, N. M., and Furuichi, Y. (1999) Mutations in RECQL4 cause a subset of cases of Rothmund-Thomson syndrome. Nat. Genet. 22, 82 – 82.
5 Siitonen, H. A., Kopra, O., Kaariainen, H., Haravuori, H., Winter, R. M., Saamanen, A. M., Peltonen, L., and Kestila, M. (2003) Molecular defect of RAPADILINO syndrome expands the phenotype spectrum of RECQL diseases. Hum. Mol. Genet. 12, 2837 – 2844.
6 Van Maldergem, L., Siitonen, H. A., Jalkh, N., Chouery, E., De Roy, M., Delague, V., Muenke, M., Jabs, E. W., Cai, J., Wang, L. L., et al. (2006) Revisiting the craniosynostosis-radial ray hypoplasia association: Baller-Gerold syndrome caused by mutations in the RECQL4 gene. J. Med. Genet. 43, 148 – 152.
7 Rothmund, A. (1868) Ueber Cataracten in Verbindung mit einer eigenthumlichen Hautdegeneration. Arch. Klin. Exp. Opthal. 4, 159 – 182.
8 Thomson, M. S. (1936) Poikiloderma congenitale. Br. J. Dermatol. *48*, 221 – 234.
9 Vennos, E. M., Collins, M., and James, W. D. (1992) Rothmund-Thomson syndrome: review of the world literature. J. Am. Acad. Dermatol. 27, 750 – 762.
10 Wang, L. L., Levy, M. L., Lewis, R. A., Chintagumpala, M. M., Lev, D., Rogers, M., Plon, S. E. (2001) Clinical manifestations in a cohort of 41 Rothmund-Thomsom patients. Am. J. Med. Genet. 102, 11 – 17.
11 Kitao, S., Lindor, N. M., Shiratori, M., Furuichi, Y., and Shimamoto, A. (1999) Rothmund-Thomson syndrome responsible gene, RECQL4: genomic structure and products. Genomics 61, 268 – 276.
12 Lindor, N. M., Furuichi, Y., Kitao, S., Shimamoto, A., Arndt, C., and Jalal, S. (2000) Rothmund-Thomson syndrome due to RECQ4 helicase mutations: report and clinical and molecular comparisons with Bloom syndrome and Werner syndrome. Am. J. Med. Genet. 90, 223 – 228.
13 Der Kaloustian, V. M., McGill, J. J., Vekemans, M., and Kopelman, H. R. (1990) Clonal lines of aneuploid cells in Rothmund-Thomson syndrome. Am. J. Med. Genet. 37, 336 – 339.
14 Vennos, E. M., and James, W. D. (1995) Rothmund-Thomson syndrome. Dermatol. Clin. 13, 143 – 150.
15 Werner, S. R., Prahalad, A. K., Yang, J., and Hock, J. M. (2006) RECQL4-deficient cells are hypersensitive to oxidative stress/damage: insights for osteosarcoma prevalence and heterogeneity in Rothmund-Thomson syndrome. Biochem. Biophys. Res. Commun. 345, 403 – 409.
16 Kellermayer, R., Siitonen, H. A., Hadzsiev, K., Kestila, M., and Kosztolanyi, G. (2005) A patient with Rothmund-Thomson syndrome and all features of RAPADILINO. Arch. Dermatol. 141, 617 – 620.
17 Baller, F. (1950) Radiosaplasie und Inzucht. Z. Menschl. Vererb. Konstitutionsl. 29, 782 – 790.
18 Ichikawa, K., Noda, T., and Furuichi, Y. (2002) Preparation of the gene targeted knockout mice for human premature aging diseases, Werner syndrome, and Rothmund-Thomson syndrome caused by the mutation of DNA helicases. Nippon Yakurigaku Zasshi 119, 219 – 226.
19 Hoki, Y., Araki, R., Fujimori, A., Ohhata, T., Koseki, H., Fukumura, R., Nakamura, M., Takahashi, H., Noda, Y., and Kito, S. (2003) Growth retardation and skin abnormalities of the Recql4-deficient mouse. Hum. Mol. Genet. 12, 2293–2299.
20 Mann, M. B., Hodges, C. A., Barnes, E., Vogel, H., Hassold, T. J., and Luo, G. (2005) Defective sister-chromatid cohesion, aneuploidy and cancer predisposition in a mouse model of type II Rothmund-Thomson syndrome. Hum. Mol. Genet. 14, 813 – 825.
21 Wang, H., and Elledge, S. J. (1999) DNA replication and checkpoint protein 1, functions with DPB11 to control DNA replication and the S-phase checkpoint in Saccaromyces cerevisiae. Proc. Natl. Acad. Sci. USA 96, 3824 – 3829.
22 Matsumoto, H., Muramatsu, S., Kamimura, Y., and Araki, H. (2002) S-Cdk-dependent phosphorylation of Sld2 essential for chromosomal DNA replication in budding yeast. Nature 415, 651 – 655.

23 Noguchi, E., Shanahan, P., Noguchi, C., and Russell, P. (2002) CDK phosphorylation of Drc1 regulates DNA replication in fission yeast. Curr. Biol. 12, 599 – 605.
24 Sangrithi, M. N., Bernal, J.A., Madine, M., Philpott, A., Lee, J., Dunphy, W. G., and Venkitaraman, A. R. (2005) Initiation of DNA replication requires the RECQL4 protein mutated in Rothmund-Thomson syndrome. Cell 121, 887 – 898.
25 Matsuno, K., Kumano, M., Kubota, Y., Hashimoto, Y.,and Takisawa, H. (2006) The N-terminal noncatalytic region of Xenopus RecQ4 is required for chromatin binding of DNA polymerase in the initiation of DNA replication. Mol. Cell. Biol. 26, 4843 – 4852.
26 Yin, J., Tae Kwon, Y., Varshavsky, A., and Wang, W. (2004) RECQL4, mutated in the Rothmund-Thomson and RAPADILINO syndromes, interacts with ubiquitin ligases UBR1 and UBR2 of the N-end rule pathway. Hum. Mol. Genet. 13, 2421 – 2430.
27 Hershko, A., Ciechanover, A., and Varshavsky, A. (2000) The ubiquitin system. Nat. Med. 6, 1073 – 1081.
28 Petkovic, M., Dietschy, T., Freire, R., Jiao, R., and Stagljar, I. (2005) The human Rothmund-Thomson syndrome gene product, RECQL4, localizes to distinct nuclear foci that coincide with proteins involved in the maintenance of genome stability. J. Cell Sci. 118, 4261 – 4269.
29 Raderschall, E., Golub, E.I., and Haaf, T. (1999) Nuclear foci of mammalian recombination proteins are located at single-stranded DNA regions formed after DNA damage. Proc. Natl. Acad. Sci. USA 96, 1921 – 1926.
30 Hashimoto, Y., and Takisawa, H. (2003) Xenopus Cut5 is essential for a CDK-dependent process in the initiation of DNA replication. EMBO J. 10, 2526 – 2535.
31 Van Hatten, R. A., Tutter, A. V., Holway, A. H., Khederian, A. M., Walter, J. C., and Michael, W. M. (2002) The Xenopus Xmus101 protein is required for the recruitment of Cdc45 to origins of DNA replication. J. Cell Biol. 159, 541 – 547.
32 Kamimura, Y., Masumoto H., Sugino A., and Araki H. (1998) Sld2, which interacts with Dpb11 in Saccharomyces cerevisiae, is required for chromosomal DNA replication. Mol. Cell. Biol. 18, 6102 – 6109.
33 Woo, L. L., Futami, K., Shimamoto, A., Furuichi, Y., and Frank, K.M. (2006) The Rothmund-Thomson gene product RECQL4 localizes to the nucleolus in response to oxidative stress. Exp. Cell Res. 312, 3443 – 3457.
34 Malanga, M. and Althaus, F. R. (2005). The role of poly(ADP-ribose) in the DNA damage signaling network. Biochem. Cell Biol. 83, 354 – 364.
35 Allinson, S. L., Dianova, I. I., and Dianov, G. L. (2003) Poly(ADP-ribose) polymerase in base excision repair: always engaged, but not essential for DNA damage processing. Acta Biochim. Pol. 50, 169 – 179.
36 Hodges, M., Tissot, C., Howe, K., Grimwade, D., and Freemont, P. S. (1998) Structure, organization, and dynamics of promyelocytic leukemia protein nuclear bodies. Am. J. Hum. Genet. 63, 297 – 304.
37 Shinohara, A., and Ogawa, T. (1999) Rad51/RecA protein families and the associated proteins in eukaryotes. Mutat. Res. 435, 13 – 21.
38 Macris, M. A., Bussen, W., Shimamoto, A., and Sung, P. (2006) Biochemical characterization of the RECQ4 protein mutated in Rothmund-Thomson syndrome. DNA Repair 5, 172 – 180.
39 Larizza, L., Magnani, I., and Roversi, G. (2006) Rothmund-Thomson syndrome and RECQL4 defect: splitting and lumping. Cancer Lett. 232, 107 – 120.
40 Sharma, S., Doherty, K. M., and Brosh, R. M., Jr (2006) Mechanisms of RecQ helicases in pathways of DNA metabolism and maintenance of genomic stability. Biochem. J. 398, 319 – 337.

Article III

Physical and functional interactions between Werner syndrome helicase and mismatch-repair initiation factors.

Nurten Saydam*, Radhakrishnan Kanagaraj*, Tobias Dietschy*, Patrick L. Garcia, Javier Peña-Diaz, Igor Shevelev, Igor Stagljar and Pavel Janscak Nucl. Acids. Res. *2007, 1–11* (***** contributed equally)

For this work, it did the experiments for figures 1 and 4.

Nucleic Acids Research Advance Access published August 22, 2007

Nucleic Acids Research, 2007, 1–11
doi:10.1093/nar/gkm500

Physical and functional interactions between Werner syndrome helicase and mismatch-repair initiation factors

Nurten Saydam[1] Radhakrishnan Kanagaraj[1], Tobias Dietschy[1,2,3], Patrick L. Garcia[1], Javier Peña-Diaz[1], Igor Shevelev[2,3], Igor Stagljar[2,3] and Pavel Janscak[1,*]

[1]Institute of Molecular Cancer Research of the University of Zurich, Switzerland and [2]Department of Biochemistry and [3]Department of Medical Genetics and Microbiology, Donnelly Centre for Cellular and Biomolecular Research, University of Toronto, Canada

Received April 26, 2007; Revised and Accepted June 7, 2007

ABSTRACT

Werner syndrome (WS) is a severe recessive disorder characterized by premature aging, cancer predisposition and genomic instability. The gene mutated in WS encodes a bi-functional enzyme called WRN that acts as a RecQ-type DNA helicase and a 3′-5′ exonuclease, but its exact role in DNA metabolism is poorly understood. Here we show that WRN physically interacts with the MSH2/MSH6 (MutSα), MSH2/MSH3 (MutSβ) and MLH1/PMS2 (MutLα) heterodimers that are involved in the initiation of mismatch repair (MMR) and the rejection of homeologous recombination. MutSα and MutSβ can strongly stimulate the helicase activity of WRN specifically on forked DNA structures with a 3′-single-stranded arm. The stimulatory effect of MutSα on WRN-mediated unwinding is enhanced by a G/T mismatch in the DNA duplex ahead of the fork. The MutLα protein known to bind to the MutSα–heteroduplex complexes has no effect on WRN-mediated DNA unwinding stimulated by MutSα, nor does it affect DNA unwinding by WRN alone. Our data are consistent with results of genetic experiments in yeast suggesting that MMR factors act in conjunction with a RecQ-type helicase to reject recombination between divergent sequences.

INTRODUCTION

Werner syndrome (WS) is an autosomal recessive disorder characterized by an early onset of age-related pathologies including graying hair, alopecia, arteriosclerosis, osteoporosis, diabetes mellitus and cancer (1). The gene mutated in WS, *WRN*, encodes a RecQ-type DNA helicase (2,3). WRN also possesses a 3′ - 5′ exonuclease activity residing in a separate domain located at the N-terminus of the protein (4,5). At the cellular level, WRN deficiency is associated with defects in DNA replication, homologous recombination (HR) and telomere maintenance (6–9). As a result, cells derived from WS patients display a high degree of genomic instability including elevated levels of chromosomal translocations and deletions (10–13). WS cells are hypersensitive to DNA-damaging agents such as 4-nitroquinoline 1-oxide, topoisomerase inhibitors and DNA cross-linkers, suggesting that WRN is actively involved in DNA repair (14–16). Several lines of evidence implicate WRN in the cellular response to DNA double-strand breaks (DSBs). WRN is rapidly recruited to the sites of ionizing radiation (IR)-induced damage (17). Moreover, it interacts physically and functionally with a number of proteins that are involved in the DSB-repair process including the MRE11-RAD50-NBS1 (MRN) complex (18), the Ku complex (19), RAD52 (20) and DNA-dependent protein kinase (21). However, the precise role for WRN in DNA repair remains to be elucidated.

The DNA mismatch-repair (MMR) system maintains genomic integrity by correcting DNA replication errors and preventing recombination between divergent sequences (22,23). Defects in a subset of MMR genes including *MSH2*, *MSH3*, *MSH6*, *MLH1* and *PMS2* are associated with hereditary non-polyposis colon cancer, highlighting the crucial role for MMR in genome maintenance (24). In the initiation step of the eukaryotic

*To whom correspondence should be addressed. Tel: +41(0)44 635 3470; Fax: +41(0)44 635 3484; Email: pjanscak@imcr.unizh.ch
Present address:
Nurten Saydam, Harvard School of Public Health, 667, Huntington Ave, Boston, USA

The authors wish it to be known that, in their opinion, the first three authors should be regarded as joint First Authors

MMR process, at least three heterodimers, namely MSH2/MSH6 (MutSα), MSH2/MSH3 (MutSβ) and MLH1/PMS2 (MutLα), are involved (22). MutSα binds to base-base mismatches and short insertion/deletion loops, while MutSβ can recognize only insertion/deletion loops containing up to 16 extra nucleotides in one strand (22). MutLα possesses an intrinsic endonuclease activity, which is activated upon mismatch recognition and introduces incisions in the discontinuous strand of the heteroduplex DNA, generating entry sites for the 5′-3′ exonuclease EXO1 (25).

Sgs1, the yeast ortholog of WRN, also contributes to the suppression of recombination between divergent DNA sequences (26). Heteroduplex rejection during repair of DSBs by the single-strand annealing pathway of HR in yeast requires the mismatch binding and ATPase functions of the Msh2p/Msh6p heterodimer and the helicase activity of Sgs1 (27,28). These findings led to the proposal that MMR proteins act in conjunction with Sgs1 to unwind DNA recombination intermediates containing mismatches (27,28).

Here we demonstrate that WRN directly interacts with MutSα, MutSβ and MutLα via distinct domains. MutSα and MutSβ are found to stimulate WRN-mediated unwinding of forked DNA duplexes with a 3′-single-stranded (ss) arm. The stimulatory effect of MutSα on WRN-mediated unwinding is enhanced by a single G/T mismatch located in the duplex ahead of the fork in a manner independent of MutLα. These data provide biochemical evidence suggesting that the rejection of homeologous recombination by MMR proteins occurs *via* helicase-mediated unwinding of recombination intermediates.

MATERIALS AND METHODS

Construction of plasmids

The bacterial expression vectors for the WRN fragments encompassing the amino acid residues 51–449, 949–1432, 500–946, 500–1149, 500–1236, respectively, fused to the C-terminus of glutathione *S*-transferase (GST) were constructed by PCR amplification of corresponding regions of the WRN cDNA and their insertion in pGEX-2TK (Amersham Biosciences) between the EcoRI and BamHI sites. The complete coding region of WRN was amplified by PCR and cloned in pACT2 (Clontech Palo Alto, CA) via SmaI site to construct a yeast two-hybrid (YTH) vector expressing WRN as a fusion with a Gal4 activation domain. MLH1 cDNA comprised of the codons 500–756 was cloned in a YTH vector pBTM116 (Clontech Palo Alto, CA) between the EcoRI and SalI sites, resulting in a fusion with a LexA DNA binding domain. The pBTM16 derivatives expressing other MLH1 variants as well as the full-length yMlh1 were previously described (29). The Gal4-hMSH2 (pLJR105), LexA-MSH3 and LexA-MSH6 bait plasmids were also described previously (30,31).

Proteins

Recombinant human WRN (3,32), MutSα (33), MutSβ (33) and MutLα (34) and *Escherichia coli* MutS (35) were produced and purified as previously described. An antibody against the N-terminal region of WRN encompassing amino acids 1–391 (ISEV-391) was raised in rabbit and purified on an antigen-coupled Sepharose 4A column (Amersham Biosciences). Control IgGs were purified from a rabbit preimmune serum on a 5 ml HiTrap protein G-Sepharose column (Amersham Biosciences).

Cell culture

The following human cell lines were used in this study: HEK 293 embryonic kidney cells and AG11395 SV40-transformed WS fibroblasts (Coriell Institute for Medical Research). The HEK 293 cells were maintained in DMEM (Gibco) supplemented with 10% fetal calf serum (Biochrome AG). The WS cells were maintained in MEM containing 15% fetal calf serum and 2 mM L-glutamine.

Immunoprecipitation assays

Cells were suspended in lysis buffer containing 20 mM Tris–HCl (pH 7.5), 150 mM NaCl, 2 mM EDTA, 0.1% (v/v) Triton X-100, 10% (v/v) glycerol and complete, EDTA-free protease inhibitor cocktail (Roche). After sonication, the suspension was centrifuged at 20 000 *g* for 30 min at 4°C. Aliquots containing 1.6 mg of protein were incubated overnight at 4°C with purified rabbit polyclonal anti-WRN IgGs (2 μg), which was followed by a 2-h incubation with protein A/G-agarose beads (Santa Cruz) at 4°C. Where required, extracts were treated with 50 U of DNaseI (Roche) for 30 min at 25°C prior to addition of antibody. After extensive washing with the lysis buffer, the immunoprecipitates were subjected to electrophoresis in a 7.5% polyacrylamide–SDS gel followed by western blotting. The blots were probed with mouse monoclonal antibodies against WRN (BD Biosciences, 611169), MSH6 (Pharmingen, clone 44), PMS2 (Pharmingen, clone 16-4), MLH1 (BD Biosciences, 554073), MSH2 (Calbiochem, clone NA 26) and MSH3 (Transduction Laboratories, clone 52). Immune complexes were detected using ECL-plus reagent (Amersham Biosciences), with horse anti-mouse IgG-horseradish peroxidase conjugate (Vector) used as a secondary antibody. In the control experiment, IgGs purified from a preimmune rabbit serum were used instead of the anti-WRN antibody.

GST pull-down assays

GST–WRN fusion proteins were produced in the *E. coli* BL21-CodonPlus(DE3)-RIL strain (Stratagene) using the expression vectors described above. The fusion proteins were bound to glutathione–sepharose beads (Amersham Biosciences) as previously described (36). The beads were incubated with 1 μg of purified MutSα, MutSβ or MutLα in 400 μl of NET-N 100 buffer [10 mM Tris HCl (pH 8.0), 1 mM EDTA, 100 mM NaCl, 0.5% (v/v) NP-40] for 2 h at 4°C. After extensive washing with NET-N 100 buffer, proteins bound to the beads were analyzed by western blotting. Membranes were probed with the monoclonal antibodies described above. MSH3 was detected with a rabbit polyclonal antibody (NTH3) raised against its first 200 amino acids (Eurogentec). In a control experiment, beads were coated with GST protein only.

ELISA-based protein binding assay

Purified recombinant WRN was diluted to a concentration of 20 nM in carbonate buffer [16 mM Na_2CO_3, 34 mM $NaHCO_3$ (pH 9.6)] and added to wells of a 96-well microtiter plate (50 µl/well). Plates were incubated overnight at 4°C. For control reactions, wells were pre-coated with an equivalent amount of bovine serum albumin (BSA). After aspiration of the samples, the wells were blocked with blocking buffer [phosphate-buffered saline, 0.5% (v/v) Tween-20 and 3% (w/v) BSA] for 2 h at 37°C (200 µl/well). Following blockage, the wells were incubated with increasing concentrations of purified recombinant MutSα, MutSβ and MutLα proteins for 1 h at 37°C. All samples were supplemented with ethidium bromide (EtBr) at a concentration of 50 µg/ml to prevent DNA-mediated interactions. Wells were washed four times with blocking buffer to eliminate unbound proteins, and incubated with the appropriate primary antibody diluted in blocking buffer (mouse monoclonal anti-MSH2 antibody for MutSα and MutSβ, and mouse monoclonal anti-MLH1 antibody for MutLα). Plates were incubated for 1 h at 37°C. After four washings with blocking buffer, horseradish peroxidase-conjugated anti-mouse secondary antibody (1:10 000 in blocking buffer) was added and the plates were incubated at 37°C for 30 min. After extensive washing with blocking buffer, the protein complexes were detected using o-Phenylenediamine dichloride (Sigma) dissolved in 0.1 M citrate-phosphate buffer (pH 5.0) containing 0.03% hydrogen peroxide (1 mg/ml). The reactions were terminated after 5 min by adding 50 µl of 2 M H_2SO_4. The plates were scanned in a microplate reader (Molecular Devices) for absorbance at 492 nm. The A_{492} values, corrected for background signal in the presence of BSA, were plotted as a function of the concentration of appropriate MMR protein using the GraphPad Prism software. To determine an apparent dissociation constant of each complex (K_d), the data points were fitted by the hyperbolic function $Y = B_{max}*X/(K_d + X)$ where B_{max} is the maximal binding and K_d is the concentration of ligand required to reach half-maximal binding.

YTH assay

YTH analysis was carried out using *Saccharomyces cerevisiae* strains L40 (*MAT*a *trp1 leu2 his3 LYS2::lexA-HIS3 URA3::lexA-lacZ*) and Y190 (*MATα*, *ura3-52, his3-200*, *lys2-801, ade2-101, trp1-901, leu2-3, 112, gal4Δ*, *gal80Δ*, *cyh*^{r}*2, LYS2::GAL1*$_{UAS}$*-HIS3*$_{TATA}$*-HIS3, URA3::GAL1*$_{UAS}$*-GAL1*$_{TATA}$*-lacZ*). The former strain was used for LexA-bait vectors while the latter strain was used for Gal4-bait vectors. Clones carrying the bait and prey plasmids were tested for β-galactosidase activity using a pellet X-gal (PXG) assay as previously described (37).

Helicase assays

Schemes of DNA substrates as well as the sequences of the constituent oligonucleotides are summarized in Supplementary Table 1. The f11-20 oligonucleotide (50-mer) was labeled at the 5′-end using T4 polynucleotide kinase (NEB) and [γ-^{32}P]ATP (Amersham Biosciences), and annealed with appropriate oligonucleotides under previously described conditions (38). The helicase reaction mixtures (10 µl) contained 50 mM Tris–HCl (pH 7.5), 50 mM NaCl, 2 mM $MgCl_2$, 50 µg/ml of BSA, 2 mM ATP, 1 mM DTT, 1 nM DNA substrate and indicated concentrations of MMR proteins (MutSα, MutSβ, MutLα and MutS) and WRN. The MMR proteins were pre-incubated with the DNA substrate on ice for 1 min prior to the addition of WRN. The reactions were incubated at 37°C for 30 min and terminated by the addition of 0.5 reaction volume of buffer S [150 mM EDTA, 2% (w/v) SDS, 30% (v/v) glycerol, 0.1% (w/v) bromophenol blue] followed by treatment with proteinase K (0.1 mg/ml) at 37°C for 10 min. The reaction products were resolved on a non-denaturing 10% polyacrylamide gel [acrylamide to bis-acrylamide, 19:1 (w/w)] run in 1xTBE buffer at 140 V. Radiolabeled DNA species were visualized by a phosphorimager and quantified using ImageQuant software (Molecular Dynamics).

RESULTS

Physical association between WRN and MMR proteins

Based on genetic studies in yeast, it has been suggested that the proteins involved in the initiation of MMR act in conjunction with RecQ DNA helicases to eliminate DNA recombination intermediates containing mismatches, which can give rise to chromosomal rearrangements (27,28). We sought to test the validity of this model biochemically using the WRN helicase, one of the five RecQ homologs identified in human cells, whose dysfunction results in chromosomal translocations and deletions. First, we performed an ELISA-based protein-binding assay to investigate whether WRN and the MMR proteins interact physically. Increasing concentrations of purified MutSα (MSH2/MSH6), MutSβ (MSH2/MSH3) and MutLα (MLH1/PMS2) proteins (Figure 1A) ranging from 0 to 80 nM were incubated in wells that had been pre-coated with WRN at a concentration of 20 nM and subsequently blocked with BSA to prevent non-specific interactions. After extensive washing, the bound MMR proteins were incubated with specific antibodies followed by a colorimetric assay to quantify the binding. In control experiments, MMR proteins were incubated in wells pre-coated only with BSA. We found that all the three MMR heterodimers were specifically bound to WRN-coated wells in a dose dependent manner, indicating a direct interaction (Figure 1B–D). Interestingly, the apparent dissociation constant of the MutSβ–WRN complex (K_d = 8.8 nM) was much lower than that estimated for the MutSα–WRN complex (K_d = 38.5 nM). The dissociation constant of the MutLα–WRN complex (K_d = 34.9 nM) was similar to that of the MutSα–WRN complex.

To test whether WRN and MMR proteins form a stable complex *in vivo*, we immunoprecipitated WRN from extracts of exponentially growing human embryonic kidney cells (HEK 293) and subjected the resulting immunoprecipitate to western blot analysis.

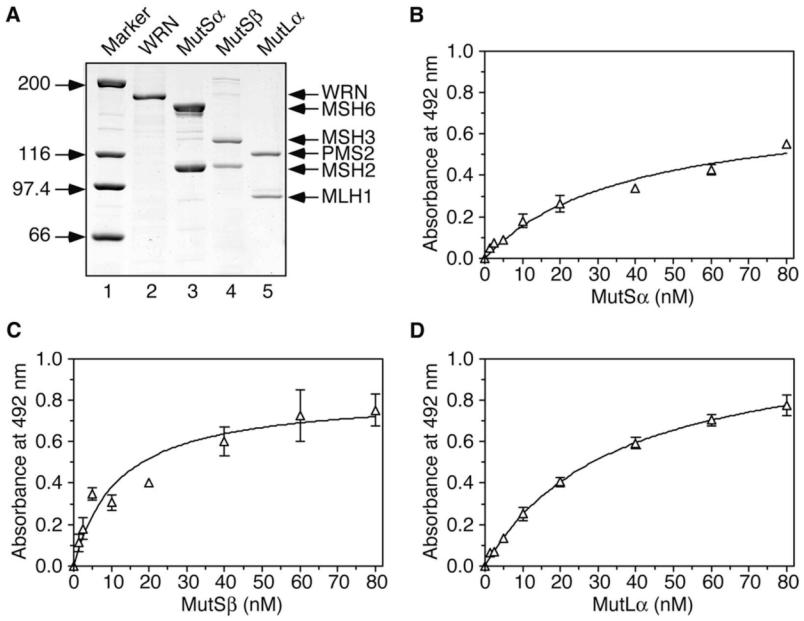

Figure 1. Direct physical interaction of WRN with MMR proteins. (**A**) SDS–PAGE analysis of purified recombinant MutSα, MutSβ, MutLα and WRN proteins produced in insect cells by means of the baculovirus system. (**B**) Binding of MutSα to WRN as a function of MutSα concentration. (**C**) Binding of MutSβ to WRN as a function of MutSβ concentration. (**D**) Binding of MutLα to WRN as a function of MutLα concentration. Increasing concentrations of MutSα, MutSβ and MutLα (0–80 nM) were incubated at 37°C for 1 h in the wells of an ELISA plate that were pre-coated with the WRN protein (20 nM) and subsequently blocked with 3% BSA. After extensive washing, the bound MMR proteins were detected by ELISA as described in Materials and Methods. The measured absorbance values were corrected by subtracting background values obtained with BSA-coated wells. The data points represent the mean of three independent experiments.

This immunoprecipitate was found to contain the MLH1 and PMS2 proteins, components of the MutLα complex, but not the MSH2 and MSH6 proteins, which form the MutSα heterodimer (Figure 2A, lanes 3 and 4). None of these MMR proteins were detected in the immunoprecipitate obtained with control IgGs (Figure 2A, lane 2). To exclude the possibility that the observed association of WRN with MLH1 and PMS2 results from independent binding of these proteins to DNA, we pre-treated the cell extracts with DNaseI. We found that this treatment did not alter the level of the MMR proteins in the WRN immunoprecipitate, suggesting that the WRN–MLH1–PMS2 complex is mediated by protein–protein interactions (Figure 2A, compare lanes 3 and 4). Furthermore, we did not detect PMS2 in an immunoprecipitate obtained with anti-WRN antibody from extracts of the WS cell line AG11395, excluding the possibility that the observed co-immunoprecipitation of MMR proteins with WRN is due to cross-reactivity of the antibody (Figure 2B).

Collectively, these data indicate that MutLα but not MutSα, forms a stable complex with WRN *in vivo*.

Mapping of protein–protein interaction domains

To identify the MutSα, MutSβ and MutLα-interaction sites on WRN, we performed affinity pull-down assays using a series of WRN fragments fused to GST. These fragments covered the entire WRN polypeptide except for the first 50 amino acids and the region spanning the amino acids 450–499 (Figure 3A and B). The GST pull-down experiments revealed that the MutSα interaction site on WRN was localized to the region between amino acids 500 and 946, which constitutes the helicase core of WRN composed of the DExH helicase and Zn-binding domains (Figure 3A and C). MutSβ was found to make contacts not only with the helicase core of WRN, but also with a region spanning amino acids 947–1149 that contains the winged-helix (WH) motif, a common interaction site for most of the WRN partners identified thus far (Figure 3A and C) (39). Notably, the binding affinity of MutSβ to the WH domain of WRN appeared to be much higher that its binding affinity to the helicase core of WRN (Figure 3C, compare lanes 4–7). The data also indicated that MutSβ binds to WRN more efficiently than MutSα (Figure 3C, top and middle panels; compare lane 1 with lanes 4–7), which is in agreement with the results of the ELISA assay (Figure 1).

MutLα was found to interact with the helicase core of WRN and with the N-terminal portion of WRN including the exonuclease domain, showing a higher binding affinity to the former domain (Figure 3A and C, bottom panel; compare lanes 3–7).

To identify the subunits of MutSα, MutSβ and MutLα that mediate the interaction with WRN, we performed a quantitative YTHassay with the full-length WRN as prey. The following interactions were examined: MSH2–WRN, MSH6–WRN, MSH3–WRN and MLH1–WRN.

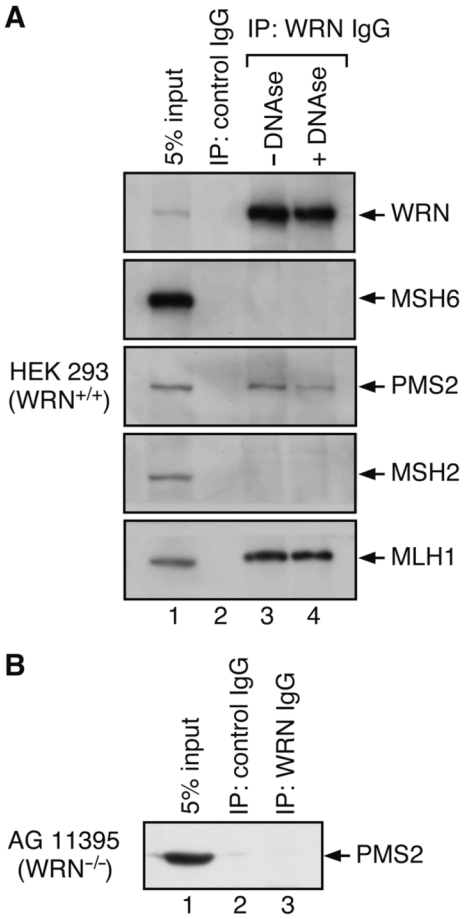

Figure 2. WRN forms a stable complex with MLH1 and PMS2 in human cells. (**A**) Western blot analysis of WRN immunoprecipitates from total extracts of HEK 293 cells (1.6 mg of protein) before (lane 3) and after (lane 4) treatment with DNaseI (50 U). Lane 1, 5% of input; lane 2, control immunoprecipitation experiment with a preimmune rabbit IgGs. Purified rabbit anti-WRN IgGs (2 μg) were used to immunoprecipitate WRN. Blots were probed with monoclonal antibodies against WRN, MSH2, MSH6, MLH1 and PMS2. (**B**) Western blot analysis of immunoprecipitate from extracts of AG11395 ($WRN^{-/-}$) cells obtained using an anti-WRN antibody. The immunoprecipitations were carried out under the same conditions as in (A). The blots were probed with a monoclonal antibody against PMS2.

We found WRN to interact with MLH1 and MSH2, but not with MSH3 and MSH6 (Figure 4A and B). This indicates that the MutSα–WRN and MutSβ–WRN interactions are mediated by MSH2, and the MutLα–WRN interaction is mediated by MLH1. However, the inability of MSH3 and MSH6 to interact with WRN in the YTH assay could be a consequence of the fact that these proteins are not soluble when expressed alone (33). This is also true for PMS2 (34). Therefore, the possibility still exists that these proteins could make additional contacts with WRN. This is particularly likely in the case of MSH3, since our GST pull-down experiments revealed that MutSβ interacts with both the helicase core and the WH domain of WRN, whereas MutSα interacts only with the helicase core of WRN (Figure 3).

In order to identify the WRN interaction domain on MLH1, we tested a series of MLH1 deletion variants for the ability to interact with the full-length WRN in YTH assay. We found that this domain is located at the C-terminus of the MLH1 polypeptide between amino acids 500 and 756 (Figure 4A and B). This is different from the location of the BLM-interaction site that was mapped to the region spanning amino acids 396–500 (29).

Stimulation of the helicase activity of WRN by MutSα and MutSβ

Next, we tested MutSα for the ability to affect the helicase activity of WRN on DNA substrates containing mismatches. In these experiments, we used a synthetic DNA duplex (49 bp) with a 3′-ss flap (19 nt) resembling a part of the structure that results from annealing of the resected arms of a broken chromosome at regions of homology. On such forked DNA structures, WRN preferentially translocates along the 3′-flap oligonucleotide to unwind the duplex ahead of the fork junction, generating a 3′-tailed duplex. This primary product can be further unwound by WRN into the component strands, as a consequence of loading of a second helicase molecule on the 3′-ssDNA tail (40). We prepared a fully matched substrate and a substrate containing a single G/T mismatch located 11 nt ahead of the ss/ds junction (Figure 5A and B, top panels). WRN alone displayed a very low helicase activity on both structures when present at the same concentration as the DNA substrate (1 nM). However, the helicase activity of WRN on these structures dramatically increased upon inclusion of an 8-fold molar excess of MutSα in the reaction (Figure 5A–D). Notably, the initial rate of the MutSα-stimulated unwinding reaction with G/T substrate was about 1.7 times higher than that measured with the G/C substrate (Supplementary Table 2).

Since MutLα is known to bind to MutSα–heteroduplex complexes (41), we investigated whether it can affect the WRN-mediated unwinding of G/T and G/C substrates induced by MutSα. We found that MutLα did not significantly alter the MutSα-dependent helicase activity of WRN on these DNA structures (Figure 5). Also, it had no effect on WRN-mediated unwinding in the absence of MutSα (Figure 7, lane 5).

To further assess the effect of MutSα on WRN-mediated unwinding of the 3′-flap duplex, we performed a protein titration experiment, in which we varied the concentration of MutSα while keeping WRN and DNA substrate at a fixed concentration of 1 nM. We found that MutSα stimulated the helicase activity of WRN in a concentration-dependent manner, exhibiting a significantly higher activity on the G/T substrate than on the homoduplex substrate (Figure 6).

To explore the specificity of the observed stimulatory effect, we tested human MutSβ as well as *E. coli* MutS for the ability to stimulate DNA unwinding by WRN. We found that MutSβ enhanced the WRN-mediated unwinding of the 3′-flap DNA duplex to a similar extent

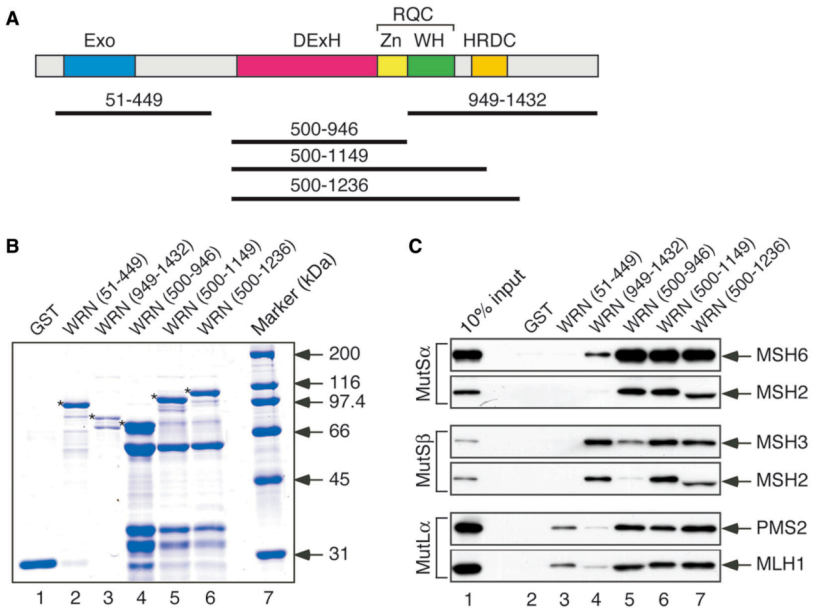

Figure 3. Mapping of MutSα, MutSβ and MutLα-interaction domains on WRN (**A**) Domain organization of the WRN protein. Exo, exonuclease domain; DExH, helicase domain; Zn, zinc-binding domain; WH, winged-helix domain; HRDC, helicase and RNaseD C-terminal domain; RQC, RecQ C-terminal region. The black lines indicate the boundaries of the various WRN fragments used in this study. (**B**) SDS–PAGE analysis of GST–WRN fragments expressed in *E. coli* and isolated using glutathione beads. Bands migrating below the WRN fragments (marked by an asterisks) were determined to be degradation products by western blot analysis using an anti-GST antibody. (**C**) GST pull-down assay. Glutathione beads coated with the indicated GST-tagged WRN fragments were incubated with purified MutSα, MutSβ or MutLα proteins expressed in insect cells using baculovirus system and the bound MMR proteins were analyzed by western blotting as described in Materials and Methods.

as seen with MutSα (Figure 7, compare lanes 2 and 3). In contrast, the *E. coli* MutS protein did not enhance the WRN-mediated DNA unwinding (Figure 7, lane 8), indicating that the observed stimulatory effect is specific to human MutS homologs. As in the case of MutSα, MutSβ-stimulated helicase activity of WRN was not influenced upon addition of MutLα (Figure 7, compare lanes 4 and 7) and it was dependent on MutSβ concentration (Supplementary Figure S1). We also found that in the presence of MutSβ, WRN unwound the G/T substrate with the same efficiency as the homoduplex substrate (Supplementary Figure S2). This is consistent with the fact that MutSβ does not bind to base–base mismatches (22) and supports the conclusion that the observed stimulatory effect of the G/T mismatch on MutSα-dependent unwinding of the 3′-flap duplex by WRN results from the specific binding of MutSα to the mismatch.

Together, the results described above indicate that MutSα and MutSβ, but not MutLα, can stimulate WRN to unwind DNA structures resembling recombination intermediates and that this stimulatory effect is enhanced by mismatches in the DNA substrate.

MutSα and MutSβ stimulate WRN helicase specifically on forked DNA duplexes with a 3′-ss arm

To gain further insights into the mechanism underlying the stimulation of the helicase activity of WRN by MutSα and MutSβ, we investigated the dependence of this reaction on the configuration of the arms of the fork. Using the same set of oligonucleotides, we prepared the following substrates: a forked duplex with both arms single stranded (splayed arm); a forked duplex with the 3′-arm single stranded and the 5′-arm double stranded (3′-flap duplex); a forked duplex with the 3′-arm double stranded and the 5′-arm single stranded (5′-flap duplex) and a forked duplex with both arms double stranded. Earlier studies revealed that WRN could unwind efficiently all these structures, indicating that it does not require the 3′-arm to be single stranded for loading at the fork (40). We found that MutSα and MutSβ strongly stimulated the WRN-mediated unwinding of the splayed arm and the 3′-flap duplex, but had no significant effect on the unwinding of the 5′-flap duplex and the fully double stranded fork (Figure 8). We also tested these proteins for the ability to stimulate the helicase activity of WRN on 3′-ssDNA-tailed duplex, which is normally a poor substrate for WRN (40). We found that neither MutSα nor MutSβ could activate WRN for unwinding of this partial DNA duplex (data not shown). Interestingly, the 3′-tail duplex resulting from unwinding of the 3′-flap structure was unwound by WRN efficiently. This discrepancy can result from the fact that WRN exists as an oligomeric structure, which would facilitate loading of a second molecule of WRN on the 3′-ssDNA generated by unwinding of the duplex ahead of the fork.

Collectively, these data indicate that MutSα and MutSβ require a forked DNA structure with 3′-ss DNA at the junction to stimulate WRN-mediated DNA unwinding.

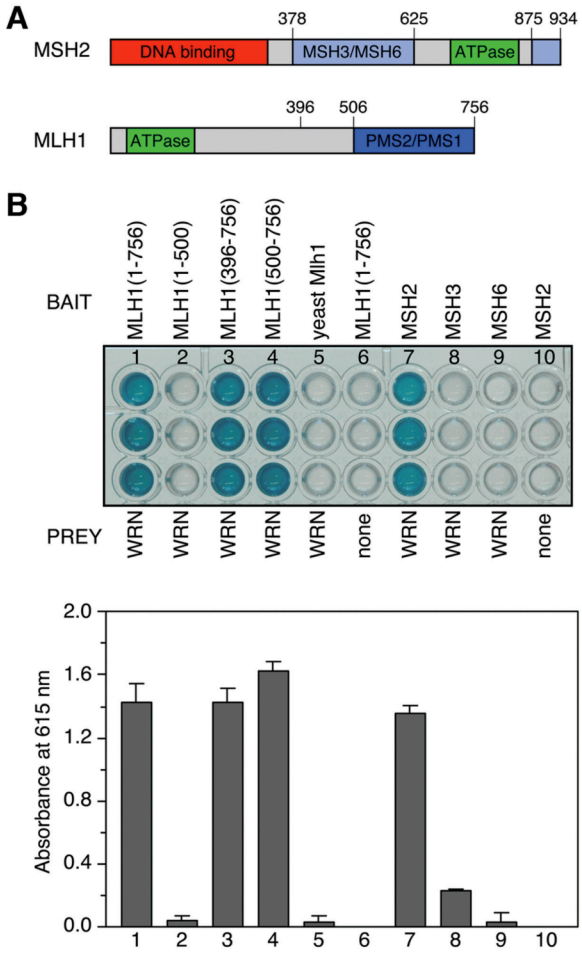

Figure 4. Interaction between WRN and MMR proteins in yeast two-hybrid system. (**A**) Domain organizations of the MSH2 and MLH1 proteins. The numbers refer to the amino acid sequence. (**B**) Quantitative yeast two-hybrid assay. The S. cerevisiae strain L40 harboring a pACT2 vector expressing the full-length WRN fused to the GAL4 activation domain was transformed with pBTM116 vectors encoding the indicated MMR proteins fused to LexA (MLH1 and its deletion derivatives, MSH3 and MSH6) or Gal4 (MSH2) DNA binding domains. Clones containing both plasmids were subjected to β-galactosidase assay on an ELISA micro-plate using 5-bromo-4-chloro-3-indolyl-β-D-galactopyranoside (X-gal) as a substrate. Top panel: An ELISA plate after a 30-min incubation at room temperature. Bottom panel: Graph showing absorbance at 615 nm measured in individual wells after 35 min, which is a measure of β-gal activity. The values represent the mean of three independent experiments.

DISCUSSION

Although WRN has been implicated in a number of DNA repair processes, the exact DNA transactions mediated by this helicase/exonuclease in the cell remain elusive. Here we show that WRN interacts physically with proteins that are involved in the initiation of MMR and the rejection of recombination between divergent sequences. Most importantly, our experiments revealed that MutSα and MutSβ can stimulate the helicase activity of WRN on forked DNA structures with a 3′-ss arm that resemble intermediates of single-strand annealing pathways of HR. In addition, we found that a single G/T mismatch located ahead of the fork junction increased the efficiency of the MutSα-dependent unwinding by WRN. These data are consistent with a model in which the MMR initiation factors prevent homeologous recombination by activating a DNA helicase for unwinding of recombination intermediates containing mismatches. This model was proposed earlier on the basis of results of *in vivo* heteroduplex rejection assays with yeast *msh2* and *sgs1* mutants (27,28). It is possible that MutSα and MutSβ bind to mismatches formed after pairing of sequences of imperfect homology and, following ATP binding, are converted into a DNA sliding clamp as proposed in the case of the MMR pathway (42). When the clamp encounters the junction between the heteroduplex and the non-homologous 3′-ss tail, it binds stably to it and recruits a DNA helicase to disrupt the joined DNA molecule. In agreement with this hypothesis, it has been demonstrated that yeast MutSβ specifically binds to forked DNA structures containing 3′- ssDNA making contacts with the sequences at the ds–ss junction (43). These studies also revealed that MutSβ holds the junction in an altered, perhaps more rigid, conformation (43). Such structural changes could facilitate the loading of the WRN helicase on the 3′- ssDNA at the junction, which is a prerequisite for duplex unwinding to occur. However, it should be noted that the MutSα-activated unwinding of a 3′-flap duplex by WRN displayed only a moderate dependence on mismatches. It is therefore possible that hereroduplex rejection *in vivo* involves some additional factors that ensure mismatch specificity of this transaction.

In our studies, we did not observe any significant modulation of WRN-mediated unwinding by MutLα, even in the presence of MutSα or MutSβ. In agreement with this finding, the yeast Mlh1 and Pms1 proteins have been shown to have only minor roles in the rejection of homeologous recombination relative to the contributions of Msh2 and Msh6 (27). Thus, it appears that the physical interaction between WRN and MutLα identified in this study has some other functional implication. Interestingly, MLH1 was shown to interact with various DNA repair factors including MRE11, BACH1, MBD4 and BLM (29,44–47). It is, therefore, possible that MLH1 plays a more general role in DNA repair processes.

A number of other functional implications for the observed interactions between WRN and the MMR factors can be discussed. Several lines of evidence suggest that WRN promotes replication of telomeric DNA by unwinding G-quadruplex structures that can readily form in G-rich telomeric DNA and impose a barrier for progression of DNA replication forks (9,48–50). Strikingly, human MutSα has been shown to bind efficiently to G-quadruplex DNA (51). Moreover, Msh2 deficiency in mice is associated with loss of telomeres and an elevated level of telomere end-to-end fusion, a phenotype similar to that manifested by WRN-deficient

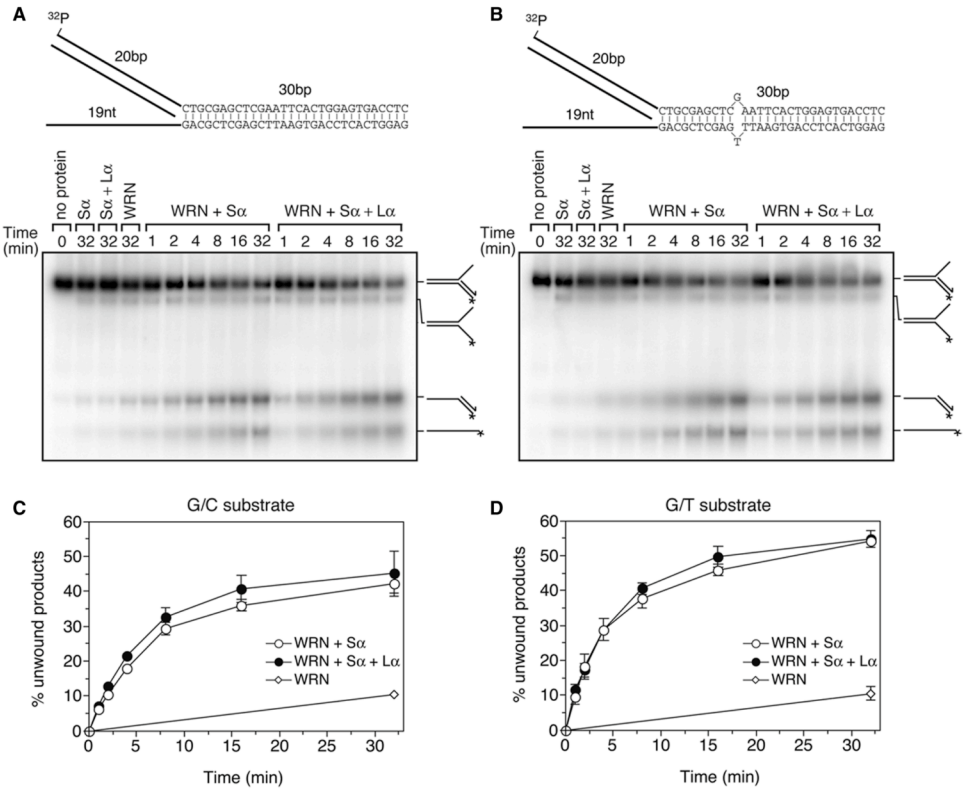

Figure 5. Kinetics of WRN-mediated unwinding of a 3′-flap DNA duplex in the presence of MutSα and MutLα. (**A**) Reactions with a homoduplex 3′ flap substrate. (**B**) Reactions with a 3′-flap duplex containing a G/T mismatch located 11 nucleotides ahead of the fork as indicated. (**C**) Quantification of the time course reactions in A. (**D**) Quantification of the time course reactions in B. All reactions contained 1 nM [^{32}P]DNA, 1 nM WRN and 8 nM MMR proteins as indicated. Aliquots at individual time points were analyzed by native PAGE followed by phosphorimaging and quantification as described in Materials and Methods section. Schemes of the substrate and the reaction products are shown on the right. The relative concentration of unwound products (3′-tailed duplex and free labeled oligonucleotide) is expressed as a percentage of total DNA.

cells (9,52). Thus, one can speculate that the MMR proteins can mediate recruitment of the WRN helicase to G-quadruplex structures formed at telomeres and hence facilitate their removal.

It has been shown that the human MutSβ and WRN are required along with PCNA, RPA and ERCC1-XPF for uncoupling of psoralen-induced inter-strand DNA crosslinks (ICLs) in cell-free extracts, suggesting a novel ICL-repair pathway in which MutSβ is essential for the recognition of ICLs, while the WRN helicase mediates unwinding of the DNA duplex adjacent to the lesion, which enables strand incision by ERCC1-XPF (53,54). Our finding that MutSβ physically interacts with WRN and stimulates its helicase activity brings further support for this model and suggests that MutSβ might recruit WRN to the ICL sites.

Earlier studies demonstrated that nuclear extracts from several fibroblastoid cell lines derived from WS patients were deficient in repair of base–base mismatches and insertion/deletion loops, suggesting that WRN could have a role in MMR (55). However, it is not certain that the MMR-deficiency of these extracts was caused solely by WRN deficiency because complementation experiments with recombinant WRN protein were not performed in this study. Moreover, in some cases, pairwise mixing of these extracts restored MMR proficiency, making the involvement of WRN in MMR rather questionable.

Recently, two other human RecQ homologs, namely RECQ1 and BLM, have been shown to interact physically and functionally with the MMR-initiation factors (29,31,47,56,57). As in the case of WRN, MutSα was found to stimulate RECQ1-mediated unwinding of a forked structure with a 3′-ss arm (56). In contrast, MutSα did not affect unwinding of forked DNA duplexes by BLM (31). Instead, MutSα was found to stimulate the ability of BLM to process Holliday junctions *in vitro* (57). Further studies will be needed to fully understand the molecular mechanisms by which the RecQ helicases and MMR factors work together to maintain genomic stability.

SUPPLEMENTARY DATA

Supplementary Data are available at NAR Online.

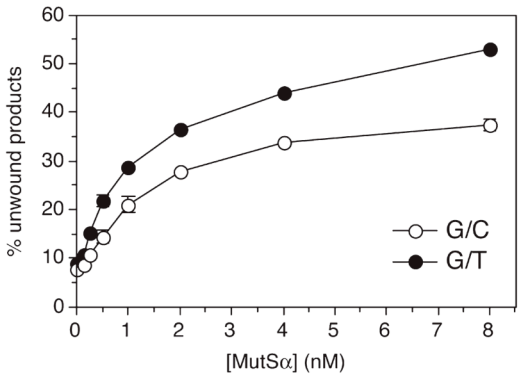

Figure 6. Helicase activity of WRN on 3′-flap duplexes with or without a G/T mismatch as a function of MutSα concentration. WRN and the DNA substrate were present at a concentration of 1 nM. The DNA substrates were the same as in Figure 5. Reactions were incubated for 30 min and analyzed by native PAGE followed by phosphorimaging as described in Materials and Methods section. The data points represent the mean of three independent experiments. The relative concentration of unwound products (3′-tailed duplex and free labeled oligonucleotide) is expressed as a percentage of total DNA.

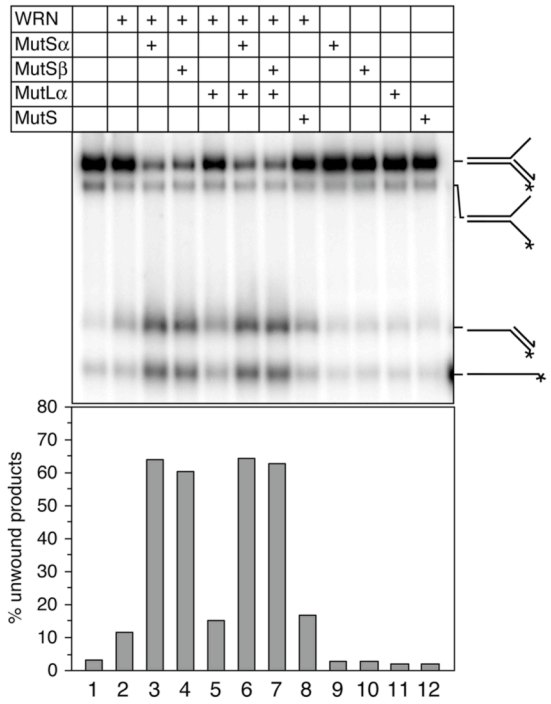

Figure 7. Effect of various MMR proteins on WRN-mediated unwinding of a 3′-flap DNA duplex. Helicase reactions contained 1 nM [^{32}P]DNA substrate and 2 nM WRN. The MMR proteins were present in a concentration of 8 nM as indicated. Reactions were incubated for 32 min and analyzed by native PAGE followed by phosphorimaging as described in Materials and Methods section (top panel). The relative concentration of unwound products (3′-tailed duplex and free labeled oligonucleotide) is expressed as a percentage of total DNA (bottom panel). Schemes of the substrate and the reaction products are shown on the right.

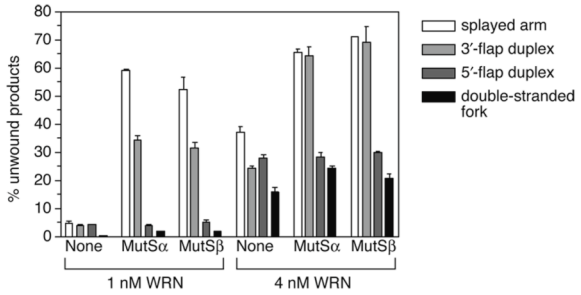

Figure 8. Stimulation of WRN-mediated unwinding of forked DNA structures by MutSα and MutSβ is dependent on the presence of 3′-single stranded DNA at the junction. Reactions with 1 nM splayed arm (white bars), 1 nM 3′-flap duplex (light gray bars), 1 nM 5′-flap duplex (dark gray bars) and 1 nM fully double-stranded fork duplex (black bars) contained 1 nM or 4 nM WRN and 8 nM MutSα or MutSβ as indicated. Reactions were incubated for 32 min and analyzed by native PAGE followed by phosphorimaging as described in Materials and Methods. The relative concentration of unwound products is expressed as a percentage of total DNA. The data points represent the mean of at least three independent experiments.

ACKNOWLEDGEMENTS

We thank Renjie Jiao for the construction of pACT2-WRN plasmid used in YTH assay, Peter Cejka for purified *E. coli* MutS protein and Lene Rasmussen for the plasmid pLJR105. We are also grateful to Josef Jiricny, Stefano Ferrari and David Lauterbach for comments on the manuscript. This work was supported by the Sassella and the Swiss National Science Foundations (Marie Heim-Vögtlin Grant Nr. PMPDA-102451 to N.S.). Funding to pay the Open Access publication charges for this article was provided by the Swiss National Science Foundation.

Conflict of interest statement. None declared.

REFERENCES

1. Martin,G.M. (1982) Syndromes of accelerated aging. *Natl. Cancer Inst. Monogr.*, **60**, 241–247.
2. Yu,C.E., Oshima,J., Fu,Y.H., Wijsman,E.M., Hisama,F., Alisch,R., Matthews,S., Nakura,J., Miki,T. *et al.* (1996) Positional cloning of the Werner's syndrome gene. *Science*, **272**, 258–262.
3. Gray,M.D., Shen,J.C., Kamath-Loeb,A.S., Blank,A., Sopher,B.L., Martin,G.M., Oshima,J. and Loeb,L.A. (1997) The Werner syndrome protein is a DNA helicase. *Nat. Genet.*, **17**, 100–103.
4. Huang,S., Li,B., Gray,M.D., Oshima,J., Mian,I.S. and Campisi,J. (1998) The premature ageing syndrome protein, WRN, is a 3′—>5′ exonuclease. *Nat. Genet.*, **20**, 114–116.
5. Kamath-Loeb,A.S., Shen,J.C., Loeb,L.A. and Fry,M. (1998) Werner syndrome protein. II. Characterization of the integral 3′ —> 5′ DNA exonuclease. *J. Biol. Chem.*, **273**, 34145–34150.
6. Fujiwara,Y., Higashikawa,T. and Tatsumi,M. (1977) A retarded rate of DNA replication and normal level of DNA repair in Werner's syndrome fibroblasts in culture. *J. Cell. Physiol.*, **92**, 365–374.
7. Rodriguez-Lopez,A.M., Jackson,D.A., Iborra,F. and Cox,L.S. (2002) Asymmetry of DNA replication fork progression in Werner's syndrome. *Aging Cell*, **1**, 30–39.
8. Saintigny,Y., Makienko,K., Swanson,C., Emond,M.J. and Monnat,R.J.Jr. (2002) Homologous recombination resolution defect in Werner syndrome. *Mol. Cell. Biol.*, **22**, 6971–6978.

9. Crabbe,L., Verdun,R.E., Haggblom,C.I. and Karlseder,J. (2004) Defective telomere lagging strand synthesis in cells lacking WRN helicase activity. *Science*, **306**, 1951–1953.
10. Fukuchi,K., Martin,G.M. and Monnat,R.J.Jr. (1989) Mutator phenotype of Werner syndrome is characterized by extensive deletions. *Proc. Natl Acad. Sci. USA*, **86**, 5893–5897.
11. Salk,D., Au,K., Hoehn,H. and Martin,G.M. (1985) Cytogenetic aspects of Werner syndrome. *Adv. Exp. Med. Biol.*, **190**, 541–546.
12. Salk,D., Au,K., Hoehn,H. and Martin,G.M. (1981) Cytogenetics of Werner's syndrome cultured skin fibroblasts: variegated translocation mosaicism. *Cytogenet. Cell. Genet.*, **30**, 92–107.
13. Crabbe,L., Jauch,A., Naeger,C.M., Holtgreve-Grez,H. and Karlseder,J. (2007) Telomere dysfunction as a cause of genomic instability in Werner syndrome. *Proc. Natl Acad. Sci. USA*, **104**, 2205–2210.
14. Poot,M., Gollahon,K.A., Emond,M.J., Silber,J.R. and Rabinovitch,P.S. (2002) Werner syndrome diploid fibroblasts are sensitive to 4-nitroquinoline-N-oxide and 8-methoxypsoralen: implications for the disease phenotype. *FASEB J.*, **16**, 757–758.
15. Poot,M., Yom,J.S., Whang,S.H., Kato,J.T., Gollahon,K.A. and Rabinovitch,P.S. (2001) Werner syndrome cells are sensitive to DNA cross-linking drugs. *FASEB J.*, **15**, 1224–1226.
16. Poot,M., Gollahon,K.A. and Rabinovitch,P.S. (1999) Werner syndrome lymphoblastoid cells are sensitive to camptothecin-induced apoptosis in S-phase. *Hum. Genet.*, **104**, 10–14.
17. Lan,L., Nakajima,S., Komatsu,K., Nussenzweig,A., Shimamoto,A., Oshima,J. and Yasui,A. (2005) Accumulation of Werner protein at DNA double-strand breaks in human cells. *J. Cell Sci.*, **118**, 4153–4162.
18. Cheng,W.H., von Kobbe,C., Opresko,P.L., Arthur,L.M., Komatsu,K., Seidman,M.M., Carney,J.P. and Bohr,V.A. (2004) Linkage between Werner syndrome protein and the Mre11 complex via Nbs1. *J. Biol. Chem.*, **279**, 21169–21176.
19. Cooper,M.P., Machwe,A., Orren,D.K., Brosh,R.M., Ramsden,D. and Bohr,V.A. (2000) Ku complex interacts with and stimulates the Werner protein. *Genes Dev.*, **14**, 907–912.
20. Baynton,K., Otterlei,M., Bjoras,M., von Kobbe,C., Bohr,V.A. and Seeberg,E. (2003) WRN interacts physically and functionally with the recombination mediator protein RAD52. *J. Biol. Chem.*, **278**, 36476–36486.
21. Karmakar,P., Piotrowski,J., Brosh,R.M.Jr, Sommers,J.A., Miller,S.P., Cheng,W.H., Snowden,C.M., Ramsden,D.A. and Bohr,V.A. (2002) Werner protein is a target of DNA-dependent protein kinase *in vivo* and *in vitro*, and its catalytic activities are regulated by phosphorylation. *J. Biol. Chem.*, **277**, 18291–18302.
22. Kunkel,T.A. and Erie,D.A. (2005) DNA mismatch repair. *Annu. Rev. Biochem.*, **74**, 681–710.
23. Jiricny,J. (2006) The multifaceted mismatch-repair system. *Nat. Rev. Mol. Cell. Biol.*, **7**, 335–346.
24. Jiricny,J. and Marra,G. (2003) DNA repair defects in colon cancer. *Curr. Opin. Genet. Dev.*, **13**, 61–69.
25. Kadyrov,F.A., Dzantiev,L., Constantin,N. and Modrich,P. (2006) Endonucleolytic function of MutLα in human mismatch repair. *Cell*, **126**, 297–308.
26. Myung,K., Datta,A., Chen,C. and Kolodner,R.D. (2001) SGS1, the *Saccharomyces cerevisiae* homologue of BLM and WRN, suppresses genome instability and homologous recombination. *Nat. Genet.*, **27**, 113–116.
27. Sugawara,N., Goldfarb,T., Studamire,B., Alani,E. and Haber,J.E. (2004) Heteroduplex rejection during single-strand annealing requires Sgs1 helicase and mismatch repair proteins Msh2 and Msh6 but not Pms1. *Proc. Natl Acad. Sci. USA*, **101**, 9315–9320.
28. Goldfarb,T. and Alani,E. (2005) Distinct roles for the *Saccharomyces cerevisiae* mismatch repair proteins in heteroduplex rejection, mismatch repair and nonhomologous tail removal. *Genetics*, **169**, 563–574.
29. Pedrazzi,G., Perrera,C., Blaser,H., Kuster,P., Marra,G., Davies,S.L., Ryu,G.H., Freire,R., Hickson,I.D. *et al.* (2001) Direct association of Bloom's syndrome gene product with the human mismatch repair protein MLH1. *Nucleic Acids Res.*, **29**, 4378–4386.
30. Rasmussen,L.J., Rasmussen,M., Lee,B., Rasmussen,A.K., Wilson,D.M.3rd, Nielsen,F.C. and Bisgaard,H.C. (2000) Identification of factors interacting with hMSH2 in the fetal liver utilizing the yeast two-hybrid system. *In vivo* interaction through the C-terminal domains of hEXO1 and hMSH2 and comparative expression analysis. *Mutat. Res.*, **460**, 41–52.
31. Pedrazzi,G., Bachrati,C.Z., Selak,N., Studer,I., Petkovic,M., Hickson,I.D., Jiricny,J. and Stagljar,I. (2003) The Bloom's syndrome helicase interacts directly with the human DNA mismatch repair protein hMSH6. *Biol Chem.*, **384**, 1155–1164.
32. Orren,D.K., Brosh,R.M.Jr, Nehlin,J.O., Machwe,A., Gray,M.D. and Bohr,V.A. (1999) Enzymatic and DNA binding properties of purified WRN protein: high affinity binding to single-stranded DNA but not to DNA damage induced by 4NQO. *Nucleic Acids Res.*, **27**, 3557–3566.
33. Palombo,F., Iaccarino,I., Nakajima,E., Ikejima,M., Shimada,T. and Jiricny,J. (1996) hMutSβ, a heterodimer of hMSH2 and hMSH3, binds to insertion/deletion loops in DNA. *Curr. Biol.*, **6**, 1181–1184.
34. Raschle,M., Marra,G., Nystrom-Lahti,M., Schar,P. and Jiricny,J. (1999) Identification of hMutLβ, a heterodimer of hMLH1 and hPMS1. *J. Biol. Chem.*, **274**, 32368–32375.
35. Lamers,M.H., Perrakis,A., Enzlin,J.H., Winterwerp,H.H., de Wind,N. and Sixma,T.K. (2000) The crystal structure of DNA mismatch repair protein MutS binding to a G x T mismatch. *Nature*, **407**, 711–717.
36. Brosh,R.M.Jr, von Kobbe,C., Sommers,J.A., Karmakar,P., Opresko,P.L., Piotrowski,J., Dianova,I., Dianov,G.L. and Bohr,V.A. (2001) Werner syndrome protein interacts with human flap endonuclease 1 and stimulates its cleavage activity. *EMBO J.*, **20**, 5791–5801.
37. Mockli,N. and Auerbach,D. (2004) Quantitative β-galactosidase assay suitable for high-throughput applications in the yeast two-hybrid system. *Biotechniques*, **36**, 872–876.
38. Janscak,P., Garcia,P.L., Hamburger,F., Makuta,Y., Shiraishi,K., Imai,Y., Ikeda,H. and Bickle,T.A. (2003) Caracterization and mutational analysis of the RecQ core of the bloom syndrome protein. *J. Mol. Biol.*, **330**, 29–42.
39. Lee,J.W., Harrigan,J., Opresko,P.L. and Bohr,V.A. (2005) Pathways and functions of the Werner syndrome protein. *Mech. Ageing Dev.*, **126**, 79–86.
40. Brosh,R.M.Jr, Waheed,J. and Sommers,J.A. (2002) Biochemical characterization of the DNA substrate specificity of Werner syndrome helicase. *J. Biol. Chem.*, **277**, 23236–23245.
41. Blackwell,L.J., Wang,S. and Modrich,P. (2001) DNA chain length dependence of formation and dynamics of hMutSα.hMutLα.heteroduplex complexes. *J. Biol. Chem.*, **276**, 33233–33240.
42. Gradia,S., Subramanian,D., Wilson,T., Acharya,S., Makhov,A., Griffith,J. and Fishel,R. (1999) hMSH2-hMSH6 forms a hydrolysis-independent sliding clamp on mismatched DNA. *Mol. Cell.*, **3**, 255–261.
43. Surtees,J.A. and Alani,E. (2006) Mismatch repair factor MSH2-MSH3 binds and alters the conformation of branched DNA structures predicted to form during genetic recombination. *J. Mol. Biol.*, **360**, 523–536.
44. Her,C., Vo,A.T. and Wu,X. (2002) Evidence for a direct association of hMRE11 with the human mismatch repair protein hMLH1. *DNA Repair (Amst.)*, **1**, 719–729.
45. Cannavo,E., Gerrits,B., Marra,G., Schlapbach,R. and Jiricny,J. (2007) Characterization of the interactome of the human MutL homologues MLH1, PMS1, and PMS2. *J. Biol. Chem.*, **282**, 2976–2986.
46. Bellacosa,A., Cicchillitti,L., Schepis,F., Riccio,A., Yeung,A.T., Matsumoto,Y., Golemis,E.A., Genuardi,M. and Neri,G. (1999) MED1, a novel human methyl-CpG-binding endonuclease, interacts with DNA mismatch repair protein MLH1. *Proc. Natl Acad. Sci. USA*, **96**, 3969–3974.
47. Langland,G., Kordich,J., Creaney,J., Goss,K.H., Lillard-Wetherell,K., Bebenek,K., Kunkel,T.A. and Groden,J. (2001) The Bloom's syndrome protein (BLM) interacts with MLH1 but is not required for DNA mismatch repair. *J. Biol. Chem.*, **276**, 30031–30035.
48. Kamath-Loeb,A.S., Loeb,L.A., Johansson,E., Burgers,P.M. and Fry,M. (2001) Interactions between the Werner syndrome helicase and DNA polymerase delta specifically facilitate copying of tetraplex and hairpin structures of the d(CGG)n trinucleotide repeat sequence. *J. Biol. Chem.*, **276**, 16439–16446.

49. Mohaghegh,P., Karow,J.K., Brosh,R.M.Jr, Bohr,V.A. and Hickson,I.D. (2001) The Bloom's and Werner's syndrome proteins are DNA structure-specific helicases. *Nucleic Acids Res.*, **29**, 2843–2849.
50. Vorlickova,M., Chladkova,J., Kejnovska,I., Fialova,M. and Kypr,J. (2005) Guanine tetraplex topology of human telomere DNA is governed by the number of (TTAGGG) repeats. *Nucleic Acids Res.*, **33**, 5851–5860.
51. Larson,E.D., Duquette,M.L., Cummings,W.J., Streiff,R.J. and Maizels,N. (2005) MutSα binds to and promotes synapsis of transcriptionally activated immunoglobulin switch regions. *Curr. Biol.*, **15**, 470–474.
52. Campbell,M.R., Wang,Y., Andrew,S.E. and Liu,Y. (2006) Msh2 deficiency leads to chromosomal abnormalities, centrosome amplification, and telomere capping defect. *Oncogene*, **25**, 2531–2536.
53. Zhang,N., Kaur,R., Lu,X., Shen,X., Li,L. and Legerski,R.J. (2005) The Pso4 mRNA splicing and DNA repair complex interacts with WRN for processing of DNA interstrand cross-links. *J. Biol. Chem.*, **280**, 40559–40567.
54. Zhang,N., Lu,X., Zhang,X., Peterson,C.A. and Legerski,R.J. (2002) hMutSbeta is required for the recognition and uncoupling of psoralen interstrand cross-links *in vitro*. *Mol. Cell. Biol.*, **22**, 2388–2397.
55. Bennett,S.E., Umar,A., Oshima,J., Monnat,R.J.Jr. and Kunkel,T.A. (1997) Mismatch repair in extracts of Werner syndrome cell lines. *Cancer Res.*, **57**, 2956–2960.
56. Doherty,K.M., Sharma,S., Uzdilla,L.A., Wilson,T.M., Cui,S., Vindigni,A. and Brosh,R.M.Jr. (2005) RECQ1 helicase interacts with human mismatch repair factors that regulate genetic recombination. *J. Biol. Chem.*, **280**, 28085–28094.
57. Yang,Q., Zhang,R., Wang,X.W., Linke,S.P., Sengupta,S., Hickson,I.D., Pedrazzi,G., Perrera,C., Stagljar,I. *et al.* (2004) The mismatch DNA repair heterodimer, hMSH2/6, regulates BLM helicase. *Oncogene*, **23**, 3749–3756.

Article IV

Acetylation of RECQL4, the Rothmund-Thomson-RAPADILINO- and Baller-Gerold-Syndrome gene product, by the histone acetyltransferase p300 regulates its subcellular localization.

Tobias Dietschy, Igor Shevelev, Raymond Mak, Mohammad Fahad Miah, Daniel Hess, Monika Fey, Pavel Janscak, Michael Hottiger and Igor Stagljar

Submitted

In this work, I have performed all experiments except those for figures 1B and 2

Acetylation of RECQL4, the Rothmund-Thomson-,RAPADILINO- and Baller-Gerold-Syndrome gene product, by the histone acetyltransferase p300 regulates its subcellular localization

Tobias Dietschy[1], Igor Shevelev[1], Raymond Mak[1], Mohammad Fahad Miah[1], Daniel Hess[2], Monika Fey[3], Pavel Janscak[4], Michael Hottiger[3] and Igor Stagljar[1*]

[1] Department of Biochemistry and Department of Medical Genetics & Microbiology, Faculty of Medicine, Terrence Donnelly Centre for Cellular and Biomolecular Research (dCCBR), University of Toronto, 160 College Street, Toronto ON, Canada, M5S 3E1

[2] Protein Analysis Facility, Friedrich Miescher Institute, Maulbeerstr.66, CH-4058 Basel

[3] Institute of Veterinary Biochemistry and Molecular Biology, University of Zürich, Winterthurerstr. 190, CH-8057 Zürich, Switzerland

[4] Institute of Molecular Cancer Research (IMCR), University of Zürich, Winterthurerstr. 190, CH-8057 Zürich, Switzerland

Running title: RECQL4 acetylation by the histone acetyltransferase p300

* Communicating author

Tel: +1 416 946 78 28

Fax: +1 416 978 82 87

Email:igor.stagljar@utoronto.ca

RECQL4 is a member of the conserved RecQ family of DNA helicases that play important roles in the maintenance of genome stability in all organisms examined. Although it was reported that genetic alterations in the *RECQL4* gene are associated with three autosomal recessive disorders called Rothmund-Thomson, RAPADILINO, and Baller-Gerold syndromes, respectively, the molecular role of RECQL4 still remains poorly understood. Here we show that RECQL4 specifically interacts with the histone acetyltransferase p300 both, *in vivo* and *in vitro*, and that p300 acetylates one or more of the lysine residues at positions 376, 380, 382, 385, and 386 of RECQL4. Furthermore, we report that these five lysine residues lie in a short motif of 30 amino acids that is essential for the nuclear localization of RECQL4. Remarkably, the acetylation of RECQL4 by p300 *in vivo* leads to a significant shift of a proportion of RECQL4 protein from the nucleus to the cytoplasm. Lastly, we demonstrate that p300 stimulates the ATPase activity of RECQL4 *in vitro*. Our results provide first evidence of a post-translational modification of the RECQL4 protein and suggest that acetylation of RECQL4 by p300 regulates the trafficking of RECQL4 between the nucleus and the cytoplasm.

Genome instability plays a major role in the development and progression of cancer. All organisms have developed pathways to mitigate DNA damage by employing enzymes involved in all DNA metabolic processes including replication, recombination, and repair (1). The fundamental importance of these enzymes, such as DNA helicases and acetyltransferases, is highlighted by the variety of genetic instability disorders arising from enzymes defective in these functions (2, 3).

One family of proteins required to maintain genome stability is the RecQ helicase family (4). Humans possess five RecQ homologues: *RECQL1*, *BLM*, *WRN*, *RECQL4*, and *RECQL5*. Five autosomal recessive disorders, characterized by genomic instability, cancer progression, and developmental abnormalities, have been associated with defects in the BLM (Bloom syndrome) (5), WRN (Werner syndrome) (6), and RECQL4 (Rothmund-Thomson (RTS), RAPADILINO, and Baller-Gerold syndromes (BGS) (7-10) gene products. RTS is an unusual autosomal recessive condition associated with poikiloderma, growth deficiency, juvenile cataracts, premature aging and a predisposition to malignant tumours, particularly osteosarcomas (11). Interestingly, mutations in the *RECQL4* gene cause only 60% of all RTS cases (12). Accordingly, RTS seems to be a heterogenous disease and mutations in other, yet unidentified gene(s) seem to be responsible for the phenotype of the remaining 40% of RTS patients. The number of mutations found in *RECQL4* is quite low, ranging from nonsense,

frameshift, and splice site mutations to intronic insertions and deletions (8). Most of them result in premature termination of protein translation yielding truncated RECQL4 proteins that often lack a large part of the helicase domain (13). Cells derived from RTS patients show genomic instability, including trisomy, aneuploidy and chromosomal rearrangements (11, 14). Additionally, RTS cells are sensitive to ionizing radiation and oxidative stress (15, 16).

RAPADILINO syndrome is another autosomal recessive disease associated with mutations in the *RECQL4* gene (8). The acronym stands for the characteristic clinical features: RAdial hypo-/aplasia, Patellae hypo-/aplasia and cleft or highly arched PAlate, DIarrhoea and DIslocated joints, LIttle size and LImb malformation, NOse slender and NOrmal intelligence. The most common mutations of the *RECQL4* gene in RAPADILINO patients represent in-frame deletions of exon 7 which do not affect the helicase domain of RECQL4 protein (8). Although RAPADILINO patients share some clinical features with RTS patients, like photosensitivity with extra pigmentation of skin and growth deficiency, there are unique diagnostic findings such as joint dislocations and patellar hypo/aplasia. In contrast to RTS, RADADILINO syndrome is more common in females, and only 7% of the current RAPADILINO patients developed malignant tumors, mainly osteosarcomas (17).

BGS is the third recently reported autosomal recessive disorder linked to mutations in the *RECQL4* gene (7). The clinical hallmarks of BGS are radial aplasia/hypoplasia and craniosynostosis**.** To date, most mutations of *RECQL4* found in BGS patients represent a R1021W missense mutation and a 2886 delta T frameshift mutation of exon 9. Surprisingly, none of the 24 BGS patients reported so far show any predisposition for cancer (7). Furthermore, the results derived from the experiments with various *RECQL4*$^{-/-}$ mice showed that these mice accumulate defects that clearly reflect the situation in humans, i.e. different mutations in the *RECQL4* gene lead to different phenotypes (18-20).

Thus, the cumulative set of data suggests that RECQL4 has roles independent of the helicase domain. Whether the role of the RECQL4 N-terminal domain is independent of the helicase domain, or if it is sufficient to perform a partial function remains to be elucidated in future experiments.

While the distinct molecular functions of BLM and WRN helicases have been widely characterized in the last decade, the precise molecular and cellular role of the RECQL4 protein has not yet been elucidated. Recent studies revealed an involvement of RECQL4 protein in DNA replication (21, 22) and repair of DNA double strand breaks (DSB) by homologous recombination (HR) (23, 24). The localization of RECQL4 in different mammalian cells has been studied extensively (9, 23, 25-27). Several cell biological and biochemical studies indicated that RECQL4 can be found both in the nucleus and cytosol of different transformed cell lines (23, 27). In the nucleus, RECQL4 forms discrete nuclear foci in response to DNA damage that coincide with those formed by promyelocytic leukaemia (PML) bodies and Rad51, further suggesting a role in DNA DSB repair by HR (23). Furthermore, upon oxidative damage, RECQL4 moves to the nucleolus in living HeLa cells and the nucleolar localization signal (NOS) was mapped to amino acids (aa) 376-386 in the RECQL4 sequence (26). Recent findings indicated that RECQL4 aa 363-492 are important for the nuclear import and localization of RECQL4 protein in different mammalian cells, while aa 420-463 encoded by exon 7 are crucial for its retention in the nucleus (25). In the cytosol, RECQL4 forms stable complexes with cytosolic ubiquitin ligases UBR1 and UBR2, which function in the N-end rule pathway (27). However, the exact mechanism of how RECQL4 is transported from the nucleus to the cytosol as well as what the function of the cytosolic RECQL4 protein is, remains totally unexplored.

Another class of enzymes, known as acetyltransferases, are also responsible for maintaining genome stability (28, 29). Histone acetyltranferases (HATs) catalyze a reversible transfer of an acetyl group from acetyl-coenzyme A to ε-NH_3^+ of lysine residues on core histone tails (30). Traditionally, HATs have been associated exclusively with the acetylation of histone tails and transcriptional regulation through chromatin remodelling. By alleviating repressive histone-DNA binding, and thus facilitating the association of transcription factors with DNA, histone acetylation can lead to increased transcriptional activity (31). One such HAT is p300/CBP which includes two distinct but related proteins p300 and CBP, and participates in many physiological processes, including proliferation, differentiation, and apoptosis (32). Although p300/CBP was originally identified as acetylating lysine residues on core histones (33, 34), in the past decade a growing body of evidence suggested that other non-histone targets, including proteins involved in the regulation of transcription such as p53, E2F1, EKLF, TFIIEβ, TFIIF, TCF, GATA1, HMGI(Y) and ACTR (35) as well as DNA repair/replication proteins such as PCNA (36), FEN-1 (37), TDG (38), APE1 (39), NEIL2 (40), DNA polymerase β

(41), and human 8-oxoguanine-DNA glycosylase (OGG1) (42) are also acetylated by p300/CBP. Acetylation by p300/CBP can modulate the activity of DNA repair/replication proteins either positively or negatively. For example, acetylation of FEN1 by p300/CBP reduces the nuclease activity of FEN1 presumably as a result of the reduced DNA binding (37). On the other hand, acetylation of TDG by p300/CBP does not affect its DNA glycosylase activity, which is stimulated by sumoylation, another covalent post-translational modification (43). Furthermore, acetylation of NEIL2, an oxidized pyrimidine-specific DNA glycosylase, was shown to inhibit its enzymatic activity (40) whereas acetylation of human OGG1 by p300/CBP significantly increases OGG1's activity *in vitro* in the presence of AP-endonuclease by reducing its affinity for the abasic (AP) site product (42). All these examples highlight the importance of p300/CBP in the DNA base excision repair process.

In spite of several recent studies showing altered DNA repair and substrate specificity of DNA repair/replication proteins due to acetylation by p300/CBP, acetylation of RECQL4 as well as its physiological relevance has not been addressed so far. In this paper, we report the physical and functional interaction between RECQL4 and p300. Overexpression of p300, but not the catalytic dead mutant (p300 ΔHAT), leads to a significant translocation of a proportion of RECQL4 protein from the nucleus to the cytoplasm. The same effect can be observed by treating the cells with histone deacetylase (HDAC) inhibitors TSA and nicotinamide, suggesting that indeed, acetylation of RECQL4 by p300 is involved in the translocation of RECQL4 towards the cytoplasm. p300 specifically acetylates RECQL4 on a stretch of Lysine residues, previously shown to function as NOS/NLS sequence of RECQL4 (25, 26). Furthermore, we demonstrate that mutation of these lysine residues to alanine (Lys 376, 380, 382, 385, 386 Ala), but not to arginine (Lys 376, 380, 382, 385, 386 Arg), completely abolishes the nuclear import of RECQL4 in human cells. Additionally, the fusion of the RECQL4 aa 376-386 to the N-terminus of β-Galactosidase leads to the nuclear import of this 100kDa protein in mammalian cells, indicating the importance of the positively charged amino acid residues for the nuclear import of the RECQL4 protein. Lastly, we show that p300 has a stimulatory effect on the RECQL4 ATPase activity *in vitro*. Taken together, our data help to understand the mechanism by which RECQL4 is translocated from the nucleus to the cytoplasm in mammalian cells.

MATERIALS AND METHODS

Expression and purification of p300- and RECQL4 GST fragments in *E.coli*

All p300 and RECQL4 protein fragments were expressed in *E. coli* [HMS174(DE3) for p300, BL21(DE3) for RECQL4; Novagen] as N-terminal fusions with glutathione-S-transferase (GST), using the plasmid vector pGEX-6P2 (GE Healthcare) with the isopropyl-β-D-thiogalactoside (IPTG)-inducible T7 promoter. Overnight cultures grown in Luria Broth at 37°C were diluted 1:100 into fresh medium and incubated until OD_{600} reached 0.6. IPTG was added to 0.5mM, and the cultures were incubated at 15°C for 20h. Cells were harvested by centrifugation and re-suspended in buffer A (50 mM Tris, 50 mM NaCl, 20% glycerol, pH 8.0 supplemented with 1μg/ml bestatin, leupeptin and pepstatin protease inhibitors) and stored at -20°C overnight (>12h). All subsequent steps were performed at 4°C or on ice. Following sonication (8 × 15s bursts with 5s cooling), lysates were clarified by centrifugation (50,000 × *g* for 45 min) and added to glutathione Sepharose 4B beads (GE Healthcare). After washing with 20 mM KH_2PO_4, 140 mM NaCl, 0.2% [v/v] Triton X-100, pH 8.0, bound proteins were eluted in buffer A containing 10 mM glutathione. Proteins were dialyzed overnight against buffer B (20 mM Tris, 200 mM NaCl, 1mM EDTA, 0.5% [v/v] NP40, 0.5% [v/v] PMSF, 20% [v/v] glycerol) and stored at -80°C.

Purification of RECQL4

The human RecQL4 cDNA was cloned into pET21b vector (Novagen). The cDNA of GST was cut from pET41a vector (Novagen) and cloned N-terminally of the RecQL4 cDNA in pET21b. RECQL4 protein was expressed in BL21(DE3)Rosetta-pLysS cells. Overnight cultures grown in Luria Broth at 37°C were diluted 1:100 into fresh medium and incubated until OD_{600} reached 0.4. IPTG was added to 0.3 mM, and the cultures were incubated at 18°C for 22h. Cells from 12 liters of culture were harvested by centrifugation, and pellet was resuspended on ice in 300 ml of NiLB (pH 8.1, 10 mM Tris-HCl, 30 mM KH_2PO_4, 0.5 M NaCl, 20 mM imidazole supplemented with 1 mM PMSF and 2 μg/ml of each bestatin, leupeptin and pepstatin). Cells were lysed by French press (2x) and sonication. After centrifugation (20,000 rpm, 2 hours, +4° C, SS-34 rotor), the supernatant was loaded on a 1 ml HisHiTrap (GE Healthcare) column. The Column

was washed by 100 ml NiLB, 30 ml NiLB containing 1 M NaCl, 30 ml NiLB with 1 % TritonX-100, 30 ml NiLB with 60 mM imidazole. Protein was eluted by 300 mM imidazole in NiLB containing 10% glycerol. RECQL4 protein containing fractions were pooled, desalted to GSTLB (GST-loading buffer, pH 7.4, containing 30 mM Tris-HCl, 150 mM NaCl, 1 mM DTT, 10 % glycerol, supplemented with 0.5 mM PMSF and 1 μg/ml of each bestatin, leupeptin and pepstatin) using a 5 ml desalting column (GE Healthcare) and applied to 1 ml GST-Sepharose HiTrap column. After washing with 50 ml GSTLB containing 0.2% Triton X-100, bound protein was eluted by GSTEB (GST-elution buffer, pH 8.1 containing 50 mM Tris-HCl, 150 mM NaCl, 10 % glycerol, 10 mM glutathione, 1 mM DTT supplemented with 0.5 mM PMSF and 1 μg/ml of each bestatin, leupeptin and pepstatin). Eluted RECQL4 Protein was dialysed overnight against buffer C (pH 8.0, 40 mM Tris-HCl, 150 mM NaCl, 1 mM DTT, 1 mM EDTA, 40 % glycerol and protease inhibitors) and stored at -80° C.

GST pull-down assays

293T whole cell extracts, containing over-expressed full-length RECQL4 or p300 (500 μg of total protein), were incubated with 10 μg of purified GST- p300 or RecQL4 protein fragments (or GST alone), 50 μl glutathione-Sepharose 4B beads (GE Healthcare), and 100 μg/ml ethidium bromide in buffer B in a total reaction volume of 600 μl. Bound proteins were eluted with 30 μl Laemmli buffer, boiled for 5 min at 100°C and subjected to western blot analysis using α-RECQL4 (Rabbit polyclonal, ab34800-100, Abcam) or p300 antibody (Mouse polyclonal, ab3164-500, Abcam).

Cellculture and indirect immunofluorescence assays

U2OS, 293T and HeLa cells were maintained in Dulbecco's Modified Eagle's Medium (Gibco) supplemented with 10% bovine fetal serum and 1% penicillin-streptomycin in 5% CO_2 atmosphere at 37°C. At 50% confluency, cells grown on glass slides were transiently transfected with 2 μg of appropriate plasmid DNA using Metafectene (Biontex).

For the indirect immunofluorescence assays, cells growing on glass slides were incubated in PBS for 5 minutes, fixed with methanol (30 min at -20°C), and washed in acetone (30 sec at -20°C). After a blocking step (5% BSA in PBS, 20 min at RT), slides were incubated with a mixture appropriate antibodies (α-His, 1:200, Goat polyclonal, sc-499-6, Santa Cruz; α-FLAG, 1:2000, Mouse polyclonal, F-1804, Sigma; α-β-Galactosidase, 1:5000, Rabbit polyclonal, ab616, Abcam). Rabbit antibodies were detected with AlexaFluor 488 conjugated goat anti-rabbit IgG (1:400 in blocking buffer, Molecular Probes), the goat antibodies were detected with AlexaFluor 546 conjugated donkey anti-goat IgG (1:400 in blocking buffer, Molecular Probes), and mouse antibodies were detected with AlexaFluor 488 conjugated donkey anti-mouse IgG (1:400 in blocking buffer, Molecular Probes). To visualize nuclear DNA, slides were incubated with DAPI (0.4 μg/ml). After washing, slides were mounted in Vectashield (Vector Laboratories) and viewed under a ZEISS Axiovert 200M Microscope. Images were processed by Axiovision software. For statistical analysis at least 200 cells were counted in two independent experiments.

Synchronization of cells and DNA damaging treatments

293T cells were grown as described above. For G1/S and S phase synchronization, cells (50% confluency) were grown for 15h in the presence of 2 mM thymidine. After washing with PBS, cells were grown for 12h in complete medium. Subsequent addition of 2 mM thymidine for another 15h led to synchronization of the cell population in G1/S transition. For synchronization in S-phase, the cells were released from double-thymidine block by washing with PBS and incubated for 4h in complete medium before harvesting. For G2/M synchronization, cells were grown in the presence of nocodazole (400 ng/ml) overnight (12h) before harvesting. To induce DNA damage, cells were treated with 10 μM Cisplatin (12h), 10 μM Etoposide (12h) or 5 μM Bleomycin (12h) before harvesting.

Co-immunoprecipitation experiments

Whole cell extract, supplemented with ethidium bromide (100 μg/ml), containing ectopically expressed His-RECQL4 (1 mg of total protein) or FLAG-p300 (1.5 mg of total protein) respectively, was incubated with 1.5μg of anti-p300 antibody (mouse polyclonal, 554215, BD Pharmingen) or 1.5μg of an anti-RECQL4 antibody (Rabbit polyclonal, ab 34800-100, Abcam), respectively. Immune complexes were bond to protein G-Sepharose Fast Flow beads (GE Healthcare) for 4h at 4°C. The final volume was raised to 1ml with IP buffer [20 mM HEPES pH 7.5, 5 mM $MgCl_2$, 80 or 120 or 160 mM NaCl, 0.1% (w/v) NP40, supplemented with 1μg/ml bestatin, leupeptin, and pepstatin]. Immunoprecipitated p300 or RECQL4 protein was visualized by western blot analysis using an anti-p300 or anti-RECQL4 antibody, respectively, and co-immunoprecipitated His-RECQL4 or FLAG-p300 protein was visualized by western blot analysis using an α-His (Goat

polyclonal, sc-499-6, Santa Cruz) or α-FLAG (Mouse, polyclonal, F-1804, Sigma) antibody, respectively.

ELISA-based protein binding

Purified recombinant p300 was diluted to a concentration of 20 nM in carbonate buffer [16 mM Na2CO3, 34 mM NaHCO3 (pH 9.6)] and added to wells of a 96-well microtiter plate (50µl/well). Plates were incubated overnight at 4°C. For control reactions, wells were pre-coated with an equivalent amount of bovine serum albumin (BSA). After aspiration of the samples, the wells were blocked with blocking buffer [phosphate-buffered saline, 0.5% (v/v) Tween 20, and 3% (w/v) BSA] for 2 hours at 37°C (200 µl/well). Following blockage, the wells were incubated with increasing concentrations of purified recombinant RECQL4 protein for 1 hour at 37°C. Wells were washed four times with blocking buffer to eliminate unbound proteins, and incubated with RECQL4 antibody (Rabbit polyclonal, 1:2000, ab34800-100, Abcam) diluted in blocking buffer. Plates were incubated for 1 hour at 37°C. After four washings with blocking buffer, horseradish peroxidase-conjugated anti-rabbit secondary antibody (1:10,000 in blocking buffer) was added and the plates were incubated at 37°C for 30 minutes. After extensive washing with blocking buffer, the protein complexes were detected using o-Phenylenediamine dichloride (Sigma) dissolved in 0.1 M citratephosphate buffer (pH 5.0) containing 0.03% hydrogen peroxide (1 mg/ml). The reactions were terminated after 10 minutes by adding 50 µl of 2 M H2SO4. The plates were scanned in a microplate reader (Molecular Devices) for absorbance at 450 nm. The A450 values, corrected for background signal in the presence of BSA, were plotted as a function of the concentration of RECQL4 protein using the GraphPad Prism software.

***In vivo* Acetylation Assay**

One milligram of total protein extracted from 293T cells, ectopically expressing RECQL4 and one of the selected histone acetyltransferases (p300, GCN5, pCAF, HAT1), was incubated for 4h at 4°C with 2 μg of an anti-His antibody (Goat polyclonal, sc-499-6, Santa Cruz) bound to protein A-Sepharose 4B beads (GE Healthcare). Immunoprecipitated RECQL4 protein was visualized by western blot analysis using the anti-His antibody. The membrane was stripped in 50 mM Tris pH8, 5 mM β-mercaptoethanol, 2% sodium dodecyl sulfate for 1h at 52°C and acetylated lysine residues were visualized by a polyclonal anti-acetylated lysine antibody (Rabbit polyclonal, 1: 1000, 9441-5, Cell Signaling).

***In vitro* Acetylation Assay**

Purified GST-RECQL4 fragments (1 □g) were incubated with 0.1 μCi [14C] acetyl coenzyme A (CFA390, Amersham Biosciences) and purified p300 (1 □g) in 30 μl HAT-Buffer (50 mM Tris [pH 8.0], 10% [v/v] glycerol, 150 mM NaCl, 1 mM DTT, 1 mM PMSF, 10 mM Na butyrate) at 30°C for 1h. The reactions were subjected to SDS-PAGE analysis. Gels were stained with Coomassie and subsequently subjected to autoradiography.

ATPase Assay

Purified full length RECQL4 (40 nM) was incubated in the presence or absence of p300 in 10 μl HAT Buffer (50 mM Tris pH 7.5, 50 mM KCl, 10% Glycerol, 1 mM DTT, 1 mM PMSF, 1 mM Na-Butyrate) at 30°C for 30 min. Where required Ac-Co-A was added to a final concentration of 50 μM. This mixture was then supplemented with M13 ssDNA plasmid (75µM Nucleotides) and 10 μl of buffer A (30 mM Tris–HCl, pH 7.5, 2.5 mM $MgCl_2$, 1 mM DTT, and 100 μg/ml BSA) containing 1 mM $[_{-}{}^{32P}]$ATP. The reactions were incubated at 37°C for 30 min and the released 32Pi was separated from the unhydrolyzed ATP by thin layer chromatography using PEI-Cellulose (Marchery-Nagel). The data was quantified using the scion image software.

Immunodepletion

Two micrograms of rabbit polyclonal anti-RECQL4 antibody (ab34800-100, Abcam) or control rabbit IgG (sc-2027, Santa Cruz) were incubated for 1 h at 4°C with 40 µl Protein G Sepharose beads (GE Healthcare). After washing three times with reaction buffer, antibody-bound beads were incubated with 100 nM RECQL4 in the reaction buffer for 1 h at 4°C. Beads were removed by centrifugation. Supernatants were assayed for ATPase activity as described above.

RESULTS

***In vivo* acetylation of RECQL4 by p300 and interaction of the full length proteins**

We wanted to investigate whether RECQL4 is acetylated in mammalian cells. To identify a potential acetyltransferase that acetylates RECQL4 *in vivo*, His-RECQL4 was overexpressed in 293T cells with each of the four major human acetyltransferases (p300, pCAF, Gcn5, and HAT1). Notably, we were forced to use overexpressed RECQL4 protein in this assay due to a low expression level of the endogenous *RECQL4* gene. An anti-His antibody was used to immunoprecipitate RECQL4 from whole cell extracts (Fig. 1A, upper left panel). A control IgG

antibody failed to precipitate RECQL4 and confirmed the specificity of the anti-His antibody for His-RECQL4 (Fig. 1A, lane 6). Acetylation status of His-RECQL4 was visualized by western blot analysis using an antibody recognizing acetylated lysines (Fig. 1A, lower left panel). Although western blot analysis revealed that all four acetyltransferases (p300, pCAF, GCN5, or HAT1) were expressed to similar levels (Fig. 1A, right panel), RECQL4 was found to be strongly acetylated only in cells overproducing p300, suggesting that p300 may be the acetylatransferase that acetylates RECQL4 *in vivo*. Additionally, neither synchronizing cells in different stages of the cell cycle (G1/S and S-phase using double thymidine block, G2/M using nocodazole) nor treatment with different DNA damaging agents (Cisplatin, Etoposide, Bleomycin) triggered RECQL4 acetylation *in vivo* (Supplementary Figure 1A/B).

We next analysed whether RECQL4 and p300 interact in human cells. For this, FLAG-p300 was transiently transfected into 293T cells and total cell extract was immunoprecipitated with anti-RECQL4 antibody and analysed by immunoblotting using an anti-FLAG antibody. We found that FLAG-p300 was efficiently co-precipitated by the anti-RECQL4 antibody (Fig. 1B, lane 3), but was not detected when the control IgG antibody was used (Fig.1B, lane 2). To further confirm the interaction between RECQL4 and p300 in human cells, the reciprocal coimmunoprecipitation experiment was also carried out using a polyclonal anti-p300 antibody. The His-RECQL4 could be specifically co-immunoprecipitated with endogenous anti-p300 antibody (Fig. 1B, lane 6), but not with the control IgG antibody (Fig. 1B, lane 5). It should be noted that cell extracts used in the above-mentioned experiments were supplemented with ethidium bromide excluding the possibilitiy that association of RECQL4 and p300 is mediated by DNA.

We next performed an ELISA-based protein-binding assay using purified recombinant proteins to determine whether RECQL4 and p300 interact directly. Increasing concentrations of purified recombinant RECQL4 ranging from 0 to 40 nM were incubated in wells that had been pre-coated with purified p300 at a concentration of 20 nM and subsequently blocked with BSA to prevent non-specific interactions. After extensive washing, the bound RECQL4 was incubated with a specific anti-RECQL4 polyclonal antibody followed by a colorimetric assay to quantify the binding. In control experiments, RECQL4 was incubated in wells pre-coated only with BSA. We found that RECQL4 specifically bound to p300-coated wells in a dose dependent manner, but was not in wells pre-coated with BSA, indicating a direct interaction in the nanomolar range (Fig. 1C). Taken together, these data indicate that p300 acetylates RECQL4 *in vivo*, that RECQL4 and p300 form a complex in human cells, and that the proteins interact directly *in vitro*.

Mapping of the RECQL4 and p300 interaction regions

To confirm the RECQL4/p300 interaction and to map the RECQL4 interaction region in p300, RECQL4 was divided into four fragments which were subsequently cloned and expressed as glutathione S-transferase (GST) fusion proteins (Fig. 2A and 2B). GST pull-down experiments with these fragments were performed using total cell extracts containing overexpressed FLAG-p300 derived from transiently transfected 293T cells. Western blot analysis of bound proteins using an anti-FLAG antibody indicated that only fragment 2 of RECQL4 was able to interact with full length p300 (Fig. 2C, lane 4). This fragment spans amino acid (aa) residues 1-408 of RECQL4 and contains the RECQL4 nucleolar localization signal (NOS) previously mapped to aa 376-386 (26) and a part of the helicase domain (see also Fig. 2A).

To map the RECQL4-interaction region in p300, p300 was also divided into several fragments labelled 1-5, which were subsequently expressed and purified as GST fusions (Fig. 2D and 2E). GST pull-down experiments were performed using whole cell extracts of 293T cells over-producing His-RECQL4. Western blot analysis of bound proteins using a specific anti-His antibody indicated that only fragment 4 of p300 was able to interact with full length RECQL4 (Figure 2F, lane6). This fragment spans aa 1459-1892 and contains a part of the p300 HAT domain that was previously shown to interact with human FEN-1 (37).

p300 enhances RECQL4 ATPase activity

The physical interaction between RECQL4 and p300 suggested the possibility that the two proteins might affect each other's activities. To test this hypothesis, we first wanted to determine whether purified p300 influences RECQL4 ATPase activity. In order to purify full length RECQL4 from *E.coli*, we constructed an expression vector in which the RECQL4 cDNA was flanked by an N-terminal GST and a C-terminal His tag (Fig. 3A). After large scale expression of RECQL4 in *E.coli*, we affinity purified the protein using glutathione-Sepharose and Nickel-NTA Agarose and analysed the peak fraction by Coomassie staining (Fig. 3B, left panel) and by western blot using anti-GST and anti-RECQL4 antibodies (Fig. 3B, right panel). In agreement with previously published data, the yield of RECQL4 protein was very low, which is presumably due to proteolysis in E. coli (44)

Furthermore, we tested whether our RECQL4 prep possessed single-strand DNA (ssDNA) and Mg^{+2} dependent ATPase activity as previously described (44). As shown in Fig. 3C, the hydrolysis of ATP by RECQL4 was indeed dependent on ssDNA and Mg^{+2}. Only minor levels of ATPase activity were observed with Ca^{+2} as a co-factor, as well as if ssDNA was substituted with dsDNA or omitted. Additionally, we immunodepleted RECQL4 from the purified peak fraction using an anti-RECQL4 antibody and assayed the supernatant for ATPase activity (Fig. 3D). A twofold reduction in ATPase activity was observed compared to untreated sample or sample immunodepleted using a control rabbit IgG. This further confirms that the ATPase activity in the peak fraction is mediated by RECQL4 protein.

To investigate whether p300 affects the RECQL4 ATPase activity, RECQL4 was incubated with recombinant p300 purified from insect cells and subsequently tested in ATPase assay (Fig. 3E and 3F). Interestingly, the ATPase activity of RECQL4 preincubated with p300 was increased twofold compared to RECQL4 alone or RECQL4 preincubated with another human acetyltransferase Gcn5 (Fig. 3E). p300 alone showed no ATPase activity, confirming that purified p300 from insect cells was not contaminated with an ATPase activity.

We next wanted to investigate whether acetylation of RECQL4 would have an effect on its ATPase activity. Purified RECQL4 was preincubated with purified p300 either in the presence or absence of Acetyl Co-enzyme A (AcCoA) and subsequently tested in ATPase assay (Fig. 3F). Again, p300 had a stimulatory effect on RECQL4 ATPase activity but acetylation of RECQL4 by p300 (RECQL4+p300+AcCoA) slightly decreased this stimulatory effect. We found that ATPase activity of RECQL4 in the presence of AcCoA was only slightly lower than that measured in its absence, indicating that p300-mediated acetylation of RECQL4 has no significant effect on its ATPase activity.

Identification of acetylation sites on RECQL4 *in vitro* and *in vivo*

Several studies revealed that p300 preferentially acetylates stretches of lysine residues of substrate proteins (37, 45-48). The RECQL4 amino acid sequence contains 32 lysine residues and the only lysine stretch is located in the previously identified nucleolar localization signal (NOS) of RECQL4 with five lysine residues at positions 376, 380, 382, 385, and 386 (26). Two His-RECQL4 NOS mutants, with all five lysine residues mutated to either alanine (K□A) or to arginine (K□R), were generated using site-directed mutagenesis in order to identify the extent of acetylation of the NOS lysine residues within RECQL4 (Fig. 4A). Wildtype (WT), K□A, and K□R His-RECQL4 were subsequently co-transfected into 293T cells in the presence or absence of p300, and immunoprecipitated from whole cell extracts using an anti-His antibody (Figure 4B, upper left panel). A control IgG serum confirmed the specificity of the anti-His antibody for His-RECQL4 in the immunoprecipitation reaction (Fig. 4B, lane 7). The extent of RECQL4 acetylation was visualized by western blot analysis using an anti-acetylated lysine antibody (Fig. 4B, lower left panel). Although co-transfection of WT His-RECQL4 and p300 resulted in acetylation of RECQL4 (Fig. 4B, lane 6), the acetylation of the K□A (Fig. 4B, lane 2) and K□R (Fig. 4B, lane 4) His-RECQL4 mutants was not detected, suggesting that at least one of the lysine residues at positions 376, 380, 382, 385, and 386 of RECQL4 is required for acetylation by p300. To further investigate which of the five lysine residues is acetylated *in vivo*, we generated single (K382R) (Fig. 4B, lanes 9 and 10), double (K385,386R) (Fig. 4B, lanes 11 and 12) and triple (K376,380,382R) (Fig. 4B, lanes 13 and 14) mutants by site directed mutagenesis. The three mutants were co-transfected in the presence or absence of p300 in 293T cells and analysed as described above (Fig. 4B, left panel). Co-transfection of all three mutants and p300 resulted in acetylation of RECQL4 (Fig. 4B, lanes 10, 12 and 14), suggesting that more than one lysine residue at the aa positions 376, 380, 382, 385, and 386 is acetylated by p300.

To confirm that the stretch of lysine residues in RECQL4 at the positions 376, 380, 382, 385, and 386 is acetylated by p300, RECQL4 was divided into several fragments, labelled A-E, that were subsequently expressed and purified as GST fusion proteins (Fig. 4C). Subsequently, p300 purified from SF9 insect cells was incubated with the above mentioned GST-RECQL4 fragments and [^{14}C] acetyl coenzyme A. The reactions were analysed by SDS PAGE. After Coomassie-staining (Fig. 4D, left panel), the gel was subjected to autoradiography and revealed that p300 was self-acetylated (28, 29) and was able to acetylate the fragment B of RECQL4 (Figure 4B, right panel9). This fragment spans amino acid residues 359-478 including the putative NOS (aa 376-386) of RECQL4. Furthermore, this fragment also contains a large part of the p300 interaction region (aa 1-408) that was mapped in the experiment shown in Fig. 4B. Importantly, there was no detectable acetylation of RECQL4 fragment C, which covers the same region as fragment B but has all five lysine residues mutated to alanines. The difference in electrophoretic mobilities of fragments B and C can be explained by the lack of positive charge in

the alanine mutant. It should be noted that Coomassie blue staining of the gel confirmed that comparable amounts of RECQL4 fragments were used in each acetylation reaction.

In order to further investigate which of the fiveRECQL4 lysine residues are acetylated by p300, purified 6xHisRECQL4aa359-478 from *E.coli* was acetylated *in vitro* by p300 in the presence of cold acetyl coemzyme A and analysed by SDS-PAGE. Subsequent in gel digestion and LC-MSMS analyses of the acetylated fragment 6xHisRECQL4aa359-478 using Lys-C, chymotrypsin and pepsin respectively, did not allow us to detect peptides covering the majority of the sequence. This could be either due to difficulties with the cleavage of this highly charged sequence or problems with the chromatography in the HPLC or the detection of the peptides in the MS. We could only detect one acetylated peptide in the Lys-C digest with the sequence K386GECFGGGGATVTTK400 and acetylation on lysine residue 386.

Thus, we conclude from the *in vivo* and *in vitro* acetylation assays that p300 acetylates RECQL4 on one or more of the lysine residues at positions 376, 380, 382, 385, and 386 of RECQL4 previously characterized NOS/NLS of the RECQL4 aa sequence.

Role of lysine residues 376, 380, 382, 385, 386 in RECQL4 localization in mammalian cells

We next investigated the functional significance of K376, K380, K382, K385, and K386 acetylation by analyzing the subcellular distribution of RECQL4 protein in human cells. To that end, we transiently overexpressed full length His-RECQL4 in HeLa cells and examined its subcellular localization by indirect immunofluorescence using an α-His antibody (Fig 5A, top panels). We found that in 70% of the cells, RECQL4 was localized predominantly in the nucleus. In 22% of the cells, RECQL4 was equally distributed between nucleus and cytoplasm, while predominant cytoplasmic localization of RECQL4 protein was observed in 8% of the cells (Fig. 5B, bars on the left). Our observation is consistent with previously published biochemical and immunofluorescence data with overexpressed and endogenous RECQL4, showing that RECQL4 is found both in the nucleus and the cytoplasm of different cell lines examined (23, 25, 27). Therefore, we considered His-RECQL4 to be an adequate tool to further characterize the cellular localization of RECQL4. We next tested the two K□A and K□R His-RECQL4 mutants for the localization in HeLa cells, since the RECQL4 N-terminal basic motif spanning aa 376-386 (KQAWKQKWRKK) was previously reported to have nucleolar localization activity (26). Each of the mutants were transiently transfected in HeLa cells and the expressed proteins were detected by indirect immunofluorescence using an α-His antibody (Fig.5A, middle/lower panels). No significant difference in subcellular localization between the RECQL4 wild type and RECQL4 K□R mutant was observed (Fig.5A/4B, middle panels/ bars in the middle). Interestingly, though, the RECQL4 K□A mutant was mostly localized to the cytoplasm of HeLa cells. Similar results were obtained using U2OS cells and cell type specific observations could therefore be excluded (Supplementary Figure 2). Importantly, our findings are contradictory to the observations by Woo *et al.* (26), who found nucleolar exclusion (but nucleoplasmic localization) of GFP-RECQL4 lacking the basic motif. To further verify the validity of our results, we cloned the nucleotides encoding the basic motif (aa 376-386) of RECQL4 (NLS *β*-Gal) or the K □ A mutant sequence (NLS K □ A *β*-Gal) N-terminally to the *E.coli β*-Galactosidase cDNA (Fig. 5C). Transiently overexpressed *E.coli β*-Galactosidase was found to be localized almost entirely to the cytoplasm in Hela cells (Fig. 5D, top, Fig. 5E, left). Intriguingly, the RECQL4 wild type basic motif fused to the *β*-Galactosidase protein was able to import this 100kDa protein to the nucleus (Fig. 5D/5E, middle), while the K □ A *β*-Gal fusion protein failed to be imported and was localized mostly to the cytoplasm (Fig. 5D, low, Fig. 5E, right). The same experiment was repeated by using 293T cells (Supplementary Figure 3). Thus, we conclude from this experiment that positively charged side chains of Lys 376, 380, 382, 385, and 386 within the N-terminal basic motif (KQAWKQKWRKK) are essential for the nuclear localization of RECQL4.

A portion of RECQL4 translocates to the cytoplasm upon acetylation by p300

We next wanted to examine the cellular localization of RECQL4 protein in human cells that express either the wild-type or mutated p300. To that end, we first transiently expressed in HeLa cells FLAG-p300 and FLAG-p300ΔHAT, a catalytic dead mutant lacking part of the HAT domain, and visualized both proteins by indirect immunofluorescence using an α-FLAG antibody. As expected, both proteins were localized entirely to the nucleus of HeLa cells (Fig. 6A). We then investigated the functional consequence of the RECQL4 acetylation *in vivo*. Immunofluorescence experiments on co-transfected HeLa cells (His-RECQL4/ FLAG-p300 and His-RECQL4/FLAG-p300ΔHAT, respectively) showed that the catalytic activity of p300 enhances about three-fold the number of cells in which RECQL4 is mainly cytoplasmic (Fig. 6B/ 6C). In accordance with this

observation, p300 catalytic activity didn't drive the accumulation of RECQL4 K□R mutant in the cytoplasm, confirming that these lysine residues are responsible for p300-induced RECQL4 relocalization (Fig. 6D/ 6E).

To further confirm that the observed cytoplasmic translocation of RECQL4 is indeed due to the acetylation, HeLa cells were transfected with His-RECQL4 or His-RECQL4 K□R mutant and incubated for 30h in the presence of the histone deacetylase inhibitors Trichostatin A (TSA) and nicotinamide (NA). As shown in Fig. 6F and 6G, TSA and NA induced a translocation of His-RECQL4 to the cytoplasm, while the localization of the His-RECQL4 K□R Mutant was not affected. These findings indicate that protein acetylation, enhanced by TSA and NA, positively regulates the translocation of RECQL4 from the nucleus to the cytoplasm. Similar results were obtained when U2OS cells were used instead of HeLa cells (data not shown).

Collectively, these data imply that the subcellular localization of RECQL4 is regulated at least in part by acetylation and that p300 acetyltransferase activity on the lysine residues within the RECQL4 basic motif (KQAWKQKWRKK) is crucial for its translocation to the cytoplasm.

DISCUSSION

Proper RECQL4 activity is required for the maintenance of genome stability as reflected by the fact that three different human disorders characterized by cancer suceptibility and premature aging have been associated with mutations in the *RECQL4* gene: Rothmund-Thomson (RTS), RAPADILINO, and Baller-Gerold (BGS) syndromes (10). Although RTS, RAPADILINO and BGS syndromes caused by mutations in RECQL4 are rare (i.e. they currently affect approximately 400 individuals in total), from a molecular biology aspect it is important to investigate how faulty RECQL4 hinders the normal processes of DNA repair and replication, and how defects in these processes lead to such a broad spectrum of clinical features, as observed in RTS, RAPADILINO and BGS patients.

Investigation of RECQL4 subcellular localization was an object of extensive studies in the last couple of years (9, 23, 25-27). Different data suggested that RECQL4 is located in the nucleus and the cytoplasm of different cell lines examined, but the molecular mechanism by which RECQL4 is translocated to the cytoplasm and the cytoplasmic function of RECQL4 remains to be elucidated. This study provides the first evidence of a physical and functional interaction between RECQL4 and the transcriptional coactivator and histone acetyltransferase p300. This interaction was confirmed with purified recombinant RECQL4 and p300 proteins indicating that the interaction is direct. The N-terminal amino acids 1-408 of RECQL4 and the amino acid residues 1459–1892 of p300 were necessary and sufficient for the interaction of RECQL4 with p300. Investigations of the biochemical consequences of RECQL4/p300 interaction revealed that p300 specifically stimulates the RECQL4 ATPase activity *in vitro*, while acetylation of RECQL4 decreases this effect.

Our findings constitute two important and novel discoveries. First, we show *in vitro* and *in vivo* that p300 specifically triggers RECQL4 protein acetylation on several lysine residues of the conserved N-terminal basic motif spanning amino acids 376-386 (KQAWKQKWRKK), and that this acetylation positively regulates the translocation of a subset of RECQL4 from the nucleus to the cytoplasm. Since p300 catalytic activity didn't drive the accumulation of RECQL4 K□R mutant in the cytoplasm, our data indicate that Lys 376, 380, 382, 385, 386 of RECQL4 positively regulate the translocation of RECQL4 from the nucleus to the cytoplasm in two different human cell lines. In addition, the exposure of these cell lines to histone deacetylase inhibitors Trichostatin A (TSA) and nicotinamide (NA), both of which increase the level of protein acetylation, induced the cytoplasmic translocation of the wild-type RECQL4 but not RECQL4 K□R mutant further confirming the importance of Lys residues 376, 380, 382, 385, 386 of RECQL4 in the cytoplasmic translocation of RECQL4.

Secondly, we show that Lys 376, 380, 382, 385, 386 of RECQL4 within the N-terminal basic motif (KQAWKQKWRKK) are essential for the nuclear localization of RECQL4. The contradictory observations by Woo *et al.* (26), who found nucleolar exclusion (but nucleoplasmic localization) of GFP-RECQL4 lacking the basic motif could be explained by the fact that deleting 10 amino acids from the original RECQL4 sequence may influence its proper native folding and localization. In accordance to our data, Burks *et al.* demonstrated that RECQL4 aa 363-492 are crucial for nuclear import and localization of GFP-RECQL4 and a conserved block of 22 amino acids (aa 365-386) was able to import GFP to the nucleus of mammalian cells (25). These authors also showed that a conserved motif (VLPLV) within RECQL4 aa 420-463 (encoded by exon 7) may play a role in nuclear retention of the RECQL4 protein.

Furthermore, we have provided evidence that the acetylation of RECQL4 does not significantly change during the cell cycle or upon cellular treatment with different DNA damaging agents

including cisplatin, etoposide, and bleomycin. Interestingly, these data differ from those obtained for WRN helicase which showed that DNA damage by either UV light or ionizing radiation induces p300-dependent WRN translocation from nucleolus to the nucleocytoplasmic foci (49). Thus, further studies are needed to understand on the molecular level which endogenous and exogenous factors are required to trigger p300-dependent acetylation of RECQL4.

How might p300 regulate subcellular localization of RECQL4? One possible scenario, as previously shown for transcription factors HMGB1 (50) and E1A (51), could be that p300-mediated acetylation negatively affects the function of the RECQL4 NLS (aa 376-386) and thus disrupts its association with the nuclear import machinery, which leads to subsequent cytoplasmic accumulation of RECQL4 protein. Supporting this hypothesis, it has been recently demonstrated that RECQL4 is found in complex with UBR1/UBR2 at least partially in cytosolic extracts of HeLa cells (27). UBR1/UBR2 belong to the family of E3 ubiquitin ligases of the N-end rule pathway, which is part of the ubiquitin proteasome system (52). It is therefore tempting to speculate that, after a portion of RECQL4 is acetylated by p300 in the nucleus, RECQL4 is translocated to the cytoplasm where the interaction with UBR1/UBR2 takes place and leads to a subsequent degradation by the proteasome of the N-end rule pathway. Finally, we note that we can not at the present time rule out the possibility that RECQL4 has some other role in the cytosol that still awaits further investigations.

1. Tuteja, N. and Tuteja, R. (2001) Unraveling DNA repair in human: molecular mechanisms and consequences of repair defect. *Crit Rev Biochem Mol Biol,* **36,** 261-90.
2. Khakhar, R.R., Cobb, J.A., Bjergbaek, L., Hickson, I.D. and Gasser, S.M. (2003) RecQ helicases: multiple roles in genome maintenance. *Trends Cell Biol,* **13,** 493-501.
3. Iyer, N.G., Ozdag, H. and Caldas, C. (2004) p300/CBP and cancer. *Oncogene,* **23,** 4225-31.
4. Hickson, I.D. (2003) RecQ helicases: caretakers of the genome. *Nat Rev Cancer,* **3,** 169-178.
5. Ellis, N.A., Groden, J., Ye, T.Z., Straughen, J., Lennon, D.J., Ciocci, S., Proytcheva, M. and German, J. (1995) The Bloom's syndrome gene product is homologous to RecQ helicases. *Cell,* **83,** 655-66.
6. Gray, M.D., Shen, J.C., Kamath-Loeb, A.S., Blank, A., Sopher, B.L., Martin, G.M., Oshima, J. and Loeb, L.A. (1997) The Werner syndrome protein is a DNA helicase. *Nature genetics,* **17,** 100-3.
7. Van Maldergem, L., Siitonen, H.A., Jalkh, N., Chouery, E., De Roy, M., Delague, V., Muenke, M., Jabs, E.W., Cai, J., Wang, L.L. *et al.* (2006) Revisiting the craniosynostosis-radial ray hypoplasia association: Baller-Gerold syndrome caused by mutations in the RECQL4 gene. *J Med Genet,* **43,** 148-52.
8. Siitonen, H.A., Kopra, O., Kaariainen, H., Haravuori, H., Winter, R.M., Saamanen, A.M., Peltonen, L. and Kestila, M. (2003) Molecular defect of RAPADILINO syndrome expands the phenotype spectrum of RECQL diseases. *Hum Mol Genet,* **12,** 2837-44.
9. Kitao, S., Shimamoto, A., Goto, M., Miller, R.W., Smithson, W.A., Lindor, N.M. and Furuichi, Y. (1999) Mutations in RECQL4 cause a subset of cases of Rothmund-Thomson syndrome. *Nature genetics,* **22,** 82-4.
10. Dietschy, T., Shevelev, I. and Stagljar, I. (2007) The molecular role of the Rothmund-Thomson-, RAPADILINO- and Baller-Gerold-gene product, RECQL4: recent progress. *Cell Mol Life Sci,* **64,** 796-802.
11. Vennos, E.M., Collins, M. and James, W.D. (1992) Rothmund-Thomson syndrome: review of the world literature. *J Am Acad Dermatol,* **27,** 750-762.
12. Kitao, S., Lindor, N.M., Shiratori, M., Furuichi, Y. and Shimamoto, A. (1999) Rothmund-thomson syndrome responsible gene, RECQL4: genomic structure and products. *Genomics,* **61,** 268-276.
13. Lindor, N.M., Furuichi, Y., Kitao, S., Shimamoto, A., Arndt, C. and Jalal, S. (2000) Rothmund-Thomson syndrome due to RECQ4 helicase mutations: report and clinical and molecular comparisons with Bloom syndrome and Werner syndrome. *Am J Med Genet,* **90,** 223-228.

14. Der Kaloustian, V.M., McGill, J.J., Vekemans, M. and Kopelman, H.R. (1990) Clonal lines of aneuploid cells in Rothmund-Thomson syndrome. *Am J Med Genet,* **37,** 336-339.
15. Vennos, E.M. and James, W.D. (1995) Rothmund-Thomson syndrome. *Dermatol Clin,* **13,** 143-150.
16. Werner, S.R., Prahalad, A.K., Yang, J. and Hock, J.M. (2006) RECQL4-deficient cells are hypersensitive to oxidative stress/damage: Insights for osteosarcoma prevalence and heterogeneity in Rothmund-Thomson syndrome. *Biochem Biophys Res Commun,* **345,** 403-409.
17. Kellermayer, R., Siitonen, H.A., Hadzsiev, K., Kestila, M. and Kosztolanyi, G. (2005) A patient with Rothmund-Thomson syndrome and all features of RAPADILINO. *Arch Dermatol,* **141,** 617-620.
18. Mann, M.B., Hodges, C.A., Barnes, E., Vogel, H., Hassold, T.J. and Luo, G. (2005) Defective sister-chromatid cohesion, aneuploidy and cancer predisposition in a mouse model of type II Rothmund-Thomson syndrome. *Hum Mol Genet,* **14,** 813-825.
19. Ichikawa K, N.T., Furuichi Y. (2002) Preparation of the gene targeted knockout mice for human premature aging diseases, Werner syndrome, and Rothmund-Thomson syndrome caused by the mutation of DNA helicases. *Nippon Yakurigaku Zasshi,* **119,** 219-26.
20. Hoki, Y., Araki, R., Fujimori, A., Ohhata, T., Koseki, H., Fukumura, R., Nakamura, M., Takahashi, H., Noda, Y. and Kito, S. (2003) Growth retardation and skin abnormalities of the Recql4-deficient mouse. *Hum Mol Genet,* **12,** 2293-2299.
21. Sangrithi, M.N., Bernal, J.A., Madine, M., Philpott, A., Lee, J., Dunphy, W.G. and Venkitaraman, A.R. (2005) Initiation of DNA replication requires the RECQL4 protein mutated in Rothmund-Thomson syndrome. *Cell,* **121,** 887-898.
22. Kumiko Matsuno, M.K., Yumiko Kubota, Yoshitami Hashimoto, and Haruhiko Takisawa (2006) The N-Terminal Noncatalytic Region of Xenopus RecQ4 Is Required for Chromatin Binding of DNA Polymerase in the Initiation of DNA Replication. *Molecular and Cellular Biology,* **26,** 4843-52.
23. Petkovic, M., Dietschy, T., Freire, R., Jiao, R. and Stagljar, I. (2005) The human Rothmund-Thomson syndrome gene product, RECQL4, localizes to distinct nuclear foci that coincide with proteins involved in the maintenance of genome stability. *J Cell Sci,* **118,** 4261-4269.
24. Kumata, Y., Tada, S., Yamanada, Y., Tsuyama, T., Kobayashi, T., Dong, Y.P., Ikegami, K., Murofushi, H., Seki, M. and Enomoto, T. (2007) Possible involvement of RecQL4 in the repair of double-strand DNA breaks in Xenopus egg extracts. *Biochim Biophys Acta,* **1773,** 556-64.
25. Burks, L.M., Yin, J. and Plon, S.E. (2007) Nuclear import and retention domains in the amino terminus of RECQL4. *Gene,* **391,** 26-38.
26. Woo, L.L., Futami, K., Shimamoto, A., Furuichi, Y. and Frank, K.M. (2006) The Rothmund-Thomson gene product RECQL4 localizes to the nucleolus in response to oxidative stress. *Exp Cell Res,* **312,** 3443-57.
27. Yin, J., Kwon, Y.T., Varshavsky, A. and Wang, W. (2004) RECQL4, mutated in the Rothmund-Thomson and RAPADILINO syndromes, interacts with ubiquitin ligases UBR1 and UBR2 of the N-end rule pathway. *Hum Mol Genet,* **13,** 2421-30.
28. Hasan, S. and Hottiger, M.O. (2002) Histone acetyl transferases: a role in DNA repair and DNA replication. *J Mol Med,* **80,** 463-74.
29. Freiman, R.N. and Tjian, R. (2003) Regulating the regulators: lysine modifications make their mark. *Cell,* **112,** 11-7.
30. Kuo, M.H. and Allis, C.D. (1998) Roles of histone acetyltransferases and deacetylases in gene regulation. *Bioessays,* **20,** 615-26.
31. Nakatani, Y. (2001) Histone acetylases--versatile players. *Genes Cells,* **6,** 79-86.
32. Goodman, R.H. and Smolik, S. (2000) CBP/p300 in cell growth, transformation, and development. *Genes Dev,* **14,** 1553-77.
33. Ogryzko, V.V., Schiltz, R.L., Russanova, V., Howard, B.H. and Nakatani, Y. (1996) The transcriptional coactivators p300 and CBP are histone acetyltransferases. *Cell,* **87,** 953-9.
34. Bannister, A.J. and Kouzarides, T. (1996) The CBP co-activator is a histone acetyltransferase. *Nature,* **384,** 641-3.
35. Kouzarides, T. (2000) Acetylation: a regulatory modification to rival phosphorylation? *Embo J,* **19,** 1176-9.

36. Hasan, S., Hassa, P.O., Imhof, R. and Hottiger, M.O. (2001) Transcription coactivator p300 binds PCNA and may have a role in DNA repair synthesis. *Nature,* **410,** 387-91.
37. Hasan, S., Stucki, M., Hassa, P.O., Imhof, R., Gehrig, P., Hunziker, P., Hubscher, U. and Hottiger, M.O. (2001) Regulation of human flap endonuclease-1 activity by acetylation through the transcriptional coactivator p300. *Mol Cell,* **7,** 1221-31.
38. Tini, M., Benecke, A., Um, S.J., Torchia, J., Evans, R.M. and Chambon, P. (2002) Association of CBP/p300 acetylase and thymine DNA glycosylase links DNA repair and transcription. *Mol Cell,* **9,** 265-77.
39. Bhakat, K.K., Izumi, T., Yang, S.H., Hazra, T.K. and Mitra, S. (2003) Role of acetylated human AP-endonuclease (APE1/Ref-1) in regulation of the parathyroid hormone gene. *Embo J,* **22,** 6299-309.
40. Bhakat, K.K., Hazra, T.K. and Mitra, S. (2004) Acetylation of the human DNA glycosylase NEIL2 and inhibition of its activity. *Nucleic Acids Res,* **32,** 3033-9.
41. Hasan, S., El-Andaloussi, N., Hardeland, U., Hassa, P.O., Burki, C., Imhof, R., Schar, P. and Hottiger, M.O. (2002) Acetylation regulates the DNA end-trimming activity of DNA polymerase beta. *Mol Cell,* **10,** 1213-22.
42. Bhakat, K.K., Mokkapati, S.K., Boldogh, I., Hazra, T.K. and Mitra, S. (2006) Acetylation of human 8-oxoguanine-DNA glycosylase by p300 and its role in 8-oxoguanine repair in vivo. *Molecular and cellular biology,* **26,** 1654-65.
43. Hardeland, U., Steinacher, R., Jiricny, J. and Schar, P. (2002) Modification of the human thymine-DNA glycosylase by ubiquitin-like proteins facilitates enzymatic turnover. *Embo J,* **21,** 1456-64.
44. Margaret A. Macris, L.K., Wendy Bussen, Akira Shimamoto, Patrick Sung (2006) Biochemical characterization of the RECQ4 protein, mutated in Rothmund-Thomson syndrome. *DNA Repair,* **5,** 172-80.
45. Faiola, F., Wu, Y.T., Pan, S., Zhang, K., Farina, A. and Martinez, E. (2007) Max is acetylated by p300 at several nuclear localization residues. *Biochem J,* **403,** 397-407.
46. Bai, Y., Srinivasan, L., Perkins, L. and Atchison, M.L. (2005) Protein acetylation regulates both PU.1 transactivation and Ig kappa 3' enhancer activity. *J Immunol,* **175,** 5160-9.
47. Topper, M., Luo, Y., Zhadina, M., Mohammed, K., Smith, L. and Muesing, M.A. (2007) Posttranslational acetylation of the human immunodeficiency virus type 1 integrase carboxyl-terminal domain is dispensable for viral replication. *J Virol,* **81,** 3012-7.
48. Hassa, P.O., Haenni, S.S., Buerki, C., Meier, N.I., Lane, W.S., Owen, H., Gersbach, M., Imhof, R. and Hottiger, M.O. (2005) Acetylation of poly(ADP-ribose) polymerase-1 by p300/CREB-binding protein regulates coactivation of NF-kappaB-dependent transcription. *The Journal of biological chemistry,* **280,** 40450-64.
49. Blander, G., Zalle, N., Daniely, Y., Taplick, J., Gray, M.D. and Oren, M. (2002) DNA damage-induced translocation of the Werner helicase is regulated by acetylation. *The Journal of biological chemistry,* **277,** 50934-40.
50. Bonaldi, T., Talamo, F., Scaffidi, P., Ferrera, D., Porto, A., Bachi, A., Rubartelli, A., Agresti, A. and Bianchi, M.E. (2003) Monocytic cells hyperacetylate chromatin protein HMGB1 to redirect it towards secretion. *Embo J,* **22,** 5551-60.
51. Madison, D.L., Yaciuk, P., Kwok, R.P. and Lundblad, J.R. (2002) Acetylation of the adenovirus-transforming protein E1A determines nuclear localization by disrupting association with importin-alpha. *The Journal of biological chemistry,* **277,** 38755-63.
52. Hershko, A., Ciechanover, A. and Varshavsky, A. (2000) The ubiquitin system. *Nature Medicine,* **6,** 1073-1081.

Figure Legend

FIG.1 p300 acetylates RECQL4 *in vivo* and the two proteins form a stable complex.
(A) Left panel: His-RECQL4 was ectopically expressed in 293T cells along with with FLAG-p300, myc-pCAF, HA-Gcn5 or FLAG-HAT1 histone acetyltransferases (HATs). His-RECQL4 was then immunoprecipitated with an α-His antibody (IP: 6xHis-RECQL4) and analyzed by Western blot (upper panel). The same nitrocellulose membrane was stripped and re-probed with an α-acetyl-lys (α-Ac-lys) antibody (lower panel). Right panel: Western blot analysis of overexpressed HATs (FLAG-p300, myc-PCAF, HA-Gcn5, and FLAG-HAT1/ FLAG-p46 heterodimer). 50 μg of total protein extract were loaded in each lane. As negative controls (-) the same amount of extracts of untransfected 293T cells was analyzed. **(B)** RECQL4 and p300 form a complex in human cells. Left panel: 293T cells were transiently transfected with FLAG-p300 expression vector. Total cell extract derived from these cells was immunoprecipitated with an α-RECQL4 antibody or control IgG, and was analyzed by SDS PAGE. One-tenth (100 μg) of the same total cell extract was used as input control (lane 1). Immunoprecipitated FLAG-p300 and RECQL4 were detected by Western blotting using an α-FLAG and α-RECQL4 antibody, respectively (lane 3). Reciprocal co-immunoprecipitation is shown in the right panel: lane 4, input; lane 5, immunoprecipitation with the control IgG; lane 6, immunoprecipitation with an α-p300 antibody using total cell extracts derived from 293T cells overexpressing His-RECQL4. **(C)** Binding of RECQL4 to p300 as a function of RECQL4 concentration. Increasing concentrations of RECQL4 (0 - 40 nM) were incubated at 37°C for 1 hour in wells of an ELISA plate that were pre-coated with the p300 protein (20nM) and subsequently blocked with 3% BSA. After extensive washing, bound RECQL4 protein was detected as described in Materials and Methods. Absorbance values measured were corrected by subtracting background values obtained with BSA-coated wells.

FIG.2 Mapping of interaction domains between p300 and RECQL4.
(A) Schematic representation of RECQL4 and its deletion variants used in this study. **(B)** SDS-PAGE analysis of bacterially expressed and purified GST-RECQL4 fragments 1-4. Gel was stained with Coomassie blue. **(C)** GST pull-down assay showing binding of FLAG-p300 to bacterially expressed GST RECQL4 fragments 1-4. GST-RECQL4 fragments bound to Glutathione-Sepharose beads were incubated with whole cell extract (1 mg of total protein) derived from 293T cells overexpressing p300. p300 binding was analyzed by western blotting using anti FLAG antibody.
(D) Schematic representation of p300 and its deletion variants. **(E)** SDS-PAGE analysis of bacterially expressed and purified GST-p300 fragments 1-5. **(F)** GST pull-down assay showing binding of His-RECQL4 to bacterially expressed GST-p300 fragments 1-5. GST-p300 fragments bound to Glutathione-Sepharose beads were incubated with whole cell extract (1 mg of total protein) derived 293T cells over-expressing RECQL4. RECQL4 binding was analyzed by western blotting using anti-His antibody.

FIG.3 p300 has a stimulatory effect on the RECQL4 ATPase activity.
(A) Schematic representation of the RECQL4 construct used for the purification of the full length protein. RECQL4 protein was expressed in *E.coli* as a double-tagged fusion protein (GST-RECQL4-His). **(B)** After purification of GST-RECQL4-His using Glutathione-Sepharose and Nickel-NTA agarose, the eluted protein was analyzed by SDS-PAGE followed by Coomassie staining (left panel) and immunoblotting using α-GST- and α-RECQL4 antibodies (right panel). The arrows indicate the full length GST-RECQL4-His protein. **(C)** ssDNA and Mg^{+2} are crucial co-factors for RECQL4 ATPase activity. Reactions containing 40 nM RECQL4, 1mM [γ -32P] ATP, 50mM KCl, and either 2.5mM Mg^{+2} or Ca^{+2}, and either M13 ssDNA or ds plasmid DNA (75μM nucleotides) were incubated at 37°C for 30 minutes. The relative amount of hydrolysed ATP was determined using thin layer chromatography and Scion Image software. **(D)** RECQL4 immunodepletion inhibits ATPase activity. Rabbit polyclonal α-RECQL4 antibody or control rabbit IgG immobilized to protein G Sepharose were used to immunodeplete RECQL4 as described in Material and Methods. Increasing amounts of each sample (white box, RECQL4 antibody; grey box, control antibody) were subsequently assayed for ATPase activity and compared with the activity of untreated RECQL4 sample (black box). **(E)** p300 stimulates RECQL4 ATPase activity. Reactions containing 40 nM RECQL4, 1mM [γ -32P] ATP, 50 mM KCl, 2mM Mg^{+2} and M13 ssDNA (75μM Nucleotides) were incubated at 37°C for 30 minutes in the

presence or absence of purified p300 (100nM) or Gcn5 (40nM). **(F)** Acetylation of RECQL4 by p300 slightly decreases its ATPase activity. RECQL4 and p300 were preincubated together in the presence or absence of cold acetyl- Coenzyme A (AcCoA) for 30 min at 30°C and the samples were subsequently assayed for ATPase activity. Same ATPase reaction conditions as in **(E)** have been used. The data points in all graphs (C-F) represent average values of at least two independent experiments.

FIG.4 Mutation of lysine residues Lys-376, Lys-380, Lys-382, Lys-385 and Lys-386 abrogates the acetylation of RECQL4 by p300 *in vitro* and *in vivo*.
(A) Amino acid sequence of RECQL4 nucleolar localization signal (NOS) sequence. Wild-type sequence is highlighted in the orange box. Lysine to alanine (K□A) mutated NOS sequence (solid outline) and lysine to arginine (K□R) mutated NOS sequence (dashed outline) were generated by site-directed mutagenesis. Mutated residues are underlined. **(B)** Left panel: Effect of mutation of lysine residues on *in vivo* acetylation of RECQL4. Using anti-α-His antibody, wild-type (WT), K□A, and K□R nucleolar localization signal mutants of His-RECQL4 were immunoprecipitated (IP) from extracts of 293T cells co-transfected with p300 expression vector (+) or control vector (-) (upper panel). Acetylated His-RECQL4 was detected by western blot analysis using anti-α-acetylated lysine antibody (lower panel). Right panel: Same as left panel but the effect of single (K382R), double (K385, 386R) and triple (K376, 380, 382R) RECQL4 NOS mutations on its *in vivo* acetylation was tested. **(C)** Schematic representation of RECQL4 and its deletion variants used in this study. Italicized numbers indicate terminal amino acid positions. Solid black box, nucleolar localization signal (NOS); striped box, NOS with five lysine to alanine point mutations; green box, RecQ DNA helicase domain. **(D)** p300 purified from insect cells was incubated with [14C] acetyl coenzyme A and purified GST-RECQL4 fragments or purified histone octamers. Left panel shows the Coomassie-stained SDS-PAGE gel, while the right panel shows the autoradiogram of the same gel. Asterisks indicate protein bands with predicted molecular weight of the corresponding purified GST-RECQL4 fragment. Double dagger indicates band with molecular weight corresponding to acetylated RECQL4-B fragment in autoradiogram.

FIG.5 Mutation of RECQL4 lysine residues Lys-376, Lys-380, Lys-382, Lys-385 and Lys-386 to alanine, but not to arginine, cause relocaliztion of RECQL4 to the cytoplasm of human cells.
(A) His-tagged RECQL4 (wt) and the indicated His-RECQL4 K□R and K□A mutants were expressed in HeLa cells and visualized by indirect immunofluorescence using an α-His antibody (middle panels, α-HisRECQL4, red). The left panels show DAPI-stained nuclei (blue) and the right panels show the merged images of α-HisRECQL4 (red) and DAPI (blue) staining. **(B)** The histograms show the percentages of transfected cells that show an equal distribution of RECQL4 between nucleus and cytoplasm (N=C), a prevalence of RECQL4 in the cytoplasm (N<C) or a prevalence of RECQL4 in the nucleus (N>C). The plotted data indicate the mean ± standard deviation of two independent transfection experiments in which more than 200 transfected cells were analyzed each time. **(C)** Schematic representation of the N-terminal β-Galactosidase fusion constructs. RECQL4 nucleotides encoding amino acids 376-386 (wt) and the indicated K□A mutant sequences were N-terminally cloned to the full length cDNA of the *E.coli* β-Galactosidase gene and the fusion proteins were transiently expressed in HeLa cells. **(D)** β-Galactosidase and the indicated N-terminal fusion constructs (NLS-β-Gal and NLS-β-Gal K□A) were transiently transfected into HeLa cells and expressed proteins were visualized by indirect immunofluorescence using an α-β-Galactosidase antibody (middle panels, α- β-Gal, red). DAPI-staining is shown in the left panels and right panels show merged pictures (Merge). **(E)** Quantitative analysis as in **(B)**.

FIG.6 p300 activity-dependent translocation of RECQL4 protein to the cytoplasm.
(A) p300 and p300 ΔHAT a catalytic dead mutant, localize to the nucleus in mammalian cells. FLAG-tagged p300 or FLAG-p300 ΔHAT proteins were transiently expressed in HeLa cells and visualized by indirect immunofluorescence using an α-FLAG antibody (middle panels). DAPI-stained nuclei are shown in the left panels, while the merged pictures (Merge) are shown by the right panels. **(B+D)** His-tagged RECQL4 **(B)** or the indicated His-RECQL4 K□R Mutant **(D)** proteins were co-expressed with FLAG-tagged p300 or FLAG-p300 ΔHAT proteins in HeLa cells. RECQL4 **(B)** and RECQL4 K□R Mutant **(D)** proteins were visualized with an α-His antibody, while p300 and p300 ΔHAT proteins were visualized with an α-FLAG antibody by

indirect immunofluorescence (middle panels). DAPI-staining shows nuclear DNA (left panels) and right panels show merged pictures (Merge). **(C+E)** Quantification of **(B+D).** The histograms show the percentages of cells out of transfected cells that show an equal distribution of RECQL4 between nucleus and cytoplasm (N=C), a prevalence of RECQL4 in the cytoplasm (N<C) or a prevalence of RECQL4 in the nucleus (N>C). **(F)** Histone deacetylase (HDAC) inhibitors trichostatin A (TSA) and nicotin amide have a slight effect on the translocation of RECQL4 to the cytoplasm.
His-RECQL4 and His-RECQL4 K□R mutant were transiently overexpressed in HeLa cells. 24 hours post transfection, TSA and nicotin amide were added for an additional 30hours.Cells were subsequently fixed and expressed proteins were visualized as mentioned above. **(G)** Quantification of **(F). (C, E, G)** The plotted data indicates the mean ± standard deviation of two independent transfection experiments in which more than 200 transfected cells were analyzed each time.

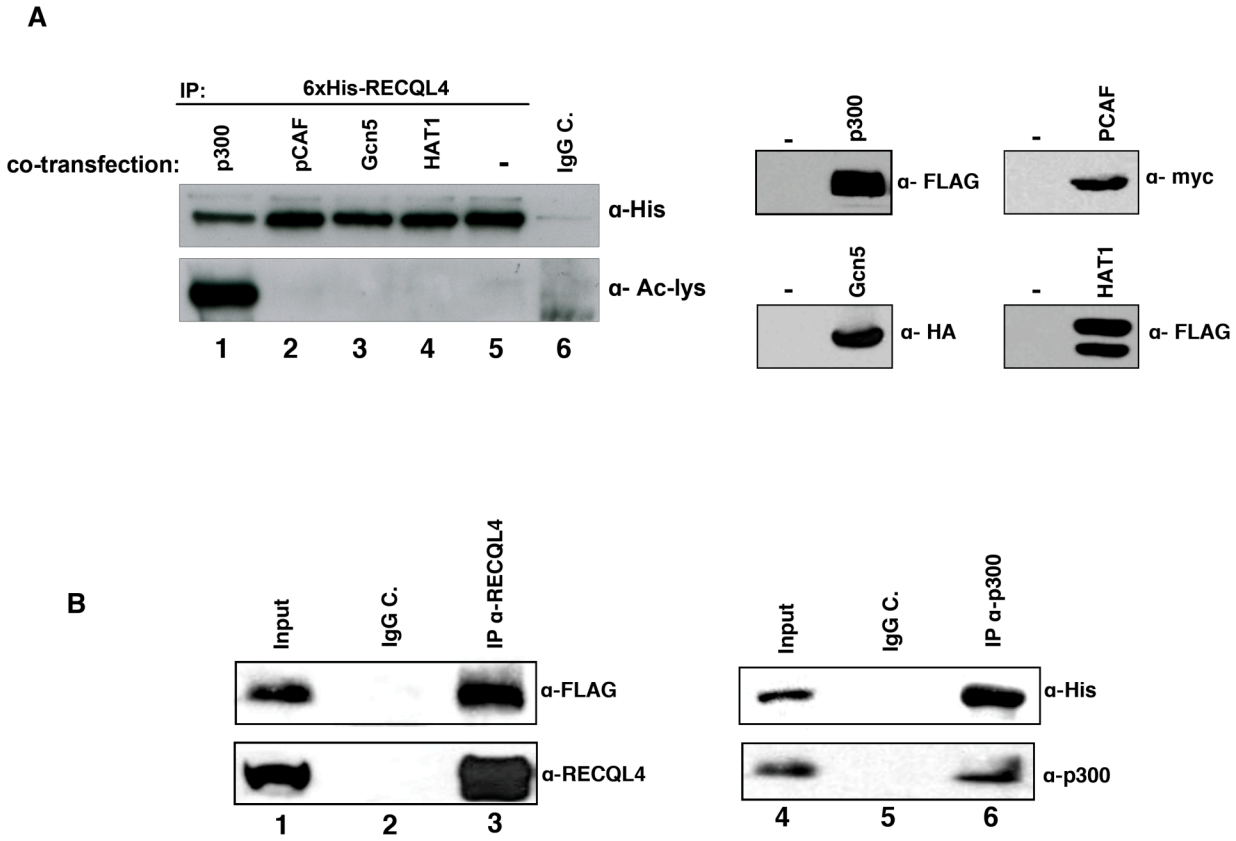
A
IP:
6xHis-RECQL4
co-transfection:
p300
pCAF
Gcn5
HAT1
-
IgG C.
α-His
α- Ac-lys
1 2 3 4 5 6
-
p300
α- FLAG
-
PCAF
α- myc
-
Gcn5
α- HA
-
HAT1
α- FLAG
B
Input
IgG C.
IP α-RECQL4
α-FLAG
α-RECQL4
1 2 3
Input
IgG C.
IP α-p300
α-His
α-p300
4 5 6
C
Abs. 450nm
0.0
0.1
0.2
0.3
0.4
0.5
0 10 20 30 40 50
RECQL4 (nM)

FIGURE 1

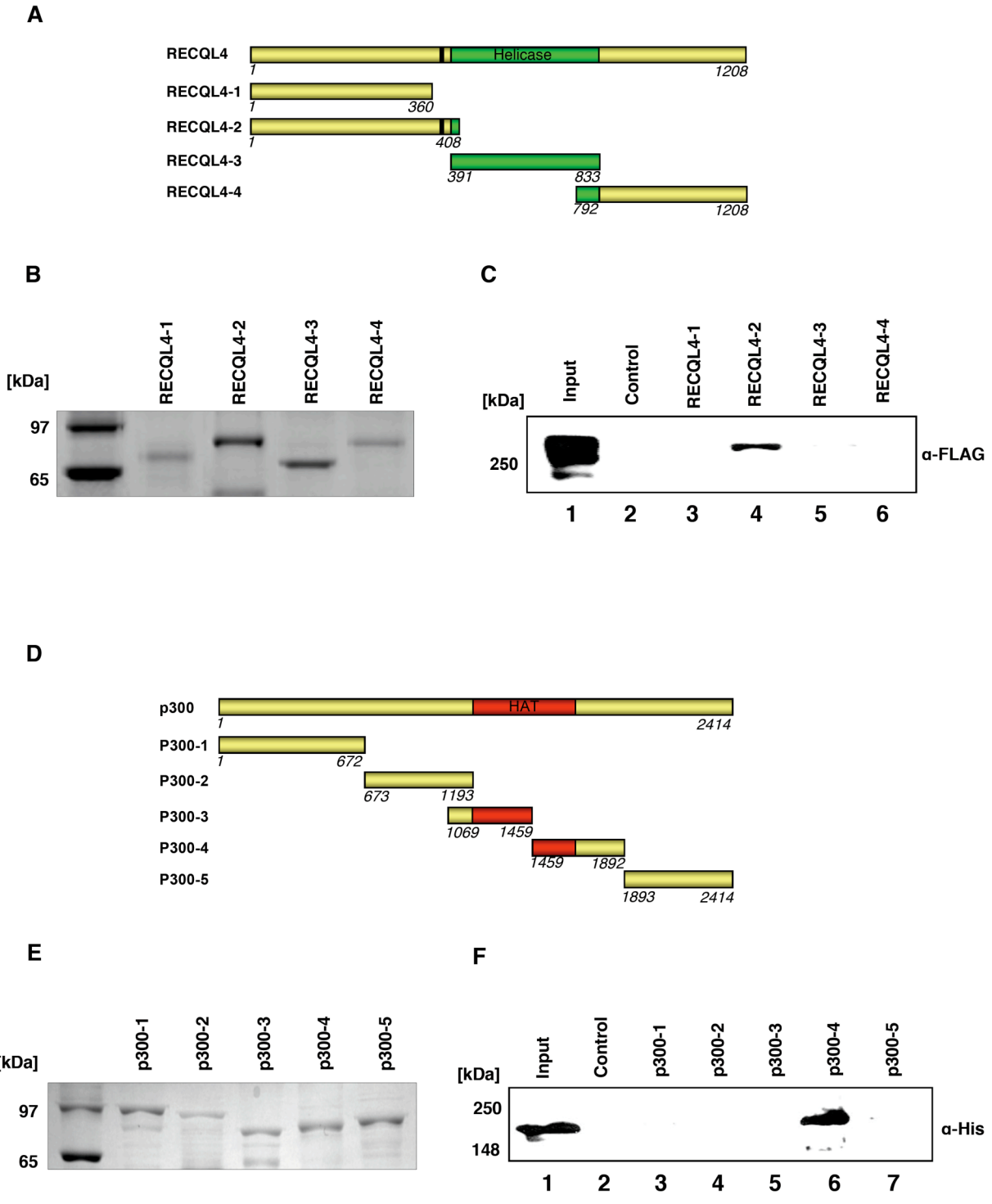
A
RECQL4
Helicase
1
1208
RECQL4-1
1
360
RECQL4-2
1
408
RECQL4-3
391
833
RECQL4-4
792
1208
B
[kDa]
RECQL4-1
RECQL4-2
RECQL4-3
RECQL4-4
97
65
C
[kDa]
Input
Control
RECQL4-1
RECQL4-2
RECQL4-3
RECQL4-4
250
α-FLAG
1 2 3 4 5 6
D
p300
HAT
1
2414
P300-1
1
672
P300-2
673
1193
P300-3
1069
1459
P300-4
1459
1892
P300-5
1893
2414
E
[kDa]
p300-1
p300-2
p300-3
p300-4
p300-5
97
65
F
[kDa]
Input
Control
p300-1
p300-2
p300-3
p300-4
p300-5
250
148
α-His
1 2 3 4 5 6 7

FIGURE 2

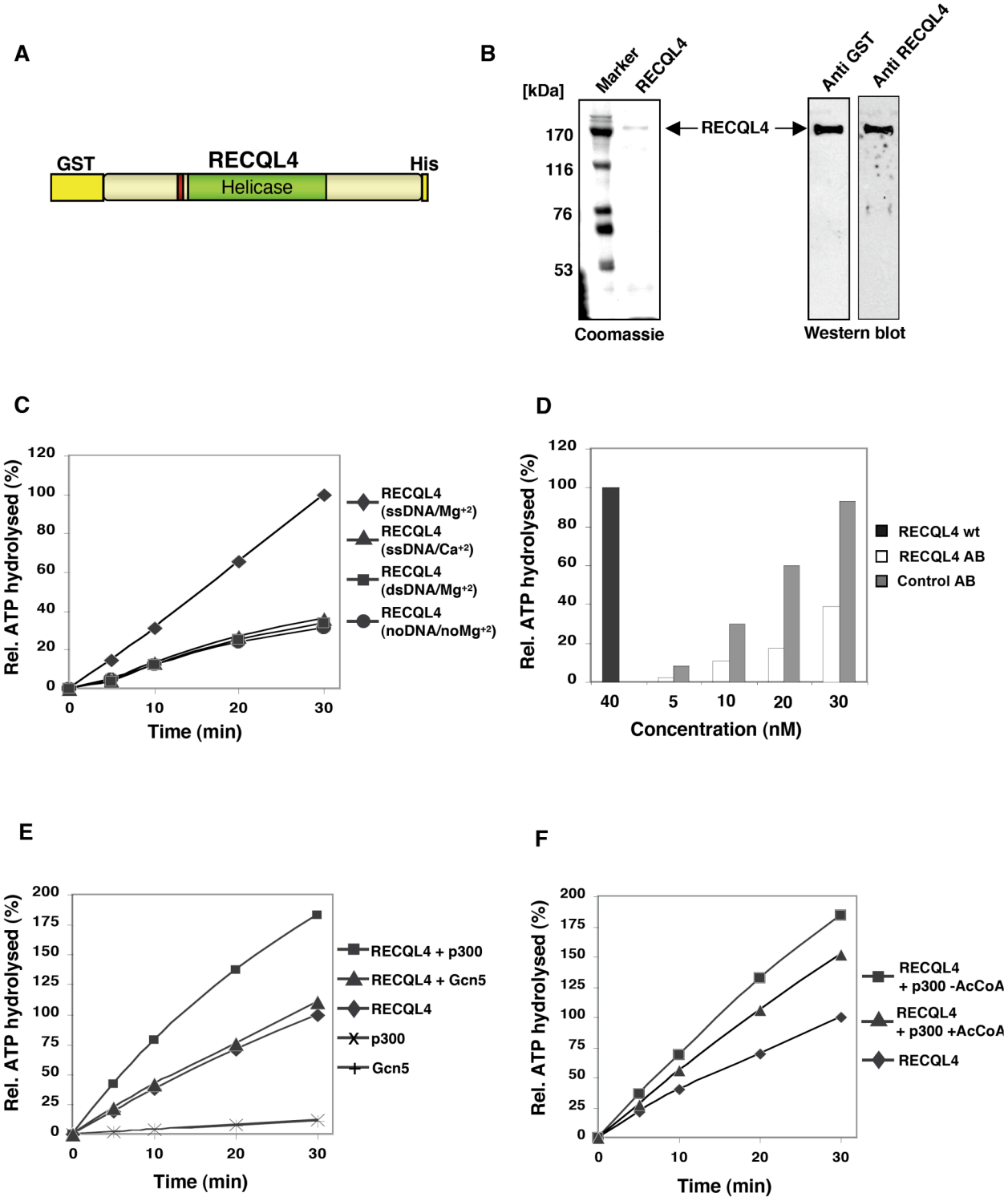
A
GST
RECQL4
Helicase
His
B
[kDa]
Marker
RECQL4
Anti GST
Anti RECQL4
170
116
76
53
RECQL4
Coomassie
Western blot
C
Rel. ATP hydrolysed (%)
Time (min)
RECQL4 (ssDNA/Mg+2)
RECQL4 (ssDNA/Ca+2)
RECQL4 (dsDNA/Mg+2)
RECQL4 (noDNA/noMg+2)
D
Rel. ATP hydrolysed (%)
Concentration (nM)
RECQL4 wt
RECQL4 AB
Control AB
E
Rel. ATP hydrolysed (%)
Time (min)
RECQL4 + p300
RECQL4 + Gcn5
RECQL4
p300
Gcn5
F
Rel. ATP hydrolysed (%)
Time (min)
RECQL4 + p300 -AcCoA
RECQL4 + p300 +AcCoA
RECQL4

FIGURE 3

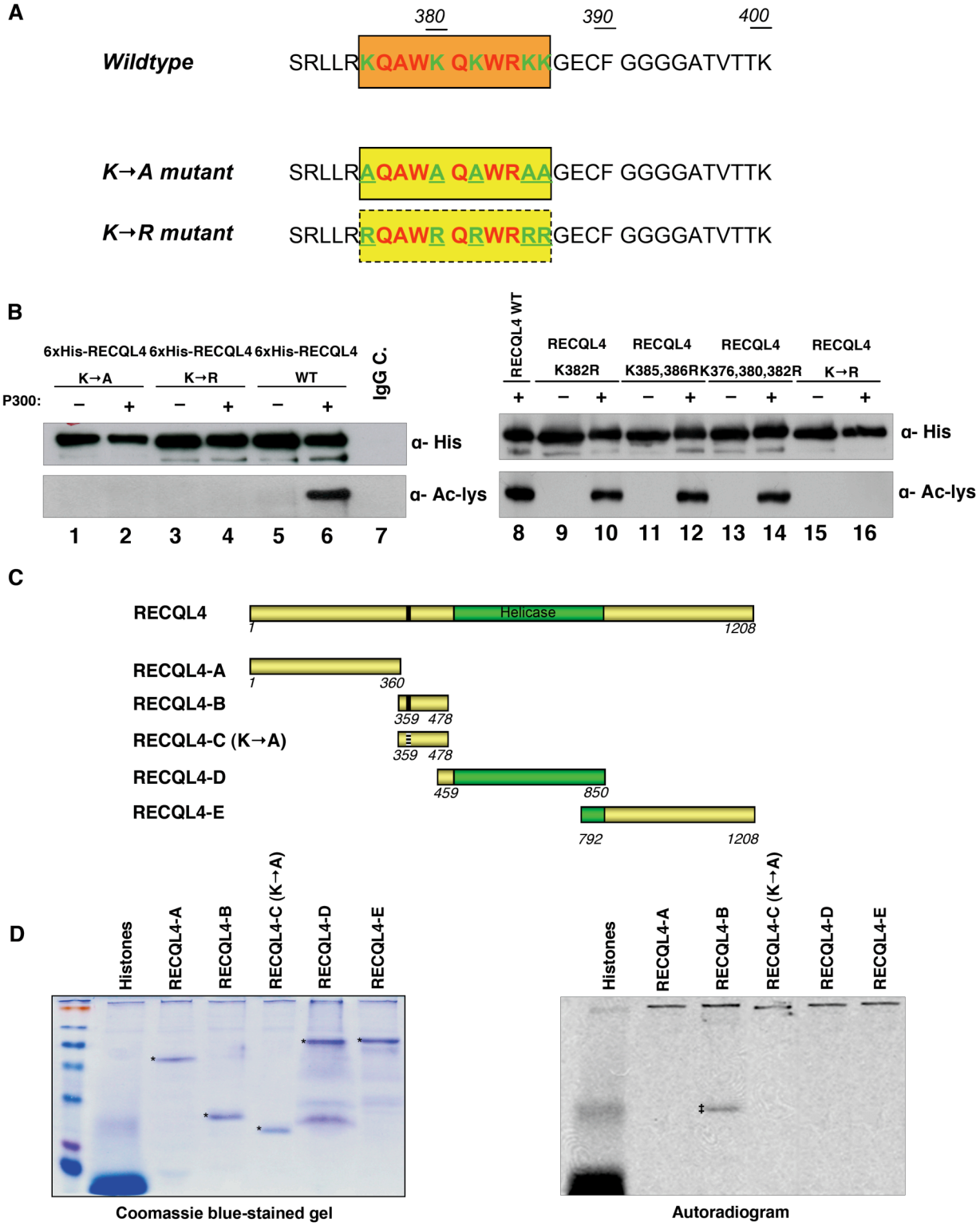
A
380
390
400
Wildtype
SRLLRKQAWK QKWRKKGECF GGGGATVTTK
K→A mutant
SRLLRAQAWA QAWRAAGECF GGGGATVTTK
K→R mutant
SRLLRRQAWR QRWRRRGECF GGGGATVTTK
B
6xHis-RECQL4 K→A
6xHis-RECQL4 K→R
6xHis-RECQL4 WT
IgG C.
P300:
α- His
α- Ac-lys
1 2 3 4 5 6 7
RECQL4 WT
RECQL4 K382R
RECQL4 K385,386R
RECQL4 K376,380,382R
RECQL4 K→R
α- His
α- Ac-lys
8 9 10 11 12 13 14 15 16
C
RECQL4
Helicase
1
1208
RECQL4-A
1
360
RECQL4-B
359 478
RECQL4-C (K→A)
359 478
RECQL4-D
459
850
RECQL4-E
792
1208
D
Histones
RECQL4-A
RECQL4-B
RECQL4-C (K→A)
RECQL4-D
RECQL4-E
Coomassie blue-stained gel
Autoradiogram

FIGURE 4

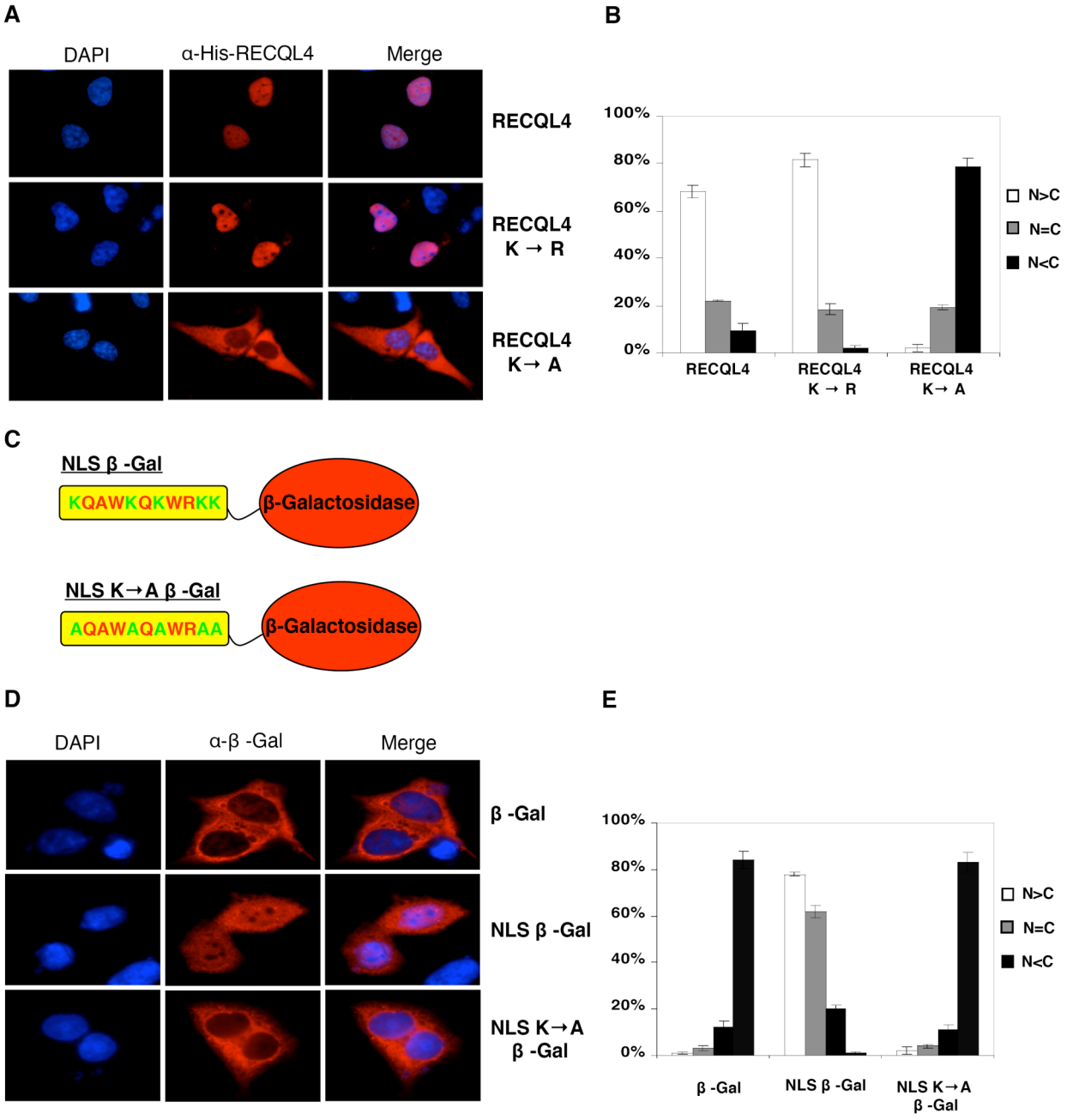
A
DAPI
α-His-RECQL4
Merge
RECQL4
RECQL4 K → R
RECQL4 K→ A
B
100%
80%
60%
40%
20%
0%
RECQL4
RECQL4 K → R
RECQL4 K→ A
N>C
N=C
N<C
C
NLS β -Gal
KQAWKQKWRKK
β-Galactosidase
NLS K→A β -Gal
AQAWAQAWRAA
β-Galactosidase
D
DAPI
α-β -Gal
Merge
β -Gal
NLS β -Gal
NLS K→A β -Gal
E
100%
80%
60%
40%
20%
0%
β -Gal
NLS β -Gal
NLS K→A β -Gal
N>C
N=C
N<C

FIGURE 5

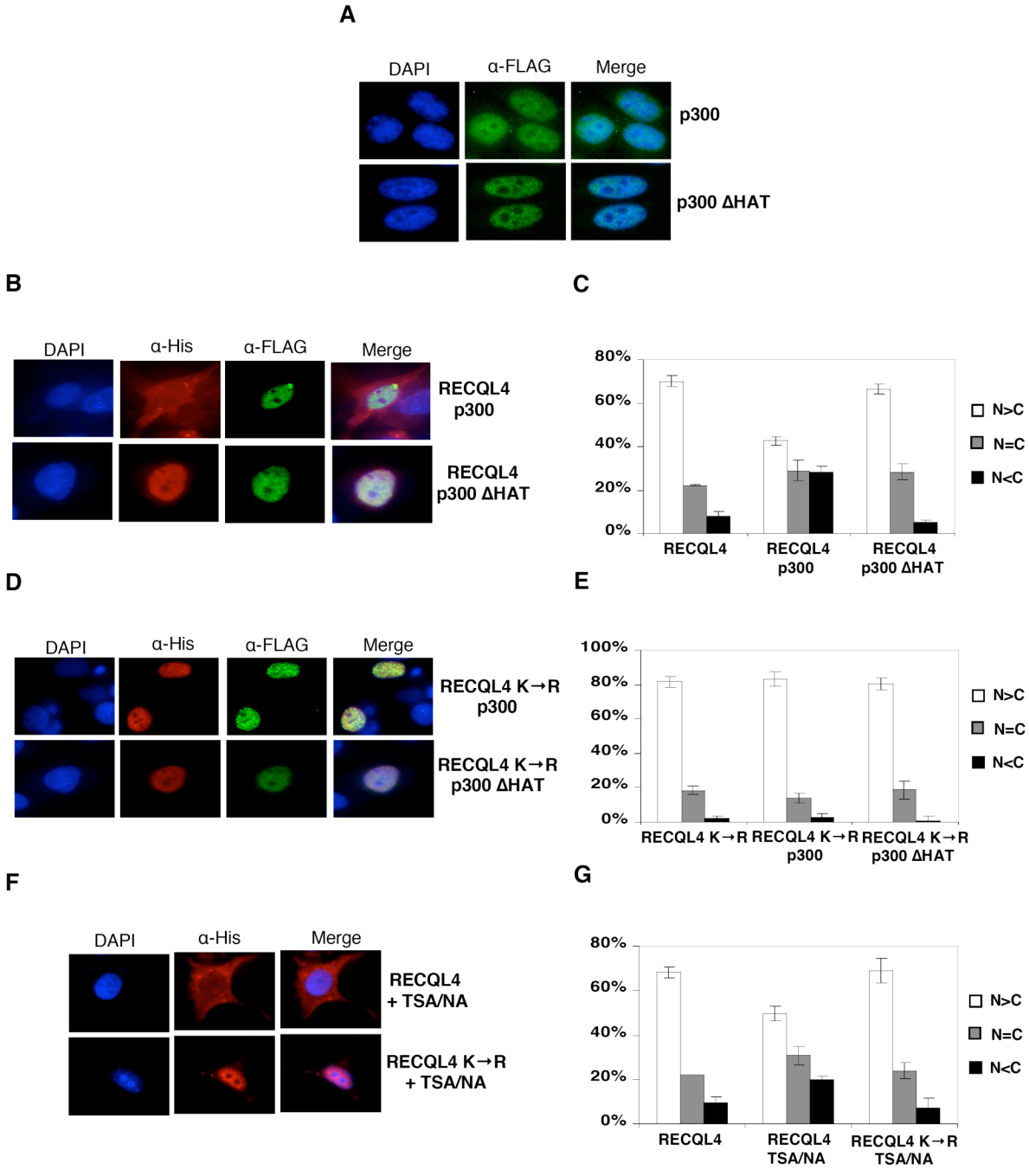
A
DAPI
α-FLAG
Merge
p300
p300 ΔHAT
B
DAPI
α-His
α-FLAG
Merge
RECQL4 p300
RECQL4 p300 ΔHAT
C
80%
60%
40%
20%
0%
RECQL4
RECQL4 p300
RECQL4 p300 ΔHAT
N>C
N=C
N<C
D
DAPI
α-His
α-FLAG
Merge
RECQL4 K→R p300
RECQL4 K→R p300 ΔHAT
E
100%
80%
60%
40%
20%
0%
RECQL4 K→R
RECQL4 K→R p300
RECQL4 K→R p300 ΔHAT
N>C
N=C
N<C
F
DAPI
α-His
Merge
RECQL4 + TSA/NA
RECQL4 K→R + TSA/NA
G
80%
60%
40%
20%
0%
RECQL4
RECQL4 TSA/NA
RECQL4 K→R TSA/NA
N>C
N=C
N<C

FIGURE 6

Supplementary Figure S1

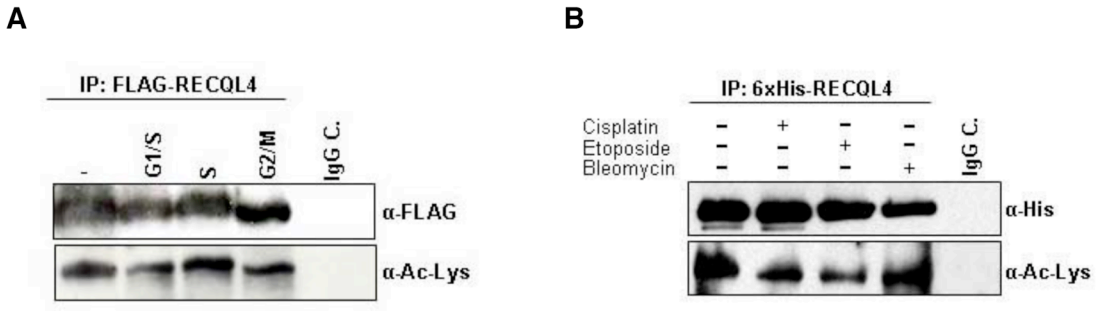

Fig. S1 Cell cycle arrest and DNA damage have no significant influence on RECQL4 acetylation
(A) FLAG-RECQL4 was transiently transfected in 293T cells and the cells were subsequently synchronized at different stages of the cell cycle as described in the material and method section. FLAG-RECQL4 was then immunoprecipitated with an α-FLAG antibody and analyzed by Western blot (upper panel). The same nitrocellulose membrane was stripped and then re-probed with an α-acetyl-lys (α-Ac-lys) antibody (lower panel).
(B) His-RECQL4 was transiently transfected in 293T cells and the cells were subsequently treated with different DNA damaging agent as described in Materials and Methods. His-RECQL4 was immunoprecipitated with an α-His antibody and analyzed by western blot. The same nitrocellulose membrane was stripped and then re-probed with an α-acetyl-lys (α-Ac-lys) antibody (lower panel).
Femto-ECL was used to detect very low amounts of acetylated RECQL4 protein (A+B, lower panels).

Supplementary Figure S2

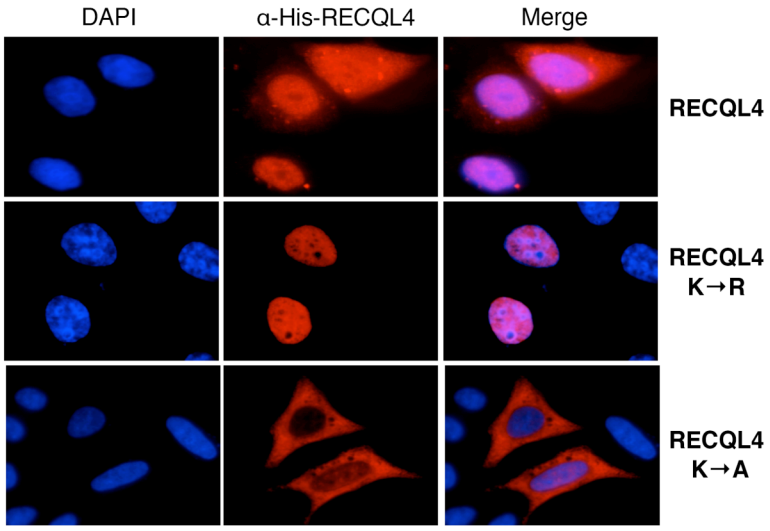

Fig. 2S Mutation of RECQL4 lysine residues Lys-376, Lys-380, Lys-382, Lys-385 and Lys-386 to alanine but not arginine relocalizes RECQL4 to the cytoplasm of U2OS cells.
His-tagged RECQL4 (wt) and the indicated His-RECQL4 K→R and K→A mutant proteins were expressed in U2OS cells by transient transfection and visualized with the His antibody by indirect immunofluorescence (middle panels, α-HisRECQL4, red). The left show the DAPI-stained nuclei (blue) and the right panels show the merged images of α-HisRECQL4 (red) and DAPI (blue) staining.

Supplementary Figure S3

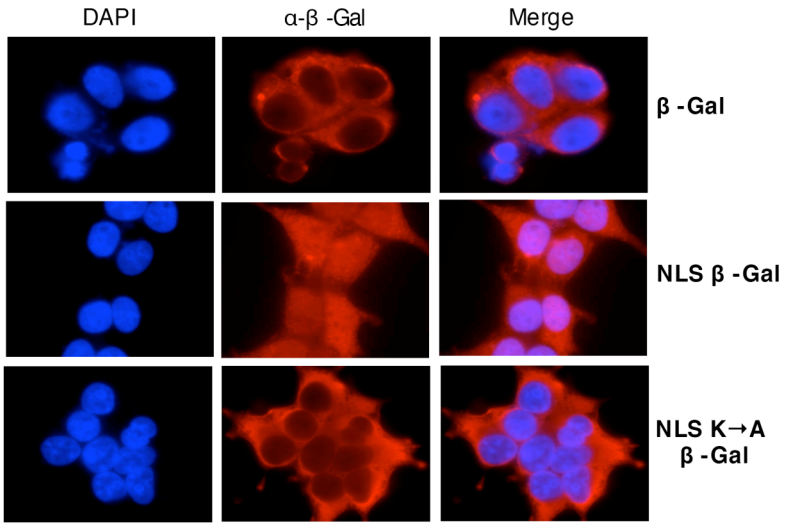

Fig. S3 RECQL4 aa 376-386 fused to β –Galactosidase leads to its import in 293T cells
β-Galactosidase and the indicated N-terminal fusion constructs (NLS-β-Gal and NLS-β-Gal K→A) were transiently transfected in 293T cells and visualized with the β-Galactosidase antibody by indirect immunofluorescence (middle panels, α- β-Gal, red). DAPI-staining shows nuclear DNA (left panels) and right panels show merged pictures (Merge).

5 Conclusion and Perspective

RECQL4 is a member of the conserved RecQ family of helicases. There are five human homologues named: *RECQL1, BLM, WRN, RECQL4, and RECQL5.* Mutations in three of the five family members, *BLM*, *WRN* and *RECQL4*, are associated with rare autosomal recessive disorders that are characterized by predisposition to cancer and premature aging (23). Interestingly, three disorders have been linked to mutations in the *RECQL4* gene: Rothmund-Thomson-, RAPADILINO-, and Baller-Gerold syndromes, thus making RECQL4 unique within the RecQ family of DNA helicases. Although these disorders represent distinct genetic entities, clinical observations have depicted highly variable expressivity and significant overlaps in the associated phenotypes. Consequently, it is extremely difficult to unravel the precise genotype-phenotype correlation in *RECQL4* related syndromes. This is likely due to the complex and multiple cellular networks RECQL4 is associated with.

RecQ helicases have been shown to unwind nuclear DNA structures resembling replication, transcription, and recombination intermediates (47). There is already much known about biochemical properties, interacting partners, and cellular localization of BLM and WRN helicase, although their exact cellular role is still under investigation. Progress in RECQL4 research is going much slower. After initial work about the cloning of the *RECQL4* gene (36) and its association with RTS (33), only a few papers about RECQL4 function have been published: It was shown that purified RECQL4 protein from *E.coli* lacks helicase activity, but possess ssDNA strand annealing and ssDNA-dependent ATPase activity (190). By amino acid homology RECQL4 contains a conserved helicase domain. Unlike other RecQ homologues, RECQL4 lacks the conserved RQC (*R*ec*Q C*-terminal) and HRDC (*h*elicase and *R*NAse *D C*-terminal) domains necessary for nucleic acid binding

and unwinding (271-274). However, it still remains possible that RECQL4 needs co-activator proteins or a particular post-translational modification in order to accomplish a DNA unwinding function. It would be interesting to test whether RECQL4 purified from mammalian or insect cells possesses helicase activity. Two reports suggest that RECQL4 is essential for DNA replication and cell proliferation. The *Xenopus* RECQL4 orthologue, *x*RTS, accumulates at origins of DNA replication and is required for binding of DNA polymerase α to chromatin (177, 178). Yin *et* al. demonstrated that RECQL4 interacts with cytoplasmic ubiquitinating proteins UBR1 and UBR2 (275) although the functional significance of this interaction is unclear. Our group recently reported that, in response to the induction of DSBs by etoposide treatment, a portion of RECQL4 and Rad51 nuclear foci colocalized, suggesting that RECQL4 plays a role in the repair of DSBs by homologous recombination (181).

Taken together, only little information is available about the cellular role of RECQL4 protein and further studies are needed to draw a more precise picture about the function of RECQL4 protein to maintain genome stability.

We investigated if RECQL4 is subject to reversible acetylation and how this post-translational modification influences RECQL4 function *in vivo*. We found that RECQL4 and the histone acetyltransferase p300 physically and functionally interact. We purified RECQL4 from *E.coli* and our experiments confirmed a previous report showing that RECQL4 is a Mg^{+2}– and ssDNA dependent ATPase (190). Surprisingly, preincubation of RECQL4 with purified p300 resulted in significant stimulation of the RECQL4 ATPase activity. However, the physiological consequence of this finding remains elusive. Further experiments could include the mapping of p300 domain that is crucial for the stimulation of RECQL4 ATPase activity. Additionally, it would be of particular interest to further investigate the consequence of p300 binding on the RECQL4 helicase activity.

RECQL4 subcellular localization was studied extensively in the last couple of years (163, 181, 186, 275, 276). RECQL4 is the only human RecQ family member that is not entirely nuclear but also located in the cytoplasm of different cell lines examined (276). So far, the molecular mechanism by which RECQL4 is translocated to the cytoplasm and the cytoplasmic function of RECQL4 remains to be elucidated.

We could show that the RECQL4 NLS is spanning amino acids 376-386 (KQAWKQKWRKK) and locates N-terminally of the helicase domain and p300 mediated acetylation of several lysine residues inside the RECQL4 NLS positively regulates the translocation of RECQL4 from the nucleus to the cytoplasm. Our findings are consistent with previously published data indicating that lysine acetylation modulates the subcellular localization of several proteins (199). Lysines are important components of NLSs (277), because the positive charge mediates the interaction with importins (278). We hypothesize, as shown for transcription factors HMGB1 (265) and E1A (267), that p300-mediated acetylation negatively affects the function of the RECQL4 NLS (aa 376-386) and thus disrupts its association with the nuclear import machinery, which leads to subsequent cytoplasmic accumulation of RECQL4 protein. However, synchronizing cells at different stages of the cell cycle or treatment with different DNA damaging agents had no influence on the acetylation level of RECQL4 and the trigger for the RECQL4 acetylation by p300 remains unknown. Further studies might address the question of how RECQL4 acetylation is stimulated *in vivo*. Additionally, investigating RECQL4 localization in cells where p300 is transiently knocked-down by siRNA might help to further understand the role of RECQL4 acetylation *in vivo*.

Shuttling of proteins between the nucleus and the cytoplasm of cells involves highly regulated protein-protein interactions between the import/export machinery and the cargo-protein. It would be of particular interest to identify the RECQL4 nuclear export signal (NES) in order to elucidate the mechanism by which

RECQL4 is exported to the cytoplasm in mammalian cells and to fully understand the dynamic process of RECQL4 shuttling.

BLM and WRN are both subject to different posttranslational modifications like phosphorylation, SUMOylation and acetylation (85-90, 146, 152-158). For example BLM is phosphorylated after treatment of cells with ionizing radiation or HU in an ATM/ATR dependent manner. These checkpoint kinases phosphorylate target protein with the consensus motif S/TQ (154). The RECQL4 aa sequence contains several putative ATM/ATR phosphorylation sites and it is therefore very likely that RECQL4 is phosphorylated by those kinases. Future experiments could address this question as following: RECQL4 protein could be immunoprecipitated from whole cell extracts and assayed for phosphorylation using and anti-phosphorylated-serine or threonine antibody. Furthermore, purified RECQL4 protein could be phosphorylated *in vitro* using purified ATM/ATR kinase and γ-ATP. Phosphorylated RECQL4 could subsequently be detected by autoradiography.

SUMO modifications, as shown for acetylation, take place at lysine residues. It would therefore be interesting to test if RECQL4 is SUMOylated *in* vivo and if SUMOylation would target the same binding sites as acetylation.

What might be the function of RECQL4 in the cytoplasm of human cells? RECQL4 is found in complex with UBR1/UBR2, two ubiquitin ligases that are part of the ubiquitin proteasome system, in cytosolic extracts of HeLa cells (275). It is therefore possible, that acetylation of RECQL4 could be a signal for its degradation in the cytoplasm. To address this question, we could test if acetylated RECQL4 preferentially binds to UBR1/UBR2 and if acetylation has an influence on RECQL4 poly-ubiquitination *in vitro* and *in vivo*. Co-immunoprecipitation experiments and subsequent mass spectrometry analysis using cytosolic extracts from human cells could help to identify novel RECQL4 interacting partners and clarify the function of cytosolic RECQL4 protein.

6 References

1. Soultanas, P. and Wigley, D.B. (2001) Unwinding the 'Gordian knot' of helicase action. *Trends in biochemical sciences,* **26,** 47-54.

2. Tuteja, N. and Tuteja, R. (2004) Unraveling DNA helicases. Motif, structure, mechanism and function. *European journal of biochemistry / FEBS,* **271,** 1849-63.

3. Abdel-Monem, M., Chanal, M.C. and Hoffmann-Berling, H. (1977) DNA unwinding enzyme II of Escherichia coli. 1. Purification and characterization of the ATPase activity. *European journal of biochemistry / FEBS,* **79,** 33-8.

4. Gorbalenya, A.E. and Koonin, E.V. (1993) Helicases: Amino acid sequence comparisons and structure-function relationships. *Current Opinion in Structural Biology,* **3,** 419-429.

5. Bird, L.E., Subramanya, H.S. and Wigley, D.B. (1998) Helicases: a unifying structural theme? *Curr Opin Struct Biol,* **8,** 14-8.

6. Singleton, M.R., Sawaya, M.R., Ellenberger, T. and Wigley, D.B. (2000) Crystal structure of T7 gene 4 ring helicase indicates a mechanism for sequential hydrolysis of nucleotides. *Cell,* **101,** 589-600.

7. Subramanya, H.S., Bird, L.E., Brannigan, J.A. and Wigley, D.B. (1996) Crystal structure of a DExx box DNA helicase. *Nature,* **384,** 379-83.

8. Hall, M.C. and Matson, S.W. (1999) Helicase motifs: the engine that powers DNA unwinding. *Mol Microbiol,* **34,** 867-77.

9. Walker, J.E., Saraste, M., Runswick, M.J. and Gay, N.J. (1982) Distantly related sequences in the alpha- and beta-subunits of ATP synthase, myosin, kinases and other ATP-requiring enzymes and a common nucleotide binding fold. *Embo J,* **1,** 945-51.

10. Pause, A. and Sonenberg, N. (1992) Mutational analysis of a DEAD box RNA helicase: the mammalian translation initiation factor eIF-4A. *Embo J,* **11,** 2643-54.

11. Marintcheva, B. and Weller, S.K. (2003) Helicase motif Ia is involved in single-strand DNA-binding and helicase activities of the herpes simplex virus type 1 origin-binding protein, UL9. *J Virol,* **77,** 2477-88.

12. Dillingham, M.S., Soultanas, P. and Wigley, D.B. (1999) Site-directed mutagenesis of motif III in PcrA helicase reveals a role in coupling ATP hydrolysis to strand separation. *Nucleic acids research,* **27,** 3310-7.

13. Ha, T., Rasnik, I., Cheng, W., Babcock, H.P., Gauss, G.H., Lohman, T.M. and Chu, S. (2002) Initiation and re-initiation of DNA unwinding by the Escherichia coli Rep helicase. *Nature,* **419,** 638-41.

14. Lohman, T.M. and Bjornson, K.P. (1996) Mechanisms of helicase-catalyzed DNA unwinding. *Annual review of biochemistry,* **65,** 169-214.

15. Maluf, N.K., Fischer, C.J. and Lohman, T.M. (2003) A Dimer of Escherichia coli UvrD is the active form of the helicase in vitro. *Journal of molecular biology,* **325,** 913-35.

16. Patel, S.S. and Picha, K.M. (2000) Structure and function of hexameric helicases. *Annual review of biochemistry,* **69,** 651-97.

17. Soultanas, P. and Wigley, D.B. (2000) DNA helicases: 'inching forward'. *Curr Opin Struct Biol,* **10,** 124-8.

18. Sharma, S., Doherty, K.M. and Brosh, R.M., Jr. (2006) Mechanisms of RecQ helicases in pathways of DNA metabolism and maintenance of genomic stability. *The Biochemical journal,* **398,** 319-37.

19. Velankar, S.S., Soultanas, P., Dillingham, M.S., Subramanya, H.S. and Wigley, D.B. (1999) Crystal structures of complexes of PcrA DNA helicase with a DNA substrate indicate an inchworm mechanism. *Cell,* **97,** 75-84.

20. Byrd, A.K. and Raney, K.D. (2004) Protein displacement by an assembly of helicase molecules aligned along single-stranded DNA. *Nature structural & molecular biology,* **11,** 531-8.

21. Byrd, A.K. and Raney, K.D. (2005) Increasing the length of the single-stranded overhang enhances unwinding of duplex DNA by bacteriophage T4 Dda helicase. *Biochemistry,* **44,** 12990-7.

22. Cobb, J.A., Bjergbaek, L. and Gasser, S.M. (2002) RecQ helicases: at the heart of genetic stability. *FEBS letters,* **529,** 43-8.

23. Hickson, I.D. (2003) RecQ helicases: caretakers of the genome. *Nature reviews,* **3,** 169-178.

24. Hickson, I.D. (2003) RecQ helicases: caretakers of the genome. *Nature reviews,* **3,** 169-78.

25. Nakayama, H., Nakayama, K., Nakayama, R., Irino, N., Nakayama, Y. and Hanawalt, P.C. (1984) Isolation and genetic characterization of a thymineless death-resistant mutant of Escherichia coli K12: identification of a new mutation (recQ1) that blocks the RecF recombination pathway. *Mol Gen Genet,* **195,** 474-80.

26. Bernstein, D.A., Zittel, M.C. and Keck, J.L. (2003) High-resolution structure of the E.coli RecQ helicase catalytic core. *EMBO J,* **22,** 4910-21.

27. Courcelle, J. and Hanawalt, P.C. (1999) RecQ and RecJ process blocked replication forks prior to the resumption of replication in UV-irradiated Escherichia coli. *Mol Gen Genet,* **262,** 543-51.

28. Hanada, K., Ukita, T., Kohno, Y., Saito, K., Kato, J. and Ikeda, H. (1997) RecQ DNA helicase is a suppressor of illegitimate recombination in Escherichia coli. *Proceedings of the National Academy of Sciences of the United States of America,* **94,** 3860-5.

29. Hishida, T., Han, Y.W., Shibata, T., Kubota, Y., Ishino, Y., Iwasaki, H. and Shinagawa, H. (2004) Role of the Escherichia coli RecQ DNA helicase in SOS signaling and genome stabilization at stalled replication forks. *Genes & development,* **18,** 1886-97.

30. Tuteja, N. and Tuteja, R. (2004) Prokaryotic and eukaryotic DNA helicases. Essential molecular motor proteins for cellular machinery. *European journal of biochemistry / FEBS,* **271,** 1835-48.

31. Yu, C.E., Oshima, J., Fu, Y.H., Wijsman, E.M., Hisama, F., Alisch, R., Matthews, S., Nakura, J., Miki, T., Ouais, S. *et al.* (1996) Positional cloning of the Werner's syndrome gene. *Science,* **272,** 258-262.

32. Ellis, N.A., Groden, J., Ye, T.Z., Straughen, J., Lennon, D.J., Ciocci, S., Proytcheva, M. and German, J. (1995) The Bloom's syndrome gene product is homologous to RecQ helicases. *Cell,* **83,** 655-666.

33. Kitao, S., Shimamoto, A., Goto, M., Miller, R.W., Smithson, W.A., Lindor, N.M. and Furuichi, Y. (1999) Mutations in RECQL4 cause a subset of cases of Rothmund-Thomson syndrome. *Nat Genet,* **22,** 82-82.

34. Siitonen, H.A., Kopra, O., Kaariainen, H., Haravuori, H., Winter, R.M., Saamanen, A.M., Peltonen, L. and Kestila, M. (2003) Molecular defect of RAPADILINO syndrome expands the phenotype spectrum of RECQL diseases. *Hum Mol Genet,* **12,** 2837-2844.

35. Van Maldergem, L., Siitonen, H.A., Jalkh, N., Chouery, E., De Roy, M., Delague, V., Muenke, M., Jabs, E.W., Cai, J., Wang, L.L. *et al.* (2006) Revisiting the craniosynostosis-radial ray hypoplasia association: Baller-Gerold syndrome caused by mutations in the RECQL4 gene. *J Med Genet,* **43,** 148-152.

36. Kitao, S., Ohsugi, I., Ichikawa, K., Goto, M., Furuichi, Y. and Shimamoto, A. (1998) Cloning of two new human helicase genes of the RecQ family: biological significance of multiple species in higher eukaryotes. *Genomics,* **54,** 443-52.

37. Puranam, K.L. and Blackshear, P.J. (1994) Cloning and characterization of RECQL, a potential human homologue of the Escherichia coli DNA helicase RecQ. *The Journal of biological chemistry,* **269,** 29838-45.

38. Seki, M., Miyazawa, H., Tada, S., Yanagisawa, J., Yamaoka, T., Hoshino, S., Ozawa, K., Eki, T., Nogami, M., Okumura, K. *et al.* (1994) Molecular cloning of cDNA encoding human DNA helicase Q1 which has homology to Escherichia coli Rec Q helicase and localization of the gene at chromosome 12p12. *Nucleic acids research,* **22,** 4566-73.

39. Cui, S., Klima, R., Ochem, A., Arosio, D., Falaschi, A. and Vindigni, A. (2003) Characterization of the DNA-unwinding activity of human RECQ1, a helicase specifically stimulated by human replication protein A. *The Journal of biological chemistry,* **278,** 1424-32.

40. Cui, S., Arosio, D., Doherty, K.M., Brosh, R.M., Jr., Falaschi, A. and Vindigni, A. (2004) Analysis of the unwinding activity of the dimeric RECQ1 helicase in the presence of human replication protein A. *Nucleic acids research,* **32,** 2158-70.

41. Sharma, S., Sommers, J.A., Choudhary, S., Faulkner, J.K., Cui, S., Andreoli, L., Muzzolini, L., Vindigni, A. and Brosh, R.M., Jr. (2005) Biochemical analysis of the DNA unwinding and strand annealing activities catalyzed by human RECQ1. *The Journal of biological chemistry,* **280,** 28072-84.

42. Muzzolini, L., Beuron, F., Patwardhan, A., Popuri, V., Cui, S., Niccolini, B., Rappas, M., Freemont, P.S. and Vindigni, A. (2007) Different quaternary structures of human RECQ1 are associated with its dual enzymatic activity. *PLoS biology,* **5,** e20.

43. Seki, T., Tada, S., Katada, T. and Enomoto, T. (1997) Cloning of a cDNA encoding a novel importin-alpha homologue, Qip1: discrimination of Qip1 and Rch1 from hSrp1 by their ability to interact with DNA helicase Q1/RecQL. *Biochem Biophys Res Commun,* **234,** 48-53.

44. Miyamoto, Y., Imamoto, N., Sekimoto, T., Tachibana, T., Seki, T., Tada, S., Enomoto, T. and Yoneda, Y. (1997) Differential modes of nuclear localization signal (NLS) recognition by three distinct classes of NLS receptors. *The Journal of biological chemistry,* **272,** 26375-81.

45. Johnson, F.B., Lombard, D.B., Neff, N.F., Mastrangelo, M.A., Dewolf, W., Ellis, N.A., Marciniak, R.A., Yin, Y., Jaenisch, R. and Guarente, L. (2000) Association of the Bloom syndrome protein with topoisomerase IIIalpha in somatic and meiotic cells. *Cancer research,* **60,** 1162-7.

46. Bloom, D. (1954) Congenital telangiectatic erythema resembling lupus erythematosus in dwarfs; probably a syndrome entity. *A.M.A,* **88,** 754-8.

47. Bachrati, C.Z. and Hickson, I.D. (2003) RecQ helicases: suppressors of tumorigenesis and premature aging. *The Biochemical journal,* **374,** 577-606.

48. http://info.med.yale.edu/pediat/pedres/.

49. McDaniel, L.D. and Schultz, R.A. (1992) Elevated sister chromatid exchange phenotype of Bloom syndrome cells is complemented by human chromosome 15. *Proceedings of the National Academy of Sciences of the United States of America,* **89,** 7968-72.

50. Poppe, B., Van Limbergen, H., Van Roy, N., Vandecruys, E., De Paepe, A., Benoit, Y. and Speleman, F. (2001) Chromosomal aberrations in Bloom syndrome patients with myeloid malignancies. *Cancer genetics and cytogenetics,* **128,** 39-42.

51. Poppe, B., Van Limbergen, H., Van Roy, N., Vandecruys, E., De Paepe, A., Benoit, Y. and Speleman, F. (2001) Chromosomal aberrations in Bloom syndrome patients with myeloid malignancies. *Cancer Genet Cytogenet,* **128,** 39-42.

52. German, J., Schonberg, S., Louie, E. and Chaganti, R.S. (1977) Bloom's syndrome. IV. Sister-chromatid exchanges in lymphocytes. *Am J Hum Genet,* **29,** 248-55.

53. Chester, N., Kuo, F., Kozak, C., O'Hara, C.D. and Leder, P. (1998) Stage-specific apoptosis, developmental delay, and embryonic lethality in mice homozygous for a targeted disruption in the murine Bloom's syndrome gene. *Genes & development,* **12,** 3382-93.

54. Luo, G., Santoro, I.M., McDaniel, L.D., Nishijima, I., Mills, M., Youssoufian, H., Vogel, H., Schultz, R.A. and Bradley, A. (2000) Cancer predisposition caused by elevated mitotic recombination in Bloom mice. *Nat Genet,* **26,** 424-9.

55. Goss, K.H., Risinger, M.A., Kordich, J.J., Sanz, M.M., Straughen, J.E., Slovek, L.E., Capobianco, A.J., German, J., Boivin, G.P. and Groden, J. (2002) Enhanced tumor formation in mice heterozygous for Blm mutation. *Science,* **297,** 2051-3.

56. Zhong, S., Hu, P., Ye, T.Z., Stan, R., Ellis, N.A. and Pandolfi, P.P. (1999) A role for PML and the nuclear body in genomic stability. *Oncogene,* **18,** 7941-7.

57. Dellaire, G. and Bazett-Jones, D.P. (2004) PML nuclear bodies: dynamic sensors of DNA damage and cellular stress. *Bioessays,* **26,** 963-77.

58. Hodges, M., Tissot, C., Howe, K., Grimwade, D. and Freemont, P.S. (1998) Structure, organization, and dynamics of promyelocytic leukemia protein nuclear bodies. *Am J Hum Genet,* **63,** 297-304.

59. Ruggero, D., Wang, Z.G. and Pandolfi, P.P. (2000) The puzzling multiple lives of PML and its role in the genesis of cancer. *Bioessays,* **22,** 827-35.

60. Yankiwski, V., Marciniak, R.A., Guarente, L. and Neff, N.F. (2000) Nuclear structure in normal and Bloom syndrome cells. *Proceedings of the National Academy of Sciences of the United States of America,* **97,** 5214-9.

61. Wang, Y., Cortez, D., Yazdi, P., Neff, N., Elledge, S.J. and Qin, J. (2000) BASC, a super complex of BRCA1-associated proteins involved in the recognition and repair of aberrant DNA structures. *Genes & development,* **14,** 927-39.

62. Franchitto, A. and Pichierri, P. (2002) Bloom's syndrome protein is required for correct relocalization of RAD50/MRE11/NBS1 complex after replication fork arrest. *The Journal of cell biology,* **157,** 19-30.

63. Meetei, A.R., Sechi, S., Wallisch, M., Yang, D., Young, M.K., Joenje, H., Hoatlin, M.E. and Wang, W. (2003) A multiprotein nuclear complex connects Fanconi anemia and Bloom syndrome. *Mol Cell Biol,* **23,** 3417-26.

64. Pichierri, P., Franchitto, A. and Rosselli, F. (2004) BLM and the FANC proteins collaborate in a common pathway in response to stalled replication forks. *The EMBO journal,* **23,** 3154-63.

65. Wu, L., Davies, S.L., Levitt, N.C. and Hickson, I.D. (2001) Potential role for the BLM helicase in recombinational repair via a conserved interaction with RAD51. *The Journal of biological chemistry,* **276,** 19375-81.

66. Bischof, O., Kim, S.H., Irving, J., Beresten, S., Ellis, N.A. and Campisi, J. (2001) Regulation and localization of the Bloom syndrome protein in response to DNA damage. *The Journal of cell biology,* **153,** 367-80.

67. Garkavtsev, I.V., Kley, N., Grigorian, I.A. and Gudkov, A.V. (2001) The Bloom syndrome protein interacts and cooperates with p53 in regulation of transcription and cell growth control. *Oncogene,* **20,** 8276-80.

68. Wang, X.W., Tseng, A., Ellis, N.A., Spillare, E.A., Linke, S.P., Robles, A.I., Seker, H., Yang, Q., Hu, P., Beresten, S. *et al.* (2001) Functional interaction of p53 and BLM DNA helicase in apoptosis. *The Journal of biological chemistry,* **276,** 32948-55.

69. Yang, Q., Zhang, R., Wang, X.W., Spillare, E.A., Linke, S.P., Subramanian, D., Griffith, J.D., Li, J.L., Hickson, I.D., Shen, J.C. *et al.* (2002) The processing of Holliday junctions by BLM and WRN helicases is regulated by p53. *The Journal of biological chemistry,* **277,** 31980-7.

70. Brosh, R.M., Jr., Li, J.L., Kenny, M.K., Karow, J.K., Cooper, M.P., Kureekattil, R.P., Hickson, I.D. and Bohr, V.A. (2000) Replication protein A physically interacts with the Bloom's syndrome protein and stimulates its helicase activity. *The Journal of biological chemistry,* **275,** 23500-8.

71. Langland, G., Kordich, J., Creaney, J., Goss, K.H., Lillard-Wetherell, K., Bebenek, K., Kunkel, T.A. and Groden, J. (2001) The Bloom's syndrome protein (BLM) interacts with MLH1 but is not required for DNA mismatch repair. *The Journal of biological chemistry,* **276,** 30031-5.

72. Sanz, M.M., Proytcheva, M., Ellis, N.A., Holloman, W.K. and German, J. (2000) BLM, the Bloom's syndrome protein, varies during the cell cycle in its amount, distribution, and co-localization with other nuclear proteins. *Cytogenetics and cell genetics,* **91,** 217-23.

73. Wu, L., Davies, S.L., North, P.S., Goulaouic, H., Riou, J.F., Turley, H., Gatter, K.C. and Hickson, I.D. (2000) The Bloom's syndrome gene product interacts with topoisomerase III. *The Journal of biological chemistry,* **275,** 9636-44.

74. Wu, L., Bachrati, C.Z., Ou, J., Xu, C., Yin, J., Chang, M., Wang, W., Li, L., Brown, G.W. and Hickson, I.D. (2006) BLAP75/RMI1 promotes the BLM-dependent dissolution of homologous recombination intermediates. *Proceedings of the National Academy of Sciences of the United States of America,* **103,** 4068-73.

75. Opresko, P.L., von Kobbe, C., Laine, J.P., Harrigan, J., Hickson, I.D. and Bohr, V.A. (2002) Telomere-binding protein TRF2 binds to and stimulates the Werner and Bloom syndrome helicases. *The Journal of biological chemistry,* **277,** 41110-9.

76. Stavropoulos, D.J., Bradshaw, P.S., Li, X., Pasic, I., Truong, K., Ikura, M., Ungrin, M. and Meyn, M.S. (2002) The Bloom syndrome helicase BLM interacts with TRF2 in ALT cells and promotes telomeric DNA synthesis. *Hum Mol Genet,* **11,** 3135-44.

77. Jiao, R., Bachrati, C.Z., Pedrazzi, G., Kuster, P., Petkovic, M., Li, J.L., Egli, D., Hickson, I.D. and Stagljar, I. (2004) Physical and functional interaction between the Bloom's syndrome gene product and the largest subunit of chromatin assembly factor 1. *Mol Cell Biol,* **24,** 4710-9.

78. Karow, J.K., Chakraverty, R.K. and Hickson, I.D. (1997) The Bloom's syndrome gene product is a 3'-5' DNA helicase. *The Journal of biological chemistry,* **272,** 30611-4.

79. Beresten, S.F., Stan, R., van Brabant, A.J., Ye, T., Naureckiene, S. and Ellis, N.A. (1999) Purification of overexpressed hexahistidine-tagged BLM N431 as oligomeric complexes. *Protein expression and purification,* **17,** 239-48.

80. Mohaghegh, P., Karow, J.K., Brosh Jr, R.M., Jr., Bohr, V.A. and Hickson, I.D. (2001) The Bloom's and Werner's syndrome proteins are DNA structure-specific helicases. *Nucleic acids research,* **29,** 2843-9.

81. van Brabant, A.J., Ye, T., Sanz, M., German, I.J., Ellis, N.A. and Holloman, W.K. (2000) Binding and melting of D-loops by the Bloom syndrome helicase. *Biochemistry,* **39,** 14617-25.

82. Cheok, C.F., Wu, L., Garcia, P.L., Janscak, P. and Hickson, I.D. (2005) The Bloom's syndrome helicase promotes the annealing of complementary single-stranded DNA. *Nucleic acids research,* **33,** 3932-41.

83. Wu, L. and Hickson, I.D. (2003) The Bloom's syndrome helicase suppresses crossing over during homologous recombination. *Nature,* **426,** 870-4.

84. Schwacha, A. and Kleckner, N. (1995) Identification of double Holliday junctions as intermediates in meiotic recombination. *Cell,* **83,** 783-91.

85. Ababou, M., Dutertre, S., Lecluse, Y., Onclercq, R., Chatton, B. and Amor-Gueret, M. (2000) ATM-dependent phosphorylation and accumulation of endogenous BLM protein in response to ionizing radiation. *Oncogene,* **19,** 5955-63.

86. Bayart, E., Dutertre, S., Jaulin, C., Guo, R.B., Xi, X.G. and Amor-Gueret, M. (2006) The Bloom syndrome helicase is a substrate of the mitotic Cdc2 kinase. *Cell cycle (Georgetown, Tex,* **5,** 1681-6.

87. Beamish, H., Kedar, P., Kaneko, H., Chen, P., Fukao, T., Peng, C., Beresten, S., Gueven, N., Purdie, D., Lees-Miller, S. *et al.* (2002) Functional link between BLM defective in Bloom's syndrome and the ataxia-telangiectasia-mutated protein, ATM. *The Journal of biological chemistry,* **277,** 30515-23.

88. Davies, S.L., North, P.S., Dart, A., Lakin, N.D. and Hickson, I.D. (2004) Phosphorylation of the Bloom's syndrome helicase and its role in recovery from S-phase arrest. *Mol Cell Biol,* **24,** 1279-91.

89. Leng, M., Chan, D.W., Luo, H., Zhu, C., Qin, J. and Wang, Y. (2006) MPS1-dependent mitotic BLM phosphorylation is important for chromosome stability. *Proceedings of the National Academy of Sciences of the United States of America,* **103,** 11485-90.

90. Eladad, S., Ye, T.Z., Hu, P., Leversha, M., Beresten, S., Matunis, M.J. and Ellis, N.A. (2005) Intra-nuclear trafficking of the BLM helicase to DNA damage-induced foci is regulated by SUMO modification. *Hum Mol Genet,* **14,** 1351-65.

91. Goto, M., Rubenstein, M., Weber, J., Woods, K. and Drayna, D. (1992) Genetic linkage of Werner's syndrome to five markers on chromosome 8. *Nature,* **355,** 735-8.

92. Hisama, F.M., Bohr, V.A. and Oshima, J. (2006) WRN's tenth anniversary. *Sci Aging Knowledge Environ,* **2006,** pe18.

93. Epstein, C.J., Martin, G.M., Schultz, A.L. and Motulsky, A.G. (1966) Werner's syndrome a review of its symptomatology, natural history, pathologic features, genetics and relationship to the natural aging process. *Medicine,* **45,** 177-221.

94. Goto, M. (1997) Hierarchical deterioration of body systems in Werner's syndrome: implications for normal ageing. *Mechanisms of ageing and development,* **98,** 239-54.

95. Martin, G.M. (1978) Genetic syndromes in man with potential relevance to the pathobiology of aging. *Birth defects original article series,* **14,** 5-39.

96. Goto, M., Miller, R.W., Ishikawa, Y. and Sugano, H. (1996) Excess of rare cancers in Werner syndrome (adult progeria). *Cancer Epidemiol Biomarkers Prev,* **5,** 239-46.

97. Martin, G.M., Oshima, J., Gray, M.D. and Poot, M. (1999) What geriatricians should know about the Werner syndrome. *Journal of the American Geriatrics Society,* **47,** 1136-44.

98. Salk, D. (1982) Werner's syndrome: a review of recent research with an analysis of connective tissue metabolism, growth control of cultured cells, and chromosomal aberrations. *Human genetics,* **62,** 1-5.

99. Poot, M., Gollahon, K.A., Emond, M.J., Silber, J.R. and Rabinovitch, P.S. (2002) Werner syndrome diploid fibroblasts are sensitive to 4-nitroquinoline-N-oxide and 8-methoxypsoralen: implications for the disease phenotype. *Faseb J,* **16,** 757-8.

100. Gray, M.D., Wang, L., Youssoufian, H., Martin, G.M. and Oshima, J. (1998) Werner helicase is localized to transcriptionally active nucleoli of cycling cells. *Exp Cell Res,* **242,** 487-94.

101. Sakamoto, S., Nishikawa, K., Heo, S.J., Goto, M., Furuichi, Y. and Shimamoto, A. (2001) Werner helicase relocates into nuclear foci in response to DNA damaging agents and co-localizes with RPA and Rad51. *Genes Cells,* **6,** 421-30.

102. Lebel, M. and Leder, P. (1998) A deletion within the murine Werner syndrome helicase induces sensitivity to inhibitors of topoisomerase and loss of cellular proliferative capacity. *Proceedings of the National Academy of Sciences of the United States of America,* **95,** 13097-102.

103. Lombard, D.B., Beard, C., Johnson, B., Marciniak, R.A., Dausman, J., Bronson, R., Buhlmann, J.E., Lipman, R., Curry, R., Sharpe, A. *et al.* (2000) Mutations in the WRN gene in mice accelerate mortality in a p53-null background. *Molecular and cellular biology,* **20,** 3286-91.

104. Wang, L., Ogburn, C.E., Ware, C.B., Ladiges, W.C., Youssoufian, H., Martin, G.M. and Oshima, J. (2000) Cellular Werner phenotypes in mice expressing a putative dominant-negative human WRN gene. *Genetics,* **154,** 357-62.

105. Lavoie, J., Carter, R., Drouin, R. and Lebel, M. (2005) Increased frequency of multiradial chromosome structures in mouse embryonic fibroblasts lacking functional Werner syndrome protein and poly(ADP-ribose) polymerase-1. *Cancer genetics and cytogenetics,* **156,** 134-43.

106. Chang, S., Multani, A.S., Cabrera, N.G., Naylor, M.L., Laud, P., Lombard, D., Pathak, S., Guarente, L. and DePinho, R.A. (2004) Essential role of limiting telomeres in the pathogenesis of Werner syndrome. *Nature genetics,* **36,** 877-82.

107. Essers, J., Theil, A.F., Baldeyron, C., van Cappellen, W.A., Houtsmuller, A.B., Kanaar, R. and Vermeulen, W. (2005) Nuclear dynamics of PCNA in DNA replication and repair. *Mol Cell Biol,* **25,** 9350-9.

108. Lebel, M., Spillare, E.A., Harris, C.C. and Leder, P. (1999) The Werner syndrome gene product co-purifies with the DNA replication complex and interacts with PCNA and topoisomerase I. *The Journal of biological chemistry,* **274,** 37795-9.

109. Rodriguez-Lopez, A.M., Jackson, D.A., Nehlin, J.O., Iborra, F., Warren, A.V. and Cox, L.S. (2003) Characterisation of the interaction between WRN, the helicase/exonuclease defective in progeroid Werner's syndrome, and an essential replication factor, PCNA. *Mechanisms of ageing and development,* **124,** 167-74.

110. Warbrick, E. (1998) PCNA binding through a conserved motif. *Bioessays,* **20,** 195-9.

111. Warbrick, E. (2000) The puzzle of PCNA's many partners. *Bioessays,* **22,** 997-1006.

112. Kusumoto, R., Muftuoglu, M. and Bohr, V.A. (2007) The role of WRN in DNA repair is affected by post-translational modifications. *Mechanisms of ageing and development,* **128,** 50-7.

113. Laine, J.P., Opresko, P.L., Indig, F.E., Harrigan, J.A., von Kobbe, C. and Bohr, V.A. (2003) Werner protein stimulates topoisomerase I DNA relaxation activity. *Cancer research,* **63,** 7136-46.

114. Pichierri, P., Franchitto, A., Mosesso, P. and Palitti, F. (2000) Werner's syndrome cell lines are hypersensitive to camptothecin-induced chromosomal damage. *Mutat Res,* **456,** 45-57.

115. Poot, M., Gollahon, K.A. and Rabinovitch, P.S. (1999) Werner syndrome lymphoblastoid cells are sensitive to camptothecin-induced apoptosis in S-phase. *Human genetics,* **104,** 10-4.

116. Kamath-Loeb, A.S., Johansson, E., Burgers, P.M. and Loeb, L.A. (2000) Functional interaction between the Werner Syndrome protein and DNA polymerase delta. *Proceedings of the National Academy of Sciences of the United States of America,* **97,** 4603-8.

117. Kamath-Loeb, A.S., Loeb, L.A., Johansson, E., Burgers, P.M. and Fry, M. (2001) Interactions between the Werner syndrome helicase and DNA polymerase delta specifically facilitate copying of tetraplex and hairpin structures of the d(CGG)n trinucleotide repeat sequence. *The Journal of biological chemistry,* **276,** 16439-46.

118. Wold, M.S. (1997) Replication protein A: a heterotrimeric, single-stranded DNA-binding protein required for eukaryotic DNA metabolism. *Annual review of biochemistry,* **66,** 61-92.

119. Brosh, R.M., Jr., Orren, D.K., Nehlin, J.O., Ravn, P.H., Kenny, M.K., Machwe, A. and Bohr, V.A. (1999) Functional and physical interaction between WRN helicase and human replication protein A. *The Journal of biological chemistry,* **274,** 18341-50.

120. Shen, J.C., Lao, Y., Kamath-Loeb, A., Wold, M.S. and Loeb, L.A. (2003) The N-terminal domain of the large subunit of human replication protein A binds to Werner syndrome protein and stimulates helicase activity. *Mechanisms of ageing and development,* **124,** 921-30.

121. Ohsugi, I., Tokutake, Y., Suzuki, N., Ide, T., Sugimoto, M. and Furuichi, Y. (2000) Telomere repeat DNA forms a large non-covalent complex with unique cohesive properties which is dissociated by Werner syndrome DNA helicase in the presence of replication protein A. *Nucleic acids research,* **28,** 3642-8.

122. Opresko, P.L., Laine, J.P., Brosh, R.M., Jr., Seidman, M.M. and Bohr, V.A. (2001) Coordinate action of the helicase and 3' to 5' exonuclease of Werner syndrome protein. *The Journal of biological chemistry,* **276,** 44677-87.

123. Brosh, R.M., Jr., von Kobbe, C., Sommers, J.A., Karmakar, P., Opresko, P.L., Piotrowski, J., Dianova, I., Dianov, G.L. and Bohr, V.A. (2001) Werner syndrome protein interacts with human flap endonuclease 1 and stimulates its cleavage activity. *Embo J,* **20,** 5791-801.

124. Bambara, R.A., Murante, R.S. and Henricksen, L.A. (1997) Enzymes and reactions at the eukaryotic DNA replication fork. *The Journal of biological chemistry,* **272,** 4647-50.

125. Kim, K., Biade, S. and Matsumoto, Y. (1998) Involvement of flap endonuclease 1 in base excision DNA repair. *The Journal of biological chemistry,* **273,** 8842-8.

126. Wu, X., Wilson, T.E. and Lieber, M.R. (1999) A role for FEN-1 in nonhomologous DNA end joining: the order of strand annealing and nucleolytic processing events. *Proceedings of the National Academy of Sciences of the United States of America,* **96,** 1303-8.

127. Dynan, W.S. and Yoo, S. (1998) Interaction of Ku protein and DNA-dependent protein kinase catalytic subunit with nucleic acids. *Nucleic acids research,* **26,** 1551-9.

128. Jeggo, P.A. (1998) DNA breakage and repair. *Advances in genetics,* **38,** 185-218.

129. Cooper, M.P., Machwe, A., Orren, D.K., Brosh, R.M., Ramsden, D. and Bohr, V.A. (2000) Ku complex interacts with and stimulates the Werner protein. *Genes & development,* **14,** 907-12.

130. Karmakar, P., Snowden, C.M., Ramsden, D.A. and Bohr, V.A. (2002) Ku heterodimer binds to both ends of the Werner protein and functional interaction occurs at the Werner N-terminus. *Nucleic acids research,* **30,** 3583-91.

131. Spilianakis, C., Papamatheakis, J. and Kretsovali, A. (2000) Acetylation by PCAF enhances CIITA nuclear accumulation and transactivation of major histocompatibility complex class II genes. *Mol Cell Biol,* **20,** 8489-98.

132. Li, B. and Comai, L. (2001) Requirements for the nucleolytic processing of DNA ends by the Werner syndrome protein-Ku70/80 complex. *The Journal of biological chemistry,* **276,** 9896-902.

133. Li, B. and Comai, L. (2002) Displacement of DNA-PKcs from DNA ends by the Werner syndrome protein. *Nucleic acids research,* **30,** 3653-61.

134. Orren, D.K., Machwe, A., Karmakar, P., Piotrowski, J., Cooper, M.P. and Bohr, V.A. (2001) A functional interaction of Ku with Werner exonuclease facilitates digestion of damaged DNA. *Nucleic acids research,* **29,** 1926-34.

135. Harrigan, J.A., Opresko, P.L., von Kobbe, C., Kedar, P.S., Prasad, R., Wilson, S.H. and Bohr, V.A. (2003) The Werner syndrome protein stimulates DNA polymerase beta strand displacement synthesis via its helicase activity. *The Journal of biological chemistry,* **278,** 22686-95.

136. Barnes, D.E. and Lindahl, T. (2004) Repair and genetic consequences of endogenous DNA base damage in mammalian cells. *Annual review of genetics,* **38,** 445-76.

137. Brosh, R.M., Jr., Karmakar, P., Sommers, J.A., Yang, Q., Wang, X.W., Spillare, E.A., Harris, C.C. and Bohr, V.A. (2001) p53 Modulates the exonuclease activity of Werner syndrome protein. *The Journal of biological chemistry,* **276,** 35093-102.

138. Spillare, E.A., Robles, A.I., Wang, X.W., Shen, J.C., Yu, C.E., Schellenberg, G.D. and Harris, C.C. (1999) p53-mediated apoptosis is attenuated in Werner syndrome cells. *Genes & development,* **13,** 1355-60.

139. Yamabe, Y., Shimamoto, A., Goto, M., Yokota, J., Sugawara, M. and Furuichi, Y. (1998) Sp1-mediated transcription of the Werner helicase gene is modulated by Rb and p53. *Mol Cell Biol,* **18,** 6191-200.

140. Johnson, F.B., Marciniak, R.A., McVey, M., Stewart, S.A., Hahn, W.C. and Guarente, L. (2001) The Saccharomyces cerevisiae WRN homolog Sgs1p participates in telomere maintenance in cells lacking telomerase. *The EMBO journal,* **20,** 905-13.

141. Opresko, P.L., Otterlei, M., Graakjaer, J., Bruheim, P., Dawut, L., Kolvraa, S., May, A., Seidman, M.M. and Bohr, V.A. (2004) The Werner syndrome helicase and exonuclease cooperate to resolve telomeric D loops in a manner regulated by TRF1 and TRF2. *Mol Cell,* **14,** 763-74.

142. Orren, D.K., Theodore, S. and Machwe, A. (2002) The Werner syndrome helicase/exonuclease (WRN) disrupts and degrades D-loops in vitro. *Biochemistry,* **41,** 13483-8.

143. Crabbe, L., Verdun, R.E., Haggblom, C.I. and Karlseder, J. (2004) Defective telomere lagging strand synthesis in cells lacking WRN helicase activity. *Science (New York, N.Y,* **306,** 1951-3.

144. Pichierri, P. and Franchitto, A. (2004) Werner syndrome protein, the MRE11 complex and ATR: menage-a-trois in guarding genome stability during DNA replication? *Bioessays,* **26,** 306-13.

145. D'Amours, D. and Jackson, S.P. (2002) The Mre11 complex: at the crossroads of dna repair and checkpoint signalling. *Nat Rev Mol Cell Biol,* **3,** 317-27.

146. Cheng, W.H., von Kobbe, C., Opresko, P.L., Fields, K.M., Ren, J., Kufe, D. and Bohr, V.A. (2003) Werner syndrome protein phosphorylation by abl tyrosine kinase regulates its activity and distribution. *Mol Cell Biol,* **23,** 6385-95.

147. Franchitto, A. and Pichierri, P. (2004) Werner syndrome protein and the MRE11 complex are involved in a common pathway of replication fork recovery. *Cell cycle (Georgetown, Tex,* **3,** 1331-9.

148. Jiao, R., Harrigan, J.A., Shevelev, I., Dietschy, T., Selak, N., Indig, F.E., Piotrowski, J., Janscak, P., Bohr, V.A. and Stagljar, I. (2007) The Werner syndrome protein is required for recruitment of chromatin assembly factor 1 following DNA damage. *Oncogene,* **26,** 3811-22.

149. Huang, S., Beresten, S., Li, B., Oshima, J., Ellis, N.A. and Campisi, J. (2000) Characterization of the human and mouse WRN 3'-->5' exonuclease. *Nucleic acids research,* **28,** 2396-405.

150. Huang, S., Li, B., Gray, M.D., Oshima, J., Mian, I.S. and Campisi, J. (1998) The premature ageing syndrome protein, WRN, is a 3'-->5' exonuclease. *Nat Genet,* **20,** 114-6.

151. Constantinou, A., Tarsounas, M., Karow, J.K., Brosh, R.M., Bohr, V.A., Hickson, I.D. and West, S.C. (2000) Werner's syndrome protein (WRN) migrates Holliday junctions and co-localizes with RPA upon replication arrest. *EMBO Rep,* **1,** 80-4.

152. Karmakar, P., Piotrowski, J., Brosh, R.M., Jr., Sommers, J.A., Miller, S.P., Cheng, W.H., Snowden, C.M., Ramsden, D.A. and Bohr, V.A. (2002) Werner protein is a target of DNA-dependent protein kinase in vivo and in vitro, and its catalytic activities are regulated by phosphorylation. *The Journal of biological chemistry,* **277,** 18291-302.

153. Pichierri, P., Rosselli, F. and Franchitto, A. (2003) Werner's syndrome protein is phosphorylated in an ATR/ATM-dependent manner following replication arrest and DNA damage induced during the S phase of the cell cycle. *Oncogene,* **22,** 1491-500.

154. Kim, S.T., Lim, D.S., Canman, C.E. and Kastan, M.B. (1999) Substrate specificities and identification of putative substrates of ATM kinase family members. *The Journal of biological chemistry,* **274,** 37538-43.

155. Yannone, S.M., Roy, S., Chan, D.W., Murphy, M.B., Huang, S., Campisi, J. and Chen, D.J. (2001) Werner syndrome protein is regulated and phosphorylated by DNA-dependent protein kinase. *The Journal of biological chemistry,* **276,** 38242-8.

156. Kawabe, Y., Seki, M., Seki, T., Wang, W.S., Imamura, O., Furuichi, Y., Saitoh, H. and Enomoto, T. (2000) Covalent modification of the Werner's syndrome gene product with the ubiquitin-related protein, SUMO-1. *The Journal of biological chemistry,* **275,** 20963-6.

157. Woods, Y.L., Xirodimas, D.P., Prescott, A.R., Sparks, A., Lane, D.P. and Saville, M.K. (2004) p14 Arf promotes small ubiquitin-like modifier conjugation of Werners helicase. *The Journal of biological chemistry,* **279,** 50157-66.

158. Blander, G., Zalle, N., Daniely, Y., Taplick, J., Gray, M.D. and Oren, M. (2002) DNA damage-induced translocation of the Werner helicase is regulated by acetylation. *The Journal of biological chemistry,* **277,** 50934-40.

159. Rothmund, A. (1868) Uber cataracten in verbindung mit einer eigenthumlichen hautdegeneration. *Arch. Klin. Exp. Opthal.,* **4,** 159-182.

160. Thomson, M.S. (1936) Poikiloderma congenitale. *Br. J. Dermatol.,* **48,** 221-234.

161. Vennos, E.M., Collins, M. and James, W.D. (1992) Rothmund-Thomson syndrome: review of the world literature. *J Am Acad Dermatol,* **27,** 750-762.

162. Wang, L.L., Levy, M.L., Lewis, R.A., Chintagumpala, M.M., Lev, D., Rogers, M., Plon, S.E. (2001) Clinical manifestations in a cohort of 41 Rothmund-Thomsom patients. *Am J Med Genet,* **102,** 11-17.

163. Kitao, S., Lindor, N.M., Shiratori, M., Furuichi, Y. and Shimamoto, A. (1999) Rothmund-thomson syndrome responsible gene, RECQL4: genomic structure and products. *Genomics,* **61,** 268-276.

164. Lindor, N.M., Furuichi, Y., Kitao, S., Shimamoto, A., Arndt, C. and Jalal, S. (2000) Rothmund-Thomson syndrome due to RECQ4 helicase mutations: report and clinical and molecular comparisons with Bloom syndrome and Werner syndrome. *Am J Med Genet,* **90,** 223-228.

165. Der Kaloustian, V.M., McGill, J.J., Vekemans, M. and Kopelman, H.R. (1990) Clonal lines of aneuploid cells in Rothmund-Thomson syndrome. *Am J Med Genet,* **37,** 336-339.

166. Vennos, E.M. and James, W.D. (1995) Rothmund-Thomson syndrome. *Dermatol Clin,* **13,** 143-150.

167. Werner, S.R., Prahalad, A.K., Yang, J. and Hock, J.M. (2006) RECQL4-deficient cells are hypersensitive to oxidative stress/damage: Insights for osteosarcoma prevalence and heterogeneity in Rothmund-Thomson syndrome. *Biochem Biophys Res Commun,* **345,** 403-409.

168. Jam, K., Fox, M. and Crandall, B.F. (1999) RAPADILINO syndrome: a multiple malformation syndrome with radial and patellar aplasia. *Teratology,* **60,** 37-8.

169. Kellermayer, R., Siitonen, H.A., Hadzsiev, K., Kestila, M. and Kosztolanyi, G. (2005) A patient with Rothmund-Thomson syndrome and all features of RAPADILINO. *Arch Dermatol,* **141,** 617-620.

170. Baller, F. (1950) Radiosaplasie und Inzucht. *Z Menschl Vererb Konstitutionsl,* **29,** 782-790.

171. Ichikawa K, N.T., Furuichi Y. (2002) Preparation of the gene targeted knockout mice for human premature aging diseases, Werner syndrome, and Rothmund-Thomson syndrome caused by the mutation of DNA helicases. *Nippon Yakurigaku Zasshi,* **119,** 219-26.

172. Hoki, Y., Araki, R., Fujimori, A., Ohhata, T., Koseki, H., Fukumura, R., Nakamura, M., Takahashi, H., Noda, Y. and Kito, S. (2003) Growth retardation and skin abnormalities of the Recql4-deficient mouse. *Hum Mol Genet,* **12,** 2293-2299.

173. Mann, M.B., Hodges, C.A., Barnes, E., Vogel, H., Hassold, T.J. and Luo, G. (2005) Defective sister-chromatid cohesion, aneuploidy and cancer predisposition in a mouse model of type II Rothmund-Thomson syndrome. *Hum Mol Genet,* **14,** 813-825.

174. Matsumoto, H., Muramatsu, S., Kamimura, Y. and Araki, H. (2002) S-Cdk-dependent phosphorylation of Sld2 essential for chromosomal DNA replication in budding yeast. *Nature,* **415,** 651-655.

175. Noguchi, E., Shanahan, P., Noguchi, C. and Russell, P. (2002) CDK phosphorylation of Drc1 regulates DNA replication in fission yeast. *Curr. Biol.,* **12,** 599-605.

176. Wang, H., and Elledge, S.J. (1999) DNA replication and checkpoint protein 1, functions with DPB11 to control DNA replication and the S-phase checkpoint in Saccaromyces cerevisiae. *Proc. Natl. Acad. Sci. USA* **96,** 3824-3829.

177. Sangrithi, M.N., Bernal, J.A., Madine, M., Philpott, A., Lee, J., Dunphy, W.G. and Venkitaraman, A.R. (2005) Initiation of DNA replication requires the RECQL4 protein mutated in Rothmund-Thomson syndrome. *Cell,* **121,** 887-898.

178. Matsuno, K., Kumano, M., Kubota, Y., Hashimoto, Y. and Takisawa, H. (2006) The N-terminal noncatalytic region of Xenopus RecQ4 is required for chromatin binding of DNA polymerase alpha in the initiation of DNA replication. *Mol Cell Biol,* **26,** 4843-52.

179. Yin, J., Tae Kwon, Y., Varshavsky, A. and Wang, W. (2004) RECQL4, mutated in the Rothmund-Thomson and RAPADILINO syndromes, interacts with ubiquitin ligases UBR1 and UBR2 of the N-end rule pathway. *Hum Mol Genet,* **13,** 2421-2430.

180. Hershko, A., Ciechanover, A. and Varshavsky, A. (2000) The ubiquitin system. *Nature Medicine,* **6,** 1073-1081.

181. Petkovic, M., Dietschy, T., Freire, R., Jiao, R. and Stagljar, I. (2005) The human Rothmund-Thomson syndrome gene product, RECQL4, localizes to distinct nuclear foci that coincide with proteins involved in the maintenance of genome stability. *J Cell Sci,* **118,** 4261-4269.

182. Raderschall, E., Golub, E.I. and Haaf, T. (1999) Nuclear foci of mammalian recombination proteins are located at single-stranded DNA regions formed after DNA damage. *Proc Natl Acad Sci USA,* **96,** 1921-1926.

183. Hashimoto, Y. and Takisawa, H. (2003) Xenopus Cut5 is essential for a CDK-dependent process in the initiation of DNA replication. *EMBO J.,* **10,** 2526-2535.

184. Van Hatten, R.A., Tutter, A.V., Holway, A.H., Khederian, A.M., Walter, J.C. and Michael, W.M. (2002) The Xenopus Xmus101 protein is required for the recruitment of Cdc45 to origins of DNA replication. *J. Cell Biol.,* **159,** 541-547.

185. Kamimura, Y., H. Masumoto, A. Sugino, and H. Araki (1998) Sld2, which interacts with Dpb11 in Saccharomyces cerevisiae, is required for chromosomal DNA replication. *Mol. Cell. Biol.,* **18,** 6102-09.

186. Woo, L.L., Futami, K., Shimamoto, A., Furuichi, Y. and Frank, K.M. (2006) The Rothmund-Thomson gene product RECQL4 localizes to the nucleolus in response to oxidative stress. *Experimental Cell Research,* **312,** 3443-3457.

187. Malanga, M. and Althaus, F.R. (2005) The role of poly(ADP-ribose) in the DNA damage signaling network. *Biochem Cell Biol,* **83,** 354-364.

188. Allinson, S.L., Dianova, I.I. and Dianov, G.L. (2003) Poly(ADP-ribose) polymerase in base excision repair: always engaged, but not essential for DNA damage processing. *Acta Biochim Pol,* **50,** 169-179.

189. Shinohara, A. and Ogawa, T. (1999) Rad51/RecA protein families and the associated proteins in eukaryotes. *Mutat Res,* **435,** 13-21.

190. Macris, M.A., Krejci, L., Bussen, W., Shimamoto, A. and Sung, P. (2006) Biochemical characterization of the RECQ4 protein, mutated in Rothmund-Thomson syndrome. *DNA Repair (Amst),* **5,** 172-80.

191. Sekelsky, J.J., Brodsky, M.H., Rubin, G.M. and Hawley, R.S. (1999) Drosophila and human RecQ5 exist in different isoforms generated by alternative splicing. *Nucleic acids research,* **27,** 3762-9.

192. Shimamoto, A., Nishikawa, K., Kitao, S. and Furuichi, Y. (2000) Human RecQ5beta, a large isomer of RecQ5 DNA helicase, localizes in the nucleoplasm and interacts with topoisomerases 3alpha and 3beta. *Nucleic acids research,* **28,** 1647-55.

193. Garcia, P.L., Liu, Y., Jiricny, J., West, S.C. and Janscak, P. (2004) Human RECQ5beta, a protein with DNA helicase and strand-annealing activities in a single polypeptide. *Embo J,* **23,** 2882-91.

194. Karow, J.K., Newman, R.H., Freemont, P.S. and Hickson, I.D. (1999) Oligomeric ring structure of the Bloom's syndrome helicase. *Curr Biol,* **9,** 597-600.

195. Xue, Y., Ratcliff, G.C., Wang, H., Davis-Searles, P.R., Gray, M.D., Erie, D.A. and Redinbo, M.R. (2002) A minimal exonuclease domain of WRN forms a hexamer on DNA and possesses both 3'- 5' exonuclease and 5'-protruding strand endonuclease activities. *Biochemistry,* **41,** 2901-12.

196. Kanagaraj, R., Saydam, N., Garcia, P.L., Zheng, L. and Janscak, P. (2006) Human RECQ5beta helicase promotes strand exchange on synthetic DNA structures resembling a stalled replication fork. *Nucleic acids research,* **34,** 5217-31.

197. Krishna, R.G. and Wold, F. (1993) Post-translational modification of proteins. *Advances in enzymology and related areas of molecular biology,* **67,** 265-98.

198. Polevoda, B. and Sherman, F. (2000) Nalpha -terminal acetylation of eukaryotic proteins. *The Journal of biological chemistry,* **275,** 36479-82.

199. Yang, X.J. (2004) Lysine acetylation and the bromodomain: a new partnership for signaling. *Bioessays,* **26,** 1076-87.

200. Mukherjee, S., Keitany, G., Li, Y., Wang, Y., Ball, H.L., Goldsmith, E.J. and Orth, K. (2006) Yersinia YopJ acetylates and inhibits kinase activation by blocking phosphorylation. *Science,* **312,** 1211-4.

201. Allfrey, V.G., Faulkner, R. and Mirsky, A.E. (1964) Acetylation and Methylation of Histones and Their Possible Role in the Regulation of Rna Synthesis. *Proceedings of the National Academy of Sciences of the United States of America,* **51,** 786-94.

202. Braunstein, M., Rose, A.B., Holmes, S.G., Allis, C.D. and Broach, J.R. (1993) Transcriptional silencing in yeast is associated with reduced nucleosome acetylation. *Genes & development,* **7,** 592-604.

203. Hebbes, T.R., Thorne, A.W. and Crane-Robinson, C. (1988) A direct link between core histone acetylation and transcriptionally active chromatin. *Embo J,* **7,** 1395-402.

204. Jaskelioff, M. and Peterson, C.L. (2003) Chromatin and transcription: histones continue to make their marks. *Nature cell biology,* **5,** 395-9.

205. Berger, S.L. (2007) The complex language of chromatin regulation during transcription. *Nature,* **447,** 407-12.

206. Kleff, S., Andrulis, E.D., Anderson, C.W. and Sternglanz, R. (1995) Identification of a gene encoding a yeast histone H4 acetyltransferase. *The Journal of biological chemistry,* **270,** 24674-7.

207. Parthun, M.R., Widom, J. and Gottschling, D.E. (1996) The major cytoplasmic histone acetyltransferase in yeast: links to chromatin replication and histone metabolism. *Cell,* **87,** 85-94.

208. Brownell, J.E., Zhou, J., Ranalli, T., Kobayashi, R., Edmondson, D.G., Roth, S.Y. and Allis, C.D. (1996) Tetrahymena histone acetyltransferase A: a homolog to yeast Gcn5p linking histone acetylation to gene activation. *Cell,* **84,** 843-51.

209. Wang, L., Mizzen, C., Ying, C., Candau, R., Barlev, N., Brownell, J., Allis, C.D. and Berger, S.L. (1997) Histone acetyltransferase activity is conserved between yeast and human GCN5 and is required for complementation of growth and transcriptional activation. *Mol Cell Biol,* **17,** 519-27.

210. Xu, W., Edmondson, D.G., Evrard, Y.A., Wakamiya, M., Behringer, R.R. and Roth, S.Y. (2000) Loss of Gcn5l2 leads to increased apoptosis and mesodermal defects during mouse development. *Nat Genet,* **26,** 229-32.

211. Yang, X.J., Ogryzko, V.V., Nishikawa, J., Howard, B.H. and Nakatani, Y. (1996) A p300/CBP-associated factor that competes with the adenoviral oncoprotein E1A. *Nature,* **382,** 319-24.

212. Bannister, A.J. and Kouzarides, T. (1996) The CBP co-activator is a histone acetyltransferase. *Nature,* **384,** 641-3.

213. Ogryzko, V.V., Schiltz, R.L., Russanova, V., Howard, B.H. and Nakatani, Y. (1996) The transcriptional coactivators p300 and CBP are histone acetyltransferases. *Cell,* **87,** 953-9.

214. Mizzen, C.A., Yang, X.J., Kokubo, T., Brownell, J.E., Bannister, A.J., Owen-Hughes, T., Workman, J., Wang, L., Berger, S.L., Kouzarides, T. *et al.* (1996) The TAF(II)250 subunit of TFIID has histone acetyltransferase activity. *Cell,* **87,** 1261-70.

215. Dunphy, E.L., Johnson, T., Auerbach, S.S. and Wang, E.H. (2000) Requirement for TAF(II)250 acetyltransferase activity in cell cycle progression. *Molecular and cellular biology,* **20,** 1134-9.

216. Sterner, D.E. and Berger, S.L. (2000) Acetylation of histones and transcription-related factors. *Microbiol Mol Biol Rev,* **64,** 435-59.

217. Fukuda, H., Sano, N., Muto, S. and Horikoshi, M. (2006) Simple histone acetylation plays a complex role in the regulation of gene expression. *Briefings in functional genomics & proteomics,* **5,** 190-208.

218. Taunton, J., Hassig, C.A. and Schreiber, S.L. (1996) A mammalian histone deacetylase related to the yeast transcriptional regulator Rpd3p. *Science,* **272,** 408-11.

219. Wu, J., Suka, N., Carlson, M. and Grunstein, M. (2001) TUP1 utilizes histone H3/H2B-specific HDA1 deacetylase to repress gene activity in yeast. *Mol Cell,* **7,** 117-26.

220. Blander, G. and Guarente, L. (2004) The Sir2 family of protein deacetylases. *Annual review of biochemistry,* **73,** 417-35.

221. Gao, L., Cueto, M.A., Asselbergs, F. and Atadja, P. (2002) Cloning and functional characterization of HDAC11, a novel member of the human histone deacetylase family. *The Journal of biological chemistry,* **277,** 25748-55.

222. Thiel, G., Lietz, M. and Hohl, M. (2004) How mammalian transcriptional repressors work. *European journal of biochemistry / FEBS,* **271,** 2855-62.

223. Hassig, C.A., Tong, J.K., Fleischer, T.C., Owa, T., Grable, P.G., Ayer, D.E. and Schreiber, S.L. (1998) A role for histone deacetylase activity in HDAC1-mediated transcriptional repression. *Proceedings of the National Academy of Sciences of the United States of America,* **95,** 3519-24.

224. Rundlett, S.E., Carmen, A.A., Kobayashi, R., Bavykin, S., Turner, B.M. and Grunstein, M. (1996) HDA1 and RPD3 are members of distinct yeast histone deacetylase complexes that regulate silencing and transcription. *Proceedings of the National Academy of Sciences of the United States of America,* **93,** 14503-8.

225. Yuan, L.W. and Giordano, A. (2002) Acetyltransferase machinery conserved in p300/CBP-family proteins. *Oncogene,* **21,** 2253-60.

226. Arany, Z., Sellers, W.R., Livingston, D.M. and Eckner, R. (1994) E1A-associated p300 and CREB-associated CBP belong to a conserved family of coactivators. *Cell,* **77,** 799-800.

227. Bordoli, L., Netsch, M., Luthi, U., Lutz, W. and Eckner, R. (2001) Plant orthologs of p300/CBP: conservation of a core domain in metazoan p300/CBP acetyltransferase-related proteins. *Nucleic acids research,* **29,** 589-97.

228. Eckner, R., Ewen, M.E., Newsome, D., Gerdes, M., DeCaprio, J.A., Lawrence, J.B. and Livingston, D.M. (1994) Molecular cloning and functional analysis of the adenovirus E1A-associated 300-kD protein (p300) reveals a protein with properties of a transcriptional adaptor. *Genes & development,* **8,** 869-84.

229. Chrivia, J.C., Kwok, R.P., Lamb, N., Hagiwara, M., Montminy, M.R. and Goodman, R.H. (1993) Phosphorylated CREB binds specifically to the nuclear protein CBP. *Nature,* **365,** 855-9.

230. Goodman, R.H. and Smolik, S. (2000) CBP/p300 in cell growth, transformation, and development. *Genes & development,* **14,** 1553-77.

231. Yuan, W., Condorelli, G., Caruso, M., Felsani, A. and Giordano, A. (1996) Human p300 protein is a coactivator for the transcription factor MyoD. *The Journal of biological chemistry,* **271,** 9009-13.

232. Kwok, R.P., Lundblad, J.R., Chrivia, J.C., Richards, J.P., Bachinger, H.P., Brennan, R.G., Roberts, S.G., Green, M.R. and Goodman, R.H. (1994) Nuclear protein CBP is a coactivator for the transcription factor CREB. *Nature,* **370,** 223-6.

233. Black, J.C., Choi, J.E., Lombardo, S.R. and Carey, M. (2006) A mechanism for coordinating chromatin modification and preinitiation complex assembly. *Mol Cell,* **23,** 809-18.

234. Neish, A.S., Anderson, S.F., Schlegel, B.P., Wei, W. and Parvin, J.D. (1998) Factors associated with the mammalian RNA polymerase II holoenzyme. *Nucleic acids research,* **26,** 847-53.

235. Nakajima, T., Uchida, C., Anderson, S.F., Lee, C.G., Hurwitz, J., Parvin, J.D. and Montminy, M. (1997) RNA helicase A mediates association of CBP with RNA polymerase II. *Cell,* **90,** 1107-12.

236. Nakajima, T., Uchida, C., Anderson, S.F., Parvin, J.D. and Montminy, M. (1997) Analysis of a cAMP-responsive activator reveals a two-component mechanism for transcriptional induction via signal-dependent factors. *Genes & development,* **11,** 738-47.

237. Cho, H., Orphanides, G., Sun, X., Yang, X.J., Ogryzko, V., Lees, E., Nakatani, Y. and Reinberg, D. (1998) A human RNA polymerase II complex containing factors that modify chromatin structure. *Molecular and cellular biology,* **18,** 5355-63.

238. Chan, H.M. and La Thangue, N.B. (2001) p300/CBP proteins: HATs for transcriptional bridges and scaffolds. *J Cell Sci,* **114,** 2363-73.

239. Vo, N. and Goodman, R.H. (2001) CREB-binding protein and p300 in transcriptional regulation. *The Journal of biological chemistry,* **276,** 13505-8.

240. Spencer, T.E., Jenster, G., Burcin, M.M., Allis, C.D., Zhou, J., Mizzen, C.A., McKenna, N.J., Onate, S.A., Tsai, S.Y., Tsai, M.J. *et al.* (1997) Steroid receptor coactivator-1 is a histone acetyltransferase. *Nature,* **389,** 194-8.

241. Yao, T.P., Ku, G., Zhou, N., Scully, R. and Livingston, D.M. (1996) The nuclear hormone receptor coactivator SRC-1 is a specific target of p300. *Proceedings of the National Academy of Sciences of the United States of America,* **93,** 10626-31.

242. Chen, H., Lin, R.J., Schiltz, R.L., Chakravarti, D., Nash, A., Nagy, L., Privalsky, M.L., Nakatani, Y. and Evans, R.M. (1997) Nuclear receptor coactivator ACTR is a novel histone acetyltransferase and forms a multimeric activation complex with P/CAF and CBP/p300. *Cell,* **90,** 569-80.

243. Kundu, T.K., Palhan, V.B., Wang, Z., An, W., Cole, P.A. and Roeder, R.G. (2000) Activator-dependent transcription from chromatin in vitro involving targeted histone acetylation by p300. *Mol Cell,* **6,** 551-61.

244. Gu, W. and Roeder, R.G. (1997) Activation of p53 sequence-specific DNA binding by acetylation of the p53 C-terminal domain. *Cell,* **90,** 595-606.

245. Cairns, B.R. (2001) Emerging roles for chromatin remodeling in cancer biology. *Trends Cell Biol,* **11,** S15-21.

246. Klochendler-Yeivin, A. and Yaniv, M. (2001) Chromatin modifiers and tumor suppression. *Biochim Biophys Acta,* **1551,** M1-10.

247. Timmermann, S., Lehrmann, H., Polesskaya, A. and Harel-Bellan, A. (2001) Histone acetylation and disease. *Cell Mol Life Sci,* **58,** 728-36.

248. Rubinstein, J.H. and Taybi, H. (1963) Broad thumbs and toes and facial abnormalities. A possible mental retardation syndrome. *American journal of diseases of children (1960),* **105,** 588-608.

249. Miller, R.W. and Rubinstein, J.H. (1995) Tumors in Rubinstein-Taybi syndrome. *Am J Med Genet,* **56,** 112-5.

250. Yang, X.J. (2004) The diverse superfamily of lysine acetyltransferases and their roles in leukemia and other diseases. *Nucleic acids research,* **32,** 959-76.

251. Gayther, S.A., Batley, S.J., Linger, L., Bannister, A., Thorpe, K., Chin, S.F., Daigo, Y., Russell, P., Wilson, A., Sowter, H.M. *et al.* (2000) Mutations truncating the EP300 acetylase in human cancers. *Nat Genet,* **24,** 300-3.

252. Ionov, Y., Matsui, S. and Cowell, J.K. (2004) A role for p300/CREB binding protein genes in promoting cancer progression in colon cancer cell lines with microsatellite instability. *Proceedings of the National Academy of Sciences of the United States of America,* **101,** 1273-8.

253. Ionov, Y., Nowak, N., Perucho, M., Markowitz, S. and Cowell, J.K. (2004) Manipulation of nonsense mediated decay identifies gene mutations in colon cancer Cells with microsatellite instability. *Oncogene,* **23,** 639-45.

254. Muraoka, M., Konishi, M., Kikuchi-Yanoshita, R., Tanaka, K., Shitara, N., Chong, J.M., Iwama, T. and Miyaki, M. (1996) p300 gene alterations in colorectal and gastric carcinomas. *Oncogene,* **12,** 1565-9.

255. Knudson, A.G., Jr. (1971) Mutation and cancer: statistical study of retinoblastoma. *Proceedings of the National Academy of Sciences of the United States of America,* **68,** 820-3.

256. Schiltz, R.L., Mizzen, C.A., Vassilev, A., Cook, R.G., Allis, C.D. and Nakatani, Y. (1999) Overlapping but distinct patterns of histone acetylation by the human coactivators p300 and PCAF within nucleosomal substrates. *The Journal of biological chemistry,* **274,** 1189-92.

257. Hasan, S., Stucki, M., Hassa, P.O., Imhof, R., Gehrig, P., Hunziker, P., Hubscher, U. and Hottiger, M.O. (2001) Regulation of human flap endonuclease-1 activity by acetylation through the transcriptional coactivator p300. *Mol Cell,* **7,** 1221-31.

258. Hasan, S., El-Andaloussi, N., Hardeland, U., Hassa, P.O., Burki, C., Imhof, R., Schar, P. and Hottiger, M.O. (2002) Acetylation regulates the DNA end-trimming activity of DNA polymerase beta. *Mol Cell,* **10,** 1213-22.

259. Tini, M., Benecke, A., Um, S.J., Torchia, J., Evans, R.M. and Chambon, P. (2002) Association of CBP/p300 acetylase and thymine DNA glycosylase links DNA repair and transcription. *Mol Cell,* **9,** 265-77.

260. Bhakat, K.K., Hazra, T.K. and Mitra, S. (2004) Acetylation of the human DNA glycosylase NEIL2 and inhibition of its activity. *Nucleic acids research,* **32,** 3033-9.

261. Chen, H., Lin, R.J., Xie, W., Wilpitz, D. and Evans, R.M. (1999) Regulation of hormone-induced histone hyperacetylation and gene activation via acetylation of an acetylase. *Cell,* **98,** 675-86.

262. Munshi, N., Merika, M., Yie, J., Senger, K., Chen, G. and Thanos, D. (1998) Acetylation of HMG I(Y) by CBP turns off IFN beta expression by disrupting the enhanceosome. *Mol Cell,* **2,** 457-67.

263. Martinez-Balbas, M.A., Bauer, U.M., Nielsen, S.J., Brehm, A. and Kouzarides, T. (2000) Regulation of E2F1 activity by acetylation. *Embo J,* **19,** 662-71.

264. Bannister, A.J., Miska, E.A., Gorlich, D. and Kouzarides, T. (2000) Acetylation of importin-alpha nuclear import factors by CBP/p300. *Curr Biol,* **10,** 467-70.

265. Bonaldi, T., Talamo, F., Scaffidi, P., Ferrera, D., Porto, A., Bachi, A., Rubartelli, A., Agresti, A. and Bianchi, M.E. (2003) Monocytic cells hyperacetylate chromatin protein HMGB1 to redirect it towards secretion. *Embo J,* **22,** 5551-60.

266. Gay, F., Calvo, D., Lo, M.C., Ceron, J., Maduro, M., Lin, R. and Shi, Y. (2003) Acetylation regulates subcellular localization of the Wnt signaling nuclear effector POP-1. *Genes & development,* **17,** 717-22.

267. Madison, D.L., Yaciuk, P., Kwok, R.P. and Lundblad, J.R. (2002) Acetylation of the adenovirus-transforming protein E1A determines nuclear localization by disrupting association with importin-alpha. *The Journal of biological chemistry,* **277,** 38755-63.

268. Santos-Rosa, H., Valls, E., Kouzarides, T. and Martinez-Balbas, M. (2003) Mechanisms of P/CAF auto-acetylation. *Nucleic acids research,* **31,** 4285-92.

269. Soutoglou, E., Katrakili, N. and Talianidis, I. (2000) Acetylation regulates transcription factor activity at multiple levels. *Mol Cell,* **5,** 745-51.

270. di Bari, M.G., Ciuffini, L., Mingardi, M., Testi, R., Soddu, S. and Barila, D. (2006) c-Abl acetylation by histone acetyltransferases regulates its nuclear-cytoplasmic localization. *EMBO Rep,* **7,** 727-33.

271. Janscak, P., Garcia, P.L., Hamburger, F., Makuta, Y., Shiraishi, K., Imai, Y., Ikeda, H. and Bickle, T.A. (2003) Characterization and mutational analysis of the RecQ core of the bloom syndrome protein. *Journal of molecular biology,* **330,** 29-42.

272. Morozov, V., Mushegian, A.R., Koonin, E.V. and Bork, P. (1997) A putative nucleic acid-binding domain in Bloom's and Werner's syndrome helicases. *Trends in biochemical sciences,* **22,** 417-8.

273. von Kobbe, C., Thoma, N.H., Czyzewski, B.K., Pavletich, N.P. and Bohr, V.A. (2003) Werner syndrome protein contains three structure-specific DNA binding domains. *The Journal of biological chemistry,* **278,** 52997-3006.

274. Wu, L., Chan, K.L., Ralf, C., Bernstein, D.A., Garcia, P.L., Bohr, V.A., Vindigni, A., Janscak, P., Keck, J.L. and Hickson, I.D. (2005) The HRDC domain of BLM is required for the dissolution of double Holliday junctions. *Embo J,* **24,** 2679-87.

275. Yin, J., Kwon, Y.T., Varshavsky, A. and Wang, W. (2004) RECQL4, mutated in the Rothmund-Thomson and RAPADILINO syndromes, interacts with ubiquitin ligases UBR1 and UBR2 of the N-end rule pathway. *Hum Mol Genet,* **13,** 2421-30.

276. Burks, L.M., Yin, J. and Plon, S.E. (2007) Nuclear import and retention domains in the amino terminus of RECQL4. *Gene,* **391,** 26-38.

277. Poon, I.K. and Jans, D.A. (2005) Regulation of nuclear transport: central role in development and transformation? *Traffic,* **6,** 173-86.

278. Conti, E., Uy, M., Leighton, L., Blobel, G. and Kuriyan, J. (1998) Crystallographic analysis of the recognition of a nuclear localization signal by the nuclear import factor karyopherin alpha. *Cell,* **94,** 193-204.

7 Appendix

Article V

The Werner syndrome protein is required for recruitment of chromatin assembly factor 1 following DNA damage

R Jiao, JA Harrigan, I Shevelev, T Dietschy, N Selak, FE Indig, J Piotrowski, P Janscak, VA Bohr and I Stagljar

Oncogene (2006), *26; 3811-22*

For this work, I was helping with Co-Ip experiments and experiments for figure 3b

Oncogene (2006), 1–12

www.nature.com/onc

ORIGINAL ARTICLE

The Werner syndrome protein is required for recruitment of chromatin assembly factor 1 following DNA damage

R Jiao[1], JA Harrigan[2,7], I Shevelev[3], T Dietschy[3], N Selak[4], FE Indig[5], J Piotrowski[2], P Janscak[6], VA Bohr[2] and I Stagljar[3]

[1]*National Laboratory of Biomacromolecules and State Key Laboratory of Brain and Cognitive Science, Institute of Biophysics, The Chinese Academy of Sciences, Beijing, China;* [2]*Laboratory of Molecular Gerontology, NIA, National Institutes of Health, Baltimore, MD, USA;* [3]*Terrence Donnelly Centre for Cellular and Biomolecular Research (dCCBR), Department of Biochemistry and Department of Medical Genetics and Microbiology, University of Toronto, Toronto, Ontario, Canada;* [4]*Friedrich Miescher Institute for Biomedical Research, Basel, Switzerland;* [5]*Research Resources Branch, NIA, National Institutes of Health, Baltimore, MD, USA and* [6]*Institute of Molecular Cancer Research, University of Zurich, Zurich, Switzerland*

The Werner syndrome protein (WRN) and chromatin assembly factor 1 (CAF-1) are both involved in the maintenance of genome stability. In response to DNA-damaging signals, both of these proteins relocate to sites where DNA synthesis occurs. However, the interaction between WRN and CAF-1 has not yet been investigated. In this report, we show that WRN interacts physically with the largest subunit of CAF-1, hp150, *in vitro* and *in vivo*. Although hp150 does not alter WRN catalytic activities *in vitro*, and the chromatin assembly activity of CAF-1 is not affected in the absence of WRN *in vivo*, this interaction may have an important role during the cellular response to DNA replication fork blockage and/or DNA damage signals. In hp150 RNA-mediated interference (RNAi) knockdown cells, WRN partially formed foci following hydroxyurea (HU) treatment. However, in the absence of WRN, hp150 did not relocate to form foci following exposure to HU and ultraviolet light. Thus, our results demonstrate that WRN responds to DNA damage before CAF-1 and suggest that WRN may recruit CAF-1, via interaction with hp150, to DNA damage sites during DNA synthesis.
Oncogene advance online publication, 18 December 2006; doi:10.1038/sj.onc.1210150

Keywords: WRN; CAF-1; DNA damage; chromatin assembly; genome stability

Correspondence: Dr I Stagljar, Terrence Donnelly Centre for Cellular and Biomolecular Research (dCCBR), Department of Biochemistry and Department of Medical Genetics & Microbiology, University of Toronto, 160 College Street, Toronto, Ontario, Canada M5S 3E1.
E-mail: igor.stagljar@utoronto.ca and Dr R Jiao, National Laboratory of Biomacromolecules and State Key Laboratory of Brain and Cognitive Science, Institute of Biophysics, The Chinese Academy of Sciences, Beijing, China.
E-mail: rjiao@sun5.ibp.ac.cn
[7]Present address: The Wellcome Trust/CRUK Gurdon Institute, University of Cambridge, Tennis Court Road, Cambridge, UK
Received 16 November 2005; revised 10 October 2006; accepted 20 October 2006

Introduction

The eukaryotic nuclear genome is assembled into the nucleoprotein structure termed chromatin. The basic repeating unit of chromatin is the nucleosome, which comprises 147 bp of DNA wrapped around an octamer of histone proteins (two molecules each of histones H3, H4, H2A and H2B) (Luger *et al*., 1997). The majority of chromatin is assembled immediately following DNA replication. This is mediated in part by the histone chaperone chromatin assembly factor 1 (CAF-1) that deposits histones H3 and H4 onto newly replicated DNA *in vitro* (Smith and Stillman, 1989). CAF-1 is a heterotrimeric protein that is highly conserved from yeast to humans (Kaufman *et al*., 1995, 1997; Tyler *et al*., 1996, 2001; Verreault *et al*., 1996). CAF-1 has been shown to localize to sites of DNA replication (Krude, 1995). Yeast lacking CAF-1 have global under-assembly of their genome into chromatin (Adkins *et al*., 2004), and reduction of CAF-1 activity in tissue culture cells leads to reduced packaging of the genome into chromatin, replication defects and S-phase arrest (Krude, 1999; Hoek and Stillman, 2003; Ye *et al*., 2003; Nabatiyan and Krude, 2004). CAF-1 has also been implicated in DNA repair via the nucleotide excision repair (NER) pathway. NER repairs single-stranded DNA lesions such as those incurred by exposure to ultraviolet light (UV) (Prakash and Prakash, 2000), and CAF-1 is capable of assembling chromatin coupled with NER *in vitro* (Gaillard *et al*., 1996). CAF-1 has also been localized to DNA templates undergoing NER, in a manner dependent upon proliferating-cell nuclear antigen (PCNA) (Moggs *et al*., 2000; Green and Almouzni, 2003). Accordingly, yeast deleted for CAF-1 components are hypersensitive to UV irradiation, indicating the importance of CAF-1 in surviving UV-induced DNA damage (Kaufman *et al*., 1997). It has been reported recently that CAF-1 has a role in the assembly of chromatin following or during the repair of double-strand DNA damage (Linger and Tyler, 2005).

Werner syndrome (WS) is an autosomal recessive disorder with distinct premature aging features and with a high incidence of age-associated diseases including cancer (soft tissue) and diabetes mellitus type II (Hickson, 2003; Bohr, 2005; Ozgenc and Loeb, 2005). The gene defective in WS, *WRN*, encodes a protein of the RecQ family of DNA helicases (Yu *et al*., 1996; Hickson, 2003; Opresko *et al*., 2003), which possesses DNA-dependent ATPase, 3′-5′ helicase and 3′-5′ exonuclease activities. The substrate specificity of WRN helicase and exonuclease activities has been determined *in vitro*, and includes a variety of intermediates produced during DNA replication, recombination and repair (Shen *et al*., 1998; Xue *et al*., 2002). WRN has been shown to predominantly localize to the nucleolus, but after certain types of DNA damage, leaves the nucleolus and forms distinct foci in the nucleoplasm (Sakamoto *et al*., 2001; Karmakar and Bohr, 2005; Li *et al*., 2005). The formation of these foci likely reflects an important stage in the DNA damage response. Although the number of WRN-containing nuclear foci increases after replication fork arrest and upon DNA damage (Szekely *et al*., 2000; Sakamoto *et al*., 2001), the significance of the formation of these foci and how they are regulated remain to be elucidated.

WRN physically and functionally interacts with proteins that appear to function at various levels in the mechanisms for maintaining the integrity of the genome and in the DNA damage response, suggesting that WRN plays more than one role in DNA repair (Hickson, 2003; Opresko *et al*., 2004b). WRN has been shown to interact with Ku and DNA-PKcs (Li and Comai, 2000; Orren *et al*., 2001; Karmakar *et al*., 2002a, b; Karmakar and Bohr, 2005; Li *et al*., 2005). Consistently, WS fibroblasts transformed with Simian Virus-40 (SV40) T antigen or immortalized by expressing human telomerase reverse transcriptase (hTERT) display a mild but distinct sensitivity to ionizing radiation compared to controls (Yannone *et al*., 2001; Cheng *et al*., 2004). WS cells also display extensive deletions at non-homologous joined ends as well as non-homologous chromosome exchanges (Oshima *et al*., 2002). These results suggest that WRN may be involved in processing ionizing radiation-induced double-strand breaks. In agreement, WRN also interacts physically with the Mre11-Rad50-NBS1 complex, which functions in homologous recombination for double-strand break processing (Cheng *et al*., 2004). WRN may also play a role in base excision repair as WRN stimulates DNA polymerase β-strand displacement synthesis via its helicase activity (Harrigan *et al*., 2003, 2006). The sensitivity of WS cells to cross-linking drugs (Poot *et al*., 2001) and a very recent report on the WRN response to UV treatment (Guay *et al*., 2006) suggest that WRN might also be involved in the repair process that removes cross-linking induced lesions. Increasing evidence also supports the hypothesis that WRN plays a direct role in telomere maintenance (Opresko *et al*., 2004a; Laud *et al*., 2005).

Here we present evidence that suggests a cross-talk between WRN and CAF-1 via its largest subunit hp150. We show that WRN interacts physically with hp150, *in vitro* and *in vivo*. In the absence of WRN, hp150 did not re-localize to form nuclear foci following treatment of cells with hydroxyurea (HU), whereas in hp150 RNAi knockdown cells, WRN did respond to the same treatment. Thus, our results indicate that before CAF-1, WRN responds to DNA damage. WRN may recruit CAF-1, via hp150, to DNA damage sites to assemble the newly synthesized DNA into chromatin following DNA synthesis, so that the epigenetic state of the chromatin is re-established, and to prevent the DNA from further damage.

Results

WRN and hp150 interact in vitro *and* in vivo

We previously reported that BLM, another member of the human RecQ helicase family, interacts physically and functionally with hp150, the largest subunit of CAF-1 (Jiao *et al*., 2004). As WRN is also involved in the maintenance of genome stability and re-localizes to sites of DNA synthesis following DNA damage similar to CAF-1 (Green and Almouzni, 2003; Jiao *et al*., 2004; Karmakar and Bohr, 2005; Li *et al*., 2005), we examined for possible interactions between WRN and CAF-1 during DNA replication and/or repair.

To test for a physical interaction between WRN and hp150 *in vitro*, we employed the Far-Western assay. As shown in Figure 1b, purified recombinant hp150 protein interacted directly with full length WRN (aa 1–1432) and two fragments WRN P1 (aa 523–1227) and WRN P2 (aa 523–1148) (lanes 1–3). These fragments comprise the helicase, RQC and HRDC (Helicase RNaseD C-terminus domain) (WRN P1), and helicase and RQC (WRN P2) domains of WRN, respectively (Figure 1e; Lee *et al*., 2005). In contrast, hp150 did not interact with the N-terminal WRN fragment, LGS-WRN (aa 1–368), which contains the exonuclease domain (Figure 1b, lane 4), nor with the unrelated bacterial helicase UvrD (Figure 1b, lane 5). In the reverse Far-Western, full-length WRN bound to hp150 and its known partner DNA polymerase β (pol β) (Figure 1c, lanes 2 and 3; Harrigan *et al*., 2003), but not to DNA polymerase lambda (pol λ) (Figure 1c, lane 1). All the purified proteins used in the Far-Western assay are shown in Figure 1a.

We next performed co-immunoprecipitation experiments to investigate whether WRN and CAF-1 formed a complex *in vivo*. In untreated HeLa cells, we were not able to detect a WRN-hp150 complex by co-immunoprecipitation using anti-hp150 antibodies (Figure 1d, lower panel, lane 3). Similarly, we did not detect a WRN and hp150 interaction in a yeast two hybrid assay (data not shown). However, in extracts from HU-treated HeLa cells, anti-hp150 antibodies co-immunoprecipitated WRN (Figure 1d, lower panel, lane 4). To eliminate the possibility that WRN and hp150 may associate through DNA, the immunoprecipitation was performed in the presence of ethidium bromide (EtBr),

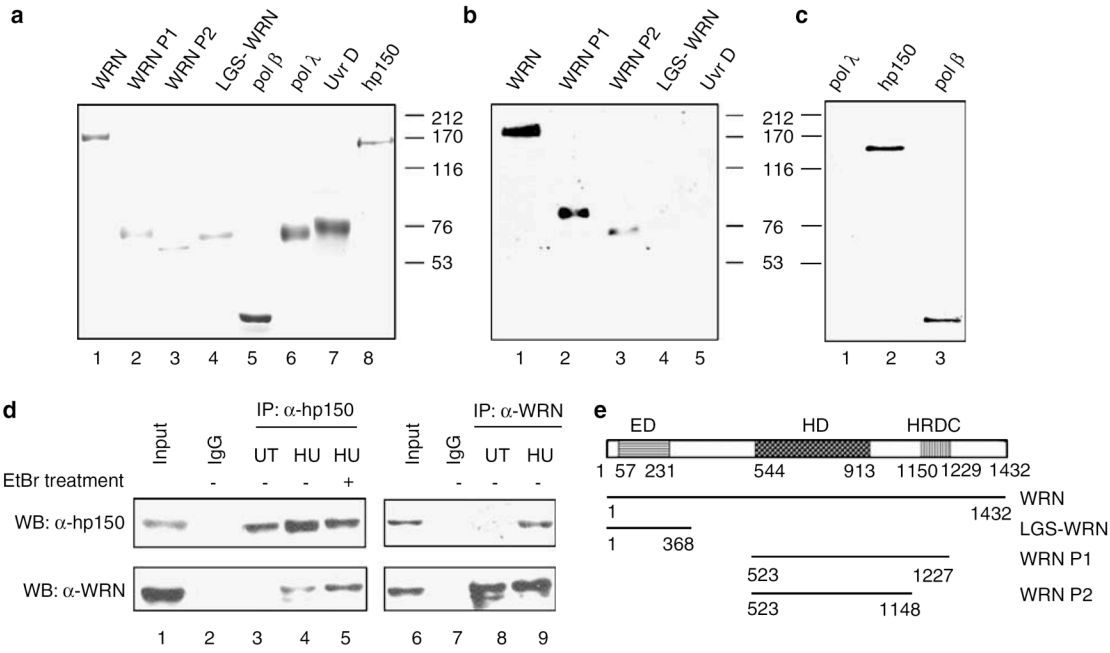

Figure 1 WRN physically interacts with the largest subunit of CAF-1, hp150, *in vitro* and *in vivo*. (**a**) SDS–PAGE and Coomassie staining showing the proteins used in the Far-Western assay. Lanes 1–8 represent, respectively, the following proteins: full-length WRN, WRN P1 (aa 523–1227), WRN P2 (aa 523–1148), LGS-WRN (aa 1–368), pol β, pol λ, UvrD and hp150. Molecular weight markers are indicated on the right. The gel was stained with Coomassie blue. (**b**) Far-Western analysis. WRN proteins (full-length and truncated) and UvrD as indicated were subjected to SDS–PAGE, transferred to a nitrocellulose membrane, and incubated with hp150. Anti-hp150 antibodies were used for detection of the hp150 interacting proteins. Molecular weight markers are indicated on the right. (**c**) pol λ, hp150, and pol β as indicated were subjected to SDS–PAGE, transferred to a nitrocellulose filter, and incubated with WRN. Anti-WRN antibodies were used for detection of the WRN interacting proteins. Molecular weight markers are indicated on the left. (**d**) Left panels: anti-hp150 antibodies (lanes 3–5) or control (IgG) antibodies (lane 2) were used to immunoprecipitate proteins from either untreated (UT) or HU-treated (HU) HeLa nuclear extracts in the absence (lanes 2–4) or presence (lane 5) of EtBr and subjected to Western blotting using anti-hp150 or anti-WRN antibodies as indicated. Right panels: anti-WRN antibodies (lanes 8–9) or control IgG antibodies (lane 7) were used to immunoprecipitate proteins from either untreated (UT) or HU-treated (HU) HeLa nuclear extracts. In both the left and right panels, 1/10 of the nuclear extracts were used as input control (lanes 1 and 6). (**e**) Representation of different WRN fragments used in the Far-Western assay. ED: exonuclease domain, HD: helicase domain, HRDC: helicase RNaseD C-terminus domain.

a DNA-intercalating agent that can dissociate proteins from DNA and has often been used to identify DNA-independent protein associations (Lai and Herr, 1992). The anti-hp150 antibody co-immunoprecipitated WRN in the presence of EtBr (Figure 1d, lower panel, lane 5), suggesting that WRN forms a DNA-independent complex with hp150. Likewise, in a reverse immunoprecipitation experiment, anti-WRN antibodies also co-immunoprecipitated hp150 from the HU-treated (Figure 1d, top panel, lane 9), but not from the untreated HeLa cells (Figure 1d, top panel, lane 8). Thus, we conclude from our Far-Western assay and co-immunoprecipitation experiments that WRN and hp150 interact directly *in vitro* and after exposure to HU *in vivo*, and that the helicase-RQC domain of WRN (aa 523–1148) is necessary and sufficient to bind hp150.

WRN and CAF-1 co-localize in human cells in response to DNA damaging agents

Based on the physical interaction between WRN and hp150 shown above, we used indirect immunofluorescence microscopy to analyze analyse whether WRN and CAF-1 co-localize in human cells. Consistent with the reports of others (Krude, 1995; Marciniak *et al*., 1998; von Kobbe *et al*., 2002), in untreated HeLa cells approximately 10% of cells contained hp150 nuclear foci while whereas only about 3% of the cells exhibited distinct nuclear foci containing WRN. The majority of WRN occupied the nucleoli (Figure 2, upper panels and Table 1). In untreated HeLa cells, we did not observe any obvious co-localization of WRN and hp150 (Figure 2, upper panels and Table 1), consistent with the immunoprecipitation experiments. However, following exposure to 10 mM HU, an agent that inhibits ribonucleotide reductase and therefore halts DNA replication fork progression, the majority of WRN re-localized from the nucleoli to the nucleoplasm to form discrete nuclear foci at sites of stalled DNA replication forks (Figure 2, middle panels; Franchitto and Pichierri, 2004). Approximately 74% of the cell population contained WRN foci with a mean number of 36 foci per cell (Table 1). Similarly, HU treatment also resulted in hp150 relocation to sites of DNA replication fork

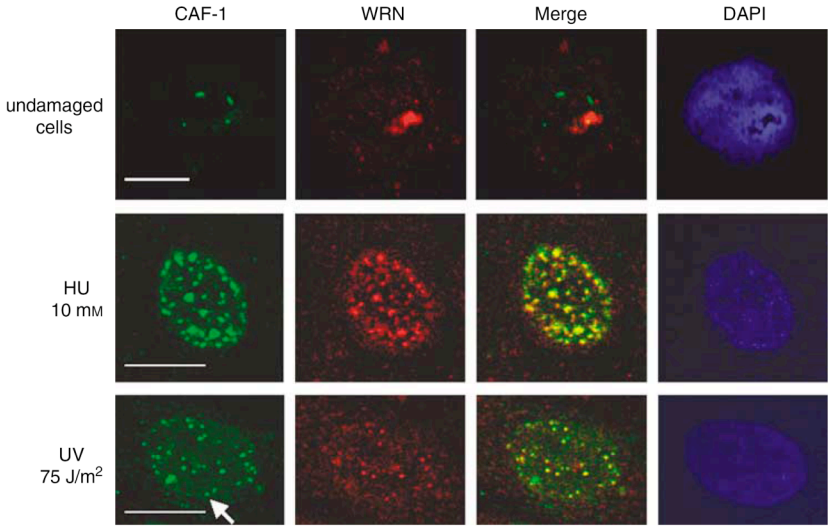

Figure 2 WRN and CAF-1 colocalize in HU- and UV-treated HeLa cells. HeLa cells cultured on slides were either untreated (upper panels) or treated with 10 mM HU (middle panel, 20 h) or 75 J/m^2 UV (lower panels, 4–6 h recovery). Following treatment, cells were processed using anti-WRN (red) and anti-hp150 (green) antibodies. In the merged pictures, yellow represents the colocalization of WRN and CAF-1. DAPI staining of the nucleus is indicated in blue. The white arrow indicates the minimum concentrated signal to be a focus. Scale bars represent 10 μm.

Table 1 WRN and CAF-1 colocalization in HeLa cells after HU and UV treatment

Treatment	*None*	*HU*	*UV*
Percentage of cells containing WRN foci	3	74	46
Percentage of cells containing CAF-1 foci	10	65	36
Mean no. of WEN foci/cell (range)	2 (0–12)	36 (0–83)	11 (0–36)
Mean no. of CAF-1 foci/cell (range)	3 (0–25)	27 (0–61)	8 (0–33)
Percentage of cells containing WEN and CAF-1 colocalizing foci			
0 (%)	99	60	79
1–5 (%)	1	9	8
More than 5 (%)	0	31	13
Mean no. of WRN and CAF-1 co-localizing foci/cell (range)	0 (0–3)	16 (0–55)	7 (0–28)

In each case, 200 cells were scored.

stalling (Figure 2, middle panels; Jiao *et al*., 2004), and 65% of cells contained CAF-1 foci with a mean number of 27 foci per cell (Table 1). Among all the cells we analyzed, 40% showed co-localization of WRN and hp150 with a mean number of 16 co-localizing foci per cell (Figure 2, middle panels and Table 1). These results suggest that WRN and CAF-1 function together in the recovery of DNA replication fork stalling. To investigate the kinetics of formation of WRN and CAF-1 foci and the co-localization of these two proteins in HeLa cells, we performed immunofluorescence studies 1, 2, 4 and 20 h after HU treatment. As shown in Figure 3a and Table 2, WRN and CAF-1 co-localized 1 h after HU treatment, however, in a lower percentage of cells and with a fewer number of co-localizing foci per cell compared to 20 h, the co-localization increased with the longer time of HU treatment, suggesting that the WRN and CAF-1 interaction is involved more in restoring stalled replication forks and/or repairing lesions induced by HU, than in establishing DNA replication forks. Table 2 also shows that the increase in WRN foci is faster than that of CAF-1 foci, especially in the first 4 h, indicating that WRN is recruited to the damaged sites earlier than CAF-1. In contrast to the observed increase of CAF-1 associated foci, the total level of CAF-1-hp150 protein did not increase in cells 20 h after HU treatment (Figure 3b). This result indicates that the increase of CAF-1 foci may reflect re-location of the protein to detergent-insoluble nuclear matrix associated regions in response to HU, rather than increased expression of the protein.

We also irradiated cells with UV, which generates the formation of covalent bonds between adjacent thymine bases, producing photoproducts. These photoproducts do not base-pair normally and, if not removed in time, may cause distortion of the DNA helix and stalling of replication forks. Four to 6 h after recovery from UV exposure, we observed WRN and hp150 co-localization

in 21% of cells with a mean number of 7 co-localizing foci per cell, while whereas 36% and 46% of the cells contained hp150 and WRN foci, respectively, each with 8 and 11 foci per cell on avarage (Figure 2, bottom panels and Table 1). Thus, our results indicate that WRN and CAF-1 may also function in a common pathway after UV treatment.

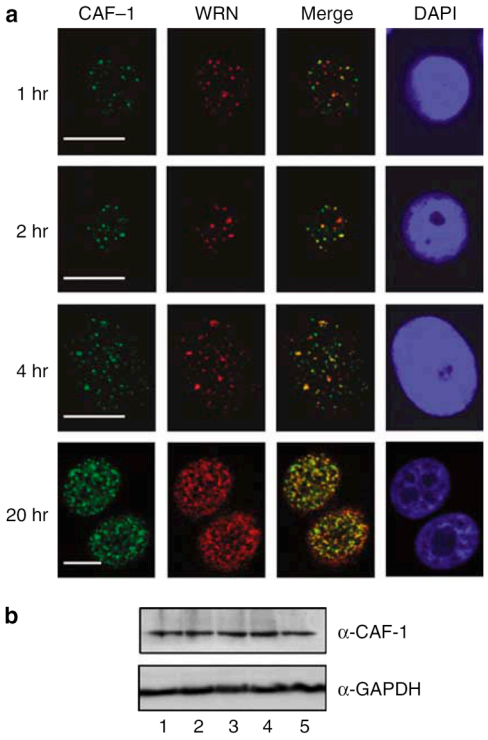

Figure 3 Kinetics of WRN and CAF-1 colocalization in HeLa cells after HU treatment. (**a**) HeLa cells cultured on slides were treated with 10 mM HU for 1, 2, 4 or 20 h, before processing with anti-WRN (red) and anti-hp150 (green) antibodies. In the merged pictures, yellow represents the colocalization of WRN and CAF-1. DAPI staining of the nucleus is indicated in blue. Scale bars represent 10 μm. (**b**) Western blot showing the amount of CAF-1-hp150 in HeLa cells at various time points after addition of HU. Lane 1, untreated. Lanes 2–5 represent the amount of CAF-1-hp150 1, 2, 4, and 20 h after HU treatment. Glyceraldehyde-3-phosphate dehydrogenase is the loading control.

The hp150 protein does not affect the enzymatic activities of WRN

Given that WRN and hp150 interacted *in vitro* and *in vivo*, and also co-localized following exposure to DNA damaging agents, we investigated whether one influenced the enzymatic activity of the other. As shown in Figure 4a, the presence of hp150 did not affect WRN helicase activity on forked DNA duplexes *in vitro* (lanes 4–8 and 10–14) compared to WRN protein alone (lanes 3 and 9). As WRN helicase activity is ATP dependent, it was not surprising that the presence of hp150 had no obvious influence on the ability of WRN to hydrolyze hydrolyse ATP (Figure 4b, lanes 2–7). Distinct from other RecQ helicases, WRN also possesses exonuclease activity. Therefore, we next examined whether this activity was altered by the presence of hp150. As shown in Figure 4c, increasing the amounts of hp150 had no effect on the exonuclease activity of WRN, either in the presence (lanes 3–8) or in the absence (lanes 10–15) of ATP. We conclude from these experiments that the catalytic activities of WRN are not affected by the presence of hp150.

CAF-1 activity is not altered in WRN deficient cells

We used an *in vitro* chromatin assembly assay coupled to DNA repair of UV-damaged DNA (Gaillard *et al*., 1996; Jiao *et al*., 2004) to detect CAF-1 activity *in vivo*. This assay takes advantage of the simultaneous analysis of DNA repair and chromatin assembly processes on the same damaged circular DNA template. Cytosolic (lacking CAF-1 proteins, Figure 5b, lane 1 and data not shown) and S100 (lacking hp150, but not hp60, Figure 5b, lane 2 and data not shown) extracts from HeLa cells were not sufficient to mediate chromatin assembly/supercoiling (Figure 5a, lanes 1 and 2). When the S100 extract was supplemented with recombinant hp150, the chromatin assembly activity was restored (Figure 5a, lane 3), demonstrating that the recombinant hp150 used in our study was functional. Likewise, when the cytosolic extract was supplemented with HeLa

Table 2 Kinetics of WRN and CAF-1 colocalization in HeLa cells after HU treatment

Hours after HU treatment	*0 h*	*1 h*	*2 h*	*4 h*	*20 h*
Percentage of cells containing WRN foci	3	8	16	27	75
Percentage of cells containing CAF-1 foci	10	13	15	18	66
Mean no. of WRN foci/cell (range)	2 (0–12)	5 (0–21)	7 (0–24)	10 (0–38)	35 (0–77)
Mean no. of CAF-1 foci/cell (range)	3 (0–25)	4 (0–24)	5 (0–27)	7 (0–31)	27 (0–58)
Percentage of cells containing WRN and CAF-1 co-localizing foci					
0 (%)	99	95	88	84	58
1–5 (%)	1	4	10	11	10
more than 5 (%)	0	1	2	5	32
Mean no. of WRN and CAF-1 colocalizing foci/cell (range)	0 (0–3)	2 (0–10)	3 (0–13)	5 (0–18)	17 (0–56)

In each case, 200 cells were scored.

nuclear extract, providing a CAF-1 source, chromatin assembly also occurred (Figure 5a, lane 4). However, one could ague that the chromatin assembly activity from HeLa nuclear extracts is not necessarily attributed to CAF-1 and may come from another chromatin assembly factor(s). To exclude this possibility, we performed RNAi experiments to knockdown endogenous hp150 before making nuclear extracts. As shown in Figure 5 (b, lane 5) transfection of hp150-specific small interfering RNA oligos efficiently eliminated hp150 protein in HeLa cells (lane 5), while whereas the control oligos did not (lane 6). Supplementing the cytosolic extracts with nuclear extracts from hp150-RNAi cells did not result in supercoiling (Figure 5a, lane 5). In contrast, nuclear extracts from control RNAi experiments clearly displayed chromatin assembly activity

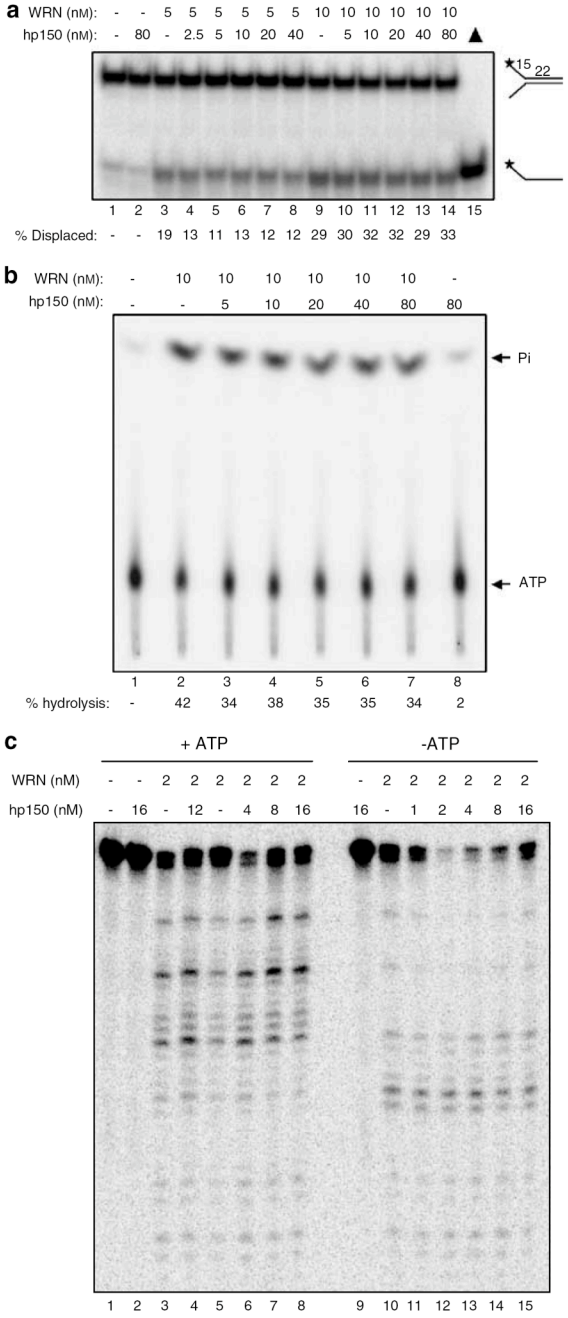

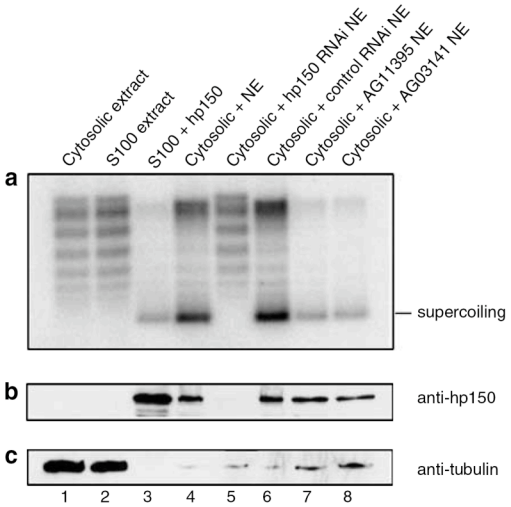

Figure 5 DNA repair-coupled chromatin assembly activity of CAF-1 does not require the presence of WRN. (**a**) Chromatin assembly assay using cytosolic, S100, or nuclear extracts (NE) as indicated and 75 ng of 500 J/m^2 UV-irradiated plasmid DNA. Lanes 1 and 2 are cytosolic and S100 extract controls. Lane 3, S100 extracts plus purified hp150. Lane 4, cytosolic plus NE. Lanes 5–8 contain cytosolic extracts plus NE from hp150 RNAi, control RNAi, WS (AG11395) or WS (AG03141) cells, respectively. (**b**) Western blot to detect the presence of hp150. Loading order is: 1, cytosolic extract; 2, S100 extract; 3, recombinant hp150;4, Normal HeLa nuclear extract; 5, HeLa nuclear extract after RNAi of hp150;6, HeLa nuclear extract after control RNAi;7, nuclear extract from WRN-deficient AG11395 cells and 8, nuclear extract from WRN deficient AG01341 cells. (**c**) Western blot to detect the presence of tubulin (loading control). The loading order is the same as in **b**.

Figure 4 WRN helicase, ATPase and exonuclease activities are not affected by hp150 *in vitro*. (**a**) Helicase assay. WRN (5 or 10 fmol) or hp150 (2.5–80 fmol) as indicated were incubated with a radiolabeled forked duplex substrate for 15 min at 37°C. Reaction products were separated on 12% native gels and visualized by a PhosphorImager. Lane 1, substrate alone.; lane 15, heat-denatured substrate. The quantification of displaced single-stranded DNA is indicated below each lane. (**b**) ATPase assay. WRN (10 nM) or hp150 (5–80 nM) as indicated were incubated with M13mp18 DNA cofactor and radiolabeled ATP for 15 min at 37°C. The percentage of ATP hydrolysis was quantified and indicated below each lane. (**c**) Exonuclease assay. WRN (2 nM) or hp150 (1–16 nM) as indicated were incubated with a radiolabeled forked duplex substrate in the absence (lanes 1–8) or presence (lanes 9–15) of ATP for 15 min at 37°C. Reaction products were separated on 14% denaturing gels and visualized by a PhosphImager. Lane 1, substrate alone.

(lane 6). Therefore, we conclude that the chromatin assembly activity from the nuclear extracts in this assay was CAF-1 specific. To this end, we examined the CAF-1 dependent chromatin assembly activity in cells lacking WRN. Using nuclear extracts from two WRN deficient cell lines, AG11395 and AG03141, we found that CAF-1 chromatin assembly activity was not affected in the absence of WRN (Figure 5a, lanes 7 and 8). Thus, these experiments indicate that CAF-1 activity is not dependent on WRN *in vivo*.

WRN is required for CAF-1 re-localization in response to HU treatment

Since the enzymatic activities of WRN and CAF-1 were not dependent on each other, yet they interacted following exposure to HU, we hypothesized that the interaction would be important in response to DNA replication fork blockage and DNA damaging signals. Similar to the situation in HeLa cells, HU treatment resulted in re-localization of WRN and hp150 to sites of stalled DNA replication forks in a normal human fibroblast cell line (Figure 6, upper panels, AG10076). In these cells, 68% contained WRN nuclear foci, 63% contained hp150 foci, whereas 36% of cells showed WRN and hp150 co-localization (Table 3 and Figure 6, upper panels). These numbers were comparable to what we observed in HeLa cells suggesting that WRN and CAF-1 behave similarly in different human cell lines.

More importantly, in the WRN deficient AG11395 cells, the profile of hp150 staining was different from normal human fibroblasts following HU and UV treatment (Figure 6). The percentage of WRN deficient cells that contained discrete nuclear hp150 foci decreased from 63 to 2–3% after HU treatment (Table 3). As expected, we did not observe nuclear staining of WRN in cells from a WS patient (Figure 6, second and last rows). Thus, our results demonstrate that the presence of WRN is required for CAF-1 to relocate in the cells after HU treatment. They also suggest that WRN may recruit CAF-1 to sites where DNA replication is stalled and that both WRN and CAF-1 are important for the recovery of stalled replication forks. This idea is confirmed by the fact that CAF-1 foci formation and CAF-1/WRN co-localization was restored following HU treatment when the WRN deficient cells were corrected with WRN expressing plasmids (Figure 6, third row and Table 3). To show that it is WRN that recruits CAF-1, and not CAF-1 that recruits WRN, we examined WRN localization in cells after HU treatment in the absence of hp150. Following transfection of RNA interfering oligos, endogenous hp150 was not detected by immunofluorescence (Figure 6 and Table 3). However, the staining of WRN, especially the relocation of WRN to partially form nuclear foci in response to HU treatment, still occurred, suggesting that CAF-1 is not required for re-localization of WRN to sites of DNA replication blocks.

Discussion

Most lines of evidence presented thus far are compatible with a multifaceted role for WRN in the resolution of alternative DNA structures in a variety of DNA synthetic processes such as replication, repair and recombination (Bohr, 2005; Ozgenc and Loeb, 2005). For example, WRN is proposed to function during DNA replication to clear the path for the replicative apparatus by resolving alternative DNA structures that would otherwise impede the progression of replication (Franchitto and Pichierri, 2004; Sharma *et al*., 2004a; Ozgenc and Loeb, 2005). On a cellular level, WS cells are

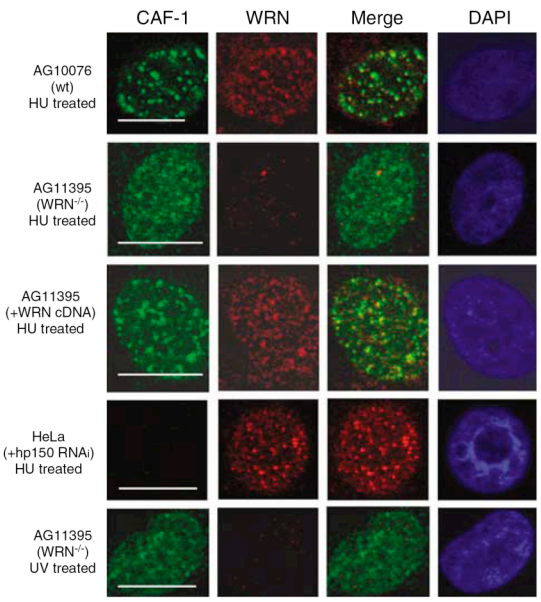

Figure 6 WRN is required for CAF-1 relocalization in response to DNA replication fork blockage by HU and UV. Wild-type (AG10076), WS (AG11395), WS cells corrected with WRN cDNA, and HeLa cells transfected with hp150 RNAi oligos as indicated were treated with HU or UV and processed for localization of hp150 (green) or WRN (red). The yellow in the merged pictures demonstrates the co-localization of WRN and CAF-1. DAPI staining indicates the nucleus (blue). Scale bars represent 10 μm.

Table 3 Colocalization of WRN and CAF-1 in response to HU treatment in WS and CAF-1 RNAi cells

Cell type	*AG10076(wt)*	*AG11395(WS)*	*AG11395 (WRN cDNA corrected)*	*AG03141 (WS)*	*Hpl5Q RNAi*
Cells containing WRN foci (%)	68	No staining	32	No staining	71
Cells containing CAF-1 foci (%)	63	3	29	2	1
Cells containing co-localizing foci (%)	36	0	18	0	0

In each case, 200 cells were scored.

hypersensitive to some, but not all, types of DNA-damaging agents. WRN is clearly involved in DNA repair processes, but more work is needed to establish its *in vivo* role in DNA transactions.

In vivo, DNA is wrapped with histones and other proteins into chromatin, a structural organization that on the one hand protects DNA from being damaged, and on the other hand inhibits DNA-dependent reactions such as replication, repair and recombination (Wolffe, 1998). More importantly, it is crucial that after every DNA transaction, the epigenetic state of the chromatin be reset so that the genome remains fully functional. Therefore, it is likely that proteins involved in DNA metabolic processes, such as WRN, coordinate with chromatin remodeling factors or chromatin assembly factors to ensure full restoration of the chromatin structure after each *in vivo* DNA transaction. The first possible connection between DNA synthesis and a protein likely to be implicated in chromatin structure restoration has been identified through studies of CAF-1. The involvement of CAF-1 in both DNA replication and nucleotide excision repair (NER) are dependent on the presence of proliferating-cell nuclear antigen (PCNA) (Shibahara and Stillman, 1999; Green and Almouzni, 2003). Here, we report the interaction of CAF-1 and the RecQ DNA helicase, WRN. We show that WRN interacts physically with the largest subunit of CAF-1, hp150, *in vitro* and *in vivo*. The results of our interaction region mapping indicate that WRN interacts with hp150 via the region (aa 523–1148) comprising the helicase and RQC domains of WRN (Figure 1e). Interestingly, this interacting domain is different from the one associating with BLM, which interacts with hp150 via two separate sites, the first located near the *N*-terminus of BLM (aa 131–333) and the second located in the middle of the helicase domain (aa 782–952) (Jiao *et al*., 2004).

Our results also show that hp150 did not affect the helicase, exonuclease or ATPase activities of WRN *in vitro*. The chromatin assembly activity of CAF-1 was also not affected in the absence of WRN *in vivo*. However, in the absence of WRN in human cells, hp150 did not relocate to form foci following treatment with HU. In hp150 RNAi knockdown cells, WRN responded normally after HU treatment, demonstrating an epistatic relationship between WRN and CAF-1 in the process of DNA replication and/or repair. Thus, before CAF-1, WRN responds to DNA damage and may recruit CAF-1 to the DNA-damaged sites during DNA synthesis in order to restore the altered chromatin structure. We note that the localization pattern of WRN in hp150 RNAi cells (HeLa) was slightly different from that of WRN in wild-type cells (AG10076) after HU treatment (Figure 6). However, by comparison with untreated HeLa cells (Figure 2), the punctuate nuclear staining (rather than nucleolar) observed after HU indicates WRN re-localization in response to HU treatment.

PCNA is essential in recruiting and modulating the activity of CAF-1, at least *in vitro*, and it is likely that WRN and PCNA act together to recruit CAF-1 in a cooperative way. It is also known that when hp150 is down-regulated, PCNA can still be recruited to sites where DNA is damaged (Green and Almouzni, 2003). It would therefore be valuable to test how CAF-1 responds to HU treatment in the absence of PCNA, unfortunately, no such PCNA-deficient cell lines are currently available. Nevertheless, we examined the PCNA localization in HU-treated HeLa cells. Figure 7 shows that PCNA colocalizes partially with both WRN and CAF-1 following HU treatment. This is in agreement with previous reports that PCNA associates with CAF-1 in DNA replication (Moggs *et al*., 2000), after UV exposure (Green and Almouzni, 2003) and in the

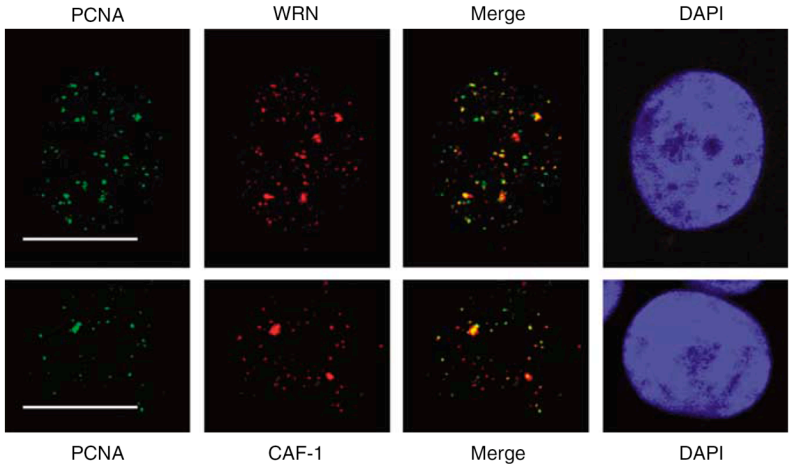

Figure 7 PCNA partially colocalizes with WRN and CAF-1 in HU -treated HeLa cells. HeLa cells cultured on slides were treated with 10 mM HU. Following treatment, cells were processed using PCNA (green) and anti-WRN (red, upper panels) or anti-CAF-1 (red, lower panels) antibodies. In the merged pictures, yellow represents the colocalization of PCNA and WRN (upper panels) or PCNA and CAF-1 (lower panels). DAPI staining of the nucleus is indicated in blue. Scale bars represent 10 μm.

process of double-strand breaks repair (Nabatiyan *et al*., 2006), and that PCNA interacts with WRN during replication (Rodriquez-Lopez *et al*., 2003). However, how WRN and PCNA coordinately interact with CAF-1 remains to be elucidated. One possibility could be that like in the case of FEN-1 (Sharma *et al*., 2005), WRN and PCNA have combined effect on the function/localization of CAF-1.

We have previously reported that CAF-1, via its largest subunit hp150, interacts physically and functionally with BLM (Jiao *et al*., 2004). Interestingly, hp150 is not the first common interaction partner of WRN and BLM. BLM and WRN both interact with replication protein A (RPA) (Garcia *et al*., 2004; Doherty *et al*., 2005), p53 (Spillare *et al*., 1999; Wang *et al*., 2001; Yang *et al*., 2002), flap endonuclease-1 (FEN-1) (Sharma *et al*., 2004a, b) and TRF2 (Opresko *et al*., 2002; Bradshaw *et al*., 2005). Moreover, BLM and WRN also interact with each other (von Kobbe *et al*., 2002). Our data suggest that it is possible that BLM, WRN and CAF-1 form a complex, at least transiently, to accomplish certain cellular functions such as the resolution of stalled replication fork intermediates. However, neither WRN nor BLM colocalized 100% with CAF-1, suggesting that the association of CAF-1 with either BLM or WRN is very dynamic. At any given time, only a proportion of WRN colocalized with CAF-1 (Table 1). Therefore, the WRN and CAF-1 interaction may also function independently from the BLM and CAF-1 interaction. This is also supported by other observations that BS cells and WS cells are sensitive to a different spectrum of DNA-damaging agents and display different phenotypes (Hickson, 2003; Jiao *et al*., 2004; Ozgenc and Loeb, 2005).

In BLM-deficient cells, the CAF-1 localization to nuclear foci following HU treatment is not as robust as in wild-type cells (Jiao *et al*., 2004). However, in WRN-deficient cells, CAF-1 did not respond normally to HU treatment (Figure 6 and Table 3). This raises the possibility that WRN plays a more important role in recruiting CAF-1 to stalled replication forks. Given the observation that in unstressed cells, BLM, but not WRN, colocalizes with CAF-1 (Jiao *et al*., 2004), it is very possible that WRN and CAF-1 interact only in DNA repair-related pathway(s), which is dependent on an activity of WRN which acts before CAF-1. Our observations are consistent with those reported by the Almouzni group that CAF-1 is not recruited to UV-damaged sites in cells from several XP complementation groups, including those deficient in the incision steps of NER (Green and Almouzni, 2003). Thus, CAF-1 functioning as a chromatin assembly factor plays an important role in restoring the structure of chromatin following DNA repair.

Materials and methods

Cell culture and transfection

HeLa, AG10076 (SV40-transformed normal human fibroblasts), AG11395 (SV40-transformed WS fibroblasts) and AG03141 (hTERT-immortalized WS fibroblasts) cells (von Kobbe *et al*., 2003) were cultured in Dulbecco's modified Eagle's medium (Life Technologies, Paisley, UK) supplemented with 10% fetal bovine serum. The WRN expression plasmid that contains the full-length human WRN cDNA cloned into the pCDNA3.1 vector (Invitrogen, Basel, Switzerland) was transfected into AG11395 cells using the conventional calcium phosphate transfection method. For HU treatment, cells were incubated with 10 mM HU for 1, 2, 4 or 20 h. UV treatment was performed with 50–100 J/m^2 at 254 nm and the recovery time was 4 h. After treatment, cells were either fixed for immunostaining or subjected to fractionation.

Far-western analysis

This assay was performed essentially as described previously (Wu *et al*., 2000; Pedrazzi *et al*., 2003). Briefly, 6 pmol of full-length WRN, truncated WRN proteins (LGS-WRN, WRN P1 and WRN P2), and control protein UvrD were subjected to sodium dodecyl sulfate–polyacrylamide gel electrophoresis (SDS–PAGE) and transferred to nitrocellulose filters. After renaturation and blocking steps, the filters were incubated for 60 min in a solution containing hp150 (1 μg/ml) in Tris-buffered saline supplemented with 0.25% milk, 0.3% Tween 20, 1 mM dithiotherlotol (DTT) and 1 mM phenylmethylsulfonyl fluoride . After extensive washing, conventional Western blotting was performed to detect the presence of hp150 (with anti-hp150 mAb, Ab-3, Oncogene research products). For the reverse direction of Far-Western analysis, filters containing hp150, pol β (positive control) and pol λ (negative control) proteins were incubated with WRN before blotting with anti-WRN antibody (ab-200, Abcam).

Preparation of nuclear extracts and co-immunoprecipitation

Nuclear extracts were prepared as follows: cells (100% confluence) were harvested, washed in phosphate-buffered saline (PBS), re-suspended in buffer A (10 mM 4-(2-hydroxyethyl)-1-piperazineethanesulfonic acid (HEPES), pH 7.9, 1.5 mM $MgCl_2$, 10 mM KCl, protease inhibitors) and then centrifuged for 1 min at 2000 r.p.m. The cell pellet was then re-suspended in buffer A+ (buffer A supplemented with 0.1% Noniodet P 40) for 5 min on ice and centrifuged at 10 000 r.p.m., for 5 min. The supernatant contained the cytosolic extract. The pellet was washed in buffer A and then re-suspended in buffer C (20 mM HEPES, pH 7.9, 420 mM NaCl, 1.5 mM $MgCl_2$, 25% glycerol, protease inhibitors) for 15 min, with rolling at 4°C. The samples were then centrifuged at 14 000 r.p.m. for 5 min. The supernatant contained the nuclear extract and the NaCl concentration was adjusted to 120 mM with buffer D (20 mM HEPES, pH 7.9, protease inhibitors). Before immunoprecipitation, nuclear extracts from HeLa cells were incubated with or without ethidium bromide (100 μg/ml) for 1 h. Two hundred microgram of nuclear extract from HeLa cells was incubated with either 2 μg anti-hp150 antibody (Ab-3, Oncogene research products) or 2 μg control IgG in IP buffer (20 mM HEPES, pH 7.5, 120 mM KCl, 5 mM $MgCl_2$, 0.1% (v/v) NP-40, protease inhibitors) at 4°C for 3 h in a total reaction volume of 200 μl. Forty microliters IP buffer-equilibrated protein G-Sepharose beads (Amersham Pharmacia Biotech, Piscataway, NJ, USA) were then added, and the mixture was incubated for 3 h at 4°C. The beads were washed five times with wash buffer (IP buffer supplemented with an additional 20 mM KCl) before the protein complexes bound to the beads were eluted and split into two portions for SDS–PAGE. 10 μg of nuclear extract were used as the input. Western blot analysis with an anti-WRN antibody (ab-200,

Abcam) and an anti-hp150 polyclonal antibody (gifts of Geneviève Almouzni) were used to detect proteins immunoprecipitated by Ab-3 (anti-hp150, Oncogene). ECL detection was performed according to the manufacturer's instructions (Amersham Pharmacia Biotech). Ab-200 (anti-WRN, Abcam) was used for the reverse IP in the above IP buffer containing 120 mM KCl.

Immunofluorescence microscopy
The indirect immunofluorescence assay was performed as described previously (Jiao *et al*., 2004; Petkovic *et al*., 2005). Briefly, cells grown on glass slides were incubated with 0.5% Triton X-100 in PBS for 5 min, fixed with 2% paraformaldehyde in PBS (20 min at room temperature (RT)), and permeabilized with 0.5% Triton X-100 in PBS (20 min at RT). After the blocking step (0.1% Tween-20, 5% bovine serum albumin (BSA) in PBS, 20 min at RT), slides were incubated with a mixture of different rabbit and mouse antibodies. Rabbit antibodies were detected with Cy3-conjugated goat anti-rabbit IgG (Jackson Laboratories, Newmarket, Suffold, England; 1:200 in blocking buffer), and mouse antibodies were detected with FITC-conjugated goat anti-mouse IgG (Jackson Laboratories 1:100 in blocking buffer). To visualize nuclear DNA, slides were incubated with 4,6-diamidino-2-phenylindole, dihydrochloride (DAPI, 0.4 μg/ml). After washing, slides were mounted with Vectashield (Vector Laboratories, Peterborough, England) and viewed under a confocal microscope Leica TCS 4D. Images were processed by Imaris software. For statistical analysis, a minimum of 200 cells was counted in two independent experiments. Anti-WRN was purchased from Abcam (rabbit Ab-200) and anti-hp150 (mAb, Ab-3) from Oncogene research product, whereas polyclonal anti-hp150 was a generous gift from Dr G Almouzni. Anti-PCNA was kindly provided by Dr U Hubscher (mAb, PC10).

Helicase assay
Helicase reactions were performed as described previously (von Kobbe *et al*., 2004). Briefly, oligonucleotide 22Fork3 was 5′ end-labeled with [^{32}P]ATP and T4 polynucleotide kinase (New England Biolabs, Ipswich, MA, USA) and annealed to 22Fork4. Reactions (20 μl) were performed in helicase reaction buffer (40 mM Tris-HCl, pH 8, 4 mM $MgCl_2$, 5 mM DTT and 0.1 mg/ml BSA) and contained ATP (2 mM), DNA substrate (1 nM) WRN and hp150 as indicated. Samples were incubated for 15 min at 37°C and terminated by the addition of stop dye (50 mM ethylenediaminetetraacetic acid (EDTA), 40% glycerol, 0.9% SDS, 0.05% bromophenol blue and 0.05% xylene cyanol). Products were run on a 12% native polyacrylamide gel and visualized using a PhosphorImager (Molecular Dynamics, Sunnyvale, CA, USA).

Exonuclease assay
Exonuclease reactions were performed as described previously (von Kobbe *et al*., 2004). Briefly, oligonucleotide 34ForkA was 5′ end-labeled and annealed to 34ForkB. Reaction (10 μl) were performed in helicase reaction buffer (see above) and contained ATP (2 mM), DNA substrate (1 nM), WRN and hp150 as indicated. Samples were incubated at 37°C for 15 min and terminated by the addition of formamide stop dye (80% formamide, 0.5X tris-borate-EDTA (TBE), 0.1% bromophenol blue and 0.1% xylene cyanol). Products were heat-denatured at 90°C for 5 min and run on a 14% denaturing polyacrylamide gel. Radioactive products were visualized using a PhosphorImager.

ATPase assay
ATPase reactions (10 μl) were performed in helicase reaction buffer (see above) and contained M13mp18 DNA cofactor (150 ng), [^{32}P]ATP (1 μCi), and ATP (50 μM). Reactions were incubated for 30 min at 37°C and terminated by the addition of 5 μl of 0.5 M EDTA. Samples were separated on a polyethylenimine/cellulose thin layer chromatography plate (Mallinckrodt Baker, Inc., Phillipsburg, NJ, USA) developed in 1 M formic acid/0.8 M LiCl. Radioactive products were visualized using a PhosphorImager.

Chromatin assembly assay
An *in vitro* chromatin assembly assay using a human cell-free system was utilized to analyse the activity of recombinant hp150 and the CAF-1 activity from various cells on DNA repair-coupled chromatin assembly (Gaillard *et al*., 1996). Briefly, UV (500 J/m^2) irradiated circular pBluescript plasmid DNA was incubated with cytosolic or S100 extract derived from HeLa cells (Martini *et al*., 1998) supplemented with nuclear extracts from either HeLa or WS cells or purified recombinant hp150 for 3 h at 37°C. The extent of supercoiling was examined by agarose gel electrophoresis followed by drying of the gel and exposure to X-ray film. Incorporation of (α-^{32}P) dCTP indicated newly synthesized DNA after NER.

RNA interference
For short interfering RNA (siRNA) experiments, siRNA oligos were from Qiagen (Basel, Switzerland) and the targeting sequences of each were control GL3 (directed against firefly luciferase): CUUACGCUGAGUACUUCGAdTdT; 150-1, AGGGGAAAGCCGAUGACAUdTdT (Hoek and Stillman, 2003). The siRNAs were transfected in HeLa cells using a 200 nM siRNA concentration with Oligofectamine (Invitrogen) according to the manufacturer's instructions and harvested after 24 h.

Acknowledgements

We thank Oleg Georgiev and Walter Schaffner for HeLa S100 extracts, Genevieve Almouzni for chromatin assembly reagents and anti-hp150 antibodies, Steve Matson for UvrD protein, and Grant Brown and Dieter Egli for comments on the manuscript. RJ is supported in part by the NSFC (Grant 30370791 and 30428029) and 973 program (2005CB522804). ISt group is financed by grants from the Canadian Government, Canadian Institute for Health Research (CIHR), Genome Canada, Novartis, Union Bank of Switzerland, Gebert Rüf Foundation, and the Swiss Cancer League (OCS-01310-02-2003).

References

Adkins MW, Howar SR, Tyler JK. (2004). Chromatin disassembly mediated by the histone chaperone Asf1 is essential for transcriptional activation of the yeast PHO5 and PHO8 genes. *Mol Cell* **14**: 657–666.

Bohr VA. (2005). Deficient DNA repair in the human progeroid disorder, Werner syndrome. *Mut Res* **577**: 252–259.

Bradshaw PS, Stavropoulos DJ, Meyn MS. (2005). Human telomeric protein TRF2 associates with genomic

double-strand breaks as an early response to DNA damage. *Nat Genet* **37**: 193–197.

Cheng WH, Von Kobbe C, Opresko PL, Arthur LM, Komatsu K, Seidman MM *et al*. (2004). Linkage between Werner syndrome protein and the Mre11 complex via Nbs1. *J Biol Chem* **279**: 21169–21176.

Doherty KM, Sommers JA, Gray MD, Lee JW, von Kobbe C, Thoma NH *et al*. (2005). Physical and functional mapping of the replication protein A interaction domain of the werner and bloom syndrome helicases. *J Biol Chem* **280**: 29494–29505.

Franchitto A, Pichierri P. (2004). Werner syndrome protein and the MRE11 complex are involved in a common pathway of replication fork recovery. *Cell Cycle* **3**: 1185–1193.

Gaillard P-H, Martini EM, Kaufman PD, Stillman B, Moustacchi E, Almouzni G. (1996). Chromatin assembly coupled to DNA repair: a new role for chromatin assembly factor I. *Cell* **86**: 887–896.

Garcia PL, Bradley G, Hayes CJ, Krintel S, Soultanas P, Janscak P. (2004). RPA alleviates the inhibitory effect of vinylphosphonate internucleotide linkages on DNA unwinding by BLM and WRN helicases. *Nucleic Acids Res* **32**: 3771–3778.

Green CM, Almouzni G. (2003). Local action of the chromatin assembly factor CAF-1 at sites of nucleotide excision repair *in vivo*. *EMBO J* **22**: 5163–5174.

Guay D, Gaudreault I, Massip L, Lebel M. (2006). Formation of a nuclear complex containing the p53 tumor suppressor, YB-1, and the Werner syndrome gene product in cells treated with UV light. *Int J Biochem Cell Biol* **38**: 1300–1313.

Harrigan JA, Opresko PL, von Kobbe C, Kedar PS, Prasad R, Wilson SH *et al*. (2003). The Werner syndrome protein stimulates DNA polymerase beta strand displacement synthesis via its helicase activity. *J Biol Chem* **278**: 22686–22695.

Harrigan JA, Wilson III DM, Prasad R, Opresko PL, Beck G, May A *et al*. (2006). The Werner syndrome protein operates in base excision repair and cooperates with DNA polymerase beta. *Nucleic Acid Res* **34**: 745–754.

Hickson ID. (2003). RecQ helicases: caretakers of the genome. *Nat Rev Cancer* **3**: 169–178.

Hoek M, Stillman B. (2003). Chromatin assembly factor 1 is essential and couples chromatin assembly to DNA replication *in vivo*. *Proc Natl Acad Sci USA* **100**: 12183–12188.

Jiao R, Bachrati CZ, Pedrazzi G, Kuster P, Petkovic M, Li J-L *et al*. (2004). Physical and functional interaction between the Bloom's syndrome gene product and the largest subunit of chromatin assembly factor 1. *Mol Cell Biol* **24**: 4710–4719.

Karmakar P, Bohr VA. (2005). Cellular dynamics and modulation of WRN protein is DNA damage specific. *Mech Ageing Dev* **126**: 1146–1158.

Karmakar P, Piotrowski J, Brosh Jr RM, Sommers JA, Miller SP, Cheng WH *et al*. (2002a). Werner protein is a target of DNA-dependent protein kinase *in vivo* and *in vitro*, and its catalytic activities are regulated by phosphorylation. *J Biol Chem* **277**: 18291–18302.

Karmakar P, Snowden CM, Ramsden DA, Bohr VA. (2002b). Ku heterodimer binds to both ends of the Werner protein and functional interaction occurs at the Werner N-terminus. *Nucleic Acids Res* **30**: 3583–3591.

Kaufman PD, Kobayashi R, Stillman B. (1997). Ultraviolet radiation sensitivity and reduction of telomeric silencing in Saccharomyces cerevisiae cells lacking chromatin assembly factor-I. *Genes Dev* **11**: 345–357.

Kaufman PD, Kobayashi R, Kessler N, Stillman B. (1995). The p150 and p60 subunits of chromatin assembly factor I: a molecular link between newly synthesized histones and DNA replication. *Cell* **81**: 1105–1114.

Krude T. (1995). Chromatin assembly factor 1 (CAF-1) colocalizes with replication foci in HeLa cell nuclei. *Exp Cell Res* **220**: 304–311.

Krude T. (1999). Chromatin assembly during DNA replication in somatic cells. *Eur J Biochem* **263**: 1–5.

Lai JS, Herr W. (1992). Ethidium bromide provides a simple tool for identifying genuine DNA-independent protein associations. *Proc Natl Acad Sci USA* **89**: 6692–6958.

Laud PR, Multani AS, Bailey SM, Wu L, Ma J, Kingsley C *et al*. (2005). Elevated telomere-telomere recombination in WRN-deficient, telomere dysfunctional cells promotes escape from senescence and engagement of the ALT pathway. *Genes Dev* **19**: 2560–2570.

Lee JW, Kusumoto R, Doherty KM, Lin GX, Zeng W, Cheng WH *et al*. (2005). Modulation of Werner syndrome protein function by a single mutation in the conserved RecQ domain. *J Biol Chem* **280**: 39627–39636.

Li B, Comai L. (2000). Functional interaction between Ku and the werner syndrome protein in DNA end processing. *J Biol Chem* **275**: 28349–28352.

Li L, Nakajima S, Komatsu K, Nussenzweig A, Shimamoto A, Oshima J *et al*. (2005). Accumulation of Werner protein at DNA double-strand breaks in human cells. *J Cell Sci* **118**: 4153–4162.

Linger JG, Tyler JK. (2005). The Yeast Histone chaperone chromatin assembly factor 1 protects against double-strand DNA-damaging agents. *Genetics* **171**: 1513–1522.

Luger K, Mader AW, Richmond RK Sargent DF, Richmond TJ. (1997). Crystal structure of the nucleosome core particle at 2.8 A resolution. *Nature* **389**: 251–260.

Marciniak RA, Lombard DB, Bradley-Johnson F, Guarente L. (1998). Nucleolar localization of the Werner syndrome protein in human cells. *Proc Natl Acad Sci USA* **95**: 6686–6692.

Martini E, Roche DMJ, Marheineke K, Verreault A, Almouzni G. (1998). Recruitment of phosphorylated chromatin assembly factor 1 to chromatin after UV irradiation of human cells. *J Cell Biol* **143**: 563–575.

Moggs JG, Grandi P, Quivy J-P, Jonsson ZO, Hübscher U, Becker PB *et al*. (2000). A CAF-1-PCNA-mediated chromatin assembly pathway triggered by sensing DNA damage. *Mol Cell Biol* **20**: 1206–1218.

Nabatiyan A, Krude T. (2004). Silencing of chromatin assembly factor 1 in human cells leads to cell death and loss of chromatin assembly during DNA synthesis. *Mol Cell Biol* **24**: 2853–2862.

Nabatiyan A, Szüts D, Krude T. (2006). Induction of CAF-1 Expression in Response to DNA Strand Breaks in Quiescent Human Cells. *Mol Biol Cell* **26**: 1839–1849.

Opresko PL, Cheng WH, Bohr VA. (2004b). Junction of RecQ helicase biochemistry and human disease. *J Biol Chem* **279**: 18099–18102.

Opresko PL, Cheng WH, von Kobbe C, Harrigan JA, Bohr VA. (2003). Werner syndrome and the function of the Werner protein; what they can teach us about the molecular aging process. *Carcinogen* **24**: 791–802.

Opresko PL, Otterlei M, Graakjaer J, Bruheim P, Dawut L, Kolvraa S *et al*. (2004a). The Werner syndrome helicase and exonuclease cooperate to resolve telomeric D loops in a manner regulated by TRF1 and TRF2. *Mol Cell* **14**: 763–774.

Opresko PL, von Kobbe C, Laine JP, Harrigan J, Hickson ID, Bohr VA. (2002). Telomere-binding protein TRF2 binds to and stimulates the Werner and Bloom syndrome helicases. *J Biol Chem* **277**: 41110–41119.

Orren DK, Machwe A, Karmakar P, Piotrowski J, Cooper MP, Bohr VA. (2001). A functional interaction of Ku with Werner exonuclease facilitates digestion of damaged DNA. *Nucleic Acids Res* **29**: 1926–1934.

Oshima J, Huang S, Pae C, Campisi J, Schiestl RH. (2002). Lack of WRN results in extensive deletion at nonhomologous joining ends. *Cancer Res* **62**: 547–551.

Ozgenc A, Loeb LA. (2005). Current advances in unraveling the function of the Werner syndrome protein. *Mut Res* **577**: 237–251.

Pedrazzi G, Bachrati CZ, Selak N, Studer I, Petkovic M, Hickson ID *et al*. (2003). The Bloom's syndrome helicase interacts directly with the human DNA mismatch repair protein hMSH6. *Biol Chem* **384**: 1155–1164.

Petkovic M, Dietschy T, Freire R, Jiao R, Stagljar I. (2005). The human Rothmund–Thomson syndrome gene product, RECQL4, localizes to distinct nuclear foci that coincide with proteins involved in the maintenance of genome stability. *J Cell Sci* **118**: 4261–4269.

Poot M, Yom JS, Whang SH, Kato JT, Gollahon KA, Rabinovitch PS. (2001). Werner syndrome cells are sensitive to DNA cross-linking drugs. *FASEB J* **15**: 1224–1226.

Prakash S, Prakash L. (2000). Nucleotide excision repair in yeast. *Mutat Res* **451**: 13–24.

Rodriquez-Lopez AM, Jackson DA, Nehlin JO, Iborra F, Warren AV, Cox LS. (2003). Characterisation of the interaction between WRN, the helicase/exonuclease defective in progeroid Werner's syndrome, and an essential replication factor, PCNA. *Mech Aging Dev* **124**: 167–174.

Sakamoto S, Nishikawa K, Heo SJ, Goto M, Furuichi Y, Shimamoto A. (2001). Werner helicase relocates into nuclear foci in response to DNA damaging agents and co-localizes with RPA and Rad51. *Genes Cells* **6**: 421–430.

Sharma S, Sommers JA, Brosh Jr RM. (2004a). *In vivo* function of the conserved non-catalytic domain of Werner syndrome helicase in DNA replication. *Hum Mol Genet* **13**: 2247–2261.

Sharma S, Sommers JA, Gary RK, Friedrich-Heineken E, Hubscher U, Brosh Jr RM. (2005). The interaction site of Flap Endonuclease-1 with WRN helicase suggests a coordination of WRN and PCNA. *Nucleic Acids Res* **33**: 6769–6781.

Sharma S, Sommers JA, Wu L, Bohr VA, Hickson ID, Brosh Jr RM. (2004b). Stimulation of flap endonuclease-1 by the Bloom's syndrome protein. *J Biol Chem* **279**: 9847–9856.

Shen JC, Gray MD, Oshima J, Loeb LA. (1998). Characterization of Werner syndrome protein DNA helicase activity: directionality, substrate dependence and stimulation by replication protein A. *Nucleic Acids Res* **26**: 2879–2885.

Shibahara K, Stillman B. (1999). Replication-dependent marking of DNA by PCNA facilitates CAF-1-coupled inheritance of chromatin. *Cell* **96**: 575–585.

Smith S, Stillman B. (1989). Purification and characterization of CAF-I, a human cell factor required for chromatin assembly during DNA replication in vitro. *Cell* **58**: 15–25.

Spillare EA, Robles AI, Wang XW, Shen JC, Yu CE, Schellenberg GD *et al*. (1999). p53-mediated apoptosis is attenuated in Werner syndrome cells. *Genes Dev* **13**: 1355–1360.

Szekely AM, Chen YH, Zhang C, Oshima J, Weissman SM. (2000). Werner protein recruits DNA polymerase delta to the nucleolus. *Proc Natl Acad Sci USA* **97**: 11365–11370.

Tyler JK, Bulger M, Kamakaka RT, Kobayashi R, Kadonaga JT. (1996). The p55 subunit of *Drosophila* chromatin assembly factor 1 is homologous to a histone deacetylase-associated protein. *Mol Cell Biol* **16**: 6149–6159.

Tyler JK, Collins KA, Prasad-Sinha J, Amiott E, Bulger M, Harte PJ *et al*. (2001). Interaction between the *Drosophila* CAF-1 and ASF1 chromatin assembly factors. *Mol Cell Biol* **21**: 6574–6584.

Verreault A, Kaufman PD, Kobayashi R, Stillman B. (1996). Nucleosome assembly by a complex of CAF-1 and acetylated histones H3/H4. *Cell* **87**: 95–104.

von Kobbe C, Harrigan JA, May A, Opresko PL, Dawut L, Cheng WH *et al*. (2003). Central role for the Werner syndrome protein/poly(ADP-ribose) polymerase 1 complex in the poly(ADP-ribosyl)ation pathway after DNA damage. *Mol Cell Biol* **23**: 8601–8613.

von Kobbe C, Harrigan JA, Schreiber V, Stiegler P, Piotrowski J, Dawut L *et al*. (2004). Poly(ADP-ribose) polymerase 1 regulates both the exonuclease and helicase activities of the Werner syndrome protein. *Nucleic Acids Res* **32**: 4003–4014.

von Kobbe C, Karmakar P, Dawut L, Opresko P, Zeng X, Brosh Jr RM *et al*. (2002). Colocalization, physical, and functional interaction between Werner and Bloom syndrome proteins. *J Biol Chem* **277**: 22035–22044.

Wang XW, Tseng A, Ellis NA, Spillare EA, Linke SP, Robles AI *et al*. (2001). Functional interaction of p53 and BLM DNA helicase in apoptosis. *J Biol Chem* **276**: 32948–32955.

Wolffe AP. (1998). *Chromatin: Structure and Function*, 3rd edn. Academic Press, New York.

Wu L, Davies DL, North PS, Goulaouic H, Riou JF, Turley H *et al*. (2000). The Bloom's syndrome gene product interacts with topoisomerase III. *J Biol Chem* **275**: 9636–9644.

Xue Y, Ratcliff GC, Wang H, Davis-Searles PR, Gray MD, Erie DA *et al*. (2002). A minimal exonuclease domain of WRN forms a hexamer on DNA and possesses both 3′–5′ exonuclease and 5′-protruding strand endonuclease activities. *Biochemistry* **41**: 2901–2912.

Yang Q, Zhang R, Wang XW, Spillare EA, Linke SP, Subramanian D *et al*. (2002). The processing of Holliday junctions by BLM and WRN helicases is regulated by p53. *J Biol Chem* **277**: 31980–31987.

Yannone SM, Roy S, Chan DW, Murphy MB, Huang S, Campisi J *et al*. (2001). Werner syndrome protein is regulated and phosphorylated by DNA-dependent protein kinase. *J Biol Chem* **276**: 38242–38248.

Ye X, Franco AA, Santos H, Nelson DM, Kaufman PD, Adams PD. (2003). Defective S phase chromatin assembly causes DNA damage, activation of the S phase checkpoint, and S phase arrest. *Mol Cell* **11**: 341–351.

Yu CE, Oshima J, Fu YH, Wijsman EM, Hisama F, Alisch R *et al*. (1996). Positional cloning of the Werner's syndrome gene. *Science* **272**: 258–262.

Article VI

The Bloom's syndrome helicase (BLM) interacts physically and functionally with p12, the smallest subunit of human DNA polymerase δ.

Nives Selak, Csanád Z. Bachrati, Igor Shevelev, Tobias Dietschy, Anette Jacob, Ulrich Hübscher, Joerg D. Hoheisel, Ian D. Hickson, and Igor Stagljar

(Submitted)

For this work, I helped with Co-Ip experiments

The Bloom's syndrome helicase (BLM) interacts physically and functionally with p12, the smallest subunit of human DNA polymerase δ

Nives Selak[1,5,†], Csanád Z. Bachrati[2,†], Igor Shevelev[3,†], Tobias Dietschy[3], Anette Jacob[4], Ulrich Hübscher[1], Joerg D. Hoheisel[4], Ian D. Hickson[2], and Igor Stagljar[3*]

[1] Institute of Veterinary Biochemistry and Molecular Biology, University of Zürich, Winterthurerstr. 190, CH-8057 Zürich, Switzerland, [2] Cancer Research UK, Weatherall Institute of Molecular Medicine, University of Oxford, John Radcliffe Hospital, Oxford OX3 9DS, UK, [3] Department of Biochemistry and Department of Medical Genetics & Microbiology, Faculty of Medicine, Terrence Donnelly Centre for Cellular and Biomolecular Research (dCCBR), University of Toronto, 160 College Street, Toronto ON, Canada, M5S 3E1, [4] Functional Genome Analysis, Deutsches Krebsforschungszentrum, Im Neuenheimer Feld 580, D-69120 Heidelberg, Germany, [5] Present address: Friedrich Miescher Institute, Maulbeerstrasse 66, CH-4058 Basel, Switzerland

† These three authors contributed equally to this study

Running title: BLM interaction with human DNA polymerase δ

* Communicating author

Tel: +1 416 946 78 28

Fax: +1 416 978 82 87

Email: igor.stagljar@utoronto.

Bloom's syndrome (BS) is a cancer predisposition disorder caused by mutation of the *BLM* gene, encoding a member of the RecQ helicase family. Although the phenotype of BS cells is suggestive of a role for BLM in repair of stalled or damaged replication forks, thus far there has been no direct evidence that BLM associates with any of the three human replicative DNA polymerases. Here, we show that BLM interacts specifically *in vitro* and *in vivo* with p12, the smallest subunit of hPOL δ. The hPOL δ enzyme, as well as the isolated p12 subunit, stimulates the DNA helicase activity of BLM. Conversely, BLM stimulates hPOL δ-mediated DNA polymerase activity. Our results provide the first functional link between BLM and the replicative machinery in human cells, and suggest that BLM might be recruited to sites of disrupted replication through an interaction with hPOL δ. Finally, our data also define a novel role for the poorly characterized p12 subunit of hPOL δ.

The faithful completion of chromosomal DNA replication is of crucial importance in determining the fidelity with which genetic information is passed from mother to daughter cells. Incomplete replication or the erroneous copying of a damaged DNA template can give rise to genome instability, accumulation of mutations and, in multicellular organisms, to neoplastic transformation (1). Chromosomal DNA replication in eukaryotic cells requires three distinct DNA polymerases named DNA polymerase α (POL α), ε (POL ε), and δ (POL δ). POL δ is probably required for replication of the leading strand and for completion of lagging strand synthesis at the replication fork, as well as for different DNA repair pathways (2). The mammalian POL δ has been studied extensively as a core enzyme consisting of 4 subunits named p125, p66, p50 and p12 (3). Two of the subunits form a tightly-associated catalytic heterodimer consisting of the catalytic p125 subunit, which has both 5' to 3' DNA polymerase and 3' to 5' exonuclease activities, and p50. The role of the p66 subunit is to bind PCNA, the homotrimeric sliding clamp that functions as a processivity factor for POL δ during DNA replication (4). A specific role for the p12 subunit has not been identified thus far, although it has been shown to interact with the p125 and p50 subunits of POL δ and PCNA (5), and data from *in vitro* DNA replication assays indicate that addition of p12 enhances the DNA polymerizing activity of the enzyme (6). The levels of p12 are regulated by the proteasome through the mechanism that is not dependent upon p12 ubiquitination (7). Apart from PCNA, no

other interacting protein has been characterized that specifically associate with p12.

The RecQ family of DNA helicases represents a group of evolutionarily conserved enzymes that are involved in the maintenance of genome stability (8;9). There are five members of this family known in humans called RECQL1, BLM, WRN, RECQL4 and RECQL5. Defects in three of these give rise to defined clinical disorders associated with cancer predisposition and various aspects of premature aging: mutations in the *WRN* and *RECQL4* genes result in Werner's syndrome (WS) and Rothmund-Thomson (RTS) syndrome, respectively, both of which feature genome instability, predisposition to some types of cancer and the early onset of several aging features. Mutations in the *BLM* gene cause Bloom's syndrome (BS), which is also associated with excessive chromosomal instability and a high incidence of cancers of all types. In contrast to WS and RTS, no obvious premature aging has been observed in BS patients (reviewed in (10). Cells derived from BS patients show a 10-fold higher frequency of reciprocal exchanges between sister chromatids (SCEs), as well as excessive chromosome breakage (11). The BLM protein is a DNA structure-specific helicase that unwinds DNA in 3' to 5' direction (12), and shows an apparent preference for unwinding of synthetic Holliday junctions, G-quadruplex (G4) DNA and D-loop DNA substrates (13;14). These substrates represent different DNA structures that can be formed *in vivo* during DNA replication and homologous recombination (HR) processes. Cell biological studies have shown that BLM is localized in the nucleus of human cells within discrete foci termed promyelocytic leukemia (PML) nuclear bodies (15). BLM also localizes to nucleoli in S phase cells (16), and to telomeres in cells lacking telomerase (17). On the basis of the aforementioned reports, it has been proposed that BLM functions at the interface of DNA replication and recombination, and facilitates the repair of damaged DNA replication forks (9;18).

A large body of evidence implicates BLM in DNA replication. First, DNA replication defects, such as a retarded rate of nascent DNA chain elongation (19) and accumulation of abnormal replication intermediates (20), have been described in BS cells. Second, BLM interacts physically and functionally with several proteins that play important roles during DNA replication, such as replication protein A (RPA) (21), FEN-1 (22), and chromatin assembly factor 1 (CAF-1) (23). Third, BLM is localized to replication foci, particularly during late S phase, and this co-localization increases in the presence of agents that inhibit DNA replication (23). Fourth, BLM expression is activated at the G1/S boundary and peaks in late S-phase/G2 (15;16;24;25). Fifth, BS cells are hyper-sensitive to agents that perturb DNA replication, such as hydroxyurea (HU) (26).

In this work, we report the physical and functional interaction of BLM with p12, the smallest subunit of human POL δ (hPOL δ). Consistent with this interaction playing an important biological function, we show that the presence of the hPOL δ enzyme, as well as the p12 subunit alone, can specifically stimulate the DNA helicase activity of BLM. We also find that BLM specifically stimulates hPOL δ-mediated DNA polymerase activity. Furthermore, we show that the co-localization of BLM and hPOL δ in nuclear foci is activated during replicative stress. Our data are consistent with a role for hPOL δ in the recruitment of BLM to sites of arrested or disrupted DNA replication forks in order for it to effect its role in fork repair and/or stabilization.

Experimental Procedures

Purification of the hPOL δ enzyme Four-subunit hPOL δ was expressed by infection of insect cells with four recombinant baculoviruses, each encoding a subunit of human POL δ. Recombinant baculoviruses encoding the hPOL δ subunits were a kind gift from Dr. Valdimir Podust. Human POL δ enzyme was purified from insect cells as described previously (6).

Purification of 6xHis-p12 protein The p12 cDNA was cloned into the pRSETb vector. The resulting pRSETb-p12 construct was verified by DNA sequencing. p12 was expressed in *E. coli* BL21(DE3) (Novagen). Expression of p12 was induced by addition of 1 mM IPTG to cultures grown at 37°C to an A_{600} of 0.4. After incubation at 37°C for 3 h, the cells were harvested by centrifugation. The *E. coli* pellet was resuspended in 30 ml of buffer A (30 mM phosphate buffer, 10 mM Tris-HCl, pH 8.0, 500 mM NaCl, 10 mM imidazole, 1 mM PMSF, 1 μM benzamidine, 5

μg/ml leupeptin and 2 μg/ml pepstatin A). The cells were disrupted with a French Press (twice) and the lysate was sonicated on ice for 1 min. After centrifugation (20000 rpm for 30 min at 4°C in a SS-34 rotor), the soluble fraction was loaded onto a 1 ml HiTrap Chelating (Ni^{+}) column pre-equilibrated with buffer A. The column was washed with 50 ml buffer A, and then with 20 ml buffer A containing 50 mM imidazole. The bound protein was eluted with 300 mM imidazole in buffer A. After desalting to buffer B (40 mM Tris-HCl pH 7.5, 50 mM NaCl, 1 mM EDTA, 1 mM 2-mercaptoethanol, 15 % (v/v) glycerol, 1 mM PMSF, 1 μM benzamidine, 5 μg/ml leupeptin and 2 μg/ml pepstatin A) using a HiTrap Desalting column, the eluate was loaded onto a 1 ml HiTrap Heparin column pre-equilibrated with buffer B. The column was washed with 20 ml buffer B, and the p12 protein was eluted with a 20 ml linear NaCl gradient (50 to 1000 mM). p12 was eluted at 300 mM NaCl as tested by SDS PAGE and Western blotting using an antibody against p12. The pool of p12 protein was diluted to 50 mM NaCl and finally loaded onto a Mono S column pre-equilibrated with buffer B. Chromatography was performed as for the HiTrap Heparin column. The yield from a 1 l culture was approximately 0.3 mg of p12 protein with a purity of over 99.5%, as judged by Coomassie Blue staining.

Production and purification of the p12 antibody To produce the p12 antibody, the 6xHis-p12 protein was expressed in *E. coli* from the pRSETb-p12 plasmid, and purified from *E. coli* using conventional chromatography (see above). Rabbits were immunized three times with 300 μg of 6xHis-p12 protein being used for each immunization. After the third immunization, the rabbit was sacrificed to obtain the serum. The p12 serum was first purified over a Protein G sepharose column, to isolate total IgG, and then purified over a column coupled to the p12 protein, to obtain the IgG_{p12}. For all subsequent studies, the anti-IgG p12 was used at concentration of 0.2 μg/ml in dilution 1:100 in TBS, 0.05% Tween20. Control IgG was purified from preimune serum using Protein G sepharose column.

Far Western Analysis Far Western assays were performed as described previously (27). Human WRN was a kind gift from Dr. Pavel Janscak, University of Zürich. Briefly, total extracts of Sf21 insect cells (0.825 μg), 0.8 μg of hPOL δ, 0.3 μg of hPOL λ and 0.2 μg of p12 were subjected to 12% SDS PAGE and transferred to a nitrocellulose filter. After blocking in 10% milk, 0.3% Tween 20 in TBS, for 1 h at RT, the filter was incubated for 2 h at 4°C with BLM (0.5 μg/ml) in TBS supplemented with 0.25% milk, 0.3% Tween 20, 1 mM DTT and 1 mM PMSF (hybridization solution). After the washing step (4x15 min, 0.25 % milk, 0.3 % Tween 20 in TBS), Western blot was performed using the anti-BLM IHIC33 antibody (28) to detect the presence of BLM. For the experiment presented in Fig. 1, BLM (1.2 μg), WRN (0.8 μg) and BSA (0.4 μg) were separated on a 7.5% SDS gel and transferred to a nitrocellulose membrane. The membrane was incubated with 6xHis-p12 in hybridization solution, with a final concentration 6xHis-p12 of 0.1μg/ml. After washing, the membrane was probed with an anti-p12 antibody (this study) to detect the presence of p12. The input samples were visualized with antibodies against BLM (IHIC33, (28)) and WRN (ab-200, Abcam). The membrane was incubated with the BLM protein in hybridization solution, with a final concentration of BLM of 0.5μg/ml. After washing, Western blot using an anti-BLM IHIC33 antibody was performed to detect the presence of BLM. The input samples were visualized with antibodies against hPOL λ (ab5954, Abcam) and p12 (this study).

Yeast two-hybrid assay Yeast two-hybrid (YTH) assays were performed as described previously (23). The activity of the reporter gene (β-galactosidase) was assessed using a liquid culture assay with *o*-nitrophenyl -D-galactopyranoside as a substrate. The constructs used to map the region of BLM that interacts with p12 have been described previously (29). The different p12 constructs were generated by PCR using pMALc2e-p12 as a template, and were cloned into the pBTM116+2 (MBN) vector. Sequences of all plasmids, primers used, and construction schemes are available upon request.

Transfections and immunoprecipitation assay The p12 cDNA was cloned into the p3xFLAG-myc-CMV-23 (Sigma) vector using plasmid pRSETb-p12 as a template and primers 5'-ggaagatctcataggggatagagatgccag -3' (*Bgl*II) and 5'- cccaagcttatgggccggaagcggctc - 3' (*Hin*dIII).

The resulting construct was sequenced. 293T cells were transiently transfected with p3xFLAG-myc-CMV-23-p12 by the calcium phosphate precipitation method. 36 h after transfection, cells were treated with 1 mM HU for 24 h, and were then harvested. Nuclear extracts were prepared from 293T cells as described previously (30). Aliquots (500 µg) of the nuclear extracts were incubated with 3 µg of anti-FLAG antibody coupled to magnetic, tosyl-activated Dynabeads (Dynal Biotech, M-280) according to manufacturer's instructions in immunoprecipitation (IP) buffer (20 mM Hepes pH 7.5, 150 mM NaCl, 5 mM $MgCl_2$, 0.1% Nonidet P 40, protease inhibitor) at 4°C for 3 h. As a control, nuclear extracts were incubated with a control rabbit IgG. The beads were washed 3 times in IP buffer, before any protein complexes bound to beads were eluted and analysed by SDS PAGE. A 50 µg portion of nuclear extract was used as input control. Subsequently, Western blot analysis was performed using the anti-FLAG (Sigma M2) and anti-BLM ab 476 antibody (abcam). C-18 (anti-BLM, Santa Cruz) was used for the reciprocal co-immunoprecipitation in the above-mentioned IP buffer containing 150 mM KCl. Nuclear extracts from BS cells were used as a negative control for the C-18 reciprocal co-immunoprecipitation.

DNA polymerase assay Reaction mixtures (final volume of 20 µl) contained 50 mM bis-Tris-HCl, pH 6.5, 6 mM $MgCl_2$, 40 µg/ml BSA, 2% glycerol, 40 µM radiolabelled dTTP, 15 µg/ml poly(dA)-oligo(dT), 10 ng/µl PCNA and 30-150 ng of hPOL δ. Reactions were incubated for 30 minutes at 37°C, and were terminated by addition of 1 ml of ice-cold 10% (w/v) trichloroacetic acid. Acid-insoluble material was analyzed by scintillation counting.

DNA polymerase primer extension assay A 18-nt primer was 5'-end labeled with ^{32}P using T4 polynucleotidekinase, purified on a Sephadex G25 microcolumn, and was then hybridized to X-poly template, essentially as described previously (31). Sequences of the primers used are available upon request. Reactions (10 µl final volume) were carried out in buffer containing 40 mM Tris-HCl buffer (pH8.0), 3 mM $MgCl_2$, 1 mM ATP, 50 mM NaCl, 2 mM DTT, 0.1mg/ml BSA, 10% glycerol, 0.15 pmol of ^{32}P-18-nt-X-poly template, 100 µM each of dATP, dGTP, dCTP, and dTTP, 10 ng of hPOL δ, and the indicated amounts of BLM, human PCNA, or *E. coli* RecQ. Reactions were incubated at 37°C for 30 min, and were terminated by rapid cooling on ice and addition of an equal volume of denaturing loading buffer. The samples were boiled, and 10 µl of sample were electrophoresed through 12.5 % polyacrylamide-8 M urea gel in 0.5xTBE buffer, and the extension products were visualized by autoradiography.

DNA helicase assays Recombinant BLM protein was purified from yeast cells as described previously (12). The splayed arm DNA substrate mimicking a replication fork was generated and purified as described previously (31). The helicase reaction was carried out in a 10 µl volume containing 1x helicase buffer [33 mM Tris-acetate (pH 7.8); 1 mM $MgCl_2$; 66 mM Na-acetate; 0.1 mg/ml BSA; 1 mM DTT; 1 mM ATP], 100 pM substrate, various concentrations of BLM and other proteins as stated in Figure Legends. The reaction was allowed to progress for 15 minutes at 37°C unless stated otherwise. Analysis of reaction products was carried out as described previously (31).

Indirect immunofluorescence analysis GM00637 transformed normal human fibroblasts were grown on coverslips and were either treated with 2.5 mM hydroxyurea for 18 hours or cultured untreated, and were then pulse-labeled with 25 µM BrdU for 5 minutes.The coverslips were then rinsed with ice-cold PBS. Soluble proteins were removed by incubating the slides in pre-extraction buffer (10 mM PIPES, 300 mM sucrose, 3 mM $MgCl_2$, 20 mM NaCl, 0.5% Triton X-100 [pH 6.8]) for 5 minutes on ice. The cells were then fixed in 4% paraformaldehyde for 20 minutes on ice. The immunostaining was performed as described earlier (32) using the IHIC34 rabbit polyclonal antibody (28) and the AlexaFluor 488 conjugated donkey anti-rabbit secondary antibody (Molecular Probes) to detect BLM, at 1:200 and 1:800 dilutions, respectively. The A-9 mouse monoclonal antibody (Santa Cruz Biotechnology Inc.) against the catalytic subunit of hPOL δ and the CY3 conjugated sheep anti-mouse secondary antibody (Sigma-Aldrich) were used to detect hPOL δ, at 1:400 and 1:1000 dilutions, respectively. BrdU incorporation was detected after repeated paraformaldehyde fixation and HCl denaturation with rat anti-BrdU primary antibody

(Abcam) and AlexaFluor 350 conjugated goat anti-rat secondary antibody (Molecular Probes), each at 1:300 dilution. Epifluorescence microscopy, image acquisition and analysis were carried out on a Nikon Eclipse 80i microscope with the Lucia G software (Laboratory Imaging s.r.o.). Grabbed images were scored manually using the Adobe Photoshop program. Foci obtained following staining with either antibody (green or red) were marked and counted. Foci were counted as co-localizing if more than 50% of the green and red signal was overlapping. Co-localization was expressed as percentage of the total number of BLM (green) or POL δ (red) foci. The total number of cells scored in each treatment was 100. Two independent experiments were conducted with nearly identical results, of which only one is presented.

RESULTS

BLM and hPOL δ interact in vitro and in vivo. To analyze the possible functional interaction of BLM and hPOL δ, we first purified both BLM and the four subunit hPOL δ enzyme (Supplementary Fig. 1). A Far-Western assay was then used to test for a specific interaction between BLM and one or more of the hPOL δ subunits. As shown in Fig. 1A, the BLM protein specifically interacted with a protein of apparent molecular mass of 14 kDa (lane 6), which corresponds to p12, the smallest subunit of hPOL δ. In contrast, BLM did not interact with any of the other 3 hPOL δ subunits, with an unrelated human DNA polymerase, hPOL λ (lane 4), or with any protein from the extract of Sf9 insect cells from which the recombinant hPOL δ enzyme was purified (lane 5). In order to confirm that BLM specifically binds to p12, the Far-Western analysis was repeated using full-length BLM and purified recombinant p12 immobilized on nitrocellulose. Clear evidence of binding was obtained (Fig. 1A, lane 9). Moreover, in a reverse Far-Western, purified p12 specifically bound to full length BLM (Fig. 1B, lane 6), but not to BSA (Fig. 1B, lane 4) or to another human RecQ helicase, WRN (Fig. 1B, lane 5). No cross-reactivity of the anti-BLM antibody with p12, or the anti-p12 antibody with BLM was detected (Fig. 1A, lanes 1-3 and 7, and Fig. 1B lanes 1-3). Taken together, these data indicate that BLM and p12 interact specifically *in vitro*.

To validate the results obtained from Far-Western assays, we next performed yeast two-hybrid (YTH) analysis. As shown in Fig. 1C, p12 interacted with full-length BLM, but not with full-length WRN or *E. coli* RecQ, indicating that the physical interaction between p12 and BLM is specific.

To gain insight into the possible association of BLM and p12 in human cells, we performed co-immunoprecipitation assays (Fig. 1D). Because the endogenous levels of p12 are very low and our newly generated anti p12 antisera did not work in immunoprecipitation assays, we were forced to use ectopically expressed p12. For this, FLAG-p12 was transiently transfected into 293T cells and the cells were subsequently synchronized in S phase by treatment with 1 mM HU for 24 hours. Synchronization of the 293T cells was confirmed by FACS analysis (data not shown). Using an anti-FLAG antibody, we were able to specifically co-immunoprecipitate BLM from HU-treated cells (Fig. 1D, lane 4), but not from unsynchronized cells (Fig. 1D, lane 3). As expected, the anti-FLAG antibody efficiently precipitated p125, the largest subunit of hPOL δ, from both HU-treated and unsynchronized cells (Fig. 1D, lanes 3 and 4, lower panel). No BLM was present in the precipitate when a control antibody was used (Fig. 1D, lane 2). A reciprocal co-immunoprecipitation experiment was also carried out, in which an anti-BLM polyclonal antibody was used to immunoprecipitate FLAG-p12 from 293T nuclear extracts. As shown in Fig. 1D, p12 could be specifically co-immunoprecipitated with endogenous BLM from the S phase-synchronized cells (lane 8), but not from unsynchronized 293T cells (lane 7). Furthermore, in addition to p12, the anti-BLM antibody efficiently co-immunoprecipitated hp150, the largest subunit of CAF-1 (Fig. 1D, lanes 7 and 8, lower panel), a protein shown previously to interact with BLM (23). Similar co-immunoprecipitation results were obtained when cell lysates were incubated with ethidium bromide, indicating that the *in vivo* interaction of p12 and BLM is unlikely to be mediated by DNA (data not shown). Finally, the specificity of co-immunoprecipitations with the anti-BLM antibody was demonstrated in a control

experiment using nuclear extracts from BS (BLM $^{-/-}$) cells: in this case, the anti-BLM antibody could not co-immunoprecipitate p12 from these cells (Fig. 1D, lane 11, lower panel), whereas it could efficiently co-immunoprecipitated p12 from S phase synchronized BS cells containing the *BLM* cDNA (BLM$^{-/-}$ + pBLM) (Fig. 1D, lane 12, lower panel). Collectively, these data indicate that BLM directly associates with the p12 subunit of hPOL δ *in vitro* and *in vivo*, and that the BLM/p12 interaction in human cells is exclusively or predominantly seen in cells in which DNA replication is arrested.

Mapping of the interacting regions on BLM and p12. BLM contains several important domains; a conserved helicase domain (aa 649-1006), an RQC domain (aa 1006-1077), and an HRDC domain (aa 1212-1292), all of which are involved in mediating protein-DNA interactions, and possibly also protein-protein interactions (Fig. 2A). To identify the region of BLM that mediates the interaction with p12, we generated a series of BLM deletion mutants and tested them for their ability to interact with full-length p12 in the YTH assay (Fig. 2A). The results indicated that p12 binds BLM in the region between amino acids 447 and 770. This fragment of BLM comprises the helicase-proximal region of the N-terminal domain and part of the helicase domain. A similar YTH approach was used to map the region of p12 that interacts with BLM. A single short region of p12, comprising amino acids 31-60, was found to be necessary and sufficient for interaction with BLM (Fig. 2B).

The hPOL δ enzyme stimulates the BLM-mediated unwinding of a model replication fork substrate. The physical interaction between BLM and hPOL δ suggested the possibility that the two proteins might functionally regulate each other's activities during DNA replication, recombination or repair. To test this hypothesis, we first determined whether the hPOL δ enzyme influences BLM helicase activity. In order to see a potential effect of hPOL δ, either positive or negative, the BLM concentration used in the helicase assays was sufficient only for partial unwinding of the substrate during a 15 minute reaction period. To prevent the potential degradation of the helicase substrate or product by the exonuclease activity of hPOL δ, the hPOL δ enzyme used carried a mutation in the exonuclease domain of p125 (D402A) and was, therefore, exonuclease defective. When hPOL δ was added to the reaction in concentrations giving molar ratios of 25-0.4 times that of the BLM concentration, we saw a significant, concentration-dependent stimulation of helicase activity (Fig. 3A, lanes 6-12). BLM alone (Fig. 3A, lane 3) and BLM incubated with heat-denatured hPOL δ (Fig. 3A, lane 5) showed the expected low level of helicase activity, and hPOL δ alone displayed no DNA helicase activity (Fig. 3A, lane 4).

Next, we analyzed the specificity of this apparent functional interaction. We found that this stimulatory effect was specific to the BLM/hPOL δ complex, as hPOL δ had no effect on another RecQ helicase, *E.coli* RecQ, in the same concentration range (Fig. 3B, lanes 7-17). Moreover, we showed that another human DNA polymerase, hPOL λ, which we had shown did not bind to BLM in Far Western analysis (Fig. 1A), did not influence BLM helicase activity (Fig. 3C, lanes 4-16). Taken together, these data indicate that hPOL δ shows a specific functional interaction with BLM.

The Far-Western and YTH analyses localized the BLM/hPOL δ interaction to the smallest p12 subunit of hPOL δ between residues 31-60 (Fig. 1 and Fig. 2). We tested, therefore, the effect of recombinant p12 subunit on the helicase activity of BLM. p12 showed a concentration-dependent stimulatory effect on BLM similar to that of the hPOL δ enzyme; however, the effective concentration range was such that there was a large molar excess of p12 over BLM was required (Fig. 4A, lanes 6-15). Interestingly, heat-denatured p12 was also able to stimulate BLM helicase activity at this high concentration (1.609 μM; Figure 4A, lane 5), which, in the light of the results showing that a small peptide is also able to stimulate the helicase activity of BLM, is not inexplicable (see below). Further examination of the stimulatory effect of p12 revealed that p12 and the hPOL δ enzyme increased the kinetics of the BLM unwinding reaction to a similar extent (Fig. 4C).

This result prompted us to test the effect on BLM activity of the tightly-defined interacting region of p12. For this, two peptides were chemically synthesized: p12$^{30-60}$ covers the BLM-

binding region, while $p12^{71-100}$ maps to a region of p12 that shows no BLM-binding, as revealed in the YTH mapping studies (Fig. 2B). Full-length p12 and $p12^{30-60}$ showed a similar degree of stimulation of BLM activity in a time-course experiment. In contrast, $p12^{71-100}$ had no effect on BLM helicase activity (Fig. 5A, B). Taken together, these results confirm that the helicase activity of BLM is stimulated by hPOL δ, and that this stimulation is dependent on the binding between the two proteins through amino acid residues 30-60 in the p12 subunit of hPOL δ.

BLM increases the DNA polymerase activity of hPOL δ. Given the data described above indicating that hPOL δ has a significant stimulatory effect on BLM helicase activity, it was important to examine whether BLM affects the polymerase activity of hPOL δ. To that end, we performed primer extension assays (Fig. 6). hPOL δ-specific polymerization activity was monitored by visualizing extension of a 5'-end labeled 18-mer primer on an 85-mer DNA template, which contains an X-junction at the 3'end. This template was chosen because we wanted to examine whether BLM can help hPOL δ to traverse X-junction at the end of template. In such an experimental set-up, BLM did not help hPOL δ to traverse X-junction structure (Fig. 6, lane 3-5). However, we found that BLM stimulated hPOL δ polymerase activity *per se*. We observed that hPOL δ was able to incorporate dNTPs up to the start of the X-junction structure (Fig. 6, lane 2). The inability of hPOL δ to extend the primer beyond the pause site indicates that the X-junction structure effectively blocked progression of hPOL δ along the template strand.

When BLM was added to the reaction in concentrations giving molar ratios of 1.5-7.5 times that of the hPOL δ concentration, we observed a significant, concentration-dependent stimulation of hPOL δ polymerase activity. Addition of BLM to reactions containing hPOL δ increased both the amount of primer extended and the maximal length of product (Fig. 6, lanes 3-5) such that the longest products represented polymerization extending beyond the position of the X-junction. This effect was similar to that produced by PCNA, although the degree of stimulation of hPOL δ by PCNA was slightly more pronounced (Fig. 6, lanes 7-9). Importantly, BLM alone showed no polymerase activity (Fig. 6, lane 6). The stimulatory effect of BLM on hPOL δ was found to be specific, as another member of the RecQ helicase family, *E. coli* RecQ, had no effect on hPOL δ polymerase activity (Fig. 6, lane 10). Taken together, these results indicated that BLM stimulates the hPOL δ -mediated DNA polymerase activity, resulting both in longer extension products and in polymerization through a region of DNA secondary structure.

BLM and hPOL δ partially co-localize in vivo in response to perturbation of DNA replication. The *in vitro* studies described above prompted us to analyze whether hPOL δ and BLM might interact *in vivo*. As indicated above (Fig. 1D), BLM and hPOL δ could be co-immunoprecipitated from 293T cells only after HU treatment, which suggested that the interaction is either S phase specific or induced specifically in response to perturbation of replication. To differentiate between these possibilities, we addressed whether BLM and hPOL δ co-localize either in unperturbed, cycling cells, or in cells blocked with HU. For this, GM00637 (BLM proficient) human fibroblast cells were plated on coverslips and treated with 2.5 mM HU for 18 hours, sufficient to block replication, as evidenced by the depression of BrdU incorporation into the nuclei (not shown). A control culture was incubated in parallel without HU treatment. In both sets of cells, BrdU was added to a final concentration of 25 μM 5 minutes before the cells were fixed. The fixed samples were stained for the presence of hPOL δ, BLM and BrdU, as described in Materials and Methods. As expected from previous analyses, BLM and hPOL δ showed a punctate nuclear pattern of localization (15;25;33). Representative images of the staining patterns are depicted in Figure 7A. The degree of co-localization of nuclear foci was then scored. This analysis revealed that, in an untreated asynchronous cell population, on average 13% of BLM foci co-localized with hPOL δ foci and 8% of hPOL δ foci co-localized with BLM (Fig. 7B, middle panels). In response to HU treatment, the degree of co-localization increased significantly: 22% of BLM foci co-localized with hPOL δ, and 17% of hPOL δ foci co-localized with BLM (Fig. 7B, top panels). This increase in the extent of co-localization might be restricted to S phase or might

be an effect of the HU-induced replication perturbation. To address this, we took advantage of the BrdU labeling of the actively replicating cells. When only the BrdU-positive subpopulation was scored in the untreated cultures, the degree of co-localization was similar to that of the whole asynchronous population: 15% of BLM foci co-localized with hPOL δ, and 9% of hPOL δ foci co-localized with BLM (Fig. 7B, bottom panels). These results indicate that BLM and hPOL δ do not normally co-localize *in vivo*, even during an unperturbed S phase, but that perturbation of DNA replication causes them to co-localize to a significant extent. Nevertheless, even after treatment of cells with HU, most BLM and hPOL δ foci still did not co-localize, indicating that a significant fraction of BLM remains distant from sites of stalled replication forks.

DISCUSSION

We have shown that the Bloom's syndrome helicase, BLM, and the major replicative DNA polymerase, hPOL δ, interact specifically *in vitro* and *in vivo.* This interaction is direct and is mediated via the so far poorly characterized p12 subunit of hPOL δ. We mapped the site of interaction of BLM with p12 to a region representing amino acids 447-770. This fragment includes the N terminal part of the BLM helicase domain and it has been shown previously that this is involved in interaction with the WRN helicase (34). In addition, we mapped the region of p12 that interacts with BLM to a short fragment comprising amino acids 30-60. Database searches revealed that this p12 fragment does not represent any known conserved protein domain and that it shows no sequence homology to any known BLM interacting partner. Of most importance, we have also shown that BLM and hPOL δ can functionally associate in that their interaction leads to stimulation of the catalytic activity of both partners.

There are a number of possible scenarios in DNA replication/repair where the productive co-operation of BLM and hPOL δ might be advantageous. Perhaps the most plausible is during the process of fork regression under circumstances where a replication fork is arrested by DNA adduct or another blockade, particularly those that block leading strand synthesis. We have shown recently that BLM can promote the regression of a model replication fork *in vitro* (35). This may be a reaction that is beneficial for DNA repair simply because, through promoting fork back-tracking, it allows access to the blocking 'lesion'. However, there is also potential for fork regression to be important in a lesion bypass pathway of DNA damage tolerance. If the lesion blocks leading strand synthesis, it appears that the synthesis of the lagging strand may continue for some distance ahead of the site of the blocked leading strand. This apparently futile uncoupling of leading and lagging strand synthesis has the potential, after fork regression, to permit template switching with the shorter leading strand being extended by copying of the longer lagging strand template. In this way, once the regressed fork is reset, the leading strand would be extended beyond the site of the lesion and normal DNA replication could commence. hPOL δ might both recruit BLM to stalled forks and then stimulate its catalytic activity once there. Conversely, BLM might play a role in assisting hPOL δ to access the regressed '4^{th} arm' and catalyze extension of the leading strand.

A striking feature of the ability of hPOL δ to stimulate the helicase activity of BLM was our finding that a short peptide (aa 30-60) representing the minimal binding region of p12 is as efficient in this stimulatory role as is the hPOL δ enzyme. This would seem to rule out many possible mechanisms for the stimulation, including recruitment of BLM to the DNA substrate. Instead, these results strongly argue for hPOL δ acting to alter the conformation of BLM in such a way as to enhance its helicase function. A major goal for the future will be to characterize in molecular detail how this short peptide can have such a marked effect on the BLM helicase.

Our data indicate that BLM and hPOL δ do not significantly co-localize in the nucleus of human cells under normal growth conditions, including within an unperturbed S-phase. This is consistent with the known localization of BLM to PML bodies and not to sites of ongoing replication. However, we were able to detect a consistent increase in the percentage of nuclear BLM foci that co-localize with hPOL δ when cells were treated with HU. Taken together, these data

indicate that this association at replication foci is driven by replication perturbation, and not by cell cycle phase *per se*. To support these results, we could show direct association of BLM with the p12 subunit of hPOL δ *in vivo* in cells which were synchronized in S phase by HU treatment. No interaction between BLM and p12 could be observed in unsynchronized cells. Our data showing that BLM and p12 co-immunoprecipitate from the nuclear extracts of the 293T cells after treatment with 1mM HU seemingly contrast with the recent data of Zhang and colleagues (36), who reported that, in HeLa and 293T cells, p12 undergoes ubiquitination and degradation 20 h after the treatment with 2 mM HU. These differences are probably the result of the different HU concentrations that have been employed in these two studies. Alternatively, it may well be that binding of BLM to p12 prevents p12 ubiquitination and degradation, which is the reason why we did not observe degradation of p12 in our experiments.

By using an oligonucleotide primer-template substrate, we have shown that BLM increases primer extension mediated by hPOL δ. In contrast, *E. coli* RecQ had no effect on DNA synthesis by hPOL δ. It has been shown previously that WRN has a stimulatory effect on the polymerization activity of *S. cerevisiae* POL δ in the absence of PCNA (37). However, WRN does not apparently have an effect on DNA synthesis catalyzed by the POL δ-PCNA complex. These results suggest that WRN may not function in processive DNA synthesis reactions during normal DNA replication; instead, WRN may function in replication restart of stalled or collapsed replication forks from which the replication machinery has dissociated (37).

Our current hypothesis is that BLM may, in a similar manner to WRN, be involved in replication restart of stalled replication forks blocked by DNA damage or unusual secondary structures in DNA template (38). One such a scenario is during the replication of ribosomal DNA in the nucleolus. Similar to telomeres, ribosomal DNA is GC rich and can adopt alternative DNA structures such as hairpins and G-quadruplexes. These structures are efficiently resolved *in vitro* by BLM and WRN (13;39-41). When overexpressed in HeLa cells, WRN can recruit the p50 and p125 subunit of hPOL δ from nucleoplasm to the nucleolus (42). In an unperturbed cell cycle, BLM is found primarily in PML nuclear bodies, except during late S phase when it co-localizes with WRN in the nucleolus (16). Additionally, BLM binds to ribosomal DNA and primarily at the non-transcribed spacer region where replication forks initiate (43). These findings suggest that BLM may be directly coupled to replication fork initiation and/or progression at particular sites of DNA synthesis. The fact that BLM and hPOL δ co-localize more prominently after blockade of replication, but that not all replication foci contain BLM under these conditions, suggests that BLM may be recruited to sites of DNA synthesis only in response to the formation of a particular DNA structure that needs BLM helicase function for its resolution. It will be interesting to address in the future whether BLM is recruited to hPOL δ foci only following post-translational modification of one or both of these factors, or whether the association is mediated by other replication factors to which BLM binds, such asRPA(21).

REFERENCES

1. Bell, S. P. and Dutta, A. (2002) *Annu.Rev.Biochem.* **71,** 333-374

2. Hubscher, U., Maga, G., and Spadari, S. (2002) *Annu.Rev.Biochem.* **71,** 133-163

3. Liu, L., Mo, J., Rodriguez-Belmonte, E. M., and Lee, M. Y. (2000) *J.Biol.Chem.* **275,** 18739-18744

4. Maga, G. and Hubscher, U. (2003) *J.Cell Sci.* **116,** 3051-3060

5. Li, H., Xie, B., Zhou, Y., Rahmeh, A., Trusa, S., Zhang, S., Gao, Y., Lee, E. Y., and Lee, M. Y. (2006) *J.Biol.Chem.* **281,** 14748-14755

6. Podust, V. N., Chang, L. S., Ott, R., Dianov, G. L., and Fanning, E. (2002) *J.Biol.Chem.* **277,** 3894-3901

7. Liu, G. and Warbrick, E. (2006) *Biochem.Biophys.Res.Commun.* **349,** 360-366

8. Bachrati, C. Z. and Hickson, I. D. (2003) *Biochem.J.* **374,** 577-606

9. Opresko, P. L., Cheng, W. H., and Bohr, V. A. (2004) *J.Biol.Chem.* **279,** 18099-18102

10. Hickson, I. D. (2003) *Nat.Rev.Cancer* **3,** 169-178

11. Ray, J. H. and German, J. (1983) The cytogenetics of the chromosome-breakage syndromes. In German, J., editor. *Chromosome mutation and neoplasia*, Alan R. Liss, Inc, New York

12. Karow, J. K., Chakraverty, R. K., and Hickson, I. D. (1997) *J.Biol.Chem.* **272,** 30611-30614

13. Mohaghegh, P., Karow, J. K., Brosh, R. M., Jr., Bohr, V. A., and Hickson, I. D. (2001) *Nucleic Acids Res.* **29,** 2843-2849

14. Bachrati, C. Z., Borts, R. H., and Hickson, I. D. (2006) *Nucleic Acids Res.* **34,** 2269-2279

15. Bischof, O., Kim, S. H., Irving, J., Beresten, S., Ellis, N. A., and Campisi, J. (2001) *J.Cell Biol.* **153,** 367-380

16. Yankiwski, V., Marciniak, R. A., Guarente, L., and Neff, N. F. (2000) *Proc.Natl.Acad.Sci.U.S.A.* **97,** 5214-5219

17. Lillard-Wetherell, K., Machwe, A., Langland, G. T., Combs, K. A., Behbehani, G. K., Schonberg, S. A., German, J., Turchi, J. J., Orren, D. K., and Groden, J. (2004) *Hum.Mol.Genet.* **13,** 1919-1932

18. Wu, L. and Hickson, I. D. (2006) *Annu.Rev.Genet.* **40,** 279-306

19. Hand, R. and German, J. (1975) *Proc.Natl.Acad.Sci.U.S.A.* **72,** 758-762

20. Lönn, U., Lönn, S., Nylen, U., Winblad, G., and German, J. (1990) *Cancer Res.* **50,** 3141-3145

21. Brosh, R. M., Jr., Li, J. L., Kenny, M. K., Karow, J. K., Cooper, M. P., Kureekattil, R. P., Hickson, I. D., and Bohr, V. A. (2000) *J.Biol.Chem.* **275,** 23500-23508

22. Sharma, S., Sommers, J. A., Wu, L., Bohr, V. A., Hickson, I. D., and Brosh, R. M., Jr. (2004) *J.Biol.Chem.* **279,** 9847-9856

23. Jiao, R., Bachrati, C. Z., Pedrazzi, G., Kuster, P., Petkovic, M., Li, J. L., Egli, D., Hickson, I. D., and Stagljar, I. (2004) *Mol.Cell.Biol.* **24,** 4710-4719

24. Sanz, M. M., Proytcheva, M., Ellis, N. A., Holloman, W. K., and German, J. (2000) *Cytogenet.Cell Genet.* **91,** 217-223

25. Dutertre, S., Ababou, M., Onclercq, R., Delic, J., Chatton, B., Jaulin, C., and Amor-Gueret, M. (2000) *Oncogene* **19,** 2731-2738

26. Davies, S. L., North, P. S., Dart, A., Lakin, N. D., and Hickson, I. D. (2004) *Mol.Cell.Biol.* **24,** 1279-1291

27. Jiao, R., Harrigan, J. A., Shevelev, I., Dietschy, T., Selak, N., Indig, F. E., Piotrowski, J., Janscak, P., Bohr, V. A., and Stagljar, I. (2006) *Oncogene* **advance online publication 18 December 2006,** doi: 10.1038/sj.onc.1210150

28. Wu, L., Davies, S. L., North, P. S., Goulaouic, H., Riou, J. F., Turley, H., Gatter, K. C., and Hickson, I. D. (2000) *J.Biol.Chem.* **275,** 9636-9644

29. Pedrazzi, G., Perrera, C., Blaser, H., Kuster, P., Marra, G., Davies, S. L., Ryu, G. H., Freire, R., Hickson, I. D., Jiricny, J., and Stagljar, I. (2001) *Nucleic Acids Res.* **29,** 4378-4386

30. Petkovic, M., Dietschy, T., Freire, R., Jiao, R., and Stagljar, I. (2005) *J.Cell Sci.* **118,** 4261-4269

31. Bachrati, C. Z. and Hickson, I. D. (2006) *Methods Enzymol.* **409,** 86-100

32. Pedrazzi, G., Bachrati, C. Z., Selak, N., Studer, I., Petkovic, M., Hickson, I. D., and Stagljar, I. (2003) *Biol.Chem.* **384,** 1155-1164

33. Ababou, M., Dutertre, S., Lecluse, Y., Onclercq, R., Chatton, B., and Amor-Gueret, M. (2000) *Oncogene* **19,** 5955-5963

34. von Kobbe, C., Karmakar, P., Dawut, L., Opresko, P., Zeng, X. M., Brosh, R. M., Jr., Hickson, I. D., and Bohr, V. A. (2002) *J.Biol.Chem.* **277,** 22035-22044

35. Ralf, C., Hickson, I. D., and Wu, L. (2006) *J.Biol.Chem.* **281,** 22839-22846

36. Zhang, S., Zhou, Y., Trusa, S., Meng, X., Lee, E. Y., and Lee, M. Y. (2007) *J.Biol.Chem.* **282,** 15330-15340

37. Kamath-Loeb, A. S., Johansson, E., Burgers, P. M. J., and Loeb, L. A. (2000) *Proc.Natl.Acad.Sci.U.S.A.* **97,** 4603-4608

38. Kamath-Loeb, A. S., Loeb, L. A., Johansson, E., Burgers, P. M. J., and Fry, M. (2001) *J.Biol.Chem.* **276,** 16439-16446

39. Fry, M. and Loeb, L. A. (1999) *J.Biol.Chem.* **274,** 12797-12802

40. Huber, M. D., Lee, D. C., and Maizels, N. (2002) *Nucleic Acids Res.* **30,** 3954-3961

41. Sun, H., Karow, J. K., Hickson, I. D., and Maizels, N. (1998) *J.Biol.Chem.* **273,** 27587-27592

42. Szekely, A. M., Chen, Y. H., Zhang, C., Oshima, J., and Weissman, S. M. (2000) *Proc.Natl.Acad.Sci.U.S.A.* **97,** 11365-11370

43. Schawalder, J., Paric, E., and Neff, N. F. (2003) *BMC.Cell Biol.* **4,** 15

FOOTNOTES

We thank Pavel Janscak for the gift of purified recombinant WRN, Vladimir Podust for the gift of recombinant baculoviruses encoding the hPOL δ subunits, and Grant Brown for critical reading of the manuscript and helpful discussions.

CZB and IDH are supported by Cancer Research UK. NS is a former graduate student in the Stagljar lab and was supported by the Swiss National Foundation Grant (Nr. 3100A0-100256/1) to ISt. The Stagljar lab is supported by grants from the Canadian Foundation for Innovation (CFI), Canadian Institute for Health Research (CIHR), National Cancer Institute of Canada (NCIC), Genome Canada and the Ontario Genomics Institute, Gebert Rüf Foundation, and Novartis.

FIGURE LEGENDS

FIG. 1. BLM and p12 of hPOL δ interact *in vitro* and *in vivo*. (A) *Left panel.* Far-Western analysis. hPOL λ, total protein extract from Sf9 insect cells, and hPOL δ enzyme were subjected to SDS-PAGE, transferred to a nitrocellulose membrane, and were incubated with purified recombinant BLM. Anti-BLM antibodies were used to permit the detection of p12 as a novel BLM-interacting protein (lane 6). Molecular weight markers are also indicated on the left. *Right panel.* Purified p12 subunit of hPOL δ was subjected to SDS-PAGE, transferred to nitrocellulose membrane, incubated with BLM, and subsequently probed with the anti-BLM antibody (lane 9).

(B) Reciprocal Far Western analysis. BSA, WRN, and BLM (left panel) were hybridized with the purified p12 and probed with the anti-p12 antibody (right panel). Anti-p12 antibodies were used to confirm that p12 specifically binds to BLM (lane 6).

(C) BLM and p12 of hPOL δ interact in the YTH assay. The L40 yeast reporter strain was co-transformed with plasmids encoding the indicated full-length "bait" (LexA-DBD) and "prey" (Gal4-AD) fusions. Two independent colonies were grown on SD agar plates lacking tryptophan and leucine, but containing X-gal, prior to assessment of β-galactosidase activity. Also shown are two negative controls, p12 co-transformed with an empty prey vector and BLM co-transformed with lamin C protein. The previously described BLM/hp150 (CAF-1) interaction (23) was used as a positive control.

(D) BLM and hPOL δ form a complex in human cells. 293T cells were transiently transfected with FLAG-p12, and were synchronized in S phase using 1 mM HU. Nuclear extracts derived from either unsynchronized (lane 3) or S-phase synchronized cells (lane 4) were immunoprecipitated with the anti-FLAG antibody or control IgG, and were analyzed by SDS PAGE. One-tenth (50 μg) of the same nuclear extract was used as input control (lane 1). Immunoprecipitated FLAG-p12 and BLM were detected by Western blotting using the anti-FLAG and anti-BLM antibody, respectively (lane 4). p125, the largest subunit of hPOL δ, was also efficiently co-immunoprecipitated using the same anti-FLAG antibody (lanes 3 and 4). Reciproical co-immunoprecipitation is shown in the middle panel: lane 5, input; lane 6, immunoprecipitation with the control IgG; lane 7, immunoprecipitation with an anti-BLM antibody (C-18) from nuclear extracts derived from unsynchronized 293T cells; lane 8, immunoprecipitation with an anti-BLM antibody (C-18) from nuclear extracts derived from the S-phase synchronized 293T cells. The known BLM interacting protein, hp150 (CAF-1) was also efficiently co-immunoprecipitated using the same anti-BLM antibody (lanes 7 and 8). Right panel shows co-immunoprecipitation with anti-BLM antibody (C-18) from BS cell nuclear extracts (BS) and BS cells containing the *BLM* cDNA (BS + pBLM). p12 could be co-immunoprecipitated in the presence of BLM from the S-phase synchronized nuclear extracts (lane 12) but not in the absence of BLM (lane 11). Lanes 9 and 10 are the inputs of the two different nuclear extracts.

FIG. 2. Interaction region mapping of BLM and p12. (A) Mapping of the BLM interaction region. The L40 yeast strain was co-transformed with plasmids encoding the indicated BLM fragments fused to Gal4-AD and the full-length p12 fused to LexA-DBD. Two independent colonies were grown on SD agar plates lacking tryptophan and leucine, but containing X-gal, prior to assessment of β-galactosidase activity. Blue coloration of colonies is a marker of interaction. Full length BLM is also shown, with a red bar indicating its conserved helicase domain, a blue bar indicating RQC and a black bar indicating the HRDC domain. Interactions between a given bait/prey pair were quantified by measurements of β-galactosidase activity. Values represent means ± S.D. of three independent experiments. **(B)** Mapping of the p12 interaction region. The L40 yeast strain was co-transformed with plasmids encoding the indicated p12 fragments fused to LexA-DBD and full length BLM fused to Gal4-AD. In both **(A)** and **(B)** the sequence boundaries of deletion mutants tested are shown with the corresponding amino acid positions indicated on the right. Values obtained from liquid β-galactosidase assay are shown on the right and represent means ± S.D. of three independent experiments.

FIG. 3. The hPOL δ enzyme specifically stimulates the BLM-mediated unwinding of the replication fork substrate in a concentration-dependent manner. (A) 1.3 nM BLM was pre-incubated with hPOL δ enzyme in various concentrations (33.5, 16.8, 8.4, 4.2, 2.1, 1, 0.5 nM; lanes 6-12, respectively) on ice for 3 minutes, and the samples were then warmed to 37°C. The unwinding reaction was initiated immediately by the addition of substrate and ATP. Flame symbol depicts heat-denatured substrate (lane 2), or BLM incubated with heat-denatured hPOL δ enzyme at the highest concentration of the titration range (33.5 nM; lane 5), as described above. **(B)** The hPOL δ enzyme does not stimulate the unwinding of the forked substrate by *E.coli* RecQ. Reactions were carried out as in (A) except using 15 pM *E.coli* RecQ in place of BLM and different concentrations of hPOL δ (33.5-0.02 nM; lanes 7-17). BLM at 1.3 nM was also included as a control with and without 33.5 nM hPOL δ (lanes 4 and 3, respectively). **(C)** Human DNA polymerase λ does not stimulate the helicase activity of BLM. Helicase reactions using 1 nM BLM and various concentrations of hPOL λ (35.16, 17.58, 8.79, 4.40, 2.20, 1.10, 0.55, 0.27, 0.14, 0.07, 0.035, 0.017 nM; lanes 4-15, respectively) were carried out as in (A). Controls and symbols used are as in (A).

FIG. 4. The small subunit of the hPOL δ enzyme, p12, is sufficient to stimulate BLM helicase activity. (A) 1.3 nM BLM was pre-incubated with various concentrations of p12 (1609, 804.5, 402.25, 201.13, 100.56, 50.28, 25.14, 12.57, 6.29, 3.14 nM; lanes 6-15, respectively) on ice for 3 minutes, and the samples were then warmed to 37°C. The unwinding reaction was initiated immediately by the addition of substrate and ATP. Controls and symbols are as in Figure 3. **(B)** 0.85 nM BLM was incubated at 37°C for 5 minutes alone (lanes 1-9), or with 20 nM hPOL δ (lanes 10-18), or 20 nM p12 (lanes 19-27). The unwinding reaction was then initiated by the addition of ATP and substrate. Samples were withdrawn at the time points indicated above the lanes. (**C)** Quantification of data from panel B.

FIG. 5. The stimulatory effect of p12 can be localized to a small peptide, spanning the region that binds BLM. (A) 0.85 nM BLM was incubated at 37°C for 5 minutes alone (lanes 1-9), or with 20 nM $p12^{71\text{-}100}$ (a peptide that shows no binding to BLM; lanes 10-18), full length hp12 (lanes 19-27) or $p12^{30\text{-}60}$ (a peptide that spans the binding region to BLM; lanes 28-36). Reactions were run as in Figure 4b. **(B)** Quantification of data from panel (A).

FIG. 6. BLM stimulates hPOL δ DNA polymerase activity. 10 ng of hPOL δ alone (lane 2) or in the presence of an increasing amount (10, 20 or 50 ng) of BLM (lanes 3-5), PCNA (lanes 7-9), or 50 ng of *E. coli* RecQ (lane 10) were tested in primer extension assays using the X-poly DNA template as described in Materials and Methods. 18 nt primer was 5' end labeled. Lane 6 contains 50 ng of BLM alone and shows that BLM does not have DNA polymerase activity. Lane 1: substrate alone; positions of oligonucleotide size-markers are indicated.

FIG. 7. BLM and hPOL δ co-localize *in vivo* and this co-localization is stimulated during replicative stress. (A) GM00637 cells were arrested with 2.5 mM hydroxyurea, and were stained as described in Materials and Methods. A representative image showing punctate BLM (green, left) and hPOL δ (red, second from left) staining and the co-localization of the two proteins (yellow signal). The right panel shows the nucleus of the same cell stained with the DNA dye Hoechst 33258. **(B)** Quantification of the extent of co-localization with (top two panels) or without (middle two panels) HU treatment. Bottom two panels show co-localization in the BrdU-positive subpopulation of cells from the middle panels. Each bar on the frequency graphs represent the number of cells with more than 0%, 5%, 10%, 15%, *etc* BLM foci co-localizing with hPOL δ (left column) or hPOL δ foci co-localizing with BLM (right column).

LEGENDS TO SUPPLEMENTARY FIGURE

Supplementary FIG. 1. Purified recombinant hPOL δ is active and dependent on PCNA. (A) Purification of hPOL δ. Coomassie Blue staining of the gel revealed that the hPOL δ enzyme (lane 1) is approximately 90% pure. Western blot analysis is shown in lane 3. Molecular weight markers are also indicated in lane 2. The nitrocellulose membrane blotted with the purified recombinant hPOL δ enzyme was cut in four pieces and hybridized with antibodies against the p125 (MBL International, K0160-3), p66 (Novus Biologicals, NB 100-476), p50 (MBL International, K0161-3), and p12 (this study) subunits of hPOL δ. The purified hPOL δ enzyme consists of all four subunits as shown by Western blot. **(B)** Polymerase activity of the hPOL δ enzyme. Different amounts (30 ng, 60 ng, 90 ng 120 ng 150 ng) of the purified recombinant hPOL δ enzyme were tested for polymerase activity in the presence and absence of PCNA (200 ng).

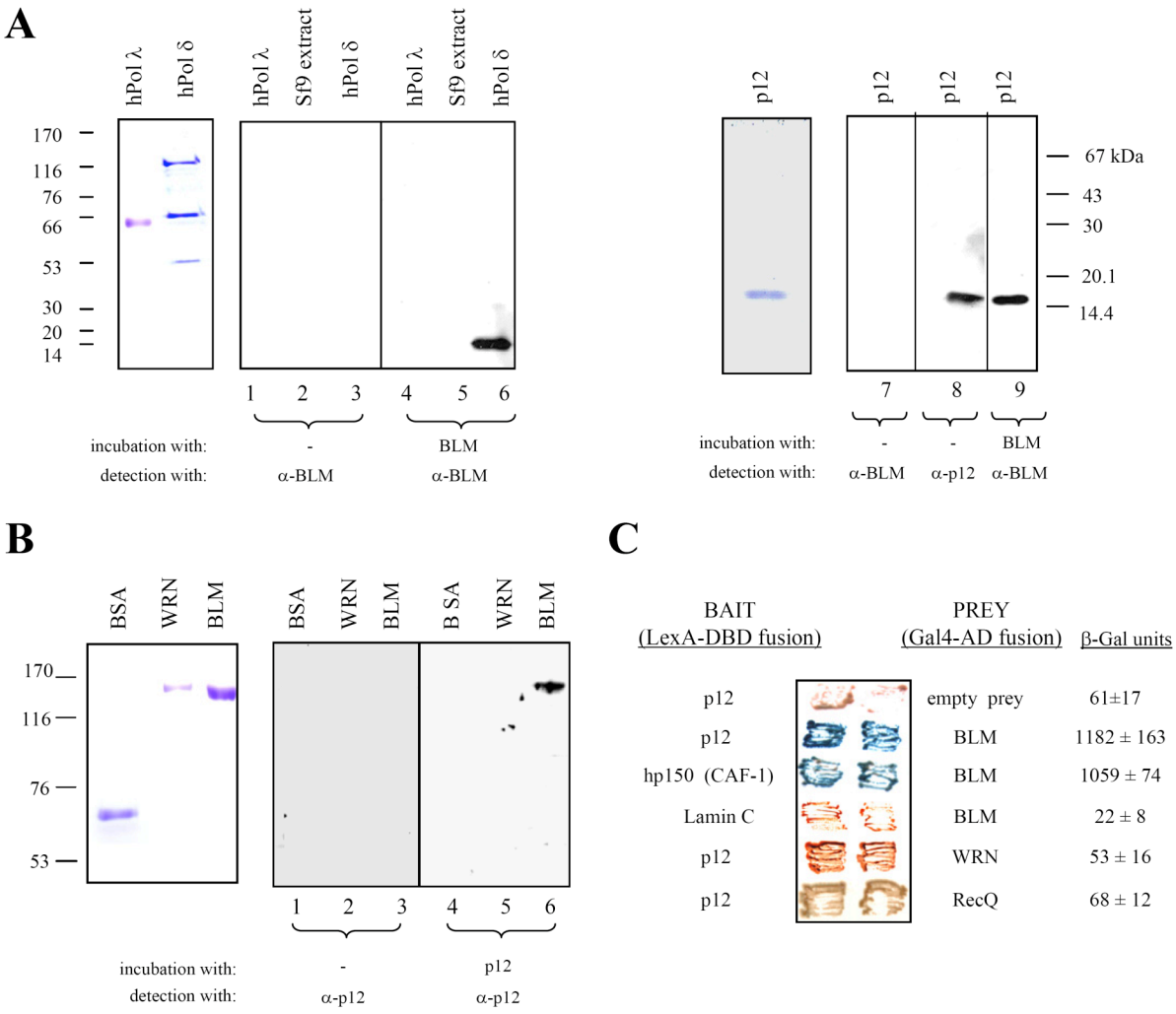
A
hPol λ
hPol δ
Sf9 extract
170
116
76
66
53
30
20
14
1 2 3 4 5 6
incubation with: - BLM
detection with: α-BLM α-BLM
p12
67 kDa
43
30
20.1
14.4
7 8 9
incubation with: - - BLM
detection with: α-BLM α-p12 α-BLM
B
BSA
WRN
BLM
B SA
170
116
76
53
incubation with: - p12
detection with: α-p12 α-p12
C
BAIT (LexA-DBD fusion)
PREY (Gal4-AD fusion)
β-Gal units
p12 empty prey 61±17
p12 BLM 1182 ± 163
hp150 (CAF-1) BLM 1059 ± 74
Lamin C BLM 22 ± 8
p12 WRN 53 ± 16
p12 RecQ 68 ± 12
D
input
IgG
IP: α- FLAG (asynchr)
IP: α- FLAG (S phase)
α-F LAG
α- BLM
α- p125
1 2 3 4
IP: α- BLM (asynchr)
IP: α- BLM (S phase)
α– BLM
α- FLAG
α- hp150 (CAF-1)
5 6 7 8
Input BLM-/-
Input BLM-/- + BLM
IP α-BLM (BLM-/-)
IP α-BLM (BLM-/- + pBLM) S phase
α- BLM
α- FLAG
9 10 11 12

Figure 1

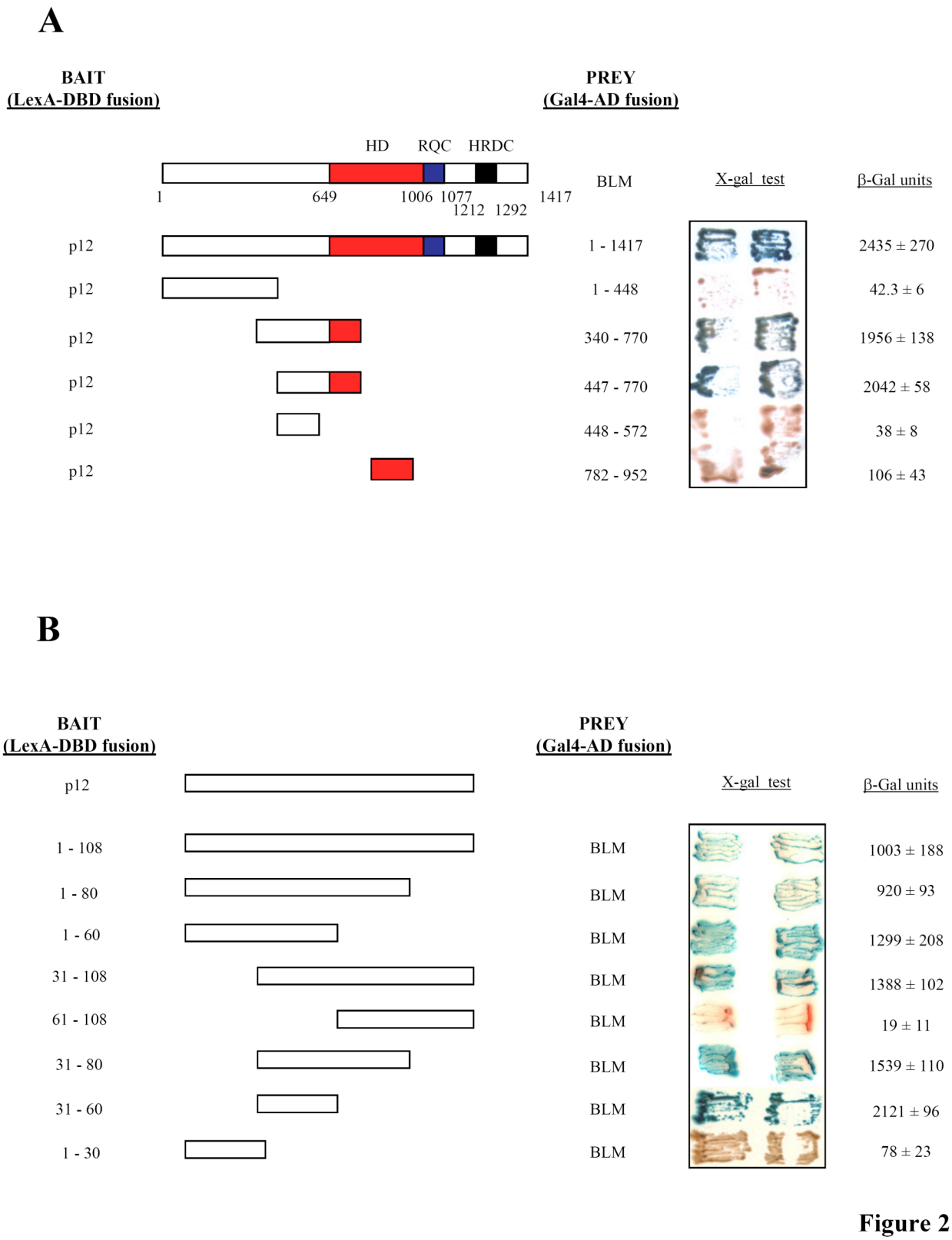
A
BAIT
(LexA-DBD fusion)
PREY
(Gal4-AD fusion)
HD
RQC
HRDC
1
649
1006
1077
1212
1292
1417
BLM
X-gal test
β-Gal units
p12
1 - 1417
2435 ± 270
p12
1 - 448
42.3 ± 6
p12
340 - 770
1956 ± 138
p12
447 - 770
2042 ± 58
p12
448 - 572
38 ± 8
p12
782 - 952
106 ± 43
B
BAIT
(LexA-DBD fusion)
PREY
(Gal4-AD fusion)
X-gal test
β-Gal units
p12
1 - 108
BLM
1003 ± 188
1 - 80
BLM
920 ± 93
1 - 60
BLM
1299 ± 208
31 - 108
BLM
1388 ± 102
61 - 108
BLM
19 ± 11
31 - 80
BLM
1539 ± 110
31 - 60
BLM
2121 ± 96
1 - 30
BLM
78 ± 23

Figure 2

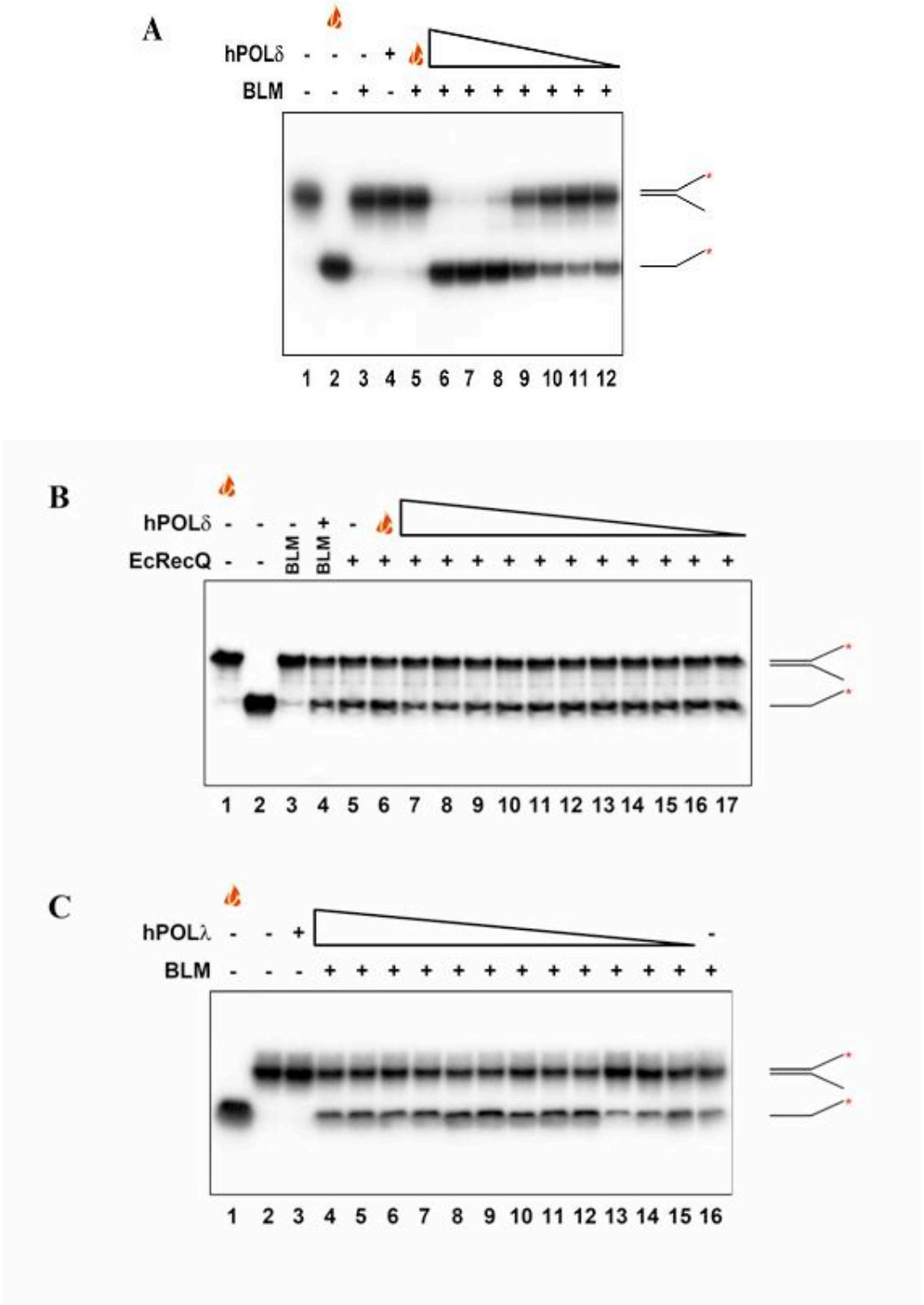
A
hPOLδ - - - + +
BLM - - + - + + + + + + + +
1 2 3 4 5 6 7 8 9 10 11 12
B
hPOLδ - - - + -
BLM BLM
EcRecQ - - + + + + + + + + + + + + +
1 2 3 4 5 6 7 8 9 10 11 12 13 14 15 16 17
C
hPOLλ - - + -
BLM - - - + + + + + + + + + + + +
1 2 3 4 5 6 7 8 9 10 11 12 13 14 15 16

Figure 3

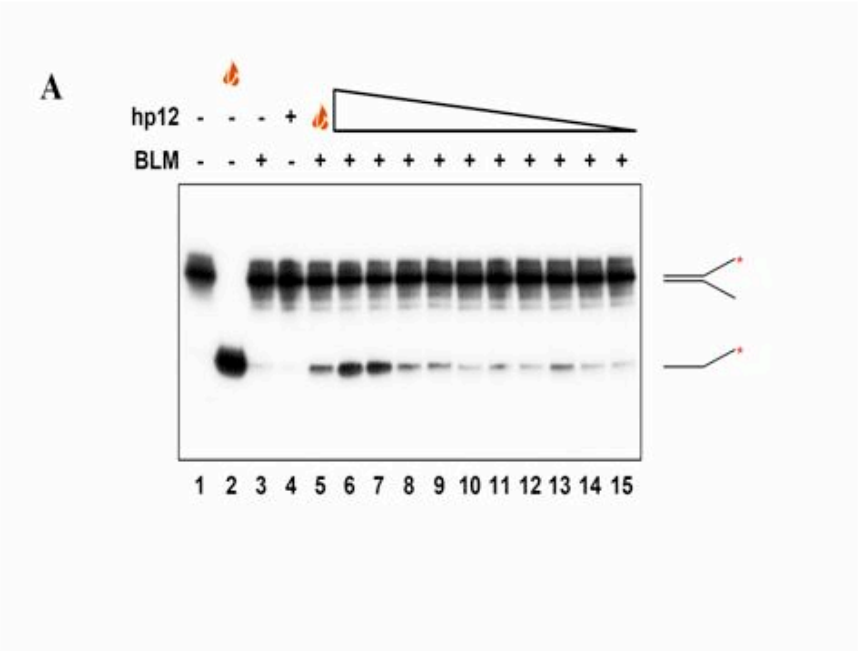
A
hp12 - - - + +
BLM - - + - + + + + + + + + + + +
1 2 3 4 5 6 7 8 9 10 11 12 13 14 15

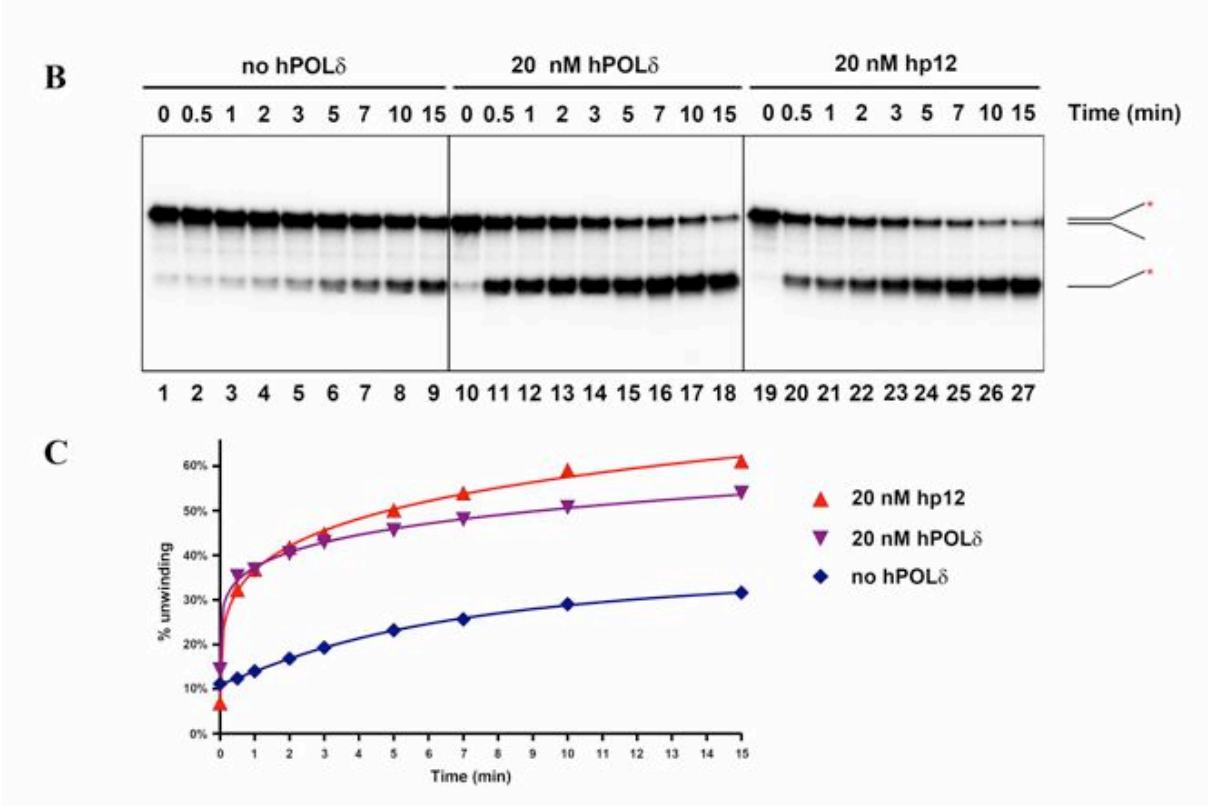
B
no hPOLδ
20 nM hPOLδ
20 nM hp12
0 0.5 1 2 3 5 7 10 15 0 0.5 1 2 3 5 7 10 15 0 0.5 1 2 3 5 7 10 15
Time (min)
1 2 3 4 5 6 7 8 9 10 11 12 13 14 15 16 17 18 19 20 21 22 23 24 25 26 27
C
% unwinding
60%
50%
40%
30%
20%
10%
0%
0 1 2 3 4 5 6 7 8 9 10 11 12 13 14 15
Time (min)
20 nM hp12
20 nM hPOLδ
no hPOLδ

Figure 4

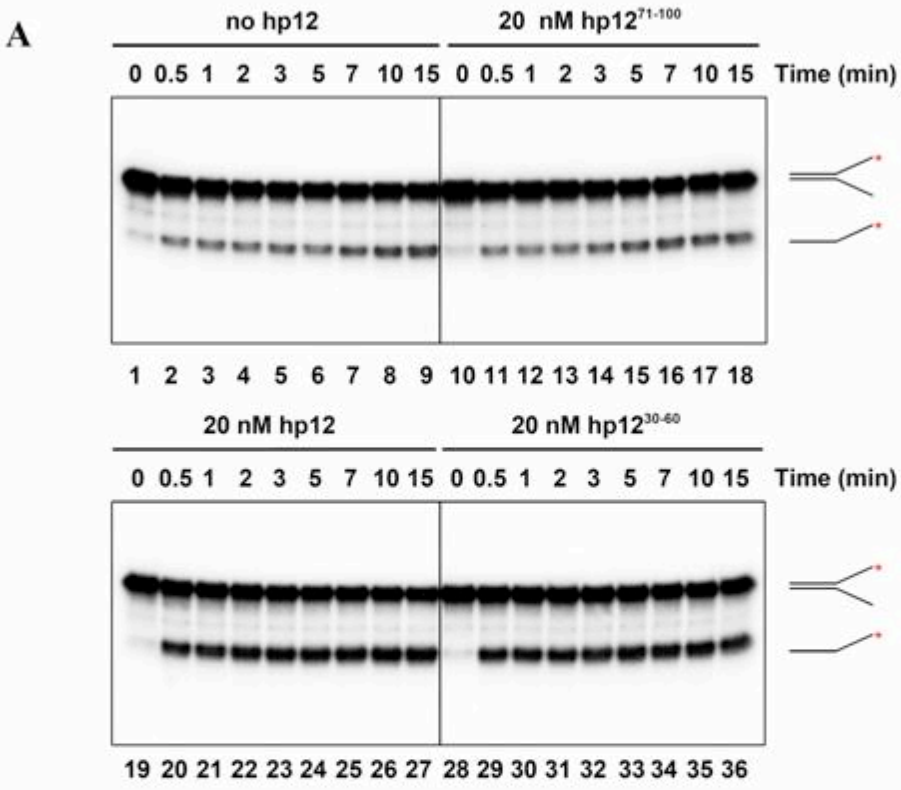
A
no hp12
20 nM hp12^71-100
0 0.5 1 2 3 5 7 10 15 0 0.5 1 2 3 5 7 10 15 Time (min)
1 2 3 4 5 6 7 8 9 10 11 12 13 14 15 16 17 18
20 nM hp12
20 nM hp12^30-60
0 0.5 1 2 3 5 7 10 15 0 0.5 1 2 3 5 7 10 15 Time (min)
19 20 21 22 23 24 25 26 27 28 29 30 31 32 33 34 35 36

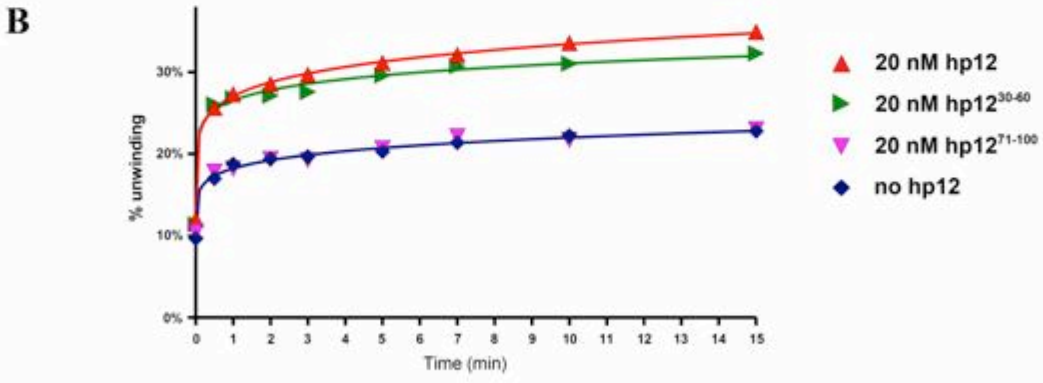
B
% unwinding
30%
20%
10%
0%
0 1 2 3 4 5 6 7 8 9 10 11 12 13 14 15
Time (min)
20 nM hp12
20 nM hp12^30-60
20 nM hp12^71-100
no hp12

Figure 5

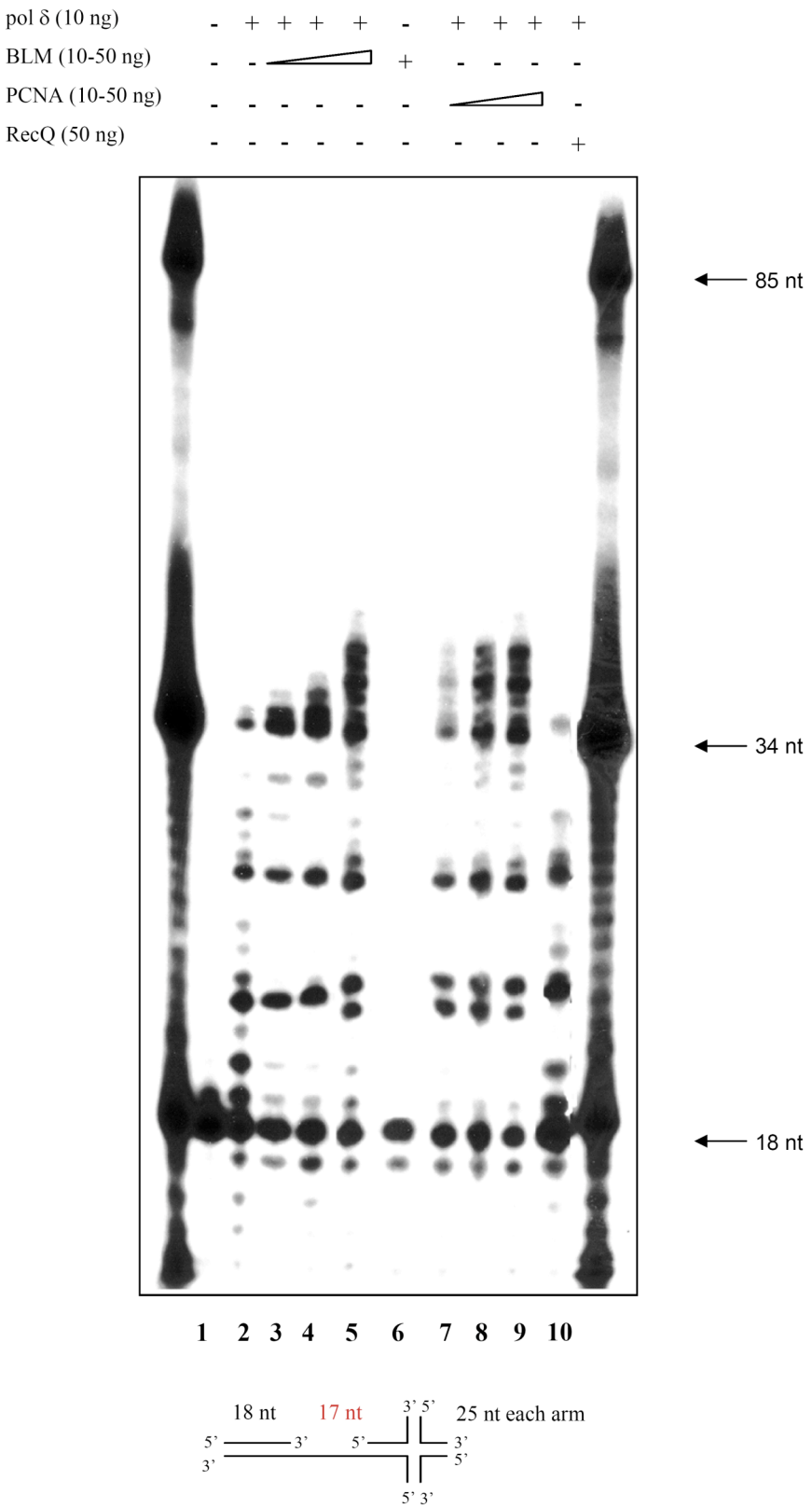
pol δ (10 ng) - + + + + - + + + +
BLM (10-50 ng) - - + - - - -
PCNA (10-50 ng) - - - - - - -
RecQ (50 ng) - - - - - - - - - +
85 nt
34 nt
18 nt
1 2 3 4 5 6 7 8 9 10
18 nt
17 nt
3' 5'
25 nt each arm
5'
3'
3'
5'
5'
3'
3'
5'
5' 3'

Figure 6

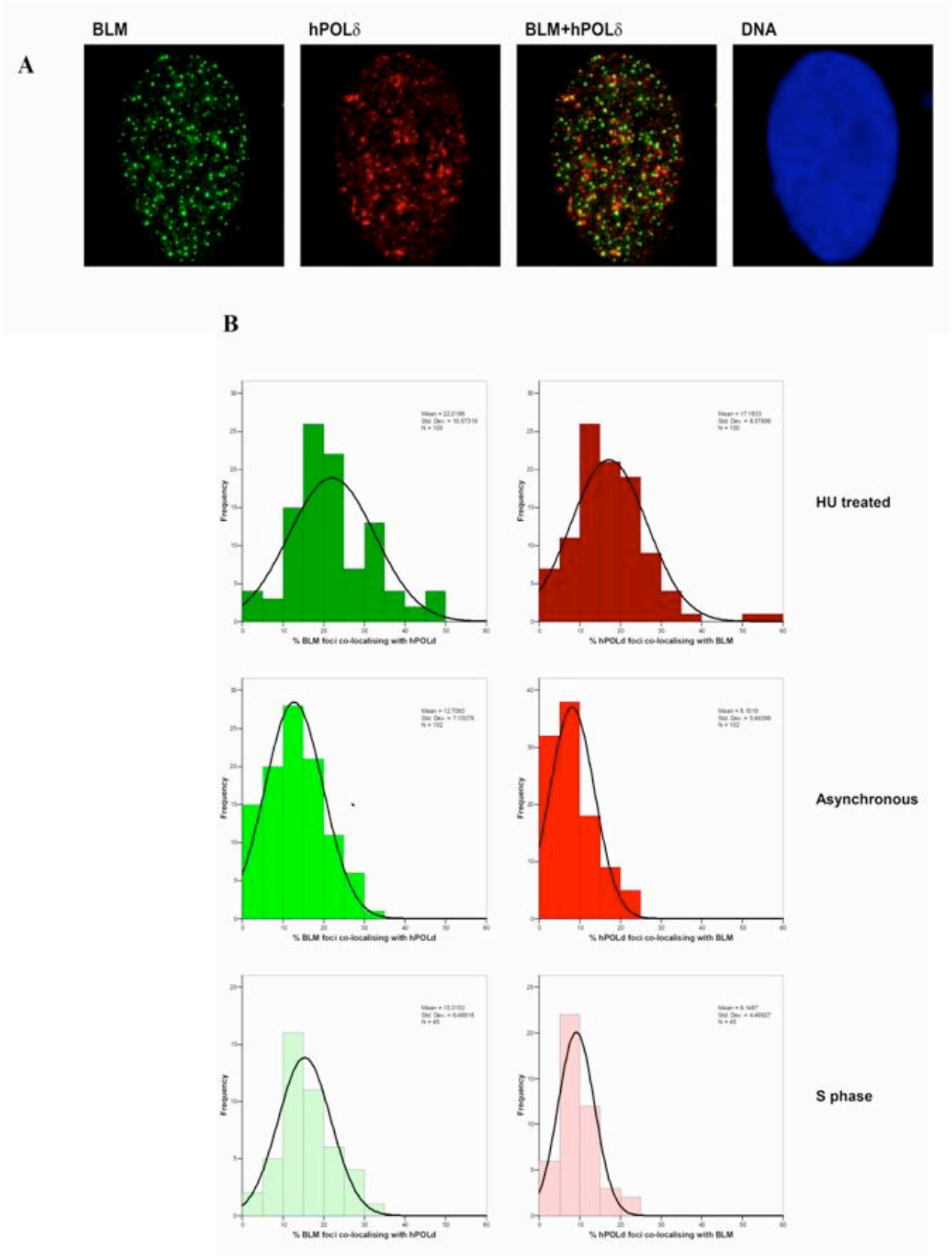
A
BLM
hPOLδ
BLM+hPOLδ
DNA
B
HU treated
Asynchronous
S phase
Frequency
% BLM foci co-localising with hPOLd
% hPOLd foci co-localising with BLM

Figure 7

A

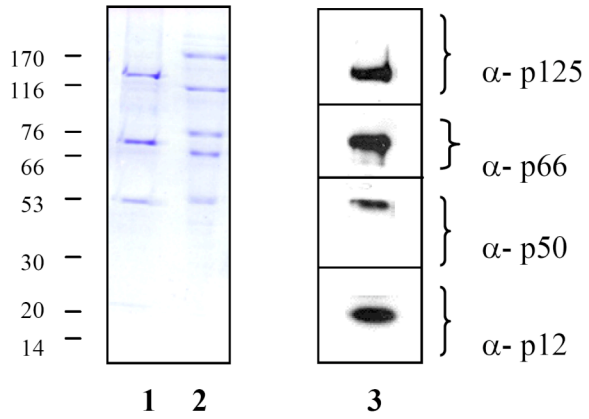

B

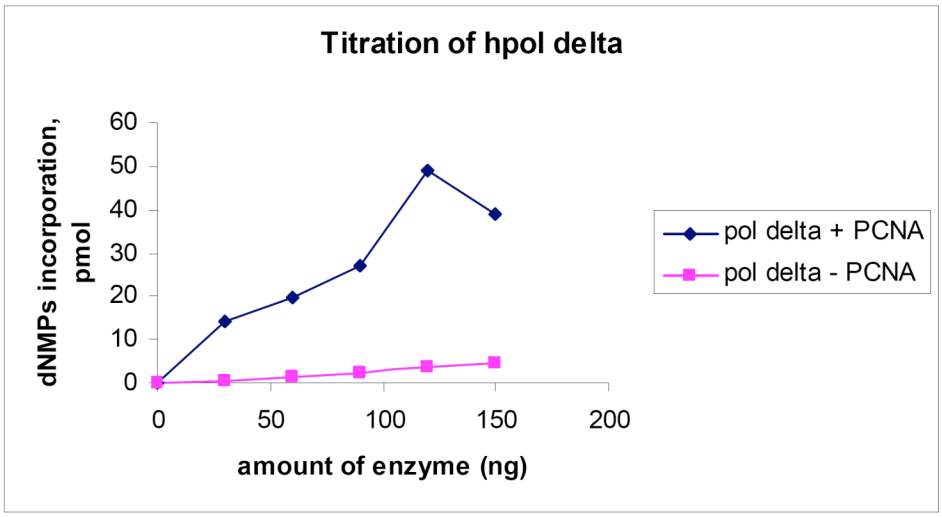

Supplementary Figure 1

8 Acknowledgements

First of all I would like to thank my supervisor Prof. Igor Stagljar for giving me the opportunity to do my PhD in his group and for his continuous support and encouragement.

I am indebted to Prof. Joe Jiricny, the director of the IMCR, who gave me the possibility to work at his Institute.

I am grateful to Dr. Pavel Janscak for accepting me in his group and for stimulating scientific discussions.

I thank Prof. Michael Hottiger for being part of my PhD-Committee and for helping me with my project.

My special thanks go to all the members the IVBMB and IMCR for great working atmosphere.

Additionally, I thank all people from the 12th Floor of the CCBR for making my year in Toronto so exciting.

I want to point out Ralph Imhof for computer support and Tania Roberts for proofreading all my manuscripts.

I also thank my parents who gave me moral and financial support during the time of my studies and PhD.

Finally I would like to thank Dr. Sandra for standing by my side and for sharing her life with me.

The Gebert Ruef Foundation is acknowledged for financial support during this PhD work.

9 Curriculum Vitae

Tobias Dietschy, dipl.mol.bio Uni ZH
Segantinistrasse 73
CH-8049 Zürich
Tel.: +41 341 22 53
tobias.dietschy@utoronto.ca

Geburtsdatum: 10.06.1977

Heimatort: Rheinfelden (AG)

Ausbildung

2006-2007	**PhD Student am Department of Biochemistry and Department of Medical Genetics and Microbioloy, University of Toronto, Canada**
2005-2006	**PhD Student am Institut für molekulare Krebsforschung, Universität Zürich**
2004-2005	**PhD Student am veterinärmedizinisch-biochemischen und molekularbiologischen Institut, Universität Zürich**
2004	**Diplom der mathematisch-naturwissenschaftlichen Fakultät der Universität Zürich**, Hauptfach Molekularbiologie
2002-2003	**Diplomarbeit im Bereich der Genomstabilität** Titel: Screening for interacting partners and purification of the human helicase RecQL4 bei **Professor Igor Stagljar**
2001-2002	**Vertiefung im Bereich Molekularbiologie und Immunologie**
1999-2001	**Grundstudium der Biologie an der Universität Zürich**
1993-1998	**Matura Gymnasium Stadelhofen-Zürich (Typus L)**

Berufliche Erfahrung

1999-2004	**The Promoter Pool**, Zürich, Promotionen und Produktvorstellungen für die Firmen **Excom** und **Orange** u.a. an verschiedenen Messen wie der **Orbit** in Basel (Teilzeitarbeit)
1995-1997	**Kiosk AG** Zürich, Arbeit als Teilzeitverkäufer

Publikationen und Konferenzen

Tobias Dietschy, Igor Shevelev, Raymond Mak, Mohammad Fahad Miah, Daniel Hess, Monika Fey, Pavel Janscak, Michael Hottiger and Igor Stagljar (2007) Acetylation of RECQL4, the Rothmund-Thomson-RAPADILINO- and Baller-Gerold-Syndrome gene product, by the histone acetyltransferase p300 regulates its subcellular localization. Submitted

Nives Selak, Csanád Z. Bachrati, Igor Shevelev, **Tobias Dietschy**, Anette Jacob, Ulrich Hübscher, Joerg D. Hoheisel, Ian D. Hickson, and Igor Stagljar (2007) The Bloom's syndrome helicase (BLM) interacts physically and functionally with p12, the smallest subunit of human DNA polymerase δ. Submitted

Tobias Dietschy, Igor Shevelev and Igor Stagljar (2007)
The molecular role of the Rothmund-Thomson-, RAPADILINO- and Baller-Gerold-gene product, RECQL4: recent progress. *Cell. Mol. Life Sci. 64, 796 – 802*

Nurten Saydam*****, Radhakrishnan Kanagaraj*****, **Tobias Dietschy***, Patrick L. Garcia, Javier Peña-Diaz, Igor Shevelev, Igor Stagljar and Pavel Janscak (2007) Physical and functional interactions between Werner syndrome helicase and mismatch-repair initiation factors. *Nucl. Acids. Res. 2007, 1–11*
(***** contributed equally)

R Jiao, JA Harrigan, I Shevelev, **T Dietschy**, N Selak, FE Indig, J Piotrowski, P Janscak, VA Bohr and I Stagljar (2006) The Werner syndrome protein is required for recruitment of chromatin assembly factor 1 following DNA damage. *Oncogene*, *1-12*

Maja Petkovic, **Tobias Dietschy**, Raimundo Freire, Renjie Jiao, and Igor Stagljar (2005) The human Rothmund-Thomson syndrome gene product, RECQL4, localizes to distinct nuclear foci that coincide with proteins involved in the maintenance of genome stability.
Journal of Cell Science 118, 4261-4269

EU-RTN Annual Meeting and Midterm Review, Amsterdam 2005
Oral Presentation

7th Charles Rodolphe Brupbacher Symposium, ETH Zürich 2005
Poster Presentation

Helicases and NTP driven nucleic acid machines, Arolla 2005
Poster Presentation

EU Young Researcher Meeting, Cambridge 2005
Oral Presentation

Sprachen

Deutsch: Muttersprache**; Englisch**: sehr gute Kenntnisse**; Französisch:** gute Kenntnisse

Informatikkenntnisse

Gute Kenntnisse in MS-Office

Persönliche Interessen

Golf spielen
Weinkunde und Kochen
Verschiedene kulturelle Reisen (1998, 2000, 2004)
Freunde